ON THE SPATIAL PROPERTIES OF FOLIAR CHEMICAL TRAITS FOR SOME COMMONLY OCCURRING EASTERN BOREAL FOREST SPECIES

By

© Travis Robert Heckford

A thesis submitted to the

School of Graduate Studies

in partial fulfillment of the requirements for the degree of

Doctor of Philosophy

Department of Biology, Faculty of Science

Memorial University of Newfoundland

April 2022

Abstract

A central focus of trait-based ecology is investigating trait-species-environment relationships. Across landscapes, foliar traits of forest species are influenced by environmental conditions that result in spatial patterns of trait variability. In this thesis, using commonly occurring boreal plant species, I infer ecological processes from the empirical spatial patterns of foliar elemental (i.e., carbon (C), nitrogen (N), and phosphorus (P)), stoichiometric (i.e., C:N, C:P, and N:P), and phytochemical traits (i.e., terpenoid concentrations of coniferous species); herein referred to as foliar ESP traits. In this thesis, I first investigated how the elemental niche of a conifer and deciduous species differ at a species level between ecoregions and at a community level across, within, and between ecoregions. Notably, I found that a species foliar elemental niche is specific to their biogeographic location, suggesting that regional environmental factors constrain eco-physiological processes that influence how species acquire and use elemental resources. Secondly, I compared multiple models to determine parsimonious predictors of foliar ESP traits using combinations of spatial covariates which include land cover (i.e., coniferous, deciduous, mixedwood), productivity (Enhanced Vegetation Index), biotic (stand height, canopy closure, age), and abiotic (elevation, aspect, slope) factors. I found that spatial-trait relationships occurred at the species level. These results suggest that the spatial patterns of foliar ESP traits are largely species-specific at the landscape extent. Thirdly, at the forest stand extent, I examined the spatial co-variance of foliar ESP traits between species. I found that in most cases, spatial correlations of foliar ESP traits differed between forest stands and that spatial aggregation/segregation patterns of foliar ESP traits varied with distance/direction. Notably, most foliar phytochemical traits of conifers exhibit strong aggregation at a close distance (0-50 metres). Finally, I summarized the main thesis takeaways that (1) foliar traits differ by biogeographical locations and in response to common community-level configurations, (2) the spatial predictors of foliar traits are species-specific, and (3) the spatial co-variance patterns of foliar traits are scale, site and species-dependent. My thesis contributes to our understanding of how traits can be used to inform different aspects of landscape functionality by bridging community, ecosystem, and landscape ecology disciplines.

General Summary

In the natural environment, the nutritional quality of plants and their foliage is influenced by factors that control how those plants acquire and use nutrients to persist in different places. Many experiments and descriptive studies have highlighted the different factors which influence nutritional plant traits. Yet few studies have investigated how these plant traits vary spatially across scales, landscapes, and between species. Identifying and relating the spatial patterns of plant traits to environmental factors is an important step towards understanding how herbivores interact with their environment and how ecosystems function. Here, I present new insights into species-trait-environmental relationships using a transferrable approach for comparisons across different ecosystems. I used chemical traits of plants, which act as universal units to compare within, across, and between different plant species. I used commonly occurring plants that are found widely throughout North American ecosystems. First, I showed how these chemical traits differed between ecosystems and in response to growing alone or together in different habitats. I found that plants have different ranges of trait variability between ecosystems that relates specificity to biogeographic location. I also showed that there are some changes in trait conditions when species occur in different combinations. Second, using this information of ecosystem-specific trait variability, I compared how different environmental factors influenced plant traits within a given ecosystem at a landscape scale. I found that plant traits are often predicted by different environmental factors, limiting our ability to generalize ideas of nutritional/resource hot spots. Third, at the stand scale, I compared the spatial co-variability of plant traits between co-occurring species and showed how these relationships changed with distance, direction, and site. I found that species with different strategies for resources often complement each other which may influence the spatial forage choices herbivores make. My results show that new insights can be gained by linking the chemical traits of species to spatial environmental conditions that reveal the spatial properties of ecosystems and landscapes. My results may also inform wildlife, habitat, and resiliency indicators of landscape management.

Acknowledgements

I would like to acknowledge that the work described in this thesis was carried out on the island of Newfoundland, the ancestral land of the Beothuk and Mi'kmaq people.

I would like to express my sincere gratitude to my supervisor, Dr. Yolanda F. Wiersma, for her unwavering support throughout my Ph.D. study and related research – your patience, kindness, and knowledge are truly inspirational. Thank you for your strong leadership and guidance throughout the researching and writing of this thesis. I could not imagine having a better supervisor and mentor for my Ph.D. study.

I would like to thank my committee members. To Dr. Shawn J. Leroux, thank you for your encouragement and support. Our many discussions helped me focus my efforts, shaped my thinking, and have inspired me to do science well. To Dr. Eric Vander Wal, thank you for your insightful comments and feedback that helped me throughout my Ph.D. study. I would also like to thank the Terrestrial Ecology Research Group students, Matteo Rizzuto, Juliana Balluffi-Fry, and Isabella Richmond for helping me with fieldwork, conceptualizing research ideas, and feedback on my thesis chapters. I am especially thankful to Matteo Rizzuto for painstakingly but diligently collecting our vegetation data in the first field season.

To the entire biology department at Memorial University of Newfoundland, thank you for providing a welcoming and supportive environment. A special thanks to the office folks of the biology department for being a rock-solid foundation. I thank all my current and past Landscape Ecology and Spatial Analysis lab mates for your helpful feedback on my research. I am grateful for your kindness and continued friendship. I would also like to extend a special thanks to Dr. Luise Hermanutz, Dr. Paul Marino, Dr. Thomas Chapman, Patrick Lauriault, and Dr. Anne McLeod, your support, encouragement, mentorship, and friendship helped me through this process, and for that, I am grateful. Last and foremost, I thank my family and friends for

supporting me. And to my partner, Tegan Padgett, thank you for always being there; I am eternally grateful. And to my son, Ruben, your arrival was the push I needed to complete this thesis, and as such, I dedicate this work to you.

This thesis would not be possible without support and funding from the Government of Newfoundland and Labrador Centre for Forest Science and Innovation, Memorial University of Newfoundland, the Research and Development Corporation of Newfoundland and Labrador, Mitacs Accelerate, Parks Canada, and the Natural Sciences and Engineering Research Council.

Table of Contents

List of Tables

List of Figures

List of Appendices

Chapter 1

Introduction and overview

1.1 The case for traits

The causes and consequences of trait variability is a fundamental focus in ecological research. Propelled by the beak traits of Darwin's finches, our push to understand trait form and function has permeated all aspects of ecology (Fajardo & Siefert, 2018; Podos & Nowicki, 2004). A central premise of trait-based ecology is that functionality, across levels of organization, is predictable using organism traits (Díaz et al., 2016; Mcgill et al., 2006). For instance, determining a species function via ecological niche uses traits to inform niche dimensions (Elton, 1927; Grinnell, 1917; Hutchinson, 1957). Community assembly hinges on a trait filter to explain species configurations, co-existence, and biodiversity patterns (Kraft et al., 2015; Vandewalle et al., 2010). Moreover, indicator traits have been proven useful for determining species responses to disturbances and reorganization processes related to the concept of ecological resiliency (Gladstone-Gallagher et al., 2019). Traits underlie population-level average fitness differences and are essential to explain co-evolutionary and speciation processes (Laughlin et al., 2020; Strauss et al., 2005). Plant traits, in particular their foliar properties, are useful predictors of ecosystem processes and feedback relationships (Grime & Pierce, 2012). Traits are the cornerstone of ecology.

1.2 Plant strategies, the leaf economic spectrum, and foliar trait variability

In plant ecology, understanding differences in trait variability across species requires the consideration of plant strategies – an overarching description of a species' approach to maximize its success in variable environments (Grime, 1974). Many definitions of plant strategies exist.

For instance, adaptive strategies describe genetic changes (Bradshaw, 1965), reproductive strategies focus on mechanisms of propagation (i.e., r/K selection theory; seed mass, number of seeds; Pianka, 1970), competitive strategies depend on resource acquisition traits (i.e., resource ratio hypothesis or R* rule; Tilman, 1982, 1985), functional trait-based strategies consider the indicator traits of life history patterns (i.e., Westoby's leaf-height-seed; Westoby, 1998), and resource allocation strategies use stress and disturbance as constraints on plant biomass production (Grime's competition-stress-disturbance triangle; Grime, 1977; Grime & Pierce, 2012). These definitions of plant strategies serve different purposes to explain the broad patterns of plant diversity. Yet, there is a common theme. Plants must make trade-offs between growth, reproduction, and maintenance in variable environments via resource allocation (Grime & Pierce, 2012). Differential resource allocation results in trait variability as plants attempt to optimize their performance by amplifying some traits via divergence of resources to other traits (Laughlin et al., 2020). For instance, when environmental conditions trigger a mast-seeding event, piñon pine (*Pinus edulis* Engelm.) will prioritize reproduction over defence via carbon (C) allocation (Redmond et al., 2019). Similar trade-offs have been observed in whitebark pine (*Pinus albicaulis* Engelm.) where nitrogen (N) and phosphorus (P) reserves are depleted from branches (i.e., growth) and allocated to cone production (i.e., reproduction; Sala et al., 2012). Using elements (i.e., C, N, and P) or elemental derivatives (i.e., primary and secondary chemical compounds) as quantifiable traits we can characterize resource-explicit strategies with trade-off linkages to environmental conditions that influence resource availability and how plants acquire and use resources.

The leaf economic spectrum functions to describe trade-offs between foliar traits in response to environmental conditions along a plant strategy continuum of resource-acquisitive to resource-conservative (Fajardo & Siefert, 2018). Species on opposite ends of the leaf economic spectrum exhibit different strategies to deal with dynamic environmental conditions (Reich, 2014). For instance, resource-acquisitive species, notably fast-growing shade intolerant species, rapidly acquire resources and have a higher competitive capacity (Reich, 2014; Wright et al., 2004). In comparison, resource-conservative species are often slow-growing, shade tolerant types where resource conservatism may promote them to eventually establish as the dominant community species (Wright et al., 2004). For example, in a mixed forest landscape, post-fire patches can favour resource-acquisitive deciduous species which rapidly acquire N and P resources for growth (Finegan, 1985). Shade tolerant resource-conservative coniferous trees may eventually re-establish and grow under the deciduous canopy, and over time, the conifers can eventually competitively exclude the deciduous species from the canopy (Finegan, 1985).

Eco-physiological traits of species with different resource strategies are particularly useful as indicator traits since trait variability directly relates to the environment (Vandewalle et al., 2010). For instance, foliar N and P traits in balsam fir (*Abies balsamea* (L.) Mill.) and red spruce (*Picea rubens* Sarg.) follow elevational gradients, while Scots pine (*Pinus sylvestris* L.) foliar C, N, and P traits shift in response to soil fertility gradients (He et al., 2019; Richardson, 2004). As well, across species with similar resource strategies, shifts in foliar traits have been observed with topographic gradients and herbivore pressure (Callis-Duehl et al., 2017). Vertical canopy variability may also occur in foliar traits. For instance, foliar N has been proposed to be proportional to light interception (Field, 1983; Hollinger, 1996), however, in conifers evidence suggests this relationship may break down as below crown shaded leaves are more efficient at capturing carbon (Richardson, 2004).

The range of foliar trait variability or plasticity depends on a species' resource strategy. Resource-acquisitive species often exhibit high foliar morphological variability compared to resource-conservative species – highly constrained growth geometry (Horn, 1971; Marshall & Monserud, 2003). As such, resource-acquisitive species may display a greater capacity for trait variability which allows them to persist within different environmental conditions where trait divergence reduces niche overlap and allows for species to co-exist (Ashton et al., 2010). Moreover, high trait variability of resource-acquisitive species is suggested to correlate with larger geographic ranges (Chacón-Madrigal et al., 2018). Thus, characterizing a species based on their resource strategies and linking environmental drivers of foliar trait variability provides a meaningful way to compare trait variability within and between species to reveal ecological generalities.

1.3 A consideration for foliar elemental, stoichiometric, phytochemical traits

Foliar elemental traits, primarily C, N, and P – as three of the most abundant elements in life forms aside from oxygen and hydrogen – and stoichiometric traits (i.e., elemental ratios of C:N, C:P, and N:P) represent universal units to compare across species with different resource strategies to reveal environmental drivers of trait variability (Meunier et al., 2017). Phytochemical traits may differ between species but species with similar resource strategies such as conifers (i.e., constituent defence strategies; see Kessler, 2015) can be used to investigate drivers of trait convergence and divergence (Champagne et al., 2018; Hunter, 2016). Foliar elemental, stoichiometric, and phytochemical (hereafter referred to as "ESP") traits are often useful indicators of ecosystem processes such as decomposition (Diaz et al., 2004), primary production (Hessen et al., 2004), evapotranspiration (Guerrieri et al., 2016), and trophic interactions (Hunter, 2016). Thus, temporal snapshots of foliar ESP traits allow us to infer ecological processes given species-specific responses to different environmental conditions.

1.4 The spatial variability of foliar ESP traits and the importance of scale

The foliar ESP traits of plants can spatially vary in response to different environmental conditions at different scales. Spatially, environmental conditions vary across landscapes. This variability can result in different mosaics creating patches of different ecological communities (i.e., seral stage stands, species configurations) or mosaics of spatial trait patterns (Pickett & Cadenasso, 1995). Different environmental conditions likely influence the spatial variability of species traits at different scales (i.e., from the tree to the stand, to the landscape, to larger regional conditions; Dézerald et al., 2018, Lavorel et al., 2011). For instance, at local scales foliar ESP traits may co-vary between co-occurring species with similar resource strategies (Buckley et al., 2016). At different distances between co-occurring species along changing environmental gradients, these relationships of trait co-variability may break down (Buckley et al., 2016; Champagne et al., 2018). At larger scales, biogeographical conditions, such as variation in temperature and precipitation regimes can influence differences in trait variability (Reich & Oleksyn, 2004). For example, plants at higher latitudes are expected to have higher concentrations of N and P attributed to lower photosynthetic gains of C in colder/wetter environments relative to N and P uptake (Woods et al., 2003). Thus, species specific spatial variability of foliar ESP traits should be considered at different scales, in order to obtain estimates of ecosystem processes that reveal differences in landscape functionality (Pickett & Cadenasso, 1995; Shen et al., 2011).

1.5 The boreal forest – a nutrient limited place

Boreal forests cover the northern circumpolar region and are characterized by cold long winters and short summers (Högberg et al., 2017). Generally, the boreal forest landscape is a mosaic of mixed coniferous and deciduous tree patches (Hansson, 1992). In North America, the boreal forest stretches across northern Canada from the Yukon to Newfoundland and Labrador – representing 25% of the world's remaining intact forests and accounting for 22% of the global carbon storage (Bonan & Shugart, 1989; Pan et al., 2011). The species composition of the boreal forest differs from west to east and south to north due to species-specific dispersal patterns and ecological requirements in response to climatic and historical patterns of glacial retreat (Hansson, 1992). The boreal is a nutrient, primarily N and P, limited system (Högberg et al., 2017). Limited N supply in boreal forests influence ecosystem processes such as decomposition via the interaction of N litter quality and temperature (Bosatta & Agren, 1991), plant productivity (Reich et al., 2012), and food web complexity (Bonan & Shugart, 1989). Resource explicit, foliar ESP traits represent meaningful units to infer spatial patterns of ecosystems processes in the boreal forest. For instance, soil N availability correlates with higher foliar N concentration in some species and increased recycling of N via litter input (Gartner & Cardon, 2004; Hobbie, 2015). However, plants with higher foliar N concentrations are preferentially foraged by boreal herbivores such as moose (*Alces alces* (Linnaeus, 1758); Balluffi-Fry et al., 2020). To deter moose browsing, plants such as white birch (*Betula papyrifera* Marshall) can increase foliar phytochemical (i.e., phenols, terpenoids) production, which can inhibit soil enzymes associated with N recycling (Adamczyk et al., 2015). Thus, within boreal forests, the spatial patterns of plant foliar ESP traits can be used to obtain estimates of critical ecosystems processes at different spatial scales.

1.6 Study location and focal species

Our study location is the island of Newfoundland. In Chapter 2, we focused on foliar trait differences between and within two ecoregions on the island of Newfoundland, the Northern Peninsula and Central Forest (differences between the two ecoregions are described in detail in Chapter 2). In Chapter 3 and Chapter 4, we focused on an ecodistrict within the Central Forest ecoregion. In the Central Forest ecoregion our data are derived from plots distributed across four chronosequenced grids which represent common stand types within this landscape (see Appendix B.2 Figure B.2.1). The grids represent different aged stands in 20 year intervals with two grids in mature and old stands (TNNP North and Dunphy’s Pond) located within Terra Nova National Park. The grids were established as part of a larger project to answer questions around herbivore space use and the spatial distribution of forage quality. Our stand types represent common habitats that are reflective of the disturbance history on the island of Newfoundland as the impacts of common disturbance agents tend to occur at the stand extent as opposed to the landscape extent (Arsenault et al., 2016). Although wildfire may have caused large landscape extent disturbance patterns, the evidence for this is limited and the return interval is suggested to operate on scales of centuries to millennia (fire cycle approximately at 769 years) and primarily in the Central Forest ecoregion. Other disturbance agents, such as spruce budworm (*Choristoneura fumiferana* Clemens) and hemlock looper (*Lambdina fiscellaria* Guenée) are suggested to have large stand level impacts that operate on decade to century return intervals (Arsenault et al., 2016).

Our study species were chosen for two reasons. The first is that they are the preferred forage for moose (*Alces alces* (Linnaeus, 1758)) and snowshoe hare (*Lepus americanus*

(Erxleben, 1777)) (Dodds, 1960). The second reason was that these plants are ubiquitous in most habitats across the study area, and across the entire island of Newfoundland (South, 1983). Throughout the thesis, where I provide the scientific names of species, I have included their authority agreements and in subsequent mentions I refer to them using their common names.

The focal species in this research included two coniferous tree species: balsam fir (*Abies balsamea* (L.) Mill.), black spruce (*Picea mariana* (Mill.) Britton, Sterns, & Poggenb), two deciduous tree species: white birch (*Betula papyrifera* Marshall), red maple (*Acer rubrum* L.), and one shrub: lowbush blueberry (*Vaccinium angustifolium* Aiton.). To control for differences in ontogeny, we focused on understory plants, sampling individuals to a maximum of 2 metres in height as these individuals constituent potential forage options for boreal herbivores. We sampled foliar material for each of our focal species that included the foliage and woody parts from lateral and terminal branches. Although our study is limited to the boreal forest system on the island of Newfoundland, Canada, our focal species co-exist across a broad geographic range (see Figure 1.1). In addition, differences in the geographic range of our focal species is related to breadth of intraspecific trait variability, which we demonstrate throughout this thesis.

Balsam fir is a small to medium-sized coniferous evergreen species that is widely distributed across northeastern North America. At maturity, tree heights range from 12 to 30 m, with diameter at breast height ranging from 30 to 75 cm (Bakuzis & Hansen, 1965). Reproduction generally begins at 20 years of age with regular seed production occurring after 30 years of age. Balsam fir forest stands typically self-replace through the development of shade tolerant juveniles within the understory (Gosse et al., 2011). Because seasonal needle losses result in the acidification of the surrounding soil, this exhibits a strong priority effect on the vegetative community composition which facilitates balsam fir community turnover and as such balsam fir is considered a foundation species (Bakuzis & Hansen, 1965). Foliage needles are flat and resinous and, although moderately palatable, they are an important source of winter and early spring forage for moose (Thompson et al., 1989).

Black spruce is a small to medium sized coniferous evergreen species that is widely distributed across North America in a variety of ecosystem types (LeBarron, 1948). At maturity tree heights range from 9-15 m, with diameter at breast height ranging from 15 to 25 cm (LeBarron, 1948). Reproduction occurs from seed dispersal both with and without fire beginning at 10 years of age (Cyr et al., 2012). In addition, vegetative reproduction occurs through layering of lower branches (LeBarron, 1939). Although many species rely on black spruce habitat types, given the low palatability of foliar material, very few species consume it (Dunn et al., 2009; Thompson et al., 1992). However, on the island of Newfoundland moose and snowshoe hare have been documented to browse black spruce in the winter and shoulder seasons (Dodds, 1960).

Red maple is a medium sized single or multi-stemmed deciduous species that is widely distributed across eastern North America (Burns & Honkala, 1990). Typically, this species matures at year 4 and is polygamo-dioecious, where some males produces no seeds and females produce seeds and some are monoecious bearing both male and female structures. At maturity, tree heights range from 18 to 27 m, with a diameter at breast height ranging from 46 to 76 m. This species may exhibit vegetation reproduction by dormant buds located at the tree base (stump) (Burns & Honkala, 1990). Leaves are relatively palatable and are an important summer forage for moose and snowshoe hare (Dodds, 1960).

White birch is a medium sized single or multi-stemmed deciduous species that is distributed across North America (Burns & Honkala, 1990). At maturity, tree heights can range from 21 to 24 m, with diameter at breast height ranging from 25 to 30 cm (Burns & Honkala, 1990). White birch is a prolific seed producer with reproduction beginning around 15 years of age and optimizing between 40 to 70 years of age (Burns & Honkala, 1990). Generally, within boreal forest ecosystems, white birch are pioneer species that readily dominate disturbed sites, forming nearly pure stands. Seasonal losses and leaf litter inputs influence the chemical composition and nutrient availability of soil resources, exhibiting strong priority effects on the white birch community turnover, and as such white birch is considered a foundation species (Schöb et al., 2012). White birch is an important source of forage material for moose, with stems serving as winter forage and leaves and stems as preferred summer forage (Wam et al., 2018).

Lowbush blueberry is a deciduous clonal shrub that exhibits a dense extensive root system (Usui et al., 2005). At maturity, shrub heights can range from 5 to 60 cm. Leaf shape ranges from broad to elliptical and fruit develop in bunches at terminal ends (Usui et al., 2005). This species grows best in the understory of forested habitats with well drained soils and is an important food sources for black bear (*Ursus americanus* (Pallas, 1780)) and snowshoe hare on the island of Newfoundland (Dodds, 1960).

1.7 Thesis overview

My thesis combines different approaches to examine the environmental drivers of foliar elemental, stoichiometric, and phytochemical traits for our focal species. Overall, my thesis is an example of integrating trait-based ecology into ecosystem and landscape ecology to demonstrate how the spatial patterning of functional traits may relate to ecosystem processes via species-trait-environmental relationships.

In Chapter 2, I constructed elemental niches for balsam fir and white birch using foliar axes of C, N, and P and investigated how ecoregion and community structure differences influenced these elemental niches. Typically, large spatial extent investigations often focus on individual elemental trait differences. Here, I show how our focal species' foliar C, N, and P traits differed together in a hypervolume niche context. Specifically, I showed that our focal species have different elemental niches in different ecoregions – due to regional biophysical factors. Furthermore, I grouped our species at the plot level by conspecific (only one of the species is present) and heterospecific (both species present) community types and compared these groups across, within, and between ecoregions for each focal species. I demonstrated that these community types differed across and within ecoregions for white birch but not for balsam fir. More notably, these community type comparisons between ecoregions showed differences that highlight large scale biophysical influences on an organism's elemental niche. This chapter may serve to guide researchers and practitioners on the use and limitations of extrapolating foliar elemental traits in different ecosystems and community types.

In Chapter 3, I took a novel spin on distribution models to map the variability of foliar ESP traits in response to remotely sensed spatial covariates (for framework see Leroux et al., 2017). More specifically, I used a multi-model approach to determine the spatial drivers of foliar ESP traits for our focal species. Using spatially explicit covariates of land cover (coniferous, deciduous, and mixedwood), productivity (Enhanced Vegetation Index), biotic (stand structure factors of age, tree height, and canopy closure), and abiotic factors (slope, aspect, and elevation), I tested different combinations of these covariates and determined parsimonious drivers of foliar ESP traits for our focal species. Model results of this chapter supported the construction of spatially explicit raster surfaces for the foliar ESP traits of our focal species. These spatially explicit predictive surfaces of resource/forage quality are used by other members of our research team to explore herbivore respond to the spatial variability of important forage traits (see section

1.8 below). Moreover, this research can act as a template for land managers to understand the spatial variability of forage and how landscapes could be structured (i.e., spatial patterns) to facilitate robust wildlife populations and habitat configurations.

In Chapter 4, I bridged community, spatial, and landscape ecology by exploring the spatial co-variance of foliar ESP traits between species. More specifically, I tested hypotheses around community assembly theory where, at the local level, filtering processes select for species with convergent resource strategies and divergent traits. I used co-dispersion analysis and determined at what distances foliar traits spatially aggregate or segregate and the overall spatial patterning of isotropy or anisotropy. I showed that the spatial patterning of traits differed by scale, direction, site age, and species-specific resource strategies. This research may be used by researchers and land managers to understand within patch variability of forage quality with linkages to herbivore foraging decisions. Lastly, in Chapter 5, I briefly summarized the main findings of my thesis and discuss potential future directions related to this work.

My thesis provides a trait-based bridge between ecosystem and landscape ecology. I used foliar chemical traits that relate to ecosystem processes such as biomass production, biogeochemical regimes, and decomposition cycles, and lean on landscape ecology concepts of pattern and process relationships to interpret the cause and consequence of foliar trait spatial patterns. Taken together, my thesis contributes to ecological theory by sharpening questions related to environmental drivers of foliar chemical traits. In particular, my thesis demonstrates the linkages of organ level traits and ecosystem/landscape functionality via species-trait-environmental relationships. First, I showed that foliar elemental niches at the species and community level (i.e., using co-occurrence of our focal species) are specific to biogeographical properties, in this case, ecoregion classifications. Secondly, I used plot data from a specific ecodistrict (i.e., an ecological sub-component of an ecoregion) and determined remotely sense covariates of foliar ESP traits. Using model estimates I spatially predicted foliar traits to reveal landscape level patterns of resource quality. Finally, I showed stand level co-variability in foliar ESP traits between species and determined the scale at which aggregation/segregation and isotropy/anisotropy trait relationships occurred. Trait-based ecology provides a framework to link organ-level traits to functionality across levels of organization. In my thesis, I show how the spatial patterns of foliar traits may influence community assembly, wildlife populations, herbivore resource selection, and ecosystem processes, while highlighting the importance of understanding habitat properties related to forage quality.

Associated data and R codes used in this thesis can be found in the data accessibility section of each chapter.

1.8 The Terrestrial Ecology Research Group

Components of my thesis fit into other projects within the Terrestrial Ecology Research Group (TERG) at Memorial University of Newfoundland. TERG is a collaboration between three principal investigators, Dr. Yolanda F. Wiersma, Dr. Shawn J. Leroux, and Dr. Eric Vander Wal with expertise spanning across landscape ecology, ecosystem ecology, and wildlife population ecology disciplines, respectively. TERG principal investigators are supervisors and/or committee members to TERG students. Each TERG student completes an individual project, however, we share data, co-author manuscripts, assist each other with field work, and meet regularly to discuss ideas, and review each other’s research progress. The overarching theme of TERG is to explore how the spatial and temporal variability of foliar ESP traits influence consumer food choices and structure food webs. In 2016, the first cohort of TERG students, including myself, Matteo Rizzuto, and Justin Strong developed the study design, set up sampling grids, and collected the vegetation data which is used widely by former and current students in TERG. The vegetation data includes sample plot descriptions of plant community structure, and foliar elemental, stoichiometric, and phytochemical data. Other students have used the work I completed in this thesis to infer consumer spatial patterns. For instance, in Chapter 3, I determined the spatial drivers of foliar ESP for our focal species and developed predictive spatial surfaces of food quality. These spatially explicit maps of forage quality allowed us to investigate additional dimensions that likely influence herbivore space use and were incorporated into the thesis chapters of other TERG members (see Balluffi-Fry et al., 2021; Richmond et al., 2021; Rizzuto et al., 2021). As part of TERG, I am the lead author of three manuscripts – appearing in this thesis – and co-author on six other manuscripts (see Balluffi-Fry et al., 2020, 2021; Richmond et al., 2020, 2021; Rizzuto et al., 2019, 2021).

1.9 Co-authorship statement

This thesis is the product of my independent research within the broader TERG research framework described above. The following provides a breakdown of each authors contribution by chapter.

Chapter 2: Ecoregion and community structure influences on the foliar elemental niche of balsam fir (*Abies balsamea* (L.) Mill.) and white birch (*Betula papyrifera* Marshall)

Yolanda F. Wiersma, Shawn J. Leroux, Eric Vander-Wal, and I designed the project. Yolanda F. Wiersma, Matteo Rizzuto, and I collected these data, as well Shawn J. Leroux, Eric Vander Wal, and Yolanda F. Wiersma contributed data from the Northern Peninsula ecoregion (as part of another project; see Leroux et al., 2017). I conducted the analysis and wrote the manuscript. All co-authors provided feedback on the analysis, interpretation of results, and edited the manuscript. This manuscript is currently under revision in the journal: *Ecology and Evolution*.

T. R. Heckford, S. J. Leroux, E. Vander Wal, M. Rizzuto, J. Balluffi-Fry, I. C. Richmond, and Y. F. Wiersma (in review). "Ecoregion and community structure influences on the foliar elemental niche of balsam fir (*Abies balsamea* (L.) Mill.) and white birch (*Betula papyrifera* Marshall)".

Chapter 3: Spatially explicit correlates of plant functional traits inform landscape patterns of resource quality

Yolanda F. Wiersma, Shawn J. Leroux, Eric Vander-Wal, Matteo Rizzuto, and I designed the project. Yolanda F. Wiersma, Matteo Rizzuto, and I collected these data. I conducted the analysis and wrote the manuscript. All co-authors provided feedback on the analysis, interpretation of results, and edited the manuscript. This manuscript is published in the journal: *Landscape Ecology*.

Heckford, T. R., Leroux, S. J., Vander Wal, E., Rizzuto, M., Balluffi-Fry, J., Richmond, I. C., & Wiersma, Y. F. (2022). Spatially explicit correlates of plant functional traits inform landscape patterns of resource quality. *Landscape Ecology* 37: 59-80 https://doi.org/10.1007/s10980-021-01334-3

Chapter 4: Local scale spatial co-dispersion patterns of plant functional traits between co-occurring species

Yolanda F. and I designed the project. Yolanda F. Wiersma, Matteo Rizzuto, and I collected these data. I conducted the analysis and wrote the manuscript. All co-authors provided feedback on the analysis, interpretation of results, and edited the manuscript. This manuscript will be submitted to the journal: *Landscape Ecology*.

Heckford, T. R., Leroux, S. J., Vander Wal, E., Rizzuto, M., Balluffi-Fry, J., Richmond, I. C., & Wiersma, Y. F. (n.d.). “Local scale spatial co-dispersion patterns of plant functional traits between co-occurring species”.

1.10 References

Adamczyk, S., Adamczyk, B., Kitunen, V., & Smolander, A. (2015). Monoterpenes and higher terpenes may inhibit enzyme activities in boreal forest soil. *Soil Biology and Biochemistry*, *87*, 59–66. https://doi.org/10.1016/j.soilbio.2015.04.006

Arsenault, A., LeBlanc, R., Earle, E., Brooks, D., Clarke, B., Lavigne, D., & Royer, L. (2016). Unravelling the past to manage Newfoundland's forests for the future. *The Forestry Chronicle*, *92*(4), 487–502.

Ashton, I. W., Miller, A. E., Bowman, W. D., & Suding, K. N. (2010). Niche complementarity due to plasticity in resource use: Plant partitioning of chemical N forms. *Ecology*, *91*(11), 3252–3260. https://doi.org/10.1890/09-1849.1

Bakuzis, E. V., & Hansen, H. L. (1965). *Balsam fir, Abies balsamea (Linnaeus) Miller: A monograph review [by] E.V. Bakuzis and H.L. Hansen, with Contributions by F.H. Kaufert [and Others]*. University of Minnesota Press. https://books.google.ca/books?id=E7n7oAEACAAJ

Balluffi-Fry, J., Leroux, S. J., Wiersma, Y. F., Heckford, T. R., Rizzuto, M., Richmond, I. C., & Vander Wal, E. (2020). Quantity–quality trade-offs revealed using a multiscale test of herbivore resource selection on elemental landscapes. *Ecology and Evolution*, *10*(24), 13847–13859. https://doi.org/10.1002/ece3.6975

Balluffi-Fry, J., Leroux, S. J., Wiersma, Y. F., Richmond, I. C., Heckford, T. R., Rizzuto, M., Kennah, J. L., & Vander Wal, E. (2021). Integrating plant stoichiometry and feeding experiments: State-dependent forage choice and its implications on body mass. *Oecologia*. https://doi.org/10.1007/s00442-021-05069-5

Bonan, G. B., & Shugart, H. H. (1989). Environmental factors and ecological processes in boreal forests. *Annual Review of Ecology and Systematics*, *20*(1), 1–28. https://doi.org/10.1146/annurev.es.20.110189.000245

Bosatta, E., & Agren, G. I. (1991). Dynamics of carbon and nitrogen in the organic matter of the soil: A generic theory. *The American Naturalist*, *138*(1), 227–245. https://doi.org/10.1086/285213

Bradshaw, A. D. (1965). Evolutionary significance of phenotypic plasticity in plants. In E. W. Caspari & J. M. Thoday (Eds.), *Advances in Genetics* (Vol. 13, pp. 115–155). Academic Press. https://doi.org/10.1016/S0065-2660(08)60048-6

Buckley, H. L., Case, B. S., & Ellison, A. M. (2016). Using codispersion analysis to characterize spatial patterns in species co-occurrences. *Ecology*, *97*(1), 32–39. https://doi.org/10.1890/15-0578.1

Buckley, H. L., Case, B. S., Zimmerman, J. K., Thompson, J., Myers, J. A., & Ellison, A. M. (2016). Using codispersion analysis to quantify and understand spatial patterns in species–environment relationships. *New Phytologist*, *211*(2), 735–749. https://doi.org/10.1111/nph.13934

Burns, R. M., & Honkala, B. H. (1990). *Silvics of North America* (Vol. 1). United States Department of Agriculture Washington, DC.

Callis-Duehl, K., Vittoz, P., Defossez, E., & Rasmann, S. (2017). Community-level relaxation of plant defenses against herbivores at high elevation. *Plant Ecology*, *218*(3), 291–304. https://doi.org/10.1007/s11258-016-0688-4

Chacón-Madrigal, E., Wanek, W., Hietz, P., & Dullinger, S. (2018). Traits indicating a conservative resource strategy are weakly related to narrow range size in a group of neotropical trees. *Perspectives in Plant Ecology, Evolution and Systematics*, *32*, 30–37. https://doi.org/10.1016/j.ppees.2018.01.003

Champagne, E., Moore, B. D., Côté, S. D., & Tremblay, J.-P. (2018). Spatial correlations between browsing on balsam fir by white-tailed deer and the nutritional value of neighboring winter forage. *Ecology and Evolution*, *8*(5), 2812–2823. https://doi.org/10.1002/ece3.3878

Cyr, D., Gauthier, S., & Bergeron, Y. (2012). The influence of landscape-level heterogeneity in fire frequency on canopy composition in the boreal forest of eastern Canada. *Journal of Vegetation Science*, *23*(1), 140–150. https://doi.org/10.1111/j.1654-1103.2011.01338.x

Dézerald, O., Srivastava, D. S., Céréghino, R., Carrias, J.-F., Corbara, B., Farjalla, V. F., Leroy, C., Marino, N. A. C., Piccoli, G. C. O., Richardson, B. A., Richardson, M. J., Romero, G. Q., & González, A. L. (2018). Functional traits and environmental conditions predict community isotopic niches and energy pathways across spatial scales. *Functional Ecology*, *32*(10), 2423–2434. https://doi.org/10.1111/1365-2435.13142

Diaz, S., Hodgson, J. G., Thompson, K., Cabido, M., Cornelissen, J. H. C., Jalili, A., Montserrat-Martí, G., Grime, J. P., Zarrinkamar, F., Asri, Y., Band, S. R., Basconcelo, S., Castro-Díez, P., Funes, G., Hamzehee, B., Khoshnevi, M., Pérez-Harguindeguy, N., Pérez-Rontomé, M. C., Shirvany, F. A., … Zak, M. R. (2004). The plant traits that drive ecosystems: Evidence from three continents. *Journal of Vegetation Science*, *15*(3), 295–304. https://doi.org/10.1111/j.1654-1103.2004.tb02266.x

Díaz, S., Kattge, J., Cornelissen, J. H. C., Wright, I. J., Lavorel, S., Dray, S., Reu, B., Kleyer, M., Wirth, C., Colin Prentice, I., Garnier, E., Bönisch, G., Westoby, M., Poorter, H., Reich, P. B., Moles, A. T., Dickie, J., Gillison, A. N., Zanne, A. E., … Gorné, L. D. (2016). The global spectrum of plant form and function. *Nature*, *529*(7585), 167–171. https://doi.org/10.1038/nature16489

Dodds, D. G. (1960). Food competition and range relationships of moose and snowshoe hare in newfoundland. *The Journal of Wildlife Management*, *24*(1), 52. https://doi.org/10.2307/3797356

Dunn, A. L., Wofsy, S. C., & Bright, A. V. H. (2009). Landscape heterogeneity, soil climate, and carbon exchange in a boreal black spruce forest. *Ecological Applications*, *19*(2), 495–504. https://doi.org/10.1890/07-0771.1

Elton, C. S. (1927). *Animal ecology*. New York, Macmillan Co.

Fajardo, A., & Siefert, A. (2018). Intraspecific trait variation and the leaf economics spectrum across resource gradients and levels of organization. *Ecology*, *99*(5), 1024–1030. https://doi.org/10.1002/ecy.2194

Field, C. (1983). Allocating leaf nitrogen for the maximization of carbon gain: Leaf age as a control on the allocation program. *Oecologia*, *56*(2), 341–347. https://doi.org/10.1007/BF00379710

Finegan, B. (1985). Forest succession. *Nature*, *315*(6021), 692–692. https://doi.org/10.1038/315692b0

Gartner, T. B., & Cardon, Z. G. (2004). Decomposition dynamics in mixed-species leaf litter. *Oikos*, *104*(2), 230–246. JSTOR.

Gladstone-Gallagher, R. V., Pilditch, C. A., Stephenson, F., & Thrush, S. F. (2019). Linking traits across ecological scales determines functional resilience. *Trends in Ecology & Evolution*, *34*(12), 1080–1091. https://doi.org/10.1016/j.tree.2019.07.010

Gosse, J., Hermanutz, L., McLaren, B., Deering, P., & Knight, T. (2011). Degradation of boreal forests by nonnative herbivores in Newfoundland’s National Parks: Recommendations for ecosystem restoration. *Natural Areas Journal*, *31*(4), 331–339. https://doi.org/10.3375/043.031.0403

Grime, J. P. (1977). Evidence for the existence of three primary strategies in plants and its relevance to ecological and evolutionary theory. *The American Naturalist*, *111*(982), 1169–1194.

Grime, P. J. (1974). Vegetation classification by reference to strategies. *Nature*, *250*, 26–31.

Grime, P. J., & Pierce, S. (2012). *The evolutionary strategies that shape ecosystems*. Wiley-Blackwell.

Grinnell, J. (1917). The niche-relationships of the california thrasher. *The Auk*, *34*(4), 427–433.

Guerrieri, R., Lepine, L., Asbjornsen, H., Xiao, J., & Ollinger, S. V. (2016). Evapotranspiration and water use efficiency in relation to climate and canopy nitrogen in U.S. forests. *Journal of Geophysical Research: Biogeosciences*, *121*(10), 2610–2629. https://doi.org/10.1002/2016JG003415

Hansson, L. (1992). Landscape ecology of boreal forests. *Trends in Ecology & Evolution*, *7*(9), 299–302. https://doi.org/10.1016/0169-5347(92)90227-3

He, P., Fontana, S., Sardans, J., Peñuelas, J., Gessler, A., Schaub, M., Rigling, A., Li, H., Jiang, Y., & Li, M.-H. (2019). The biogeochemical niche shifts of *Pinus sylvestris var. Mongolica* along an environmental gradient. *Environmental and Experimental Botany*, *167*, 103825. https://doi.org/10.1016/j.envexpbot.2019.103825

Hessen, D. O., Ågren, G. I., Anderson, T. R., Elser, J. J., & de Ruiter, P. C. (2004). Carbon sesquestration in ecosystems: The role of stoichiometry. *Ecology*, *85*(5), 1179–1192. https://doi.org/10.1890/02-0251

Hobbie, S. E. (2015). Plant species effects on nutrient cycling: Revisiting litter feedbacks. *Trends in Ecology & Evolution*, *30*(6), 357–363. https://doi.org/10.1016/j.tree.2015.03.015

Högberg, P., Näsholm, T., Franklin, O., & Högberg, M. N. (2017). Tamm Review: On the nature of the nitrogen limitation to plant growth in Fennoscandian boreal forests. *Forest Ecology and Management*, *403*, 161–185. https://doi.org/10.1016/j.foreco.2017.04.045

Hollinger, D. Y. (1996). Optimality and nitrogen allocation in a tree canopy. *Tree Physiology*, *16*(7), 627–634. https://doi.org/10.1093/treephys/16.7.627

Horn, H., S. (1971). *The adaptive geometry of trees* (Vol. 3). Princeton University Press.

Hunter, M. D. (2016). *The phytochemical landscape: Linking trophic interactions and nutrient dynamics*. Princeton University Press.

Hutchinson, G. E. (1957). Concluding remarks. *Cold Spring Harbor Symposia on Quantitative Biology*, *22*(0), 415–427. https://doi.org/10.1101/SQB.1957.022.01.039

Kessler, A. (2015). The information landscape of plant constitutive and induced secondary metabolite production. *Current Opinion in Insect Science*, *8*, 47–53. https://doi.org/10.1016/j.cois.2015.02.002

Kraft, N. J. B., Adler, P. B., Godoy, O., James, E. C., Fuller, S., & Levine, J. M. (2015). Community assembly, coexistence and the environmental filtering metaphor. *Functional Ecology*, *29*(5), 592–599. https://doi.org/10.1111/1365-2435.12345

Laughlin, D. C., Gremer, J. R., Adler, P. B., Mitchell, R. M., & Moore, M. M. (2020). The net effect of functional traits on fitness. *Trends in Ecology & Evolution*, *35*(11), 1037–1047. https://doi.org/10.1016/j.tree.2020.07.010

Lavorel, S., Grigulis, K., Lamarque, P., Colace, M.-P., Garden, D., Girel, J., Pellet, G., & Douzet, R. (2011). Using plant functional traits to understand the landscape distribution of multiple ecosystem services. *Journal of Ecology*, *99*(1), 135–147. https://doi.org/10.1111/j.1365-2745.2010.01753.x

LeBarron, R. K. (1939). The role of forest fires in the reproduction of black spruce. *Proceedings of the Minnesota Academy of Science*, *7*, 10–14.

LeBarron, R. K. (1948). *Silvicultural management of black spruce in Minnesota*. U.S. Department of Agriculture.

Leroux, S. J., Wal, E. V., Wiersma, Y. F., Charron, L., Ebel, J. D., Ellis, N. M., Hart, C., Kissler, E., Saunders, P. W., Moudrá, L., Tanner, A. L., & Yalcin, S. (2017). Stoichiometric distribution models: Ecological stoichiometry at the landscape extent. *Ecology Letters*, *20*(12), 1495–1506. https://doi.org/10.1111/ele.12859

Little, E. L., Jr. (1971). *Atlas of United States Trees, Volume 1: Conifers and Important Hardwoods* [Map]. U.S. Department of Agriculture.

Marshall, J. D., & Monserud, R. A. (2003). Foliage height influences specific leaf area of three conifer species. *Canadian Journal of Forest Research*, *33*(1), 164–170. https://doi.org/10.1139/x02-158

Mcgill, B., Enquist, B., Weiher, E., & Westoby, M. (2006). Rebuilding community ecology from functional traits. *Trends in Ecology & Evolution*, *21*(4), 178–185. https://doi.org/10.1016/j.tree.2006.02.002

Meunier, C. L., Boersma, M., El-Sabaawi, R., Halvorson, H. M., Herstoff, E. M., Van de Waal, D. B., Vogt, R. J., & Litchman, E. (2017). From elements to function: Toward unifying ecological stoichiometry and trait-based ecology. *Frontiers in Environmental Science*, *5*(18). https://doi.org/10.3389/fenvs.2017.00018

Pan, Y., Birdsey, R. A., Fang, J., Houghton, R., Kauppi, P. E., Kurz, W. A., Phillips, O. L., Shvidenko, A., Lewis, S. L., Canadell, J. G., Ciais, P., Jackson, R. B., Pacala, S. W., McGuire, A. D., Piao, S., Rautiainen, A., Sitch, S., & Hayes, D. (2011). A large and persistent carbon sink in the world's forests. *Science*, *333*(6045), 988–993. https://doi.org/10.1126/science.1201609

Pianka, E. R. (1970). On r- and K-Selection. *The American Naturalist*, *104*(940), 592–597. https://doi.org/10.1086/282697

Pickett, S. T. A., & Cadenasso, M. L. (1995). Landscape ecology: Spatial heterogeneity in ecological systems. *Science*, *269*(5222), 331–334. https://doi.org/10.1126/science.269.5222.331

Podos, J., & Nowicki, S. (2004). Beaks, adaptation, and vocal evolution in darwin's finches. *BioScience*, *54*(6), 501–510. https://doi.org/10.1641/0006-3568(2004)054[0501:BAAVEI]2.0.CO;2

Prasad, A. M., & Iverson, L. R. (2003). *Little's range and FIA importance value database for 135 eastern US tree species* [Map]. http://www.fs.fed.us/ne/delaware/4153/global/littlefia/index.html

Redmond, M. D., Davis, T. S., Ferrenberg, S., & Wion, A. P. (2019). Resource allocation trade-offs in a mast-seeding conifer: Piñon pine prioritizes reproduction over defence. *AoB PLANTS*, *11*(plz070). https://doi.org/10.1093/aobpla/plz070

Reich, P. B. (2014). The world-wide ‘fast-slow’ plant economics spectrum: A traits manifesto. *Journal of Ecology*, *102*(2), 275–301. https://doi.org/10.1111/1365-2745.12211

Reich, P. B., Frelich, L. E., Voldseth, R. A., Bakken, P., & Adair, E. C. (2012). Understorey diversity in southern boreal forests is regulated by productivity and its indirect impacts on resource availability and heterogeneity: Productivity-diversity in boreal forests. *Journal of Ecology*, *100*(2), 539–545. https://doi.org/10.1111/j.1365-2745.2011.01922.x

Reich, P. B., & Oleksyn, J. (2004). Global patterns of plant leaf N and P in relation to temperature and latitude. *Proceedings of the National Academy of Sciences*, *101*(30), 11001–11006. https://doi.org/10.1073/pnas.0403588101

Richardson, A. D. (2004). Foliar chemistry of balsam fir and red spruce in relation to elevation and the canopy light gradient in the mountains of the northeastern United States. *Plant and Soil*, *260*(1), 291–299. https://doi.org/10.1023/B:PLSO.0000030179.02819.85

Richmond, I. C., Balluffi-Fry, J., Vander Wal, E., Leroux, S. J., Rizzuto, M., Heckford, T. R., Kennah, J. L., Riefesel, G. R., & Wiersma, Y. F. (2021). Individual snowshoe hares manage risk differently: Integrating stoichiometric distribution models and foraging ecology. *Journal of Mammalogy*. https://doi.org/10.1093/jmammal/gyab130

Richmond, I. C., Leroux, S. J., Vander Wal, E., Heckford, T. R., Rizzuto, M., Balluffi-Fry, J., Kennah, J. J., & Wiersma, Y. F. (2020). Temporal variation and its drivers in the elemental traits of four boreal plant species. *Journal of Plant Ecology, 14,* 398–413.

Rizzuto, M., Leroux, S. J., Vander Wal, E., Richmond, I. C., Heckford, T. R., Balluffi-Fry, J., & Wiersma, Y. F. (2021). Forage stoichiometry predicts the home range size of a small terrestrial herbivore. *Oecologia*, *197*(2), 327–338. https://doi.org/10.1007/s00442-021-04965-0

Rizzuto, M., Leroux, S. J., Wal, E. V., Wiersma, Y. F., Heckford, T. R., & Balluffi-Fry, J. (2019). Patterns and potential drivers of intraspecific variability in the body C, N, and P composition of a terrestrial consumer, the snowshoe hare (Lepus americanus). *Ecology and Evolution*, *9*(24), 14453–14464. https://doi.org/10.1002/ece3.5880

Sala, A., Hopping, K., McIntire, E. J. B., Delzon, S., & Crone, E. E. (2012). Masting in whitebark pine (*Pinus albicaulis*) depletes stored nutrients. *New Phytologist*, *196*(1), 189–199. https://doi.org/10.1111/j.1469-8137.2012.04257.x

Schöb, C., Butterfield, B. J., & Pugnaire, F. I. (2012). Foundation species influence trait-based community assembly. *New Phytologist*, *196*(3), 824–834. https://doi.org/10.1111/j.1469-8137.2012.04306.x

Shen, W., Lin, Y., Jenerette, G. D., & Wu, J. (2011). Blowing litter across a landscape: Effects on ecosystem nutrient flux and implications for landscape management. *Landscape Ecology*, *26*(5), 629–644. https://doi.org/10.1007/s10980-011-9599-x

South, R. G. (1983). *Biogeography and ecology of the island of Newfoundland* (Vol. 48). Dr. W. Junk Publishers, The Hague, The Netherlands.

Strauss, S. Y., Sahli, H., & Conner, J. K. (2005). Toward a more trait-centered approach to diffuse (co)evolution. *New Phytologist*, *165*(1), 81–90. https://doi.org/10.1111/j.1469-8137.2004.01228.x

Thompson, I. D., Curran, W. J., Hancock, J. A., & Butler, C. E. (1992). Influence of moose browsing on successional forest growth on black spruce sites in Newfoundland. *Forest Ecology and Management*, *47*(1–4), 29–37.

Thompson, I. D., McQueen, R. E., Reichardt, P. B., Trenholm, D. G., & Curran, W. J. (1989). Factors influencing choice of balsam fir twigs from thinned and unthinned stands by moose. *Oecologia*, *81*(4), 506–509. https://doi.org/10.1007/BF00378960

Tilman, D. (1982). *Resource competition and community structure* (Vol. 17). Princeton University Press. https://doi.org/10.2307/j.ctvx5wb72

Tilman, D. (1985). The resource-ratio hypothesis of plant succession. *The American Naturalist*, *125*(6), 827–852.

Usui, M., Kevan, P. G., & Obbard, M. (2005). Pollination and breeding system of lowbush blueberries, *vaccinium angustifolium ait. And v. Myrtilloides michx.* (Ericacaeae), in the boreal forest. *The Canadian Field-Naturalist*, *119*(1), 48. https://doi.org/10.22621/cfn.v119i1.80

Vandewalle, M., de Bello, F., Berg, M. P., Bolger, T., Dolédec, S., Dubs, F., Feld, C. K., Harrington, R., Harrison, P. A., Lavorel, S., da Silva, P. M., Moretti, M., Niemelä, J., Santos, P., Sattler, T., Sousa, J. P., Sykes, M. T., Vanbergen, A. J., & Woodcock, B. A. (2010). Functional traits as indicators of biodiversity response to land use changes across ecosystems and organisms. *Biodiversity and Conservation*, *19*(10), 2921–2947. https://doi.org/10.1007/s10531-010-9798-9

Wam, H. K., Felton, A. M., Stolter, C., Nybakken, L., & Hjeljord, O. (2018). Moose selecting for specific nutritional composition of birch places limits on food acceptability. *Ecology and Evolution*, *8*(2), 1117–1130. https://doi.org/10.1002/ece3.3715

Westoby, M. (1998). A leaf-height-seed (LHS) plant ecology strategy scheme. *Plant and Soil*, *199*(2), 213–227. https://doi.org/10.1023/A:1004327224729

Woods, H. A., Makino, W., Cotner, J. B., Hobbie, S. E., Harrison, J. F., Acharya, K., & Elser, J. J. (2003). Temperature and the chemical composition of poikilothermic organisms. *Functional Ecology*, *17*(2), 237–245. https://doi.org/10.1046/j.1365-2435.2003.00724.x

Wright, I. J., Reich, P. B., Westoby, M., Ackerly, D. D., Baruch, Z., Bongers, F., Cavender-Bares, J., Chapin, T., Cornelissen, J. H., & Diemer, M. (2004). The worldwide leaf economics spectrum. *Nature*, *428*(6985), 821–827.

1.11 Figures

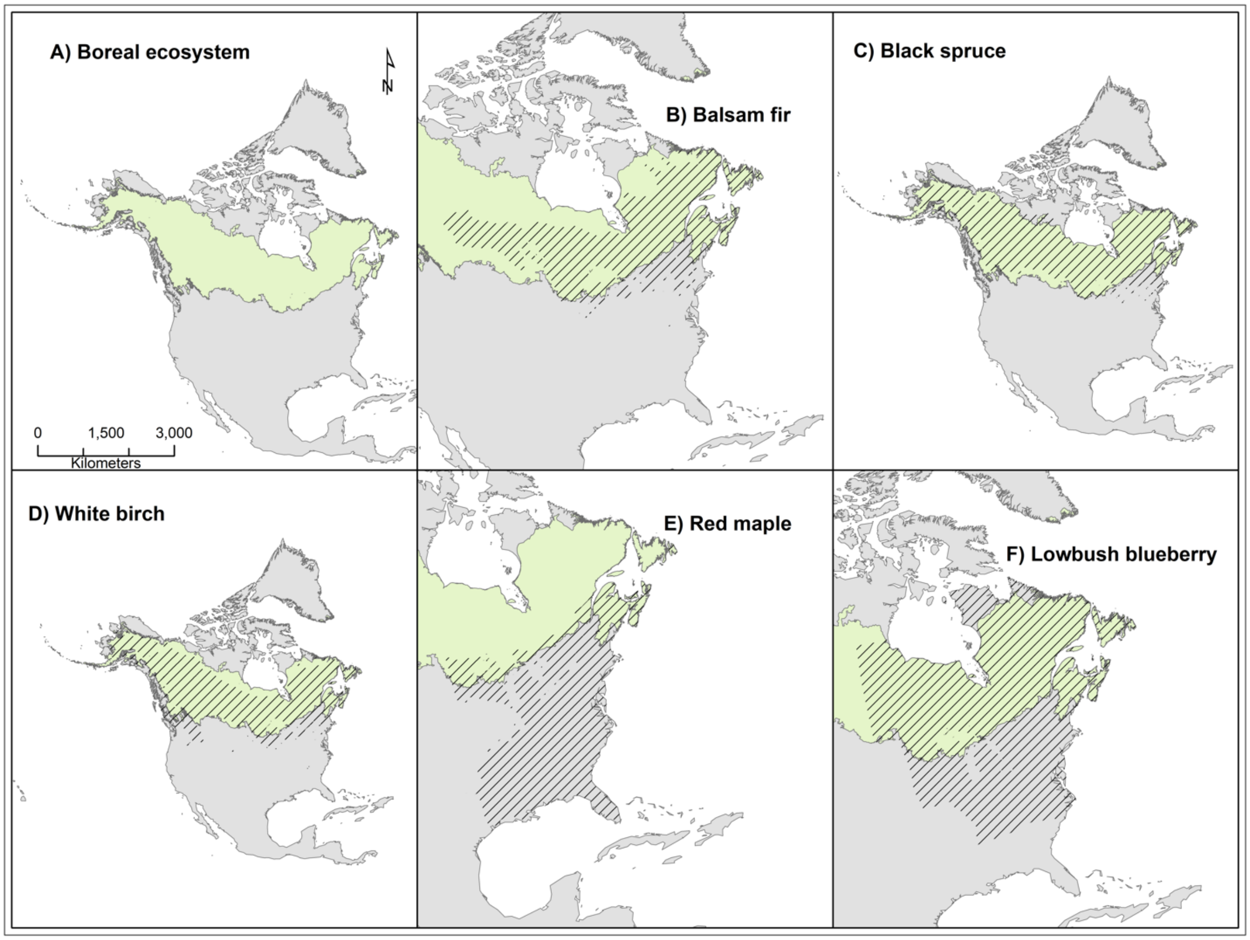

Figure 1.1 Distribution maps of our focal species with reference to the boreal biome in North America; dashed lines represent species ranges (Little, 1971; Prasad & Iverson, 2003). Forests within the boreal biome (A) stretch across North America from Alaska to Newfoundland and Labrador. The geographic range of (B) balsam fir is largely limited to eastern North America while (C) black spruce and (D) white birch are continuous throughout the boreal. The geographic range for (E) red maple and (F) lowbush blueberry extends further south than our other focal species and are limited to eastern North America.

Chapter 2

Ecoregion and community structure influences on the foliar elemental niche of balsam fir (*Abies balsamea* (L.) Mill.) and white birch (*Betula papyrifera* Marshall)

Authors: Travis R Heckford[1], Shawn J. Leroux[1], Eric Vander Wal[1], Matteo Rizzuto[1], Juliana Balluffi-Fry[2], Isabella C. Richmond[1], Yolanda F. Wiersma[1]

Author Affiliations

1: Department of Biology, Memorial University of Newfoundland. 230 Elizabeth Avenue, St. John's, Canada.

2: Department of Biological Sciences, University of Alberta, Edmonton, Canada

A version of this paper is in revision in *Ecology and Evolution* as

T. R. Heckford, S. J. Leroux, E. Vander Wal, M. Rizzuto, J. Balluffi-Fry, I. C. Richmond, and Y. F. Wiersma (in review). "Ecoregion and community structure influences on the foliar elemental niche of balsam fir (*Abies balsamea* (L.) Mill.) and white birch (*Betula papyrifera* Marshall)".

2.1 Abstract

Context: Foliar elemental niches, defined by axes of carbon (C), nitrogen (N), and phosphorus (P) concentrations reflect how species allocate resources under different environmental conditions related to ecoregions and community types.

Methods: At a species level we compared foliar elemental niches of balsam fir (*Abies balsamea* (L.) Mill.) and white birch (*Betula papyrifera* Marshall) between ecoregions. At the community level, we compared foliar elemental niches of conspecific (i.e., same species occurrence) and heterospecific groups (i.e., co-occurrence of both species) across, within, and between ecoregions. Between ecoregions at the species and community level, we expected foliar elemental niches to be different and driven by regional biophysical effects on foliar N and P concentrations. At the community level, we expected niche displacement and expansion patterns for fir and birch, respectively – patterns that reflect their resource strategy.

Results: At the species level, foliar elemental niches between ecoregions differed significantly for fir ($F = 14.591$, p-value = 0.001) and birch ($F = 75.998$, p-value = 0.001) with higher foliar N and P in the northern ecoregion. At the community level, across ecoregions, the foliar elemental niche of birch differed significantly between heterospecific and conspecific groups ($F = 4.075$, p-value = 0.021) and both species displayed niche expansion patterns in response to heterospecific conditions (fir niche volume increased by 35.49% and birch by 68.92%). Within the northern ecoregion, heterospecific conditions elicited niche expansion responses (niche volume increased for fir by 29.04% and birch by 66.48%) and in the southern ecoregion we found contraction (birch niche volume decreased by 3.66%) and neutral effects (fir = no change). Foliar elemental niches of conspecific community types between ecoregions yielded significant differences for fir and birch ($F = 7.581$, p-value = 0.005 and $F = 8.038$, p-value = 0.001) as did heterospecific comparisons ($F = 6.943$, p-value = 0.004, and $F = 68.702$, p-value = 0.001, respectively).

Conclusions: Our results suggest species may exhibit biogeographical specific elemental niches – driven by biophysical differences at the ecoregion scale. We also demonstrate how a species resource strategy influences elemental niche shifts in response to different community settings. Our study highlights how biogeographical differences may influence foliar elemental traits and how this may link to ecosystem and landscape functionality.

2.2 Introduction

How we measure and conceptualize a species niche has changed over time. From its original inception of a trait-habitat match (Grinnell, 1917) our idea of a species niche grew to incorporate species-environmental feedbacks (Elton, 1927) and their multi-dimensional resource-environmental relationships (Hutchinson, 1957). By combining these niche concepts, we can assess species' Intraspecific Trait Variability (ITV) in response to environmental and resource gradients in multidimensional space (Blonder, 2017; Gravel et al., 2019; Soberón, 2007). This approach has provided insights into the structure of food webs (Newsome et al., 2007), foraging behaviours (Hette-Tronquart, 2019), social interactions (Bergmüller & Taborsky, 2010), community assembly (Bulleri et al., 2016), species networks (Godoy et al., 2018), spatial patterns (Dézerald et al., 2018; Godsoe et al., 2017), and biogeochemical-environmental relationships (Kearney et al., 2013; Peñuelas et al., 2019; Urbina et al., 2017). However, a potential limitation to comparing niches across different species to reveal environmental relationships is that niche axes which define a species' ecological role or uniqueness may be constructed using traits which are absent in other species such as differences in root growth patterns; vegetative vs. reproductive traits; or trait differences across trophic groups.

Elemental traits represent universal traits to construct niche axes and compare within and between species to reveal how species respond to and exist within variable environments. Although organisms are composed of an elementome of approximately 25 elemental traits (Kaspari & Powers, 2016), carbon (C), nitrogen (N), and phosphorus (P) are the three most proportionately abundant elements (Sterner & Elser, 2002). The concentration of C, N, and P in foliar material provides important linkages to ecological processes (Cherif et al., 2017). For instance, the availability of N and P soil resources regulate C sequestration by influencing an individual’s growth and reproductive potential via N and P contributions to enzymes, nucleic acids, and membrane lipids (Elser et al., 2000). Foliar C, N, and P can also indicate nutrient co-limitation dynamics at the community-level where species resource requirements vary in response to competitive effects – adjustments to balance the supply and demand of elemental resources (see Harpole et al., 2011). At broad scales, foliar C, N, and P can be used to infer ecosystem functionality via species-level elemental plasticity and biogeochemical contributions to nutrient cycling (see Zhang et al., 2018). Recent work highlights the growing interest in using C, N, and P niche axes to assess stoichiometric and trait co-variability patterns between species, trophic groups, and in response to different environmental conditions (i.e., stoichiometric niche, González et al., 2017; and biogeochemical niche He et al., 2019; Peñuelas et al., 2019). Thus, foliar C, N, and P represent universal species-level traits to construct niche dimensions and assess ITV that link individuals to environmental conditions across scales such as biogeographical and community level gradients (Leal et al., 2017).

Plants that are distributed across large scale biogeographic gradients such as ecoregions, likely alter their resource strategies (resource acquisition and use) in response to differing biophysical constraints of temperature, precipitation, and soil nutrient/moisture regimes (Šímová et al., 2011). For instance, the temperature-plant physiological hypothesis suggests plants at higher latitudes contain greater foliar N and P elemental concentrations (Reich & Oleksyn, 2004). This is attributed to lower photosynthetic gains of C in colder temperatures relative to N and P uptake (Woods et al., 2003). As well, low foliar P can indicate stressful environmental conditions species might experience on the edge of their range, such as drought (He et al., 2019). By evaluating foliar elemental concentrations along niche axes, we can reveal how changes in C, N, and P via ITV and trait co-variability patterns may occur in response to large scale biogeographical environmental classification schemas (i.e., ecozone, ecoregion, ecodistrict), and their associated biophysical and climate factors (Ecological Stratification Working Group, 1996; MacKenzie & Meidinger, 2018) to derive generalities around ecosystem processes at regional scales.

Across, within, and between biogeographical areas, trees often occur in spatial associations (i.e., patches) of conspecific and heterospecific communities (i.e., trees in pure and mixed wood forest stands; Hansson, 1992; Pastor et al., 1999). In these communities, differing mechanisms of dispersal, nutrient use, herbivory, and disturbance interact to influence the recruitment of juvenile trees that will eventually replace adults (Birch et al., 2019; Gray & He, 2009). As stands develop, horizontal and vertical community structure differs, and this can influence the presence and abundance of recruiting trees via light availability and litter-biochemical soil interactions on seedling establishment (Klinka et al., 1996). In conspecific and heterospecific communities, variability in community structure can arise from differing types (i.e., needleleaf and broadleaf), amounts, and chemical compositions (i.e., low C:N) of foliar litter input (Gartner & Cardon, 2004; Hobbie, 2015). This in turn influences microbial community composition and regulates decomposition and nutrient recycling processes (Krishna & Mohan, 2017; Prieto et al., 2019). For example, in conspecific communities, positive feedbacks have been observed for biogeochemical processes of nutrient recycling via nutrient retrieval (Florence & McGuire, 2020). In comparison, heterospecific associations often promote diversification of microbial communities in response to differing types of litter input which in turn increases the competition for nutrient retrieval (Krishna & Mohan, 2017; Reynolds et al., 2003). Thus, trees in conspecific and heterospecific communities experience different community structural and nutrient feedback conditions that regulate N and P uptake and C sequestration, and this is reflected in foliar C, N, and P concentrations (Reich et al., 2009; Urbina et al., 2017).

Recent work demonstrates the linkages of foliar elemental niche patterns to different community types. For example, Urbina et al., (2017), characterized biogeochemical niche shifts as either an expansion, contraction, or displacement responses relative to a conspecific (i.e., community occurrence of the same species) niche space patterns using a principal component analysis. As well, different niches can be compared by assessing hypervolume patterns of niche similarity via size, overlap, and nestedness (for Jaccard hypervolume comparisons see Blonder et al., 2014). For instance, González et al., (2017), constructed niche hypervolumes centered around averaged stoichiometric coordinates and compared how these niche hypervolumes differed in shape, size, and location allowing them to reveal how and why intraspecific trait variability differed between trophic and latitudinal gradients. These examples demonstrate approaches to compare how the elemental niches of species may differ across biogeographic regions and in response to different community compositions such as when they occur in groups of the same species (i.e., conspecific) and when they co-occur in groups of mixed species (i.e., heterospecific).

Framing species by their resource strategies in terms of how they acquire and use C, N and P provides a link to compare and contrast species elemental niches in response to different environmental conditions. Conceptually, C, N, and P likely differs among plants species along a spectrum of conservative to acquisitive resource strategies. (Craine, 2005). These strategies describe how species make different resource acquisition and use trade-offs to optimize performance in variable environments. Moreover, species with different resource strategies often require different elemental concentrations (i.e., homeostasis for proper physiological function) and exhibit different stoichiometric plasticity (variability of elemental ratios) related to environmental conditions (Fajardo & Siefert, 2018; Leal et al., 2017; Stearns, 1989). For instance, coniferous species with conservative resource strategies, produce long lived needles and often exhibit low needle morphological variability and highly constrained growth geometry (Horn, 1971). Thus, conifers often exhibit a high elemental homeostasis and low stoichiometric plasticity where foliar C, N, and P concentrations are constrained by a narrow range of eco-physiological conditions (Marshall & Monserud, 2003). In comparison, fast growing, shade-intolerant deciduous species with acquisitive resource strategies, such as those that produce and shed seasonal foliar material often display low elemental homeostasis and high stoichiometric plasticity via variable leaf morphology (i.e., more flexibility in how they use N and P resources; Middleton et al., 2012). By characterizing the resource strategies of species in terms of their elemental homeostasis and stoichiometric plasticity, we can formulate how foliar elemental traits may differ across biogeographic gradients and in response to different community compositions to reveal species-trait generalities at large and local spatial extents.

Here we construct niche dimensions using foliar C, N, and P traits for balsam fir (*Abies balsamea* (L.) Mill.) and white birch (*Betula papyrifera* Marshall), two widespread North American boreal forest species. We investigate elemental niche differences at the species level between two ecoregions and at the community level by comparing conspecific and heterospecific niches across, within, and between ecoregions. These species exhibit different resource strategies (i.e., coniferous and deciduous) and have contrasting foliar elemental homeostasis and stoichiometric plasticity characteristics that may be influenced by large scale (i.e., ecoregion biophysical conditions) and local scale (i.e., community level dynamics) processes (Hausch et al., 2018; Richardson, 2004). At the species level, we compare foliar elemental niches between two ecoregions. For both of our focal species we hypothesize (H1) northern ecoregion foliar elemental niches will be larger in volume driven by increased foliar N and P concentrations (following the temperature-plant physiology hypothesis; see Reich & Oleksyn, 2004), compared to their niche volumes in the southern ecoregion. At the community level, we group our species into conspecifics (i.e., occurring without the other species at the plot level) and heterospecific (both species co-occur at the plot level) groups. For each of our focal species, we compare foliar elemental niches of conspecific against heterospecific community types across, within, and between ecoregions. For across ecoregion comparisons (i.e., conspecific vs heterospecific irrespective of ecoregion) species niche patterns should reflect their resource strategy. We hypothesize (H2) that balsam fir, given limited foliar stoichiometric plasticity, will exhibit a niche displacement pattern, where the proportionality of foliar elements remains similar but occupy different niche space (i.e., heterospecific niche displaced relative to conspecific niche position). We hypothesize (H3) that white birch, given a high degree of stoichiometric plasticity, will exhibit a niche expansion pattern where heterospecific conditions increase the variability of foliar elemental traits and thus increased niche volume for heterospecific groups relative to conspecific groups. For within ecoregion comparisons (i.e., conspecific vs heterospecific for a given ecoregion), again, species niche patterns should reflect their resource strategy, and we hypothesize niche displacement (H4) and niche expansion (H5) for balsam fir and white birch, respectively, as described above. For between ecoregion comparisons (i.e., conspecific vs conspecific between ecoregion), we hypothesize (H6) that conspecific and heterospecific northern ecoregion niches should operate within a larger trait space (i.e., niche volume) driven by N and P increases (following the temperature-plant physiology hypothesis; see Reich &

Oleksyn, 2004) for both balsam fir and white birch (see Figure 2.1 for a conceptual description of our hypotheses).

2.3 Materials and methods

2.3.1 Study area

Our study areas consisted of two ecoregions on the island of Newfoundland: (1) the Northern Peninsula and (2) the Central Newfoundland Forest ecoregions (see Appendix A.1 Figure A.1.1 for a study area map). Ecoregions are distinct areas characterized by major physiographic and minor macroclimatic differences; including vegetative, soil, water, fauna, and land-use differences (Ecological Stratification Working Group, 1996). Our ecoregions and corresponding sampling sites are approximately 2 latitudinal degrees apart (a 300 km distance). The Northern Peninsula ecoregion has a mean annual temperature of 3^{o}C, with mean summer and winter temperatures of 11^{o}C and -4.5^{o}C, respectively, and a mean annual precipitation of 1000-1100 mm (South, 1983). Balsam fir is the dominant tree species in this ecoregion on well to moderately drained sites, whereas black spruce (*Piceae mariana* (Mill.) Britton, Sterns, & Poggenb) and white birch are important co-dominant species (South, 1983). The soil type is generally humo-ferric podzols (South, 1983). The Central Newfoundland Forest ecoregion (hereafter referred to as Central Forest ecoregion), has a mean annual temperature of 4.5^{o}C, with mean summer and winter temperatures of 12.5^{o}C and -3.5^{o}C, respectively, and a mean annual precipitation of 1000-1300 mm (South, 1983). The forests of this ecoregion are dominated by closed stands of balsam fir with co-dominants of white birch, black spruce, trembling aspen (*Populus tremuloides* Michx.), and eastern larch (*Larix laricina* (Du Roi) K. Koch) (South, 1983). Generally, the soil type is humo-ferric podzols with gleyed podzols and brunisolic and gleysolic soils (South, 1983). These two ecoregions also differ in terms of shoulder season temperature and precipitation, soil-topographic relationships, and historical disturbance patterns (e.g., insect outbreak, wind, and fire) (Arsenault et al., 2016; South, 1983).

2.3.2 Plant sampling

During the summer months, between June and August, we collected samples of balsam fir and white birch from the Northern Peninsula and Central Forest ecoregions in 2015 and 2016, respectively (data in 2015 were collected as part of a study described by Leroux et al., 2017). Samples consisted of the forage material from juvenile trees (i.e., foliage and incidental woody bits) between 0-2 meters in height, the vertical range commonly used by moose (*Alces alces* (Linnaeus, 1758)) and snowshoe hare (*Lepus americanus* (Erxleben, 1777)). Samples were collected from a variety of stand types under the canopy and are representative of various canopy closure conditions. The variability of foliar elemental traits likely influences animal space use decisions, and this study is part of a larger research project focused on understanding elemental-trophic linkages (see Balluffi-Fry et al., 2020; Rizzuto et al., 2021). Although the sampling design differed between 2015 and 2016 in terms of plot size (2015 and 2016 plot radius were 10 m and 11.3 m, respectively) and the spatial arrangement of plots, the sampling units of C, N, P are the same. More specifically, in 2015, we randomly placed sample plots stratified by forest age within different forest types (coniferous, deciduous and mixed wood) at a minimum of 500 m apart and within 200 m of resource roads. In 2016, we set up four grids stratified by forest age and dominant forest-type and sampled along meandering transects at each grid with plots spaced 75 m apart and 37 m spacing at grid corners. At the plot level, we collected samples in both 2015 and 2016 in the same manner. We divided each sample plot into four quadrants and if present, we collected foliage from balsam fir and white birch individuals in each quadrant. We moved clockwise between each quadrant and collected foliage until a suitable amount of wet weight was collected (approx. 10 g). Lastly, we combined foliage samples from individuals by species per plot using representative foliage material until we achieved a mass suitable to determine C, N, and P concentrations (approx. 10 g; Northern Peninsula data used in this study are from Leroux et al., 2017). See Figure 3.1 from Chapter 3 for an example of how plot level foliar material was collected in our Central Forest ecoregion; sample collection was similar in the Northern Peninsula ecoregion.

Since we used data collected from Leroux et al. (2017) in an *ad hoc* opportunity, the sampling design is unbalanced between the two ecoregions being compared. In total we had 390 balsam fir and 229 white birch samples. Below we present the sample sizes for our species groupings from the total sample size. For our species level comparisons between ecoregions, we had 295 Northern Peninsula and 95 Central Forest samples of balsam fir and 158 Northern Peninsula and 71 Central Forest samples of white birch (i.e., n used to inform H1). At the plot level we determined the conspecific or heterospecific conditions based on the presence/absence of either balsam fir or white birch. For instance, a plot was considered conspecific if it only had one of the species present and heterospecific if it had both species present. For our community level comparisons across ecoregions, we had 189 conspecific and 201 heterospecific samples of balsam fir (i.e., n used to inform H2) and 28 conspecific vs 201 heterospecific samples of white birch (i.e., n used to inform H3). For our community level comparisons of balsam fir within and between ecoregions, we had 142 conspecific and 153 heterospecific samples in the Northern Peninsula ecoregion and 47 conspecific and 48 heterospecific samples in the Central Forest ecoregion (i.e., n used to inform H4/H6). For our community level comparisons of white birch within and between ecoregions, we had 5 conspecific and 153 heterospecific samples in the

Northern Peninsula ecoregion and 23 conspecific and 48 heterospecific samples in the Central Forest ecoregion (i.e., n used to inform H5/H6).

2.3.3 Lab analysis

Foliage samples were processed by the Agriculture Food Lab (AFL) at the University of Guelph. Total C and N concentration (as % dry) were determined using an Elementar Vario Macro Cube. Total P concentration (as % dry) was determined using a microwave acid digestion CEM MARSxpress microwave system and brought to volume using Nanopure water. The clear extract supernatant was further diluted by 10 to accurately fall within calibration range and reduce high level analyte concentration entering the inductively coupled plasma mass spectrometry detector (ICP-MS; see Poitevin, 2016).

2.3.4 Analysis and interpretation

For each of our focal species we made four comparisons. At the species level, we compared foliar elemental niches across ecoregions (i.e., Northern Peninsula and Central Forest; H1). We then compared community types of conspecific and heterospecific groups across (H2/H3), within (H4/H5), and between (H6) ecoregions. For each comparison we performed several different analyses to characterize and assess niche differences. Using the *factoextra* R package, we performed a PCA to characterize niche response patterns as either a displacement, contraction, or expansion via the position, shape, and size of the two 95% probability ellipses relative to each other and quantified using additional measures described below (Peñuelas et al., 2019; Urbina et al., 2017). Using the *vegan* R package (Oksanen et al., 2020), we computed the multivariate homogeneity of variances (MHD) for niche spatial median/centroid. Using these data, we computed a permutation test for homogeneity of multivariate dispersion (PT-MHD) and report the *F*-value and *p*-value for 999 permutations. This test permutes model residuals and generates the distribution of F for a null hypothesis where no difference in dispersion exists. If the *p*-value from the PT-MHD test is significant then heterogeneity in dispersion exists. The PT-MHD test is useful for assessing bias of PERMANOVA results when comparing groups with unequal size sample. PERMANOVA tests are sensitive to unequal sample sizes and require groups to exhibit homogeneous dispersion (Anderson, 2006). We used 999 permutations and Bray-Curtis distances and calculated pair-wise comparisons of niches and reported R^2, F statistic, and *p*-value PERMANOVA results. For each PERMANOVA comparison significant niche differences occur when p-value ≤ 0.05 (see Appendix A.2 Table A.2.1 for full PERMANOVA results). In addition, we used the hypervolume R package (Blonder et al., 2014), and constructed a hypervolume for each niche based on Gaussian kernel density estimation with a probability density enclosed by a 95% probability boundary. Using these hypervolume niche comparisons we reported the Jaccard similarity index to aid in our interpretation of niche differences (Blonder, 2017).

We used publicly accessible code from González et al. (2017), and evaluated niche volume, overlap, nestedness, shape, and assessed for sample size effects given the number of individuals in our ecoregion and community type groupings (see Appendix A.3 Figure A.3.1). Niche size/volume, a convex hull calculation, represents the variability of foliar C, N, and P concentrations or ITV. Niche overlap is the ratio of shared volume between each niche, presented as a percentage (i.e., the sum of two volumes minus the intersecting volume). The degree of niche overlap indicates the similarity or difference of C, N, and P traits between them. Moreover, niche nestedness represents the extent of niche overlap, using the ratio of the overlapping niche volume relative to the minimal volume occupied to produce a value on a scale of 0 to 1, with 0 indicating no nestedness and 1 indicating complete nestedness. Niche overlap and nestedness metrics describe niche position and size between groups. Niche nestedness helps to discriminate between different niche overlap patterns such as, overlap when sharing a similar proportion of niche volume and overlap when one niche occupies a subset of another niche volume. Lastly, we assessed for sample size effects on niche volume using a representative subsampling approach as opposed to rarefaction which has been shown to potentially underestimate the hypothetical true niche volumes for uncommon or less abundant species (González et al., 2017; Willis, 2019). Following González et al. (2017). We subsampled an increasing number of individuals at specified intervals depending on the number of samples we had for a given niche (or group). For each interval we calculated niche volumes using 999 randomized permutations and quantified variability using 95% confidence intervals and continued until all individuals for a given niche were sampled (see Appendix A.3 Figure A.3.1).

We determined ITV responses for each of our focal species comparisons by subtracting niche volumes against each other. For between ecoregion comparisons, we subtracted Central Forest niche volumes from Northern Peninsula niche volumes. For across ecoregion comparisons, we subtracted conspecific niche volumes from heterospecific niche volumes. For within ecoregion comparisons, we subtracted conspecific niche volumes from heterospecific niche volumes for each ecoregion. For between ecoregion comparisons, we subtracted Central Forest niche volumes of conspecific and heterospecific against their corresponding community type niche volume in the Northern Peninsula ecoregion. Lastly, to assess latitudinal patterns we took the difference between means of foliar C, N, and P traits and compared conspecific and heterospecific community types between our Northern Peninsula and Central Forest ecoregions.

We depicted niche hypervolumes in three-dimensional data space, using spherical representations centered around the averaged C, N, and P coordinates as opposed to polygonal features, where many edges, vertices, and faces make it difficult to visually discern general patterns (González et al. 2017). See Appendix A.4 Table A.4.1 for each niche sample size, Shapiro-Wilk test of multivariate normality for each niche, and volume as determined using niche metrics from González et al., 2017.

2.4 Results

2.4.1 Sample size effects

Our representative subsampling analysis to evaluate sample size effects on niche volume demonstrated potential limitations for small sample size groups. In Appendix A.3 Figure A.3.1, we showed mean niche volume curves with increasing sample size until all individuals have been sampled. In most cases, variation in the relationship between niche volume and sample size decreased with increasing sample size. At an inflection point, it appears to asymptote which indicates sample saturation. Where subsampling results showed linear relationships (i.e., sample saturation does not occur), we have limited confidence where these niches are used in species and community level comparisons. More specifically, these less reliable niches included the following: white birch conspecific (across ecoregion comparison; n = 28); Northern Peninsula conspecific (n = 5); Central Forest conspecific (n = 21); and Central Forest heterospecific (n = 48); these niches showed linear relationships between niche volume and increasing sample size (see Appendix A.3 Figure A.3.1). In total five out of our twelve comparisons may be impacted by low sample size niches.

2.4.2 Species level: between ecoregions

Our hypothesis for both balsam fir and white birch that elemental niches for individuals from our northern ecoregion will be larger in volume relative to their southern ecoregion niche is supported by our results (H1). Our PCA revealed that individuals from the Northern Peninsula ecoregion occupy larger foliar elemental trait space compared to individuals from the Central Forest ecoregion (Figure 2.2a, b). For balsam fir, variance explained by axes 1 and 2 was 56.5% and 31.7%, respectively (Figure 2.2a) and for white birch variance explained by axes 1 and 2 was 64.4% and 30.7%, respectively (Figure 2.2b). PERMANOVA results indicated significant differences between Northern Peninsula and Central Forest elemental niches for balsam fir (*F* = 14.592, *p*-value = 0.001) and white birch (*F* = 75.999, *p*-value = 0.001; see Table 2.1). However, our permutation test for homogeneity of multivariate dispersion (PT-MHD) were significant for both balsam fir (*F* = 57.683, *p*-value = 0.001) and white birch (*F* = 9.174, *p*-value = 0.005); as an assumption for PERMANOVAs this potentially limits our interpretation (Table 2.1). The Jaccard similarity index indicated a low degree of niche similarity between Northern Peninsula and Central Forest niches for balsam fir (0.281) and white birch (0.163; see Table 2.1). For balsam fir, our niche volume metrics indicated low overlap (10.714%), moderate nestedness (0.393), and increased ITV via niche volume (+70.97%) for the Northern Peninsula niche (see Figure 2.3a). For white birch, niche volume metrics indicated a low overlap (5.166%), low nestedness (0.067), and increased ITV (+46.65%) via niche volume for the Northern Peninsula niche (see Figure 2.3b and Table 2.1). Lastly, foliar N and P were greater for the Northern Peninsula ecoregion for balsam fir by a difference of 0.164% and 0.049% and for white birch, 1.143% and 0.127%, respectively. For balsam fir and white birch foliar C was greater in the Central Forest ecoregion by 0.205% and 0.545%, respectively (Table 2.2a). In addition, these results were supported by our niche sample size analysis as all four niches used in these comparisons are of adequate sample size (Appendix A.3 Figure A.3.1). As well, see Appendix A.5 Figure A.5.1 for a pairwise scatter plot comparison of foliar C, N, and P between ecoregions for balsam fir and white birch.

2.4.3 Community level: across ecoregions

We found mixed support for our hypotheses that balsam fir (H2) heterospecific niches should exhibit a niche displacement pattern and that white birch (H3) heterospecific niches should exhibit a niche expansion pattern relative to their conspecific niche. Our PCA showed a high degree of similarity between heterospecific and conspecific niches for balsam fir (Figure 2.2c). In contrast we observed a potential expansion effect for white birch heterospecific niche relative to the conspecific niche (Figure 2.2d). PERMANOVA results reaffirmed our mixed support as balsam fir conspecific and heterospecific niches were not significantly different (F = 0.646, *p*-value = 0.458), however white birch niches were (F = 4.075, *p*-value = 0.021; Table 2.1). In addition, non-significant PT-MHD results and similar MHD results support PERMANOVA interpretations (Table 2.1). The Jaccard similarity index was moderately high for both balsam fir (0.709) and white birch (0.552). For balsam fir, our niche volume metrics indicated moderate overlap (43.860%), moderate nestedness (0.276), and increased ITV via niche volume (+35.49%) for the heterospecific niche (see Figure 2.4a). For white birch, niche volume metrics indicated a low overlap (21.718%), high nestedness (0.623), and increased ITV (+68.92%) via niche volume for the heterospecific niche (see Figure 2.4b and Table 2.1). Lastly, our white birch comparison is less reliable due to a low sample size for the conspecific niche (Appendix A.3 Figure A.3.1). As well, see appendix A.5 Figure A.5.2 for a pairwise scatter plot comparison of foliar C, N, and P via conspecific vs heterospecific groups across ecoregions for balsam fir and white birch.

2.4.4 Community level: within ecoregions

We found mixed support for our hypotheses that balsam fir (H4) under heterospecific conditions should exhibit a niche displacement pattern and that white birch (H5) should exhibit a niche expansion pattern relative to their conspecific niche within a given ecoregion. Our PCA showed a high degree of similarity between heterospecific and conspecific niches for balsam fir (Figure 2.2e). In comparison we observed a potential expansion effect for white birch heterospecific niche relative to the conspecific niche (Figure 2.2f). PERMANOVA results reaffirmed our mixed support as balsam fir conspecific and heterospecific niches were not significantly different in the Northern Peninsula (F = 0.450, p-value = 0.570), and Central Forest (F = 0.306, p-value = 0.726) ecoregion. For white birch conspecific and heterospecific niches were not significantly different in the Northern Peninsula ecoregion (F = 0.480, p-value = 0.577), however these niches were significantly different in the Central Forest ecoregion (F = 9.163, p-value = 0.001; Table 2.1). Non-significant PT-MHD results and similar MHD results support PERMANOVA interpretations (Table 2.1), except for white birch conspecific and heterospecific niche comparisons in the Central Forest (F = 5.495, p-value = 0.017). The Jaccard similarity index was moderately high for both balsam fir in the Northern Peninsula and Central Forest ecoregion (0.672 and 0.566, respectively) and similarly for white birch (0.534, and 0.334, respectively; Table 2.1). For balsam fir, in the Northern Peninsula and Central Forest ecoregions our niche volume metrics indicated moderate overlap (40.426% and 50%, respectively), moderate to low nestedness (0.251 and 0, respectively), and increased ITV via heterospecific niche volume in the Northern Peninsula ecoregion (+29.04%) and with no difference in the Central Forest ecoregion (Figure 2.5a). For white birch, in the Northern Peninsula and Central Forest ecoregions our niche volume metrics indicated low to moderate overlap (0.457% and 43.396%, respectively), high to low nestedness (0.995 and 0.127, respectively), and increased ITV via heterospecific niche volume in the Northern Peninsula ecoregion (+66.48%) and decreased in the Central Forest ecoregion (-3.66%; see Figure 2.5b, Table 2.1). Lastly, our white birch comparisons are less reliable due to a low sample size for Northern Peninsula conspecific, Central Forest conspecific and heterospecific niches (Appendix A.3 Figure A.3.1). See Appendix A.5 Figure A.5.3 for a pairwise scatter plot comparison of foliar C, N, and P via conspecific vs heterospecific groups within and between ecoregions for balsam fir and white birch.

2.4.5 Community level: between ecoregions

Our hypotheses for both balsam fir and white birch that conspecific and heterospecific niches for our northern ecoregion should operate within a larger trait space (i.e., increased niche volume) were supported by our results. Our PCA showed that community level niches in the Northern Peninsula ecoregion exhibited a larger range of variability than those community niches found in the Central Forest ecoregion (Figure 2.2e, f). PERMANOVA results reaffirmed our hypothesis support as significant differences for balsam fir conspecific (F = 7.581 and p-value = 0.005) and heterospecific (F = 6.943 and p-value = 0.004) niches were detected between ecoregions. Similarly, significant differences for white birch conspecific (F = 8.038 and p-value = 0.001) and heterospecific (F = 68.702 and p-value = 0.001) niches were detected between ecoregions (Table 2.1). Although we determined similar MHD results for our comparisons we found significant PT-MHD results for balsam fir conspecific (F = 25.902 and p-value = 0.001 and heterospecific niches (F = 31.428 and p-value = 0.001) and for white birch heterospecific niches (F = 13.415 and p-value = 0.001) between ecoregions. The Jaccard similarity index was low for balsam fir conspecific (0.266) and heterospecific (0.249) niches between ecoregions, with similar results for white birch conspecific (0.132) and heterospecific (0.093) niches. For balsam fir, both conspecific and heterospecific niches between ecoregions exhibited low overlap (15.385% and 9.091%, respectively), moderate/low nestedness (0.346 and 0.409, respectively), and increased ITV via niche volume in the Northern Peninsula ecoregion (+29.04% and +58.07%, respectively; see Figure 2.5a). For white birch, both conspecific and heterospecific niches between ecoregions exhibited low overlap (0% and 2.449%, respectively), low nestedness (0 and 0.079, respectively), and increased ITV via northern heterospecific niches (+57.02%) and decreased northern conspecific niches (-13.12%; Figure 2.5b). Lastly, balsam fir foliar N and P were greater for the Northern Peninsula ecoregion for both conspecific (0.176% and 0.046%, respectively) and heterospecific (0.15% and 0.053%, respectively) niches, while foliar C was higher in the Central Forest ecoregion for both conspecific (0.24%) and heterospecific (0.173%) niches (Table 2.2b). White birch foliar N and P were greater for the Northern Peninsula ecoregion for both conspecific (1.26% and 0.146%, respectively) and heterospecific (1.214% and 0.141%, respectively) niches, while foliar C was higher in the Central Forest ecoregion for both conspecific (0.085%) and heterospecific (0.755%) niches (Table 2.2b). Lastly, our white birch comparisons are less reliable due to a low sample size for Northern Peninsula conspecific, Central Forest conspecific and heterospecific niches (Appendix A.3 Figure A.3.1). See Appendix A.5 Figure A.5.3 for a pairwise scatter plot comparison of foliar C, N, and P via conspecific vs heterospecific groups within and between ecoregions for balsam fir and white birch.

2.5 Discussion

Constructing niche axes using foliar C, N, and P traits, allows us to relate variability in species resource strategies to different environmental conditions. In this study, we advance the application of the elemental niche to describe species differences in response to environmental conditions (see González et al., 2017; He et al., 2019; Peñuelas et al., 2019; Sardans et al., 2021). Specifically, we focus on the species level by comparing foliar elemental niches between ecoregions and at the community level by comparing conspecific and heterospecific niches across, within, and between ecoregions. We find evidence to support H1 that at a species level both balsam fir and white birch exhibit larger elemental niches that are statistically different between ecoregions. At a community level between ecoregions we find no support for balsam fir (H2) niche displacement patterns, however we do find evidence to support white birch (H3) niche expansion. At a community level within ecoregions, we find no evidence to support balsam fir (H4) niche displacement or white birch (H5) niche expansion patterns in the Northern Peninsula ecoregion, however, we do find statistical support for white birch niche expansion in the Central Forest ecoregion. Lastly, at the community level we find evidence to support H6, that conspecific groups and heterospecific groups are statistically different for both species between ecoregions. Our results suggest that elemental niche differences for our focal species largely occur in response to broad scale biophysical conditions.

2.5.1 Biogeographical niche patterns

As expected, individuals from our northern ecoregion contain greater amounts of N and P and exhibited a wider elemental niche plasticity compared to their southern counterparts for species level (H1) and community level (H6) comparisons (Figure 2.2, Figure 2.3, and Figure 2.5). Ecoregions are distinguished by their biophysical properties which include major physiographic and minor macro-climatic differences (Ecological Stratification Working Group, 1996). The mean annual summer and winter temperatures between the Northern Peninsula and Central Forest ecoregion differ by 1.5^{o}C and 1^{o}C, respectively. These differences likely contribute to the increased N, P, and elemental niche plasticity we observed in our focal species. The effects of temperature on plant growth rates and underlying biochemical and physiological processes are well documented (Gillooly et al., 2001). Indeed, several studies have shown how a 2 to 5^{o}C temperature decreases can result in a 3% increase of N and P in plants and this aligns well with our results (Table 2.2; for synthesis see Woods et al., 2003). Furthermore, our results provide support for the temperature-plant physiology hypothesis (Reich & Oleksyn, 2004); plants at higher latitudes in colder environments contain greater amounts of N and P.

Moreover, although we did not compare foliar elemental niche differences between our focal species with respect to ecoregions, there are general patterns of note. Balsam fir and white birch occupy different C, N, and P trait space at a species level (Figure 2.3a, b) and community level between ecoregions (Figure 2.5a, b). Across these scales, balsam fir foliar C, N, and P is tightly clustered compared to a white birch where foliar C, N, and P is highly plastic (density contours from pair-wise trait comparisons show similar patterns of species trait plasticity; see Appendix A.5 Figure A.5.1 and Figure A.5.3). These species have different geographic distributions (see Appendix A.1 Figure A.1.1 for species distribution maps). Thus, the variability of foliar C, N, and P niche breadth may relate to their biological tolerances of temperature changes across the variable environments of their geographic range (i.e., stenothermal vs eurythermal species; van Dijk et al., 1999). Foliar elemental niche differences or changes in C, N, and P variability may provide linkages to describe the realized niche of species in response to different environmental conditions species experience across their geographic range (fundamental niche; Carscadden et al., 2020). Future studies may consider comparing interspecific niche variability to reveal species differences in resource use patterns.

Furthermore, these results allow us to generalize how the forage of our focal species contribute to dynamics at higher trophic levels and ecosystem processes. Moose on the island of Newfoundland preferentially browse juvenile balsam fir and white birch (Dodds, 1960). In different ecoregions, differing N and P forage quality may translate to different rates of browsing and nutritional conditions of moose with implications for population dynamics and space-use foraging decisions (Hoy et al., 2021). Over space and time, differing foliar N and P contributions to litter quality via leaf senescence and herbivore fecal depositions will likely influence biogeochemical processes and feedbacks (Shen et al., 2011). These linkages to ecosystem processes provide a functional picture of how the ebb and flow of N and P influence the ecology of landscape via spatial flows of N and P through herbivory, leaf litter contributions, and dissolved nutrients in hydrological systems.

2.5.2 Community level niche patterns

Although we expected to reveal heterospecific niche patterns of displacement (H2/H4) for balsam fir using a Principal Components Analysis coupled with a PERMANOVA test, we did not observe significance in these patterns. For instance, conspecific and heterospecific niches of balsam fir across and within ecoregion comparisons differed only slightly (Figure 2.2c, e). This suggests that balsam fir likely maintains a highly rigorous elemental homeostasis regardless of community level conditions. However, between ecoregion comparisons show that these community level niches operate in different elemental trait space. Thus, under elementally different community-litter-nutrient scenarios trade-offs are likely made between growth, reproduction, and survival that balance the allocation of C, N, and P to maintain a foliar elemental equivalence that is reflective of large-scale biogeographical conditions (Dumais & Prevost, 2014). As well, white birch sheds its foliar material annually, with differential litter contributions depending on the amount and size of birch present. This may provide an adequate supply of N and P coupled with early season retrieval that allows balsam fir to maintain an elemental equivalence in heterospecific communities (Giordano, 2013; Persson et al., 2010). Alternatively, other local factors not considered in this study, such as light and topographic position, may be important drivers of foliar C, N and P (Macek et al., 2019). Moreover, across eastern boreal landscapes, the occurrence of balsam fir and white birch in pure and mixedwood stands can be used to represent patches (i.e., coniferous, deciduous, and mixedwood patches; see Hansson, 1992; Pastor et al., 1999). Thus, our results highlight how emergent stand scale patterns of resource quality in term of forage may inform landscape patterns. For instance, if balsam remains elementally similar across these differing community types, this provides an invariant parameter to characterize animal foraging behaviours (Duparc et al., 2020) and potentially the movement of energy and matter across spatial scales (Dézerald et al., 2018).

In comparison, we expected white birch to exhibit a niche expansion pattern in response to heterospecific conditions relative to their corresponding conspecific niche at the species level (H3) and community level (H5). Although we did observe a significant niche expansion pattern at the species level, at the community level heterospecific niches contracted, including a significant contraction for the Central Forest ecoregion. This was unexpected. We hypothesized white birch would exhibit greater elemental plasticity under heterospecific community types regardless of spatial extent. Yet, we observe two different types of heterospecific niche responses depending on spatial scale. As well, the ITV differed between our species and community level comparisons. Furthermore, we suspect the low sample size of our Northern Peninsula ecoregion population produced an artificial increase given the high overlap between conspecific and heterospecific niches.

Overall our results suggest that white birch foliar C, N, and P is likely influenced by both regional (biogeographical) and localized conditions (Cornell & Lawton, 1992; Lu et al., 2011). For instance, balsam fir produces durable, long-lived, lignified foliar tissue with limited seasonal litter contributions of recalcitrant material which is known to reduce soil decomposition rates (Bardgett et al., 1998), alter microbial community structure, and change nutrient pathways (Hobbie, 2015). Thus, recalcitrant litter contributions may reduce white birch nutrient retrieval and N/P use-efficiencies, thus producing the niche contraction patterns we observed (Figure 2.2f; He et al., 2010; Krishna & Mohan, 2017). Moreover, our focal species differ in terms of their palatability. For instance, balsam fir exhibits a constant chemical defence profile while white birch exhibits compensatory strategies of allocating N and P to phytochemical production in response to herbivory (Bennett & Wallsgrove, 1994). In heterospecific patches, palatable species, such as white birch, may experience greater top-down pressure via herbivory (Agrawal et al., 2006). Under these heterospecific community conditions the interaction of nutrient availability (Coley et al., 1985) and herbivory (Daufresne & Loreau, 2001) events may elicit a reduction in white birch foliar C, N and P. As well, white birch is a can behave similar to a clonal species when mycorrhizal relationships are present and can allocate resources through root connections to other individuals (Deslippe & Simard, 2011; Simard et al., 1997). Thus, differing litter-nutrient input conditions, herbivorous interactions due to palatability, and the extent of mycorrhizal connections, may collectively influence the foliar C, N, and P of white birch and explain the different niche patterns we observed at the species and community level (Figure 2.2d, f).

2.5.3 Study limitations

Our study compares data from two research projects with differing sampling designs using an *ad hoc* approach and as such there are certain limitations to consider when interpreting our results. First, although we collected data/foliar samples in a similar way between these two projects there are differences in terms of the spatial distribution of sample plots (as described above in the Plant Sampling 2.3.2 section) that may influence the spatial autocorrelation of samples and thus our interpretation of the findings. However, the two projects do target similar forest units: coniferous, deciduous, and mixedwood across a range of representative age classes. Second, our sampling of foliar material occurred in two different years with the Northern Peninsula sampled in 2015 and the Central Forest sampled in 2016. Despite the potential for temporal differences in foliar C, N, and P between these ecoregions, we suspect the observed effect is due to biogeographical differences. In 2017 we resampled balsam fir and white birch foliar C, N, and P in the Central Forest ecoregion at the same sample sites. Using 2017 foliar C, N, and P we constructed conspecific and heterospecific niches and compared them with 2016 conspecific and heterospecific niches. We tested these temporal foliar elemental niches using the same approach described above. Where PERMANOVA results differed significantly for balsam fir 2016 (n = 95) and 2017 (n = 30) and white birch 2016 (n = 71) and 2017 (n = 41) temporal foliar elemental niches, PT-MHD also differed significantly. Thus, we are unable to rely on PERMANOVA results (see Appendix A.6 Figure A.6.1 for PCA; Figure A.6.2 for spherical niches; Figure A.6.3 for scatter plot kernel density comparisons; and Table A.6.1, Table A.6.2, and Table A.6.3 for niche sample size, statistical summary, and PERMANOVA results, respectively). Overall, given our temporal comparisons we suspect the effect observed in this study is likely due to biogeographical differences (for temporal comparisons of foliar stoichiometric traits see Richmond et al., 2020).

The inference for some of our comparisons is likely hindered due to small and unbalanced sample sizes, which may influence trait data dispersion patterns and the output of PERMANOVA tests (Mcardle & Anderson, 2001). To assess this limitation, we subsampled an increasing number of individuals at specified intervals and calculated 999 randomized permutations and 95% confidence of niche volumes at each interval (see Appendix A.3 Figure A.3.1). In the results section, we highlight these less reliable niches. Which include white birch across ecoregion (n = 28), Northern Peninsula conspecific (n = 5), and Central Forest conspecific (n = 21) and heterospecific niches (n = 48). These niches do not saturate and as such comparisons using these niches are less reliable. More importantly our sample size analysis demonstrates a threshold requirement of sample sizes needed to test for foliar elemental niche differences. As such, our work could help guide future research projects aimed at investigating environmental drivers of foliar niche variability across spatial scales by ensuring they have sufficient sample sizes. Lastly, given that we only control for environmental variability at the ecoregion level or community level and a whole suite of interactions conditions may influence the foliar elemental niches of species, we are unsure if our statistical relevance provides meaningful biological relevance. Future work may consider how similar environmental factors influence the foliar niches of these species between and within these ecoregions.

2.6 Conclusion

Organisms are collections of elements, predominately C, N, and P (Kaspari & Powers, 2016). For plants, C, N, and P are interconnected and needed in sufficient proportions for proper physiological functioning (Sterner & Elser, 2002). Life history and leaf attributes determine foliar intraspecific variability of C, N, and P traits (Sardans et al., 2021). A species elemental homeostasis and stoichiometric plasticity constrict an individual’s eco-physiological response and tolerance to differing environmental conditions (Asner et al., 2016; Peñuelas et al., 2019). Thus, constructing niche dimensions along C, N, and P resource axes allows us to assess how plants respond to different environmental conditions, revealing differences in resource acquisition and use (Fajardo & Siefert, 2018; González et al., 2017). Although there are numerous ways to construct and assess niche dimensions, our work compliments existing work that explicitly uses a plant elemental/stoichiometric framework (González et al., 2017; Peñuelas et al., 2019; Urbina et al., 2017). Here, we investigate elemental niches between ecoregions at the species level, and across, within, and between ecoregions at the community level. At the species level, we find large scale biophysical signals that elemental niches are specific to biogeographical conditions and that our focal species operate within larger trait spaces in our northern ecoregion. Our results provide evidence to potentially support eco-physiological patterns in response to biogeographic differences that are consistent with temperature-physiological effects on plants (Reich & Oleksyn, 2004). This geographic specificity suggests that species may exhibit elemental homeostatic conditions that are constrained by large scale biogeographical properties. Our findings suggest that using foliar elemental traits from one biogeographic area to predict their condition in another area may yield erroneous results given species specific differences to temperature/precipitation conditions (van Dijk et al., 1999; Woods et al., 2003). Moreover, studies aimed at predicting global trends via elemental niches or foliar traits should be cautious about the strength of local effects (Butler et al., 2017). At the community level, we found that species specific responses to heterospecific conditions for both balsam fir and white birch, however the patterns observed differed from our predictions and in most cases were statistically insignificant. In general, we found that balsam fir maintains a rigorous elemental homeostasis in conspecific and heterospecific groups. These results allow us to potentially form generalizations about the tolerances of coniferous/conservative strategy species and how they use and allocate resources in different biogeographical locations and under different community type scenarios. In comparison white birch did not exhibit a consistent response to heterospecific conditions with an expansion pattern observed across ecoregions and a contraction pattern observed within and between ecoregions. These results suggest other mechanisms across spatial scales likely influence how white birch uses and allocates elemental resources such as the spatial variability of mycorrhizal relationships (Simard 2009). As well, sample size issues limit the reliability of white birch niche comparisons at the community level and subsequent interpretations of those results. In this study we did not examine ecoregion specific or common environmental factors between ecoregions which may drive differences in foliar elemental niches. For instance, the different parent material, soil type, and soil texture in these ecoregions may influence the availability of nutrients for uptake via soil pH ranges (Finlay 1995). In addition, the historical disturbance ecology of an ecoregion, or even localized disturbance events can have long legacy effects that determine nutrient hot spots and community structure (Korell et al. 2017). Thus, since our study only partially explained some of the variability in foliar elemental concentrations other environmental factors may be more biologically relevant. Future work may consider how differing environmental gradients such as soil structure, disturbance, ontogeny, and finer resolutions of community composition (including species dominance effects related to the biomass-ratio hypothesis; see Tardif et al., 2014) influence the elemental niche of species.

2.7 Data Availability

All data and code used in the analyses are available via a Figshare repository at: https://doi.org/10.6084/m9.figshare.8247134.v1

2.8 References

Agrawal, A. A., Lau, J. A., & Hambäck, P. A. (2006). Community heterogeneity and the evolution of interactions between plants and insect herbivores. *The Quarterly Review of Biology*, *81*(4), 349–376. https://doi.org/10.1086/511529

Anderson, M. J. (2006). Distance-based tests for homogeneity of multivariate dispersions. *Biometrics*, *62*(1), 245–253. https://doi.org/10.1111/j.1541-0420.2005.00440.x

Arsenault, A., LeBlanc, R., Earle, E., Brooks, D., Clarke, B., Lavigne, D., & Royer, L. (2016). Unravelling the past to manage Newfoundland’s forests for the future. *The Forestry Chronicle*, *92*(4), 487–502.

Asner, G. P., Knapp, D. E., Anderson, C. B., Martin, R. E., & Vaughn, N. (2016). Large-scale climatic and geophysical controls on the leaf economics spectrum. *Proceedings of the National Academy of Sciences*, *113*(28), E4043–E4051. https://doi.org/10.1073/pnas.1604863113

Balluffi-Fry, J., Leroux, S. J., Wiersma, Y. F., Heckford, T. R., Rizzuto, M., Richmond, I. C., & Vander Wal, E. (2020). Quantity–quality trade-offs revealed using a multiscale test of herbivore resource selection on elemental landscapes. Ecology and Evolution, 10(24), 13847–13859. https://doi.org/10.1002/ece3.6975

Bardgett, R. D., Wardle, D. A., & Yeates, G. W. (1998). Linking above-ground and below-ground interactions: How plant responses to foliar herbivory influence soil organisms. *Soil Biology and Biochemistry*, *30*(14), 1867–1878. https://doi.org/10.1016/S0038-0717(98)00069-8

Bennett, R. N., & Wallsgrove, R. M. (1994). Secondary metabolites in plant defence mechanisms. *New Phytologist*, *127*(4), 617–633. https://doi.org/10.1111/j.1469-8137.1994.tb02968.x

Bergmüller, R., & Taborsky, M. (2010). Animal personality due to social niche specialisation. *Trends in Ecology & Evolution*, *25*(9), 504–511. https://doi.org/10.1016/j.tree.2010.06.012

Birch, J. D., Lutz, J. A., Simard, S. W., Pelletier, R., LaRoi, G. H., & Karst, J. (2019). Density-dependent processes fluctuate over 50 years in an ecotone forest. *Oecologia*, *191*(4), 909–918. https://doi.org/10.1007/s00442-019-04534-6

Blonder, B. (2017). Hypervolume concepts in niche- and trait-based ecology. *Ecography*. https://doi.org/10.1111/ecog.03187

Blonder, B., Lamanna, C., Violle, C., & Enquist, B. J. (2014). The *n* -dimensional hypervolume: The n-dimensional hypervolume. *Global Ecology and Biogeography*, *23*(5), 595–609. https://doi.org/10.1111/geb.12146

Bulleri, F., Bruno, J. F., Silliman, B. R., & Stachowicz, J. J. (2016). Facilitation and the niche: Implications for coexistence, range shifts and ecosystem functioning. *Functional Ecology*, *30*(1), 70–78. https://doi.org/10.1111/1365-2435.12528

Butler, E. E., Datta, A., Flores-Moreno, H., Chen, M., Wythers, K. R., Fazayeli, F., Banerjee, A., Atkin, O. K., Kattge, J., Amiaud, B., Blonder, B., Boenisch, G., Bond-Lamberty, B., Brown, K. A., Byun, C., Campetella, G., Cerabolini, B. E. L., Cornelissen, J. H. C., Craine, J. M., … Reich, P. B. (2017). Mapping local and global variability in plant trait distributions. *Proceedings of the National Academy of Sciences*, *114*(51), E10937–E10946. https://doi.org/10.1073/pnas.1708984114

Carscadden, K. A., Emery, N. C., Arnillas, C. A., Cadotte, M. W., Afkhami, M. E., Gravel, D., Livingstone, S. W., & Wiens, J. J. (2020). Niche breadth: Causes and consequences for ecology, evolution, and conservation. *The Quarterly Review of Biology*, *95*(3), 179–214. https://doi.org/10.1086/710388

Cherif, M., Faithfull, C., Guo, J., Meunier, C. L., Sitters, J., Uszko, W., & Rivera Vasconcelos, F. (2017). An operational framework for the advancement of a molecule-to-biosphere stoichiometry theory. *Frontiers in Marine Science*, *4*, 286. https://doi.org/10.3389/fmars.2017.00286

Coley, P. D., Bryant, J. P., & Chapin, F. S. I. (1985). Resource availability and plant antiherbivore defense. *Science*, *230*(4728), 5.

Cornell, H. V., & Lawton, J. H. (1992). Species interactions, local and regional processes, and limits to the richness of ecological communities: A theoretical perspective. *The Journal of Animal Ecology*, *61*(1), 1. https://doi.org/10.2307/5503

Craine, J. M. (2005). Reconciling plant strategy theories of Grime and Tilman. *Journal of Ecology*, *93*(6), 1041–1052. https://doi.org/10.1111/j.1365-2745.2005.01043.x

Daufresne, T., & Loreau, M. (2001). Plant–herbivore interactions and ecological stoichiometry: When do herbivores determine plant nutrient limitation? *Ecology Letters*, *4*(3), 196–206.

Deslippe, J. R., & Simard, S. W. (2011). Below-ground carbon transfer among *Betula nana* may increase with warming in Arctic tundra. *New Phytologist*, *192*(3), 689–698. https://doi.org/10.1111/j.1469-8137.2011.03835.x

Dézerald, O., Srivastava, D. S., Céréghino, R., Carrias, J.-F., Corbara, B., Farjalla, V. F., Leroy, C., Marino, N. A. C., Piccoli, G. C. O., Richardson, B. A., Richardson, M. J., Romero, G. Q., & González, A. L. (2018). Functional traits and environmental conditions predict community isotopic niches and energy pathways across spatial scales. *Functional Ecology*, *32*(10), 2423–2434. https://doi.org/10.1111/1365-2435.13142

Dodds, D. G. (1960). Food competition and range relationships of moose and snowshoe hare in newfoundland. *The Journal of Wildlife Management*, *24*(1), 52. https://doi.org/10.2307/3797356

Dumais, D., & Prevost, M. (2014). Physiology and growth of advance *Picea rubens* and *Abies balsamea* regeneration following different canopy openings. *Tree Physiology*, *34*(2), 194–204. https://doi.org/10.1093/treephys/tpt114

Duparc, A., Garel, M., Marchand, P., Dubray, D., Maillard, D., & Loison, A. (2020). Through the taste buds of a large herbivore: Foodscape modeling contributes to an understanding of forage selection processes. *Oikos*, *129*(2), 170–183. https://doi.org/10.1111/oik.06386

Ecological Stratification Working Group. (1996). *A national ecological framework for Canada*. Centre for Land and Biological Resources Research, Research Branch, Agriculture and Agri-Food Canada.

Elser, J. J., Fagan, W. F., Denno, R. F., Dobberfuhl, D. R., Folarin, A., Huberty, A., Interlandi, S., Kilham, S. S., McCauley, E., Schulz, K. L., Siemann, E. H., & Sterner, R. W. (2000). Nutritional constraints in terrestrial and freshwater food webs. *Nature*, *408*(6812), 578–580. https://doi.org/10.1038/35046058

Elton, C. S. (1927). *Animal ecology*. New York, Macmillan Co.

Fajardo, A., & Siefert, A. (2018). Intraspecific trait variation and the leaf economics spectrum across resource gradients and levels of organization. *Ecology*, *99*(5), 1024–1030. https://doi.org/10.1002/ecy.2194

Finlay, R. D. (1995). Interactions between soil acidification, plant growth and nutrient uptake in ectomycorrhizal associations of forest trees. *Ecological Bulletins*, *44*, 197–214

Florence, A. M., & McGuire, A. M. (2020). Do diverse cover crop mixtures perform better than monocultures? A systematic review. *Agronomy Journal*, *112*(5), 3513–3534. https://doi.org/10.1002/agj2.20340

Gartner, T. B., & Cardon, Z. G. (2004). Decomposition dynamics in mixed-species leaf litter. *Oikos*, *104*(2), 230–246. JSTOR.

Gillooly, J. F., Brown, J. H., West, G. B., Savage, V. M., & Charnov, E. L. (2001). Effects of size and temperature on metabolic rate. *Science*, *293*(5538), 2248–2251. https://doi.org/10.1126/science.1061967

Giordano, M. (2013). Homeostasis: An underestimated focal point of ecology and evolution. *Plant Science*, *211*, 92–101. https://doi.org/10.1016/j.plantsci.2013.07.008

Godoy, O., Bartomeus, I., Rohr, R. P., & Saavedra, S. (2018). Towards the integration of niche and network theories. *Trends in Ecology & Evolution*, *33*(4), 287–300. https://doi.org/10.1016/j.tree.2018.01.007

Godsoe, W., Jankowski, J., Holt, R. D., & Gravel, D. (2017). Integrating biogeography with contemporary niche theory. *Trends in Ecology & Evolution*, *32*(7), 488–499. https://doi.org/10.1016/j.tree.2017.03.008

González, A. L., Dézerald, O., Marquet, P. A., Romero, G. Q., & Srivastava, D. S. (2017). The multidimensional stoichiometric niche. *Frontiers in Ecology and Evolution*, *5*, 110. https://doi.org/10.3389/fevo.2017.00110

Gravel, D., Baiser, B., Dunne, J. A., Kopelke, J.-P., Martinez, N. D., Nyman, T., Poisot, T., Stouffer, D. B., Tylianakis, J. M., Wood, S. A., & Roslin, T. (2019). Bringing Elton and

Grinnell together: A quantitative framework to represent the biogeography of ecological interaction networks. *Ecography*, *42*(3), 401–415. https://doi.org/10.1111/ecog.04006

Gray, L., & He, F. (2009). Spatial point-pattern analysis for detecting density-dependent competition in a boreal chronosequence of Alberta. *Forest Ecology and Management*, *259*(1), 98–106. https://doi.org/10.1016/j.foreco.2009.09.048

Grinnell, J. (1917). The niche-relationships of the California thrasher. *The Auk*, *34*(4), 427–433.

Hansson, L. (1992). Landscape ecology of boreal forests. *Trends in Ecology & Evolution*, *7*(9), 299–302. https://doi.org/10.1016/0169-5347(92)90227-3

Harpole, W. S., Ngai, J. T., Cleland, E. E., Seabloom, E. W., Borer, E. T., Bracken, M. E. S., Elser, J. J., Gruner, D. S., Hillebrand, H., Shurin, J. B., & Smith, J. E. (2011). Nutrient co-limitation of primary producer communities. *Ecology Letters*, *14*(9), 852–862. https://doi.org/10.1111/j.1461-0248.2011.01651.x

Hausch, S., Vamosi, S. M., & Fox, J. W. (2018). Effects of intraspecific phenotypic variation on species coexistence. *Ecology*, *99*(6), 1453–1462. https://doi.org/10.1002/ecy.2346

He, P., Fontana, S., Sardans, J., Peñuelas, J., Gessler, A., Schaub, M., Rigling, A., Li, H., Jiang, Y., & Li, M.-H. (2019). The biogeochemical niche shifts of *Pinus sylvestris var. Mongolica* along an environmental gradient. *Environmental and Experimental Botany*, *167*, 103825. https://doi.org/10.1016/j.envexpbot.2019.103825

He, W.-M., Yu, F.-H., & Zhang, L.-L. (2010). Physiological integration impacts nutrient use and stoichiometry in three clonal plants under heterogeneous habitats. *Ecological Research*, *25*(5), 967–972. https://doi.org/10.1007/s11284-010-0724-0

Hette-Tronquart, N. (2019). Isotopic niche is not equal to trophic niche. *Ecology Letters*, ele.13218. https://doi.org/10.1111/ele.13218

Hobbie, S. E. (2015). Plant species effects on nutrient cycling: Revisiting litter feedbacks. *Trends in Ecology & Evolution*, *30*(6), 357–363. https://doi.org/10.1016/j.tree.2015.03.015

Horn, H., S. (1971). *The adaptive geometry of trees* (Vol. 3). Princeton University Press.

Hutchinson, G. E. (1957). Concluding remarks. *Cold Spring Harbor Symposia on Quantitative Biology*, *22*(0), 415–427. https://doi.org/10.1101/SQB.1957.022.01.039

Kaspari, M., & Powers, J. S. (2016). Biogeochemistry and geographical ecology: Embracing all twenty-five elements required to build organisms. *The American Naturalist*, *188*(S1), S62–S73. https://doi.org/10.1086/687576

Kearney, M. R., Simpson, S. J., Raubenheimer, D., & Kooijman, S. A. L. M. (2013). Balancing heat, water and nutrients under environmental change: A thermodynamic niche framework. *Functional Ecology*, *27*(4), 950–966. https://doi.org/10.1111/1365-2435.12020

Klinka, K., Chen, H. Y. H., Wang, Q., & de Montigny, L. (1996). Forest canopies and their influences on understory vegetation in early-seral stands on west Vancouver Island. *Science*, *70*(3), 193–200.

Korell, L., Lang, B. R., Hensen, I., Auge, H., & Bruelheide, H. (2017). Interactions count: Plant origin, herbivory and disturbance jointly explain seedling recruitment and community structure. *Scientific Reports*, *7*(8288), 1–13.Krishna, M. P., & Mohan, M. (2017). Litter decomposition in forest ecosystems: A review. *Energy, Ecology and Environment*, *2*(4), 236–249. https://doi.org/10.1007/s40974-017-0064-9

Leal, M. C., Seehausen, O., & Matthews, B. (2017). The ecology and evolution of stoichiometric phenotypes. *Trends in Ecology & Evolution*, *32*(2), 108–117. https://doi.org/10.1016/j.tree.2016.11.006

Leroux, S. J., Wal, E. V., Wiersma, Y. F., Charron, L., Ebel, J. D., Ellis, N. M., Hart, C., Kissler, E., Saunders, P. W., Moudrá, L., Tanner, A. L., & Yalcin, S. (2017). Stoichiometric distribution models: Ecological stoichiometry at the landscape extent. Ecology Letters, 20(12), 1495–1506. https://doi.org/10.1111/ele.12859

Lu, J., Jiang, L., Yu, L., & Sun, Q. (2011). Local factors determine plant community structure on closely neighbored islands. *PLoS ONE*, *6*(5), e19762. https://doi.org/10.1371/journal.pone.0019762

Macek, M., Kopecký, M., & Wild, J. (2019). Maximum air temperature controlled by landscape topography affects plant species composition in temperate forests. *Landscape Ecology*, *34*(11), 2541–2556. https://doi.org/10.1007/s10980-019-00903-x

MacKenzie, W. H., & Meidinger, D. V. (2018). The biogeoclimatic ecosystem classification approach: An ecological framework for vegetation classification. *Phytocoenologia*, 203–213. https://doi.org/10.1127/phyto/2017/0160

Marshall, J. D., & Monserud, R. A. (2003). Foliage height influences specific leaf area of three conifer species. *Canadian Journal of Forest Research*, *33*(1), 164–170. https://doi.org/10.1139/x02-158

Mcardle, B. H., & Anderson, M. J. (2001). Fitting multivariate models to community data: A comment on distance-based redundancy analysis. *Ecology*, *82*(1), 8.

Merems, J. L., Shipley, L. A., Levi, T., Ruprecht, J., Clark, D. A., Wisdom, M. J., Jackson, N. J., Stewart, K. M., & Long, R. A. (2020). Nutritional-landscape models link habitat use to condition of mule deer (*odocoileus hemionus*). *Frontiers in Ecology and Evolution, 8*. https://doi.org/10.3389/fevo.2020.00098

Middleton, E. M., Sullivan, J. H., Bovard, B. D., Deluca, A. J., Chan, S. S., & Cannon, T. A. (2012). Seasonal variability in foliar characteristics and physiology for boreal forest species at the five Saskatchewan tower sites during the 1994 Boreal Ecosystem-Atmosphere Study. *Journal of Geophysical Research: Atmospheres*, 28831–28844. https://doi.org/10.1029/97JD02560@10.1002/(ISSN)2169-8996.BOREAS2

Newsome, S. D., Martinez del Rio, C., Bearhop, S., & Phillips, D. L. (2007). A niche for isotopic ecology. *Frontiers in Ecology and the Environment*, *5*(8), 429–436. https://doi.org/10.1890/060150.1

Oksanen, J., Blanchet, G. F., Friendly, M., Kindt, R., Legendre, P., McGlinn, D., Minchin, P. R., O'Hara, R. B., Simpson, G. L., Solymos, P., Stevens, M. H. H., Szoecs, E., & Wagner, H. (2020). *Vegan: Ecological diversity* (R package version 2.5-7.) [Computer software]. https://CRAN.R-project.org/package=vegan

Pastor, J., Cohen, Y., & Moen, R. (1999). Generation of spatial patterns in boreal forest landscapes. *Ecosystems*, *2*(5), 439–450. https://doi.org/10.1007/s100219900092

Peñuelas, J., Fernández-Martínez, M., Ciais, P., Jou, D., Piao, S., Obersteiner, M., Vicca, S., Janssens, I. A., & Sardans, J. (2019). The bioelements, the elementome, and the biogeochemical niche. *Ecology*, *100(5)*, e02652. https://doi.org/10.1002/ecy.2652

Persson, J., Fink, P., Goto, A., Hood, J. M., Jonas, J., & Kato, S. (2010). To be or not to be what you eat: Regulation of stoichiometric homeostasis among autotrophs and heterotrophs. *Oikos*, *119*(5), 741–751. https://doi.org/10.1111/j.1600-0706.2009.18545.x

Poitevin, E. (2016). Official methods for the determination of minerals and trace elements in infant formula and milk products: A review. *Journal of AOAC International*, *99*(1), 42–52. https://doi.org/10.5740/jaoacint.15-0246

Prieto, I., Almagro, M., Bastida, F., & Querejeta, J. I. (2019). Altered leaf litter quality exacerbates the negative impact of climate change on decomposition. *Journal of Ecology*, *107*(5), 2364–2382. https://doi.org/10.1111/1365-2745.13168

R. Hoy, S., Forbey, J. S., Melody, D. P., Vucetich, L. M., Peterson, R. O., Koitzsch, K. B., Koitzsch, L. O., Von Duyke, A. L., Henderson, J. J., Parikh, G. L., & Vucetich, J. A. (2021). The nutritional condition of moose co-varies with climate, but not with density, predation risk or diet composition. *Oikos*, *n/a*(n/a). https://doi.org/10.1111/oik.08498

Reich, P. B., & Oleksyn, J. (2004). Global patterns of plant leaf N and P in relation to temperature and latitude. *Proceedings of the National Academy of Sciences*, *101*(30), 11001–11006. https://doi.org/10.1073/pnas.0403588101

Reich, P. B., Oleksyn, J., & Wright, I. J. (2009). Leaf phosphorus influences the photosynthesis–nitrogen relation: A cross-biome analysis of 314 species. *Oecologia*, *160*(2), 207–212. https://doi.org/10.1007/s00442-009-1291-3

Reynolds, H. L., Packer, A., Bever, J. D., & Clay, K. (2003). Grassroots ecology: Plant-microbe-soil interactions as drivers of plant community structure and dynamics. *Ecology*, *84*(9), 2281–2291. https://doi.org/10.1890/02-0298

Richardson, A. D. (2004). Foliar chemistry of balsam fir and red spruce in relation to elevation and the canopy light gradient in the mountains of the northeastern United States. *Plant and Soil*, *260*(1), 291–299. https://doi.org/10.1023/B:PLSO.0000030179.02819.85

Richmond, I. C., Leroux, S. J., Vander Wal, E., Heckford, T. R., Rizzuto, M., Balluffi-Fry, J., Kennah, J. J., & Wiersma, Y. F. (2020). Temporal variation and its drivers in the elemental traits of four boreal plant species. Journal of Plant Ecology, 14, 398–413.

Rizzuto, M., Leroux, S. J., Vander Wal, E., Richmond, I. C., Heckford, T. R., Balluffi-Fry, J., & Wiersma, Y. F. (2021). Forage stoichiometry predicts the home range size of a small terrestrial herbivore. Oecologia, 197(2), 327–338. https://doi.org/10.1007/s00442-021-04965-0

Sardans, J., Vallicrosa, H., Zuccarini, P., Farré-Armengol, G., Fernández-Martínez, M., Peguero, G., Gargallo-Garriga, A., Ciais, P., Janssens, I. A., Obersteiner, M., Richter, A., & Peñuelas, J. (2021). Empirical support for the biogeochemical niche hypothesis in forest trees. *Nature Ecology & Evolution*, *5*(2), 184–194. https://doi.org/10.1038/s41559-020-01348-1

Shen, W., Lin, Y., Jenerette, G. D., & Wu, J. (2011). Blowing litter across a landscape: Effects on ecosystem nutrient flux and implications for landscape management. *Landscape Ecology*, *26*(5), 629–644. https://doi.org/10.1007/s10980-011-9599-x

Simard, S. W. (2009). Mycorrhizal networks and complex systems: Contributions of soil ecology science to managing climate change effects in forested ecosystems. *Canadian Journal of Soil Science*, *89*(4), 369–382. https://doi.org/10.4141/cjss08078

Simard, S. W., Jones, M. D., Durall, D. M., Perry, D. A., Myrold, D. D., & Molina, R. (1997). Reciprocal transfer of carbon isotopes between ectomycorrhizal *Betula papyrifera* and *Pseudotsuga menziesii*. *The New Phytologist*, *137*(3), 529–542.

Šímová, I., Storch, D., Keil, P., Boyle, B., Phillips, O. L., & Enquist, B. J. (2011). Global species-energy relationship in forest plots: Role of abundance, temperature and species climatic tolerances. *Global Ecology and Biogeography*, *20*(6), 842–856. https://doi.org/10.1111/j.1466-8238.2011.00650.x

Soberón, J. (2007). Grinnellian and Eltonian niches and geographic distributions of species. *Ecology Letters*, *10*(12), 1115–1123. https://doi.org/10.1111/j.1461-0248.2007.01107.x

South, R. G. (1983). *Biogeography and ecology of the island of Newfoundland* (Vol. 48). Dr. W. Junk Publishers, The Hague, The Netherlands.

Stearns, S. C. (1989). Trade-offs in life-history evolution. *Functional Ecology*, *3*(3), 259–268. https://doi.org/10.2307/2389364

Sterner, R. W., & Elser, J. J. (2002). *Ecological stoichiometry: The biology of elements from molecules to the biosphere*. Princeton University Press.

Tardif, A., Shipley, B., Bloor, J. M. G., & Soussana, J.-F. (2014). Can the biomass-ratio hypothesis predict mixed-species litter decomposition along a climatic gradient? Annals of Botany, 113(5), 843–850. https://doi.org/10.1093/aob/mct304

Urbina, I., Sardans, J., Grau, O., Beierkuhnlein, C., Jentsch, A., Kreyling, J., & Peñuelas, J. (2017). Plant community composition affects the species biogeochemical niche. *Ecosphere*, *8*(5), e01801. https://doi.org/10.1002/ecs2.1801

van Dijk PL, null, Tesch, null, Hardewig, null, & Portner, null. (1999). Physiological disturbances at critically high temperatures: A comparison between stenothermal antarctic and eurythermal temperate eelpouts (Zoarcidae). *The Journal of Experimental Biology*, *202 Pt 24*, 3611–3621.

Wam, H. K., Felton, A. M., Stolter, C., Nybakken, L., & Hjeljord, O. (2018). Moose selecting for specific nutritional composition of birch places limits on food acceptability. *Ecology and Evolution*, *8*(2), 1117–1130. https://doi.org/10.1002/ece3.3715

Willis, A. D. (2019). Rarefaction, alpha diversity, and statistics. *Frontiers in Microbiology*, *10*, 2407. https://doi.org/10.3389/fmicb.2019.02407

Woods, H. A., Makino, W., Cotner, J. B., Hobbie, S. E., Harrison, J. F., Acharya, K., & Elser, J. J. (2003). Temperature and the chemical composition of poikilothermic organisms. *Functional Ecology*, *17*(2), 237–245. https://doi.org/10.1046/j.1365-2435.2003.00724.x

Zhang, J., Zhao, N., Liu, C., Yang, H., Li, M., Yu, G., Wilcox, K., Yu, Q., & He, N. (2018). C:N:P stoichiometry in China's forests: From organs to ecosystems. *Functional Ecology*, *32*(1), 50–60. https://doi.org/10.1111/1365-2435.12979

2.9 Tables

Table 2.1 Summary of niche comparison results for balsam fir and white birch. Results for balsam fir and white birch are separated within the table. The first column describes the level of comparison. Between ecoregion is our species level comparison and community type (CT) comparisons are presented for CT: across ecoregion, CT: within ecoregion, and CT: between ecoregion. In the second column we present the Multivariate Homogeneity test of Dispersion (MHD) values as the average distance to median for each niche; we denote Northern Peninsula and Central Forest ecoregions as NP and CF, respectively; we denote conspecific and heterospecific community types as con and hetero, respectively. In the third column we present results for Permutation test for Homogeneity of Multivariate Dispersion (PT-MHD) and report the *F* value and *p*-value for the niche comparisons of dispersion. In the fourth column we present Permutational Multivariate Analysis of Variance (PERMANOVA) results and report the R^2, *F* statistic, and *p*-value for niche comparisons. In the fifth column we present our hypervolume similarity assessment and report the Jaccard similarity index. In the sixth column we report niche metrics of percent overlap (%), nestedness (i.e., varies between 0 and 1, where 0 = no overlap and 1 = a smaller niche occupying space within a larger niche) and ITV as the difference between relative niche volumes as a percentage. The sign reported in the ITV column indicates if ITV increased (+) or decreased (-) and the following describes how ITV was determined. For species level comparisons we subtracted Central Forest niches from Northern Peninsula niches. For community level comparisons across ecoregions we subtracted conspecific niches from the heterospecific niches. Similarly, for within ecoregion comparisons we subtracted conspecific niches from the heterospecific niches for a given ecoregion. For community level comparisons of between ecoregions Central Forest conspecific were subtracted from Northern Peninsula conspecifics and similarly for heterospecific comparisons. Bolded *p*-value indicate significant results where *p ≤ 0.05*.

Balsam fir	MHD		PT-MHD		PERMANOVA			Hypervolume	Niche volume metrics		
Between ecoregion	**NP**	**CF**	*F* value	*p*-value	R2	*F* statistic	*p*-value	Jaccard	Overlap	Nestedness	ITV (%)
	0.011	0.005	57.683	**0.001**	0.036	14.592	**0.001**	0.281	10.714%	0.393	+70.97
CT: across ecoregion	**Con**	**Hetero**	*F* value	*p*-value	R2	*F* statistic	*p*-value	Jaccard	Overlap	Nestedness	ITV
	0.009	0.010	0.065	0.805	0.002	0.646	0.458	0.709	43.860%	0.276	+ 35.49
CT: within ecoregion	**Con**	**Hetero**	*F* value	*p*-value	R2	*F* statistic	*p*-value	Jaccard	Overlap	Nestedness	ITV
Northern Peninsula	0.011	0.011	0.140	0.716	0.002	0.450	0.570	0.672	40.426%	0.251	+ 29.04
Central Forest	0.005	0.005	0.051	0.836	0.003	0.306	0.726	0.566	50.000%	0.000	0.000
CT: between ecoregion	**NP**	**CF**	*F* value	*p*-value	R2	*F* statistic	*p*-value	Jaccard	Overlap	Nestedness	ITV
Conspecific	0.011	0.005	25.902	**0.001**	0.039	7.581	**0.005**	0.266	15.385%	0.346	+ 29.03
Heterospecific	0.011	0.004	31.428	**0.001**	0.034	6.943	**0.004**	0.249	9.091%	0.409	+ 58.07

White birch	MHD		PT-MHD		PERMANOVA			Hypervolume	Niche volume metrics		
Between ER	**NP**	**CF**	*F* value	*p*-value	R2	*F* statistic	*p*-value	Jaccard	Overlap	Nestedness	ITV
	0.014	0.010	9.174	**0.005**	0.251	75.999	**0.001**	0.163	5.166%	0.067	+46.65
CT: across ecoregions	**Con**	**Hetero**	*F* value	*p*-value	R2	*F* statistic	*p*-value	Jaccard	Overlap	Nestedness	ITV
	0.013	0.015	0.731	0.404	0.018	4.075	**0.021**	0.552	23.718%	0.623	+ 68.92
CT: within ecoregions	**Con**	**Hetero**	*F* value	*p*-value	R2	*F* statistic	*p*-value	Jaccard	Overlap	Nestedness	ITV
Northern Peninsula	0.012	0.014	0.120	0.750	0.003	0.480	0.577	0.534	0.457%	0.995	+ 66.48
Central Forest	0.012	0.008	5.495	**0.017**	0.117	9.163	**0.001**	0.334	43.396%	0.127	- 3.66
CT: between ecoregions	**NP**	**CF**	*F* value	*p*-value	R2	*F* statistic	*p*-value	Jaccard	Overlap	Nestedness	ITV
Conspecific	0.012	0.012	0.068	0.803	0.236	8.038	**0.001**	0.132	0.000%	0.000	- 13.12
Heterospecific	0.014	0.008	13.415	**0.001**	0.257	68.702	**0.001**	0.093	2.449%	0.079	+ 57.02

Table 2.2 Northern and southern ecoregions differences for each foliar elemental trait. Average values with standard errors are presented for foliar C, N, and P concentrations (%) for species level comparisons between ecoregion (a) and community level comparisons between ecoregion (b/c). Central Forest was subtracted from Northern Peninsula to determine differences in percent foliar elemental traits.

a) Species level: between ecoregion	Balsam fir			White birch		
Ecoregion	C	N	P	C	N	P
Northern Peninsula	52.122 ± 0.074	1.029 ± 0.009	0.125 ± 0.002	49.836 ± 0.115	2.784 ± 0.037	0.282 ± 0.005
Central Forest	52.327 ± 0.046	0.865 ± 0.018	0.076 ± 0.003	50.381 ± 0.096	1.641 ± 0.055	0.155 ± 0.008
Difference	-0.205	0.164	0.049	-0.545	1.143	0.127

b) Community level: between ecoregion	Conspecific			Heterospecific		
Balsam fir	C	N	P	C	N	P
Northern Peninsula	52.075 ± 0.107	1.016 ± 0.013	0.125 ± 0.002	52.166 ± 0.103	1.04 ± 0.013	0.126 ± 0.003
Central Forest	52.315 ± 0.065	0.84 ± 0.024	0.079 ± 0.005	52.339 ± 0.066	0.89 ± 0.026	0.073 ± 0.004
Difference	-0.240	0.176	0.046	-0.173	0.150	0.053

c) Community level: between ecoregion	Conspecific			Heterospecific		
White birch	C	N	P	C	N	P
Northern Peninsula	49.86 ± 0.548	3.07 ± 0.179	0.334 ± 0.021	49.835 ± 0.118	2.775 ± 0.037	0.281 ± 0.005
Central Forest	49.945 ± 0.192	1.81 ± 0.117	0.188 ± 0.014	50.59 ± 0.095	1.56 ± 0.055	0.14 ± 0.008
Difference	-0.085	1.260	0.146	-0.755	1.214	0.141

2.10 Figures

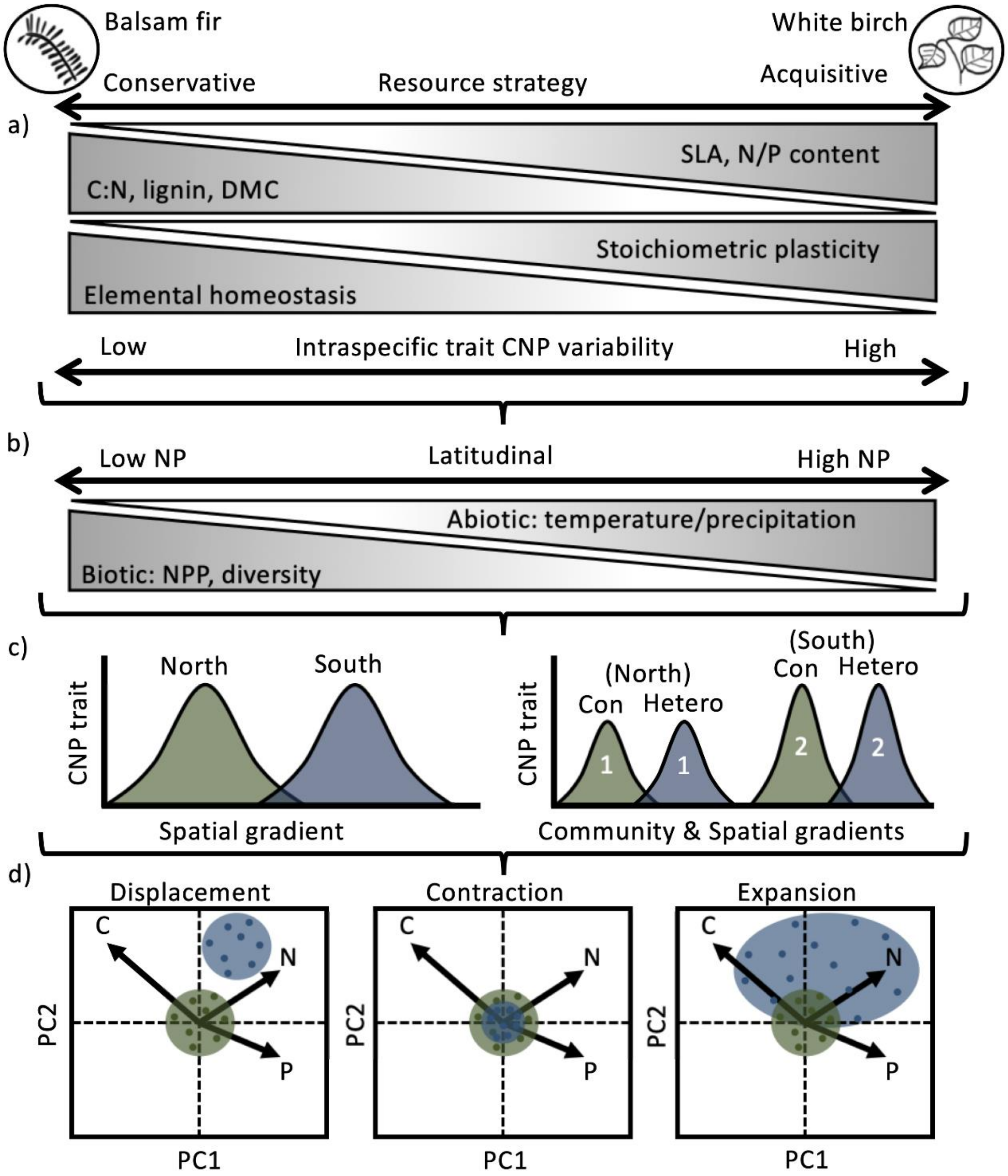

Figure 2.1 Conceptual diagram for foliar elemental niche differences. Our two focal species, balsam fir and white birch are depicted at the top of the diagram operating on different ends of a resource strategy. Differences in conservative and acquisitive foliar traits relate to life history strategies of resource acquisition, use, and storage (a). For instance, slow growing conservative

species which produce long lived foliar material often exhibit high foliar C:N, lignin, and dry matter content (DMC) as durable foliar traits as opposed to traits of high specific leaf area (SLA) and N/P concentration for fast growing acquisitive species which shed foliar material annually. Although we highlight other foliar traits in this diagram, our study focuses on foliar elemental traits of C, N, and P as they relate to elemental homeostasis and stoichiometric plasticity. Due to resource acquisition and use tactics, conservative species often exhibit low stoichiometric plasticity and high elemental homeostasis as compared to the high stoichiometric plasticity and low elemental homeostasis of acquisitive species. Furthermore, internal elemental demands and eco-physiological constraints limit the intraspecific trait variability (ITV) of foliar C, N, and P. And as a filter for community assembly, traits, and their intraspecific variability are used to explain niche mechanisms of biotic interactions such as trait conditions under different community settings. As well, latitudinal patterns of foliar N and P are often associated with gradients of temperature and precipitation with lower photosynthetic grains of C in colder temperatures relative to N and P uptake (b). This suggests that populations in northern biogeographic locations should have higher foliar N and P content relative to southern populations. Here, we use foliar C, N, and P traits as it relates directly to resource use and niche mechanisms to assess how the elemental niche of balsam fir and white birch differs at a species level and community level. At the species level (c), we expect both our focal species to exhibit larger elemental niche volumes in our northern ecoregion (Northern Peninsula) compared to their niche volumes in our southern ecoregion (Central Forest). At a community level, we group our focal species by conspecific (occurring in monocrop groups) and heterospecific (both focal species co-occur) groups. We expect their elemental niches to be different when in a conspecific (Con; green) as opposed to a heterospecific (Hetero; blue) community types (c). We make these community level comparisons across, within, and between ecoregions. For each comparison we expect balsam fir to elicit a niche displacement pattern (d) and white birch to elicit a niche expansion pattern – these potential patterns reflect their resource strategies, elemental homeostasis, and stoichiometric plasticity described above via Principal Component Analysis (PCA; Peñuelas et al., 2019; Urbina et al., 2017).

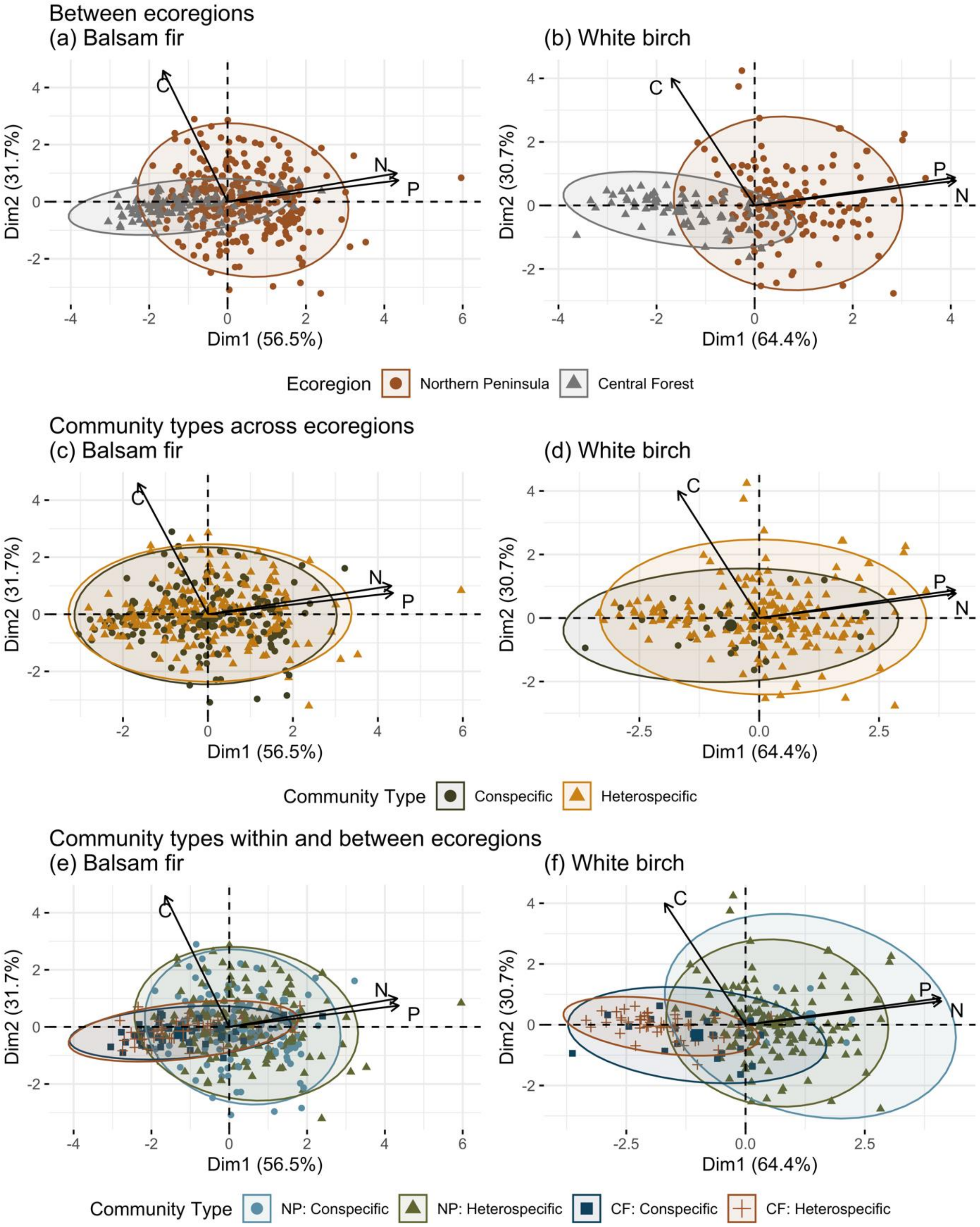

Figure 2.2 Principal component analysis (PCA) for balsam fir (a) and white birch (b) at the species level between ecoregions and at the community level across (c and d), within and

between (e and f) ecoregions. For each plot, ellipses with a 95 % probability are shown for each comparison and colour-coded for ecoregions (a and b), conspecific and heterospecific groups (c and d), and conspecific and heterospecific groups by ecoregions (e and f). In addition, different symbology is used in these plots to showcase the variability of individuals from different groups. In both cases dimension 1 explains 56.5 and 64.4 % while dimension 2 explains 31.7 and 30.7 % of the variance for balsam fir and white birch, respectively. In both cases N and P highly influence dimension 1 while C influences dimension 2.

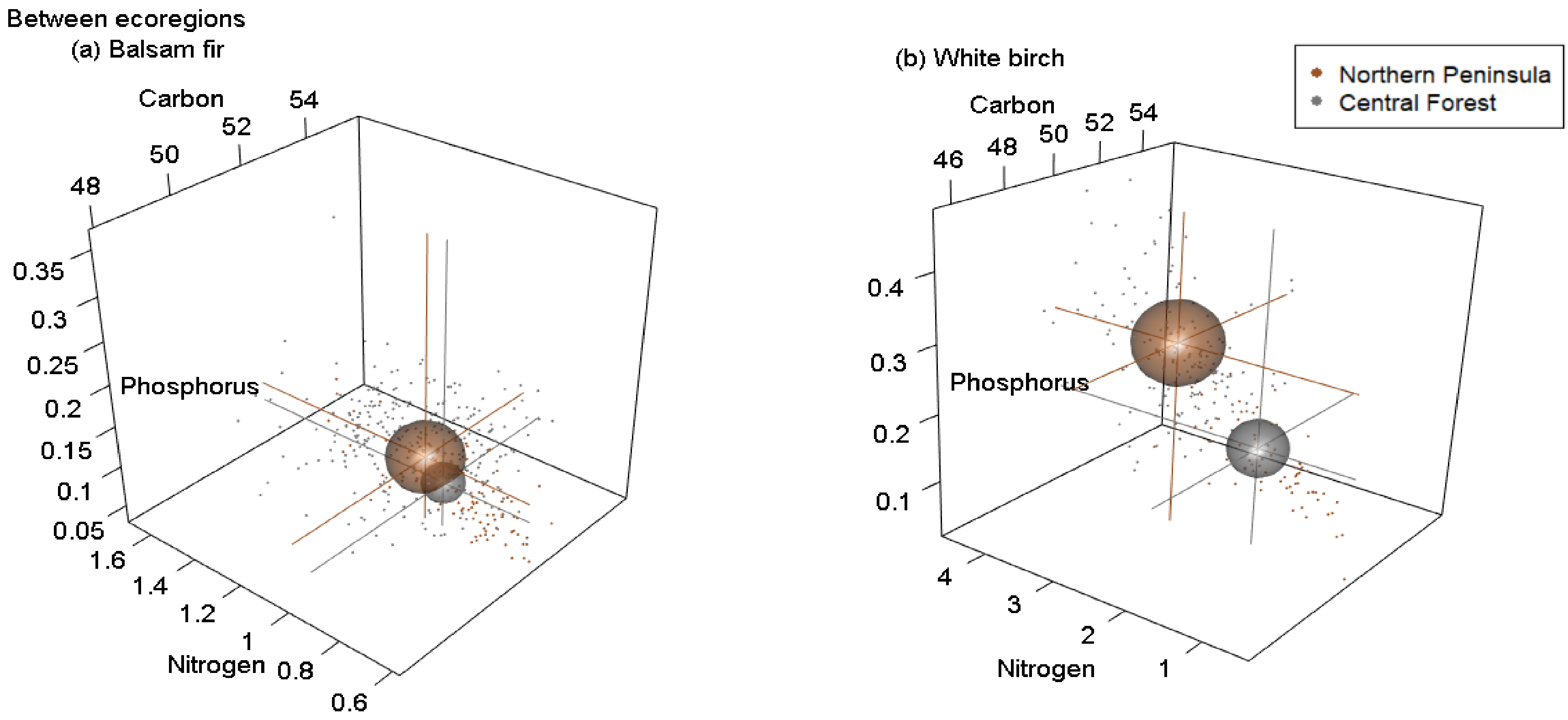

Figure 2.3 Spherical representations of niche hypervolumes at the species level for between ecoregion comparisons for balsam fir (a) and white birch (b). Plot size represents the total stoichiometric volume of C, N, and P for each focal species. Corresponding drop lines to axes indicate the average C, N, and P value for each niche.

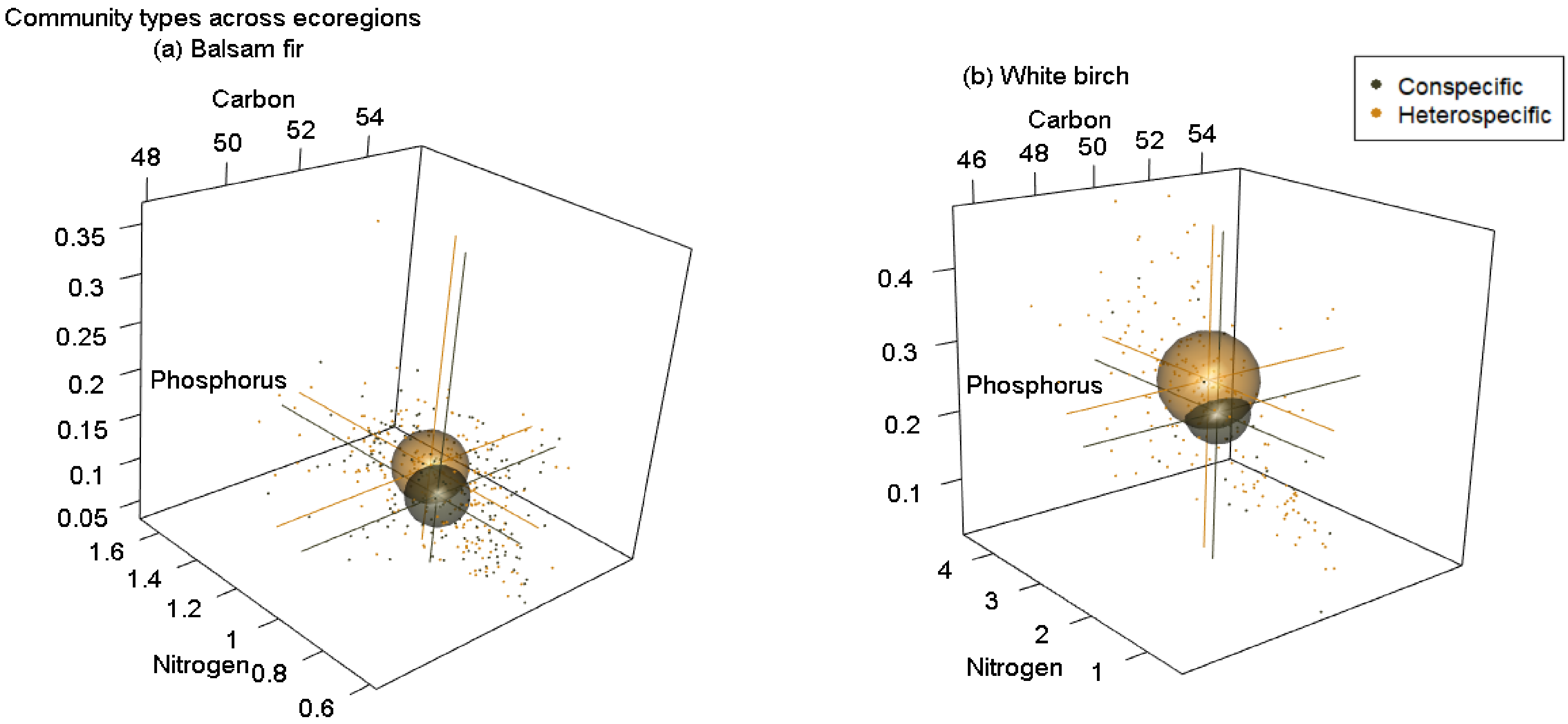

Figure 2.4 Spherical representations of niche hypervolumes at the community level for across ecoregion comparisons for balsam fir (a) and white birch (b). Plot size represents the total stoichiometric volume of C, N, and P for each focal species. Corresponding drop lines to axes indicate the average C, N, and P value for each niche. Plots are rotated in different ways to best show the differences between spheres.

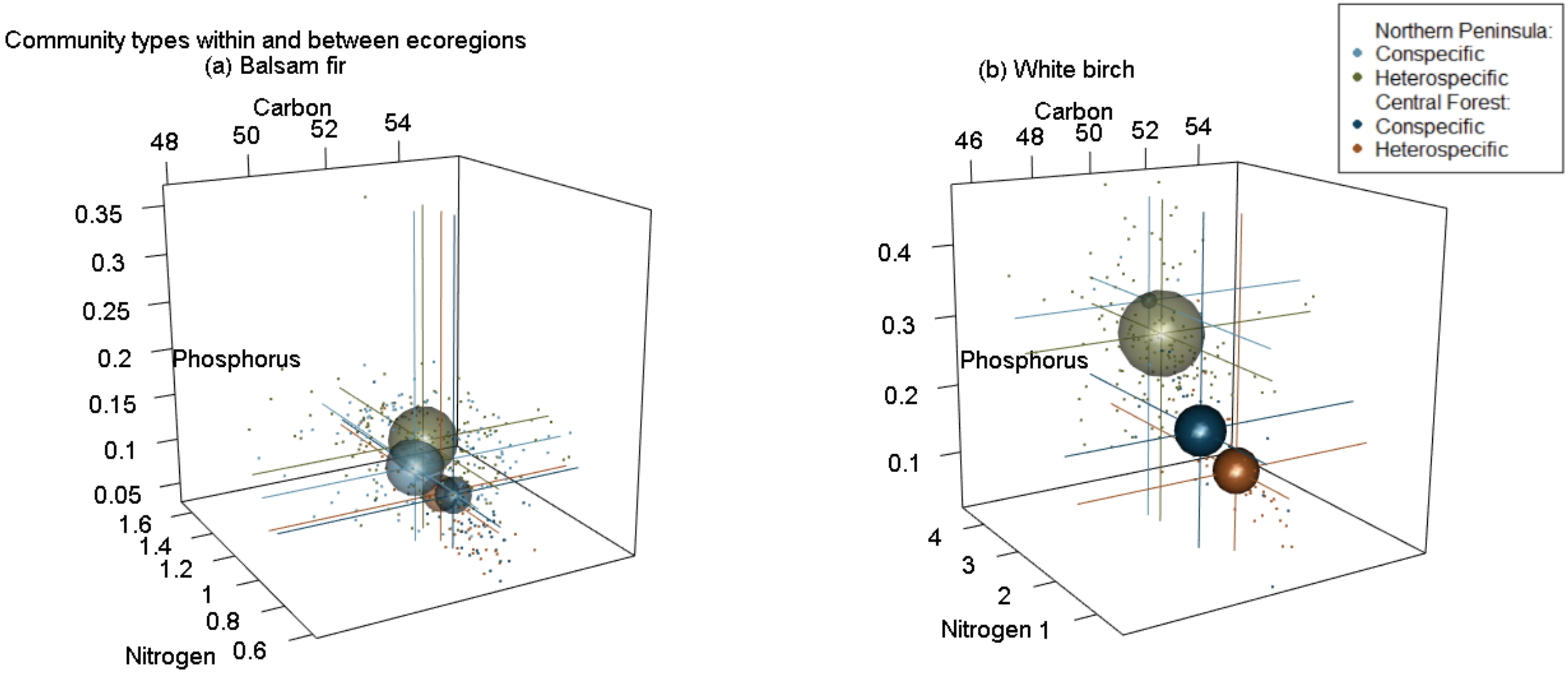

Figure 2.5 Spherical representations of niche hypervolumes at the community level for within and between ecoregion comparisons for balsam fir (a) and white birch (b). Plot size represents the total stoichiometric volume of C, N, and P for each focal species. Corresponding drop lines to axes indicate the average C, N, and P value for each niche. Note that for white birch, the Northern Peninsula conspecific niche is nested completely within the Northern Peninsula heterospecific niche.

Chapter 3

Spatially explicit correlates of plant functional traits inform landscape patterns of resource quality

Authors: Travis R Heckford[1], Shawn J. Leroux[1], Eric Vander Wal[1], Matteo Rizzuto[1], Juliana Balluffi-Fry[2], Isabella C. Richmond[1], Yolanda F. Wiersma[1]

Author Affiliations

1: Department of Biology, Memorial University of Newfoundland. 230 Elizabeth Avenue, St. John's Canada

2: Department of Biological Sciences, University of Alberta, Edmonton, Canada

A version of this paper is published in *Landscape Ecology* as

Heckford, T. R., Leroux, S. J., Vander Wal, E., Rizzuto, M., Balluffi-Fry, J., Richmond, I. C., & Wiersma, Y. F. (2022). Spatially explicit correlates of plant functional traits inform landscape patterns of resource quality. *Landscape Ecology* 37:59-80https://doi.org/10.1007/s10980-021-01334-3

3.1 Abstract

Context: Spatially explicit correlates of foliar elemental, stoichiometric, and phytochemical (ESP) traits represent links to landscape patterns of resource quality.

Objectives: We investigate spatial correlates for multiple foliar ESP traits at the species level and across species at the trait level for five boreal forest understory plants.

Methods: On the island of Newfoundland, Canada, we collected plot-level foliar material from four chronosequenced forest grids. We integrated plot-level response variables of foliar elemental (C, N, P, percent and quantity), stoichiometric (C:N, C:P, N:P), and phytochemical (terpenoids) traits, with spatial predictors available for the whole landscape to test multiple competing hypotheses. These hypotheses included the effects of land cover (e.g., coniferous, deciduous, mixedwood), productivity (e.g., enhanced vegetation index), biotic (e.g., stand age/height, canopy closure) and abiotic (e.g., elevation, aspect, slope) factors.

Results: Spatial correlates of foliar ESP traits were generally species specific. However, at the trait level, some species shared spatial predictors, notably for foliar percent carbon, C:P, N:P, sesquiterpene traits. Here we highlight that foliar C, C:P, and sesquiterpene traits between different species were explained by abiotic spatial correlates alone. Similarly, foliar terpenoid traits between different species were related to a combination of abiotic and biotic factors.

Conclusions: Spatial-trait relationships mainly occur at the species level, with some commonalities at the trait level. By linking plot-level foliar ESP traits to spatial predictors, we can map plant chemical composition patterns that influence landscape-scale ecosystem processes which can be used to inform sustainable landscape management.

3.2 Introduction

A number of environmental factors have been shown to influence the intraspecific variability of foliar traits in plants. For example, overstory vegetation (i.e., landcover; Hallett & Hornbeck, 1997; Hollinger, 1996), site productivity (Li et al., 2020; Radwan & Harrington, 2011; Zhang et al., 2017), community structure (Peñuelas et al., 2019; Perry et al., 2013; Sedio et al., 2017), and topographic conditions (Müller et al., 2017) can influence trait variability directly via resource availability and indirectly via the different strategies by which plants use resources under different environmental conditions. Chemical traits such as elemental properties (% and quantity Carbon, Nitrogen, and Phosphorus), stoichiometric ratios (elemental concentrations on a biomass basis, specifically molar C:N, N:P, and C:P ratios), and phytochemical or secondary carbon based compounds (terpenoids, phenols) are often useful indicators of ecosystem processes (hereafter we refer to foliar elemental, stoichiometric, and phytochemical traits as ‘ESP’ traits). For instance, variability in foliar ESP traits has been linked to ecosystem estimates of decomposition (Diaz et al., 2004), carbon sequestration/net ecosystem productivity (Harpole et al., 2011; Hessen et al., 2004), evapotranspiration (Liu et al., 2019), and food web complexity (Bryant et al., 1983; Hunter, 2016). Variation in foliar ESP traits is particularly important because it can relate ecosystem biogeochemical properties to changes in environmental conditions. For example, natural and anthropogenic disturbances may have landscape-scale consequences through their effects on water and energy exchanges, which can be reflected in foliar ESP traits (Asner et al., 2015; Lavorel et al., 2011). Thus, linking foliar traits to environmental conditions is an important focus in ecology to build a solid generalization of ecosystem processes at landscape extents (Chapin, 2003; Weih et al., 2014). For instance, since environmental factors vary across landscapes, we can use these environmental gradients to assess the response of species-level intraspecific trait variability to reveal how the spatial patterns these traits create lend themselves to the concept of landscape functionality (Harvey et al., 2017; Schmitz et al., 2018). Indeed, many studies have investigated plot-level correlates of trait variability, however, very few have extracted covariate values from remotely sensed products and used these values to derive spatial predictions of trait variability (see Lavorel et al., 2011; Leroux et al., 2017). Linking plot-level foliar traits to spatially continuous remotely sensed predictors will fill an important gap in the study of the causes and consequences of variation in foliar traits across landscapes.

Across a landscape, different environmental conditions influence the trade-offs plants make between resource acquisition and use, and as such, the intraspecific variability of foliar ESP traits (Lavorel et al., 2011). For instance, foliar N is suggested to be proportional to light interception as a function of carbon capture and growth (Field, 1983; Hollinger, 1996). Plants growing under different overstory vegetation (e.g., deciduous, coniferous, and mixedwood land cover types), which experience varied light conditions via vertical and horizontal canopy complexity, may redistribute foliar N and P resources to optimize growth while stabilizing for competitive interactions (Hassell et al., 1994). As well, nutrient recycling pathways may vary by landcover types via litter inputs, canopy light, temperature, and precipitation controls (Barron-Gafford et al., 2012; Philben et al., 2016) which can influence soil productivity (Krishna & Mohan, 2017), N and P resource availability (Gartner & Cardon, 2004; Knops et al., 2002), and plant N and P use efficiencies (Ashton et al., 2010). Moreover, topographic gradients of elevation, aspect, and slope further define light, temperature, and precipitation inputs and influence soil nutrient processes (Macek et al., 2019). As such, these environmental conditions may influence how plants allocate resources to different traits to optimize performance in variable conditions (Müller et al., 2017). Many different environmental factors likely influence resource trade-offs by plants and their foliar ESP traits, with the range of intraspecific variability constrained by a species resource strategy (Grime & Pierce, 2012). Thus, across the landscape, spatial gradients of environmental conditions influence the resource trade-offs that plants make. This allows for a novel spin on distribution models, whereby the variability of foliar ESP traits is mapped in response to gradients of spatial covariates. However, to make these spatial predictions of foliar trait patterns, we must first identify which spatial covariates influence the variability of foliar traits at a species level, which allows us to compare these drivers across species to derive generalizations of trait distributional patterns.

Although many studies have investigated the variability of plant functional traits along local spatial gradients for individual species or functional groups (Peñuelas et al., 2019; Perry et al., 2013), very few studies have identified which remotely sensed spatial correlates influence multiple foliar traits for different species that are indicative of forage quality. By deriving remote sensed correlate values for georeferenced plot data, we can use these correlates to map landscape patterns of resource quality via trait variability. For instance, Leroux et al. (2017) constructed stoichiometric distribution models by fitting multiple spatial correlates for white birch *(Betula papyrifera* Marshall) foliar elemental quantity and stoichiometric ratios, creating a predictive surface of forage quality and quantity and related these spatial trait patterns to moose (*Alces alces* (Linnaeus, 1758)) space use. Other studies have also linked herbivore body condition to the spatial patterns of forage quality by using plant functional groups (Merems et al., 2020). However, many studies have shown that forage choice, even for a generalist herbivore, is often species and bite-specific (Duparc et al., 2020). For instance, Wilson et al. (2019) showed that differences in the nutrient content of plant species can influence bite-scale forage selection patterns. Thus, spatial models for multiple forage species and different resource traits could reveal herbivore space use trade off decisions at fine (bite scale) and coarse (habitat/home range scale) extents. In fact, community assembly theory posits that, in a given setting, trait divergence should occur between co-occurring species which operates to reduce niche overlap (Vellend, 2016). Thus, foliar traits across species may differ in response to different environmental conditions and this species-trait specificity may explain aspects of variability related to ecosystem processes and trophic dynamics (Wilkes et al., 2020).

Identifying the spatial correlates of foliar traits linked to ecosystem processes is an important topic in landscape ecology (Pickett & Cadenasso, 1995; Turner, 1989). For instance, the distribution and movement of energy and matter over time determines landscape functionality via pattern and process relationships (Lavorel et al., 2011; Shen et al., 2011; Turner, 2005). Foliar ESP traits provide a direct link to thermodynamics and entropy processes at landscape extents (Elser & Hamilton, 2007; Vranken et al., 2015). For example, foliar N and P concentration and N:P ratios have been linked to primary productivity (Elser et al., 2010), while stoichiometric traits have been associated with nutrient limitation and community structure processes (Harpole et al., 2011; Urbina et al., 2017). Phytochemical defense traits have been linked to trophic interactions, spatial flows of energy and matter, and nutrient recycling processes (Hunter, 2016). At the landscape level, spatial covariates of land cover, productivity, forest structure, and topography are known correlates of foliar ESP trait variability. For example, balsam fir (*Abies balsamea* (L.) Mill.) and red spruce (*Picea rubens* Sarg.) foliar N and P have been shown to follow elevational gradients (Richardson, 2004), while Scots pine (*Pinus sylvestris* L.) shifts foliar stoichiometric content in response to soil nutrients (i.e., site level productivity; He et al., 2019), and eucalyptus (*Eucalyptus urophylla* S.T.Blake) foliar P decreases with stand age (Fan et al., 2015). A species level approach to identifying spatial correlates of foliar ESP traits will allow us to obtain refined estimates that are comparable across species and traits to derive potential generalities. Moreover, we can use these spatial correlates to develop predictive spatial models to better understand the ecology of landscapes (see Leroux, 2018; Leroux et al., 2017).

Here, we investigate which environmental factors drive the spatial variability of foliar elemental, stoichiometric, and phytochemical (ESP) traits at a species level for five common boreal plants, and we compare these factors across these species to determine if there are shared community level correlates of traits. To do so we use spatially explicit covariates to investigate correlates of foliar ESP traits for five commonly occurring juvenile boreal forest species. Our spatial predictors of land cover (i.e., coniferous, deciduous, mixedwood), productivity (i.e., enhanced vegetation index), biotic factors (i.e., structural conditions of stand age, height, and canopy closure), and abiotic factors (i.e., elevation, aspect, and slope), represent known and/or suggested correlates of foliar ESP traits (see Table 3.1). Our aim is to identify parsimonious relationships for plot level foliar ESP trait variability in response to different combinations of spatial correlates and to assess our results for covariate generalities at the species and trait level. Our approach identifies spatial covariates which can be used to construct predictive spatial surfaces of foliar trait variability. These surfaces provide the next step to link spatial patterns to ecosystem processes involving the distribution of energy and matter in foliar material. This work contributes to concept of landscape functionality and may help inform sustainable landscape management.

3.3 Methods

3.3.1 Study site and focal species description

Our study area is located on the eastern side of the island of Newfoundland, Canada; ecodistrict 468 (Figure 3.1a; a detailed description of Figure 3.1 is provided in Appendix B.1). Here, the bedrock is generally a mixture of crystalline Paleozoic strata with upland dominated by hummocky to ridged sandy morainal depositions (South, 1983). The natural disturbance pattern in this area favours a dominant vegetative cover of intermediate-aged, closed canopy forest stands of balsam fir and black spruce (*Picea mariana* (Mill.) Britton, Sterns, & Poggenb) on steep, moist, upland areas. Alternatively, disturbed areas are dominated by white birch, trembling aspen (*Populus tremuloides* Michx.), and black spruce with drier sites consisting of black spruce and heaths of kalmia (*Kalmia angustifolia* L.) (South, 1983). On average this region experiences annual temperature of 4.5^{o}C, with a summer and winter mean of 12.5^{o}C and -3.5^{o}C, and mean annual precipitation of 100-300 cm (South, 1983).

Our understory focal species consisted of two coniferous tree species: balsam fir, black spruce, two deciduous tree species: red maple (*Acer rubrum* L.), white birch, and one herbaceous plant: lowbush blueberry (*Vaccinium angustifolia* Aiton.). Our focal species commonly occur across the study region and are largely co-distributed geographically across North America. Moreover, our focal species represent common forage for the dominant herbivores within the boreal system: moose (*Alces alces* (Linnaeus, 1758)) and snowshoe hare (*Lepus americanus* (Erxleben, 1777)). As such, their foliar traits provide us with a useful measure of resource distribution by which we can potentially infer spatial patterns of herbivory similar to what has been done in other regions (see Balluffi-Fry et al., 2020).

3.3.2 Sampling design

In black spruce leading stands, which is the predominant forest type for this region (South, 1983), we set up four chronosequenced meandering transect grids, covering 25 ha, and differing in age by 20 year intervals (Figure 3.1b; centroid locations for each grid: Bloomfield 48.34°N, -53.98°W; Unicorn 48.63°N, -54.01°W; Terra Nova North 48.62°N, -53.97°W; Dunphy's Pond 48.49°N, -54.05°W). There is considerable variability in forest stand conditions (i.e., tree age, height, and canopy closure) across each grid, which allowed us to capture a representative snapshot of forest heterogeneity in this region (see Appendix B.2, Figure B.2.1 for a comparison of forest structure sampled versus available on the landscape). These grids were originally designed for snowshoe hare live trapping to investigate animal spatial ecology related to spatial variability of foliar ESP resources. Each grid is comprised of 50 sampling locations (Figure 3.1b).

3.3.3 Data collection

For each of our study species we assessed foliar traits of elemental concentration (i.e., percent and quantity C, N, and P) and stoichiometric ratio (i.e., C:N, C:P, and N:P). For our coniferous species, balsam fir and black spruce that have constituent phytochemical defence strategies, we assessed foliar phytochemical traits of terpene, monoterpene, monoterpenic alcohol, monoterpenic ester, sesquiterpene, and phytochemical diversity. The following sections describe how we collected shrub belt, foliar material, and biomass data.

3.3.3.1 Shrub belt

At each sample location, we set up a 22.6 m diameter circular plot (Figure 3.1c). Within each plot, we collected density estimates for each of our study species along a 22.6 m long and 1 m wide shrub belt transect (Figure 3.1c). Moving in a north to south direction, along the belt, for each of our study species encountered we measured height and basal diameter, and the distance at which an individual was encountered, for a maximum of five individuals per height class: 0-50 cm, 51-100 cm, 101-150 cm, and 151-200 cm, denoted as A, B, C, and D respectively (Figure 3.1d). We restricted our sampling to species within 0-2 m heights as these individuals represent the available forage for common boreal herbivores such as moose and snowshoe hare.

3.3.3.2 Foliar material

Within each circular plot, we collected representative foliar material from each intercardinal corner. Starting in the NE corner, we clipped foliar material and then moved to the next corner and clipped a similar amount of foliar material, we continued this process, moving clockwise between the plot corners, until we acquired approximately 20 g of foliar material. Our sampled foliar material consisted of terminal and lateral leaves and connected stem/stock, i.e., we attempted to mimic the parts of a plant a herbivore (moose/snowshoe hare), might consume. Stem/stock parts are often incidental components of summer forage, as such our samples primarily focused on terminal and lateral leaves. We also measured height and basal diameter (used for augmenting shrub belt data described below) of each individual sampled. Samples of balsam fir (n = 95), black spruce (n = 157), red maple (n = 91), white birch (n = 71), and lowbush blueberry (n = 160) were frozen at -20°C until they were sent for foliar elemental analysis at the Agriculture Food Lab (AFL) at the University of Guelph Ontario, Canada. Foliar C and N was determined using an Elementar Vario Macro Cube. Foliar P was determined using a microwave acid digestion CEM MARSxpress microwave system and brought to volume using Nanopure water. The clear extract supernatant was further diluted by 10 to accurately fall within calibration range and reduce high level analyte concentration entering the inductively coupled plasma mass spectrometry (ICP-MS) detector (Poitevin, 2016). Foliar phytochemical analysis for balsam fir (n = 104) and black spruce (n = 163) was performed at the Laboratorie PhytoChemia Inc. in Quebec, Canada. Foliar terpenoid composition was determined using a gas chromatography solvent extraction with an internal standard and a correction factor (Cachet et al., 2016). The number of elemental/stoichiometric and phytochemical samples differ due to the amount of foliar material needed for each analysis. Less foliar material is needed to perform the phytochemical analysis; thus, we were able to have more samples processed. See Appendix B.3, Table B.3.1 for a complete list of individual terpenoid compounds found in our balsam fir and black spruce foliar samples.

3.3.3.3 Biomass

To determine the foliar biomass of new growth material for our focal species we collected all of the new growth foliar material from approximately 50 individuals. We collected these individuals along the periphery of our study grids, in randomly selected locations to avoid destructive sampling of foliage in our long-term monitoring grids. We sampled individuals evenly across height classes to obtain a representative sample. More specifically, for height classes A, B, C, D for balsam fir we had 20, 16, 12, and 2 samples (n = 50); for black spruce we had 20, 20, 20, and 20 samples (n = 80); for white birch we had 14, 18, 9, and 9 samples (n = 50); for red maple we had 17, 16, 18, and 6 samples (n = 57); and for lowbush blueberry we had 31, and 19 samples (n = 50) respectively. In addition, we measured the height and basal diameter for each sample (Figure 3.1d). Biomass samples were dried at 50˚C for 2-3 days. We used the resulting dry weights to perform allometric modelling (described below).

3.3.4 Constructing foliar ESP response variables

Following Leroux et al., (2017), we used three pieces of information to construct foliar ESP distribution models; shrub belt data to determine plot level species density, foliar material to extract elemental percentages (i.e., % C, N, and P) and phytochemical composition (raw basis mg/g), and biomass data to fit allometric models. We fit allometric models using biomass as a function of height and basal diameter for each of our study species (goodness of fit adjusted R^2 for balsam fir (0.82), black spruce (0.80), red maple (0.83), white birch (0.79), and lowbush blueberry (0.47); see Appendix B.4, Figure B.4.1 for plots). The estimates of allometric correlates allowed us to parameterize shrub belt density data and predict plot level biomass estimates based on density of species in their respective height classes (Figure 3.1d,f). We then summed height class biomass estimates at the plot level. In the few instances where we did not encounter a species on the shrub belt but had collected foliar material within that plot, we augmented shrub belt data by adding the total number of individuals sampled for foliar material as a ceiling estimate of abundance for a given height class at that plot (see Appendix B.5, Table B.5.1 for details). To acquire foliar elemental quantity traits, we divided plot level biomass by the plot area (401.15 m^2) multiplied by foliar elemental percentages. To acquire foliar stoichiometric traits, we divided foliar elemental quantity traits of C, N and P by their respective molar masses and divided the resulting values together to get ratios of C:N, C:P, and N:P (Figure 3.1f). Similarly, to acquire phytochemical traits, we divided plot level biomass by the plot area (401.15 m^2) multiplied by our phytochemical raw measures. Our terpene variable is the sum of all phytochemical compounds at the plot level. Phytochemical diversity is calculated using a Shannon Diversity Index for all compounds identified per species (i.e., using our balsam fir phytochemical matrix, sites x by individual phytochemical compounds, we calculated alpha diversity; this was performed again for black spruce).

3.3.5 Spatial predictors

Based on *a priori* hypotheses we used remotely-sensed spatially explicit covariates of land cover, productivity, biotic and abiotic factors, at a resolution of 30 m, to predict ESP trait distribution across the study area (see Table 3.1 for hypothesis rationale and Appendix B.6 for additional covariate details). We investigated the relationship between all possible combinations of the four covariates including a null model (n = 16 total models per response variable, see Table 3.2 for complete model list). In addition, we confirmed the absence of collinearity among our spatial covariates. Our land cover covariate was derived from the Commission for Environmental Cooperation (Commission for Environmental Cooperation, 2017) and consists of three categorical conditions: coniferous, deciduous, and mixedwood. We used the Enhanced Vegetation Index (EVI, 30 m resolution) as a proxy of productivity, because it does not saturate as easily as the Normalized Difference Vegetation Index under wet boreal forest conditions (see Appendix B.7, Figure B.7.1 for temporal interpolation; Vermote et al., 2016). Using Forest Resource Inventory (FRI, originally digitized at a 1:12,500 scale and rasterized to a 30 m resolution) spatial datasets provided by the Provincial Government of Newfoundland (digitization date of 2011) and the Federal Government of Canada (digitization date of 1996) we derived three biotic covariates of stand height, age, and canopy closure, each having four factor levels. Our abiotic factors were derived from a Canadian Digital Elevation Model (*Canadian Digital Elevation Model: Product Specifications-Edition 1.1.*, 2016, originally a 20 m resolution rasterized to a 30 m resolution) and included covariates of elevation, aspect, and slope.

3.3.6 Statistical analyses

Data processing and statistical analyses were done using R and ESRI ArcGIS software (*ESRI*, 2020; R Core Team, 2020). We overlaid remotely sensed and grid-based GIS data on our georeferenced plot data and extracted the value of each remotely sensed covariate (i.e., land cover, productivity, biotic and abiotic factors) for each plot. Using plot level foliar data, we fit General Linear Models (GLM) with the response variables of foliar percent elemental traits (C, N, P as a %), quantity elemental traits (C, N, P as g/m^2), stoichiometric traits (molar ratios C:N, C:P, and N:P), phytochemical traits for our coniferous species which includes terpene, monoterpene, monoterpenic alcohol, monoterpenic ester, sesquiterpene, and phytochemical diversity on a raw (mg/g) and biomass basis (mg/m^2) against explanatory spatial predictors of landcover, productivity, biotic and abiotic factors. We ranked models based on Akaike Information Criterion corrected for small sample size (AIC$_c$) and only considered models within < 2 ΔAIC$_c$ and those above the null model as having evidence to support a spatial relationship. In addition, we removed models with uninformative parameters (following Leroux, 2019). If more than one model was within a < 2 ΔAIC$_c$ we averaged model coefficients and extracted full coefficient estimates for use in the construction of distribution models (see Appendix B.1; Burnham & Anderson, 2002). We constructed spatial surfaces of foliar ESP traits by summing top model or the averaged coefficients estimates for top competing models, multiplied against their corresponding spatial covariate, i.e., binary spatial rasters for landcover and biotic factors and continuous spatial rasters for productivity and abiotic factors. By computing these model equations with remotely sensed and grid-based GIS covariates we are able to create predictive spatial surfaces of foliar trait variability.

We begin each section of the results by reporting patterns and pseudo R^2 assessments of top ranked models (ΔAIC$_c$ < 2, excluding the null model results) across all five species and sub-components of foliar traits: elemental (%C, %N, %P, and quantity C, N, and P), stoichiometric (C:N, C:P, N:P ratios), and phytochemical (terpene, monoterpene, monoterpenic alcohol, monoterpenic ester, sesquiterpene, and diversity). In addition, for each section, we report patterns of top ranked models at the species level. Additional supporting results are reported in the appendices, including an AIC_c table (Appendix B.8, Table B.8.1), table of coefficient slopes and significance (Appendix B.9, Table B.9.1), distribution plots of pseudo R^2 for traits (Appendix B.10, Figure B.10.1), a comparison of observed versus spatially predicted values (Appendix B.11, Figure B.11.1), and model coefficient estimate tables for top ranked models of traits %C, %N, and %P (Appendix B.12, Tables B.12.1, B.12.2, and B.12.3), quantity C, N, and P (Table B.12.4) stoichiometric ratios of C:N, C:P and N:P (Table B.12.5, B.12.6, and B.12.7) and phytochemical groups: terpene and monoterpene (Table B.12.8), monoterpenic alcohol and ester (Table B.12.9), and sesquiterpenes and phytochemical diversity (Table B.12.10). We included the predictive distribution maps of only a subset of the models (Figure 3.5); as there were 41 combinations of species-ESP trait models.

3.4 Results

3.4.1 Foliar percent elemental traits

Across all species for foliar percent elemental traits (Figure 3.2a), eleven models supported these data (R^2 min = 0.046, max = 0.646, mean = 0.286). At the trait level (Figure 3.2a), four models explained foliar percent carbon data (R^2 min = 0.092, max = 0.646, mean = 0.372), five models explained foliar percent nitrogen data (R^2 min = 0.071, max = 0.360, mean = 0.233) and six models explained foliar percent phosphorus data (R^2 min = 0.046, max = 0.472, mean = 0.242). At the species level (Figure 3.2c) we identified different top ranked models for foliar percent elemental traits for all species except white birch foliar percent N and P. Notably, there are different patterns of top ranked model coefficient relationships among species. For balsam fir, our abiotic model explained foliar percent C and P, while N is explained by the land cover, EVI, and abiotic model. For black spruce, our biotic and abiotic model explained foliar percent C and P, although our land cover, biotic, and abiotic model is within $\Delta AIC_c < 2$ for foliar percent C (model averaged trait distribution map is shown in Figure 3.5b). In addition, we found evidence for a EVI and biotic model to explain black spruce foliar percent N. For red maple, foliar percent C is explained by our abiotic model, foliar percent N by our land cover and biotic model, and foliar percent P by two competing top models (1) EVI, and (2) EVI and abiotic. For white birch the only trait for which a parsimonious explanation was determined was foliar percent C, explained by our biotic model. For lowbush blueberry, foliar percent C is explained by our land cover, biotic, and abiotic model. In contrast foliar percent N is explained by two competing top models of (1) EVI, and (2) land cover and EVI, and foliar percent P by is explained by two competing top models of (1) EVI and biotic, and (2) biotic.

3.4.2 Foliar quantity elemental traits

Across all species (Figure 3.2b) for foliar elemental quantity traits, two out of the fifteen potential models explained foliar elemental quantity traits (across all traits R^2 min = 0.183, max = 0.350, mean = 0.263) of C (R^2 min = 0.193, max = 0.350, mean = 0.271), N (R^2 min = 0.183, max = 0.345, mean = 0.264), and P (R^2 min = 0.188, max = 0.321, mean = 0.254). This is, however, only for balsam fir and lowbush blueberry (Figure 3.2d). At the species level, balsam fir foliar quantity C, N, and P is explained by our biotic and abiotic model. For lowbush blueberry, foliar quantity C, N, and P is explained by our land cover and abiotic model.

3.4.3 Foliar stoichiometric traits

Across all species (Figure 3.3a) twelve of the potential fifteen models explained foliar stoichiometric traits (across all traits R^2 min = 0.070, max = 0.427, mean = 0.262). At the trait level (Figure 3.3a), foliar C:N is explained by five top ranked models (R^2 min = 0.089, max = 0.385, mean = 0.253). Foliar C:P is explained by four top ranked models (R^2 min = 0.070, max = 0.336, mean = 0.234). Foliar N:P is explained by six top ranked models (R^2 min = 0.076, max = 0.427, mean = 0.284).

Again, model specificity is variable at the species level (Figure 3.3b), although some geographic commonalities existed in terms of top model covariates and coefficient relationships. For balsam fir, foliar C:N is explained by our land cover, EVI, and abiotic model, foliar C:P by our abiotic model, and foliar N:P by two top models (1) abiotic model, and (2) EVI and abiotic model although the null model here was within $\Delta AIC_c < 2$. For black spruce, foliar C:N is explained by our EVI and biotic model (a spatial predictive model is shown in Figure 3.5b), foliar C:P by our biotic and abiotic model, and foliar N:P by our EVI, biotic and abiotic model. For red maple, foliar C:N is explained by our land cover and biotic model, while our abiotic model explains foliar C:P, however the null model here was within $\Delta AIC_c < 2$. In addition, red maple foliar N:P is explained by our land cover and biotic model. For lowbush blueberry, foliar C:N is explained by our EVI model, foliar C:P by competing models of (1) biotic, and (2) EVI and biotic, and foliar N:P by four competing top models of (1) EVI, biotic and abiotic, (2) EVI and biotic, (3) land cover, EVI, biotic and abiotic, and (4) land cover, EVI and biotic. For white birch, the null model was the top ranked model for all foliar stoichiometric traits.

3.4.4 Foliar phytochemical traits

Across all species (Figure 3.4a) eight of the potential fifteen models explained foliar phytochemical traits on a raw and biomass basis (across all traits R^2 min = 0.017, max = 0.272, mean = 0.138). At the trait level, terpene raw is explained by three top ranked models (R^2 min = 0.047, max = 0.270, mean = 0.191), in comparison terpene on a biomass basis is explained by one top ranked model (R^2 = 0.270). Monoterpene raw is explained by four top ranked models (R^2 min = 0.041, max = 0.244, mean = 0.121), in comparison monoterpene on a biomass basis is explained by one top ranked model (R^2 = 0.272). Monoterpenic alcohol raw is explained by two top ranked models (R^2 min = 0.046, max = 0.233, mean = 0.139). Monoterpenic ester raw is explained by one top ranked model (R^2 = 0.265), and monoterpenic ester on a biomass basis is also explained by one top ranked model (R^2 = 0.265). Sesquiterpene raw is explained by seven top ranked models (R^2 min = 0.040, max = 0.194, mean = 0.098), while sesquiterpene on a biomass basis is explained by two top ranked models (R^2 min = 0.023, max = 0.242, mean = 0.132). Phytochemical diversity on a raw basis is explained by four top ranked models (R^2 min = 0.017, max = 0.122, mean = 0.060).

At the species level (Figure 3.4b), balsam fir and black spruce share some geographic commonalities in terms of top model covariates and coefficient relationships for foliar phytochemical traits. For balsam fir, foliar terpene raw is explained by our EVI model and terpene on a biomass basis by our biotic and abiotic model. In comparison black spruce foliar terpene raw is explained by two competing top models of (1) EVI, biotic and abiotic, and (2) biotic and abiotic (a model averaged predictive model shown in Figure 3.5d). Three competing top models of (1) EVI and abiotic, (2) abiotic, and (3) EVI explained balsam fir foliar monoterpene raw, while our biotic and abiotic model explained monoterpene on a biomass basis. In comparison, black spruce foliar monoterpene raw is explained by our biotic and abiotic model. Balsam fir foliar monoterpenic alcohol raw, although the null model is within $\Delta AIC_c < 2$, is explained by our land cover model, while black spruce foliar monoterpenic alcohol raw is explained by our biotic and abiotic model. Balsam fir foliar monoterpenic ester on a biomass basis is explained by our biotic and abiotic model. While black spruce foliar monoterpenic ester raw is explained by our biotic and abiotic model. Balsam fir foliar sesquiterpene raw is explained by three competing top models of (1) EVI and abiotic, (2) EVI, and (3) abiotic. Balsam fir sesquiterpene on a biomass basis is explained by two competing top models of (1) EVI, and (2) biotic and abiotic, although the null model is within $\Delta AIC_c < 2$. In contrast, black spruce foliar sesquiterpene is explained by four competing top models of (1) land cover, EVI and abiotic, (2) abiotic, (3) biotic and abiotic, and (4) EVI and abiotic. Lastly, balsam fir foliar phytochemical diversity is explained by our abiotic model, although the null model is within $\Delta AIC_c < 2$, while black spruce foliar phytochemical diversity is explained by three competing top models of (1) land cover, (2) biotic, and (3) EVI.

3.5 Discussion

Our study identifies remotely sensed, spatially explicit correlates of foliar ESP (Elemental, Stoichiometric and Phytochemical) traits that provide a starting point to investigate organism-driven ecosystem processes at the landscape extent. Here, we use differing combinations of spatially explicit covariates: land cover, productivity (EVI), biotic (forest structure: age, height, canopy closure), and abiotic (elevation, aspect, slope) factors, to identify which combinations of these covariates drive plot-level foliar ESP traits for our focal species at the landscape extent. In addition, we compare trait spatial correlates across species to determine if there are commonalities. Our study demonstrates that remotely sensed products can be integrated with plot-level data to study trait-space relationships. In addition, we find that not all traits, across species, are driven by the same spatial covariates. Although many studies have demonstrated community level coordination of foliar traits (Callis-Duehl et al., 2017; Descombes et al., 2017;

Fyllas et al., 2020; Jiang et al., 2016), our findings suggest that trait spatial patterns are largely species specific.

Our study focuses on the identification of remotely sensed spatial correlates of plot level foliar ESP traits. By using model derived coefficient estimates for remotely sensed covariates we can develop predictive species-specific spatial distribution models of trait variability which can allow us to obtain spatially explicit estimates of landscape processes (e.g., see Figure 3.5, Pickett and Cadenasso, 1995; Shen et al., 2011; Turner, 1989). Since foliar ESP traits are often useful indicators of primary productivity, community structure, nutrient cycling, and trophic interactions, we can further investigate these linkages to reveal process and pattern relationships that contribute to the description of landscape functionality (Brauer et al., 2012; Hunter, 2016). For instance, the spatial co-location of foliar resource convergence and divergence likely influences where, how, and why herbivores make foraging trade-offs decision between multiple forage species (Balluffi-Fry et al., 2020; Haynes & Cronin, 2004; Hunter, 2016). By developing spatial distribution models for multiple species and their traits (see Figure 3.5 for an example) we can create maps that aid in identifying resource hot spots of ecosystem services (Bernhardt et al., 2017; Lavorel et al., 2011; McClain et al., 2003), provide additional spatial dimensions to explain herbivore foraging and pollinator space use patterns (Balluffi-Fry et al., 2020; Filipiak, 2018; Rizzuto et al., 2019), and inform sustainable landscape management related to changes in biogeochemical processes (Shepard et al. 2013; see also Appendix B.13 Figure B.13.1 for a spatial correlation matrix of observed versus predicted ESP surfaces).

3.5.1 Foliar percent elemental traits

For foliar percent elemental traits of C, N, and P, we find mixed support for general patterns, as our results support species-specific spatial covariate trait relationships. For instance, abiotic covariates occurred more often as a top model, reinforcing a Humboltian perspective of plant distributional patterns influenced by soil and climate (Pausas & Bond, 2019). Other top ranked models, however, with biotic components, suggest that land cover type, site productivity, and forest structure have an influence on the spatial variability of foliar percent elemental traits. Across species, the EVI covariate did not occur in top ranked models for foliar percent carbon, although land cover, biotic and abiotic correlates did. Foliar percent C, N and P are often a useful measure of site level productivity, and EVI is a measure of productivity from space, however, a difference in scale here is likely why EVI is not a spatial driver of these foliar traits, i.e., local scale feedbacks influence plant productivity. Our results suggest that land cover and biotic factors of forest structure likely have more of an influence on these foliar traits at the landscape extent (Rijkers et al., 2000). However, we did find that different combinations of EVI, biotic, and abiotic correlates influence foliar percent P at the trait level; suggesting that land cover type may not regulate phosphorus pathways. The weathering of rocks and soil particles that contribute to soil P availability (i.e., EVI as a proxy for productivity/soil fertility) and P acquisition and nutrient uplift likely depends on competitive interactions influenced by different community types (i.e., biotic factors), and soil and water movement that facilitate anion and cation exchanges from soils particles to roots (Smith et al., 2000).

At the species level, general correlates of foliar percent C, N, P concentrations are more evident. For example, our models of (1) abiotic and (2) land cover, biotic and abiotic were the top models for foliar percent carbon in red maple and balsam fir and for lowbush blueberry and black spruce, respectively. This suggests that species with differing leaf strategies (i.e., long lived versus seasonal foliar material) may have similar spatial predictors that influence their foliar carbon concentration. Moreover, red maple foliar percent N concentration showed specificity to deciduous land cover and open canopy conditions, which may suggest increased N use efficiency in areas where deciduous leaf litter feedbacks ameliorate microbial community associated with plant functional types (Hobbie, 2015). These patterns provide evidence that biotic interactions may have important consequences for intraspecific variability of plant traits at the landscape extent. Not all correlates within top models were, however, significant. Notably, elevation and slope were important for species foliar percent carbon, supported by models with abiotic correlates. Together elevation and slope often have an influence on soil nutrient retention due to drainage properties (Müller et al., 2017). In addition, age classes (a biotic correlate) was important for black spruce foliar percent carbon, thus as the dominant tree species in this area, optimal carbon sequestration potential may occur under black spruce canopy community types across various seral stages (Dunn et al., 2009). We failed to find evidence to support models for foliar percent N and P of white birch. White birch can behave similar to a clonal species when mycorrhizal relationships are present and these root extensions connect neighbouring individuals and other trees which can facilitate the sharing of elemental resources to enhance the nutrient use efficiencies of connected species (Bittebiere et al., 2019; Cornelissen and Cornwell, 2014; Simard et al., 1997). These root connections of nutrient sharing, coupled with high plasticity of intraspecific variability in foliar percent elemental traits likely explain why we failed to detect a spatial signal for white birch with our covariates (Pyakurel and Wang, 2014; Wam et al., 2018). Overall, on the landscape, different spatial correlates of foliar resource quality (i.e., C, N, and P), result in spatially heterogeneous species-specific resource hot spots. This may have far reaching implications for consumer dynamics and ecosystem processes (Haynes and Cronin, 2004; Wam et al., 2018).

3.5.2 Foliar quantity elemental traits

We only found support for spatial correlates of foliar quantity elemental traits for two out of our five study species, balsam fir and lowbush blueberry. Notably, for balsam fir the biotic and abiotic model explained foliar quantity C, N, and P traits. In comparison, for lowbush blueberry, the land cover and abiotic model explained foliar quantity C, N, and P traits. Collectively, these covariate combinations suggest that community type along with the structural properties of community conditions and abiotic factors influence the amount of foliar quantity C, N, and P resources. Across the landscape, these spatial covariates allow us to map the distribution of foliar quantity C, N, and P to detect areas of plant performance (i.e., optimal growth), resource abundance, and biogeochemical hot spots associated with nutrient uplift and storage (McClain et al., 2003; Tang et al., 2018). In addition, foliar quantity C is often related to leaf dry matter content, where increased dry matter correlates with decreased leaf palatability (Adler et al., 2014) and as such is a suggested driver of herbivore foraging trade-offs between quantity and quality (Champagne et al., 2018; Wam et al., 2018). The lack of evidence, however, to support foliar quantity elemental traits in our other study species constrains our ability to form generalizations of species spatial patterns and the correlates that drive them, and as such suggests that these traits are either driven by different covariates or inference may be limited to smaller spatial extents (Smithwick et al., 2003).

3.5.3 Foliar stoichiometric traits

Across five species at the trait level, we have limited evidence to support generalizations of spatial foliar stoichiometric relationships. More notable are the foliar stoichiometric patterns that emerge at the species level. For instance, foliar C:P and N:P between balsam fir and red maple share similar predictors. However, for red maple, elevation and slope were determined to be key correlates, in comparison, aspect was a significant correlate for balsam fir. This suggests that although these traits share similar predictors, the impact of these correlates differ, likely due to species and community level differences of nutrient co-limitation (Brauer et al., 2012). In contrast, lowbush blueberry and black spruce share a similar predictor for foliar N:P and similar responses to significant correlates of EVI, age class (i.e., biotic factor), elevation, and slope. Here, although lowbush blueberry and black spruce occupy different ecological niches, they appear to respond to similar constraints of nutrient co-limitation, and thus may be nutrient limited under similar conditions. Similar to foliar percent and quantity elemental traits, we did not find evidence of a spatial correlates for white birch foliar stoichiometric traits. Although communities are often spatially structured by nutrient co-limitation (Harpole et al., 2011), when present, species that can have mycorrhizal relationships, such as white birch, may transfer nutrients among connected individuals and this may diminish co-limitation effects and constrain our ability to detect spatial predictors of foliar C:N, C:P, and N:P in white birch (Alpert, 1991; Li et al., 2004; Zhang and He, 2009). Collectively, this information is vital to informing resource hot spots, and mechanisms of nutrient co-limitation that structure biological communities (Gimona & van der Horst, 2007; Harpole et al., 2011). For instance, foliar N:P range maps for balsam fir and red maple provide nutrient use efficiency contours from which we can make spatial comparisons of species interactions that scale to the community structure level and aid us in identifying multi-species foliar resource hot spots. Moreover, by describing the spatial patchiness of resources we can inform herbivore foraging decisions and begin to make novel spatially explicit predictions associated with movement and behavioural trade-offs (see Balluffi-Fry et al., 2020; Leroux et al., 2017; Rizzuto et al., 2019).

3.5.4 Foliar phytochemical traits

Across our two coniferous species, at the trait level we potentially have support to form generalizations of geographic commonalities of foliar phytochemical traits. For all traits, except foliar sesquiterpene and phytochemical diversity, the biotic and abiotic model was determined to be an important spatial driver. This may suggest that structural properties of habitats (i.e., stand age, tree heights, and canopy conditions) and topographic conditions interact to determine foliar phytochemical traits. This is to some extent expected, given that phytochemical traits are influenced by the spatial association of other species and their responses to the presence of herbivores (Champagne et al., 2018). On the island of Newfoundland, moose often forage on balsam fir and not black spruce (Gosse et al., 2011). Given the presented commonalities, consumption of balsam fir may elicit a non-consumptive phytochemical response in black spruce, thus further decreasing its potential palatability and aligning their foliar phytochemical composition (however, see Hussain et al., 2019).

At the species level, general patterns of foliar phytochemical trait correlates are less evident. Given the predominance of our phytochemical groups in both balsam fir and black spruce, we expected that similar spatial covariates should yield similar results between species. Our results, however, suggest foliar phytochemical traits exhibit species specificity to many different correlates. For instance, balsam fir and black spruce foliar terpene had differing predictors and differing significant correlates. Although some similarities between these two species exist, they are for traits on a different basis (i.e., raw vs biomass). For example, balsam fir foliar monoterpene on a biomass basis and black spruce foliar monoterpene on raw basis shared predictors; however, their response to specific correlates differed. For balsam fir, EVI as a remotely sensed proxy for productivity correlates to foliar terpene and monoterpene traits, suggesting optimal nutrient conditions may invoke a strong defence position (Lindroth et al., 2002). However, there are potential confounding effects. Increased phytochemical production, in species with constituent strategies (i.e., maintained baseline phytochemical production), may occur in response to the presence and or interaction of an herbivore (Kessler, 2015), which in turn can influence top-down nutrient dynamics (Hunter, 2016) in positive or negative ways depending on the soil condition and litter feedbacks (Hemming & Lindroth, 1999; Hobbie, 2015). As well, when we relativized phytochemical variables on a biomass basis, for balsam fir, support for foliar terpene, monoterpene, and monoterpenic ester traits was explained by the same combination of spatial covariates; abiotic and biotic. In contrast, we had no evidence to support spatial relationships of black spruce foliar phytochemical traits on a biomass basis. More notably, between the two species, abiotic covariates appear to influence foliar sesquiterpene. Here, the intraspecific variability of phytochemical groups and a measure of compound diversity are often used as a proxy to indicate plant-herbivore interactions, herbivore diversity, and trophic specialization (Richards et al., 2015). From our results, we find evidence to map phytochemical terpene groups and diversity, with some similarities in covariate specificity between two species with similar life histories and phylogenetic relatedness (i.e., both from the Pinaceae family). The spatial variability of foliar phytochemical composition provides us with a spatially explicit way to unravel the consequences and species interactions of herbivore foraging patterns with links to nutrient cycling processes (i.e., soil trampling, nutrient transfer, and changes in plant species composition Champagne et al., 2018; Gosse et al., 2011; Hunter, 2016).

3.5.5 Implications of ESP spatial trait distributions beyond the boreal

Foliar ESP traits represent a common currency of species (Elser & Hamilton, 2007). These traits are often used as indicators for differing ecological conditions with consequences that reach across levels of biological organization (Fajardo & Siefert, 2018). For instance, global patterns of N and P are associated with latitudinal gradients, with northern plants having higher concentrations of N and P related to plants at the equator (Reich & Oleksyn, 2004). By identifying the spatially explicit correlates of foliar N and P, we can map resource hot spots at landscape extents and compare how the distribution of these resources influence primary production (Smithwick et al., 2003), nutrient uplift (Jobbágy & Jackson, 2004), herbivore space use and forage selection (Duparc et al., 2020), and community assembly processes (Harpole et al., 2011; Jung et al., 2010) in different ecosystems. Moreover, we can begin to evaluate the spatial flows of elements across the landscape (for example see Shen et al., 2011). Indeed, many studies have identified environmental correlates of foliar ESP traits in different ecosystems (see Table 3.1 for a non-exhaustive list of studies). Although the focus of many of these studies was not to link trait variability to remotely sensed spatial correlates, these data may be re-purposed to do so. By re-purposing existing plot level foliar trait data and using remotely sensed correlates, ecologists can investigate the spatial patterns of traits for different species in a variety of ecosystems. In doing so, we can begin to understand different trait-based aspects related to the ecology of landscapes. This can help us understand how and where humans are altering biogeochemical processes, with implications for ecosystem restoration (Smith et al., 2020; Vitousek et al., 1997; Wiederholt et al., 2019). Furthermore, future studies may consider different sampling designs. In our study we sampled across four chronosequenced grids that were set up to relate forage trait variability to herbivore space use patterns. Although we used a grid-based approach to sample, and our design captures landscape scale and local scale variation on forest community structure, however future studies may consider sampling across all available habitats on the landscape including wetland habitats, ecotone areas, and riparian zones, to derive spatially continuous predictions.

3.6 Conclusion

By identifying remotely-sensed spatially explicit correlates for plot-level foliar ESP traits at the species level, we can develop distribution models of intraspecific trait variability across landscapes (for an example see Figure 3.5). These distribution models allow us to explore the consequences of trait spatial heterogeneity, and the processes that drive them, with implications for landscape functionality (Harvey et al., 2019). For example, we can test hypotheses about herbivore resource selection across scales (Balluffi-Fry et al., 2020), infer landscape functionality via pattern and process relationships (Turner, 1989), or explore how the spatial distribution of matter and energy feedbacks on landscape structure with implications for the management of biogeochemical processes (Lovell & Johnston, 2009; Shen et al., 2011). In addition, our work described here may be of use to carbon modelling approaches which largely focus on sequestration and storage, or Net Ecosystem Production (NEP), and overlook carbon dynamics at the interface of ecological interactions (Schmitz et al., 2018). Knowing how much carbon is sequestered, lost through respiration, or through pathways of non-photosynthetic carbon, foliar carbon reabsorption, and foliar carbon loss through consumptive activities allows for the refinement of carbon cycling models (Dirnböck et al., 2020). Given the importance of the circumboreal ecosystems in carbon cycles, our work here can help understand how carbon dynamics may manifest in other parts of the boreal. Here, we investigated the correlates of foliar ESP traits for commonly occurring, yet geographically widespread boreal species using accessible spatial covariates. We found some geographic commonalities in spatial covariates at the trait and species level from which we can make generalities about physiological links to ecosystem processes and landscape function (see Hobbie, 2015; Li et al., 2004; McClain et al., 2003; Poorter and Bongers, 2006). In addition, we also identify the directionality and significance of certain spatial correlates which may aid researchers that are asking similar questions elsewhere. Our results suggest there are specificities in spatial predictors at the species level, and that different plants respond differently to environmental conditions. How different species of plants respond in different parts of the world merits further work like this that combines trait-based ecology using plant stoichiometry with spatial modelling to describe the ecology of the landscape.

3.7 Data Availability

All data and R code used in the analyses are available via a Figshare repository at: https://doi.org/10.6084/m9.figshare.11911455.v1.

3.8 References

Adler, P. B., Salguero-Gómez, R., Compagnoni, A., Hsu, J. S., Ray-Mukherjee, J., Mbeau-Ache, C., & Franco, M. (2014). Functional traits explain variation in plant life history strategies. *Proceedings of the National Academy of Sciences of the United States of America*, *111*(2), 740–745. https://doi.org/10.1073/pnas.1315179111

Ågren, G. I. (1988). Ideal nutrient productivities and nutrient proportions in plant growth. *Plant, Cell & Environment*, *11*(7), 613–620.

Alpert, P. (1991). Nitrogen sharing among ramets increases clonal growth in fragaria chiloensis. *Ecology*, *72*(1), 69–80. https://doi.org/10.2307/1938903

Ashton, I. W., Miller, A. E., Bowman, W. D., & Suding, K. N. (2010). Niche complementarity due to plasticity in resource use: Plant partitioning of chemical N forms. *Ecology*, *91*(11), 3252–3260. https://doi.org/10.1890/09-1849.1

Asner, G. P., Anderson, C. B., Martin, R. E., Tupayachi, R., Knapp, D. E., & Sinca, F. (2015). Landscape biogeochemistry reflected in shifting distributions of chemical traits in the Amazon forest canopy. *Nature Geoscience*, *8*(7), 567–573. https://doi.org/10.1038/ngeo2443

Balluffi-Fry, J., Leroux, S. J., Wiersma, Y. F., Heckford, T. R., Rizzuto, M., Richmond, I. C., & Vander Wal, E. (2020). Quantity–quality trade-offs revealed using a multiscale test of herbivore resource selection on elemental landscapes. *Ecology and Evolution*, *10*(24), 13847–13859. https://doi.org/10.1002/ece3.6975

Balzotti, C. S., Asner, G. P., Taylor, P. G., Cleveland, C. C., Cole, R., Martin, R. E., Nasto, M., Osborne, B. B., Porder, S., & Townsend, A. R. (2016). Environmental controls on canopy foliar nitrogen distributions in a Neotropical lowland forest. *Ecological Applications*, *26*(8), 2451–2464. https://doi.org/10.1002/eap.1408

Barron-Gafford, G. A., Scott, R. L., Jenerette, G. D., Hamerlynck, E. P., & Huxman, T. E. (2012). Temperature and precipitation controls over leaf- and ecosystem-level CO2 flux along a woody plant encroachment gradient. *Global Change Biology*, *18*(4), 1389–1400. https://doi.org/10.1111/j.1365-2486.2011.02599.x

Becknell, J., M., & Powers, J., S. (2014). Stand age and soils as drivers of plant functional traits and aboveground biomass in secondary tropical dry forest. *Canadian Journal of Forest Research*. https://doi.org/10.1139/cjfr-2013-0331

Bernhardt, E. S., Blaszczak, J. R., Ficken, C. D., Fork, M. L., Kaiser, K. E., & Seybold, E. C. (2017). Control points in ecosystems: Moving beyond the hot spot hot moment concept. *Ecosystems*, *20*(4), 665–682. https://doi.org/10.1007/s10021-016-0103-y

Bittebiere, A.-K., Saiz, H., & Mony, C. (2019). New insights from multidimensional trait space responses to competition in two clonal plant species. *Functional Ecology*, *297–307*. https://doi.org/10.1111/1365-2435.13220

Blanes, M. C., Viñegla, B., Merino, J., & Carreira, J. A. (2013). Nutritional status of *Abies pinsapo* forests along a nitrogen deposition gradient: Do C/N/P stoichiometric shifts modify photosynthetic nutrient use efficiency? *Oecologia*, *171*(4), 797–808. https://doi.org/10.1007/s00442-012-2454-1

Booker, F. L., & Maier, C. A. (2001). Atmospheric carbon dioxide, irrigation, and fertilization effects on phenolic and nitrogen concentrations in loblolly pine (*Pinus taeda*) needles. *Tree Physiology*, *21*(9), 609–616. https://doi.org/10.1093/treephys/21.9.609

Brauer, V. S., Stomp, M., & Huisman, J. (2012). The nutrient-load hypothesis: Patterns of resource limitation and community structure driven by competition for nutrients and light. *The American Naturalist*, *179*(6), 721–740. https://doi.org/10.1086/665650

Bryant, J. P., Chapin, F. S., & Klein, D. R. (1983). Carbon/nutrient balance of boreal plants in relation to vertebrate herbivory. *Oikos*, *40*(3), 357. https://doi.org/10.2307/3544308

Burnham, K. P., & Anderson, D. R. (2002). *Model selection and multimodel inference: A practical information-theoretic approach*. Springer-Verlag.

Cachet, T., Brevard, H., Chaintreau, A., Demyttenaere, J., French, L., Gassenmeier, K., Joulain, D., Koenig, T., Leijs, H., Liddle, P., Loesing, G., Marchant, M., Merle, Ph., Saito, K., Schippa, C., Sekiya, F., & Smith, T. (2016). IOFI recommended practice for the use of predicted relative-response factors for the rapid quantification of volatile flavouring compounds by GC-FID. *Flavour and Fragrance Journal*, *31*(3), 191–194. https://doi.org/10.1002/ffj.3311

Callis-Duehl, K., Vittoz, P., Defossez, E., & Rasmann, S. (2017). Community-level relaxation of plant defenses against herbivores at high elevation. *Plant Ecology*, *218*(3), 291–304. https://doi.org/10.1007/s11258-016-0688-4

Canadian Digital Elevation Model: Product Specifications-Edition 1.1. (2016). [Map]. Natural Resources Canada.

Champagne, E., Moore, B. D., Côté, S. D., & Tremblay, J.-P. (2018). Spatial correlations between browsing on balsam fir by white-tailed deer and the nutritional value of neighboring winter forage. *Ecology and Evolution*, *8*(5), 2812–2823. https://doi.org/10.1002/ece3.3878

Chapin, F. S. (2003). Effects of plant traits on ecosystem and regional processes: A conceptual framework for predicting the consequences of global change. *Annals of Botany*, *91*(4), 455–463. https://doi.org/10.1093/aob/mcg041

Commission for Environmental Cooperation. (2017). *Land cover map of North American at 30 m resolution* (1st ed.) [Map]. Canada Centre for Remote Sensing.

Cornelissen, J. H. C., & Cornwell, W. K. (2014). The Tree of Life in ecosystems: Evolution of plant effects on carbon and nutrient cycling. *Journal of Ecology*, *102*(2), 269–274. https://doi.org/10.1111/1365-2745.12217

Couture, J. J., Holeski, L. M., & Lindroth, R. L. (2014). Long-term exposure to elevated CO2 and O3 alters aspen foliar chemistry across developmental stages. *Plant, Cell & Environment*, *37*(3), 758–765. https://doi.org/10.1111/pce.12195

Descombes, P., Marchon, J., Pradervand, J.-N., Bilat, J., Guisan, A., Rasmann, S., & Pellissier, L. (2017). Community-level plant palatability increases with elevation as insect herbivore abundance declines. *Journal of Ecology*, *105*(1), 142–151. https://doi.org/10.1111/1365-2745.12664

Diaz, S., Hodgson, J. G., Thompson, K., Cabido, M., Cornelissen, J. H. C., Jalili, A., Montserrat-Martí, G., Grime, J. P., Zarrinkamar, F., Asri, Y., Band, S. R., Basconcelo, S., Castro-Díez, P., Funes, G., Hamzehee, B., Khoshnevi, M., Pérez-Harguindeguy, N., Pérez-Rontomé, M. C., Shirvany, F. A., … Zak, M. R. (2004). The plant traits that drive ecosystems: Evidence from three continents. *Journal of Vegetation Science*, *15*(3), 295–304. https://doi.org/10.1111/j.1654-1103.2004.tb02266.x

Dirnböck, T., Kraus, D., Grote, R., Klatt, S., Kobler, J., Schindlbacher, A., Seidl, R., Thom, D., & Kiese, R. (2020). Substantial understory contribution to the C sink of a European temperate mountain forest landscape. *Landscape Ecology*, *35*(2), 483–499. https://doi.org/10.1007/s10980-019-00960-2

Dunn, A. L., Wofsy, S. C., & Bright, A. V. H. (2009). Landscape heterogeneity, soil climate, and carbon exchange in a boreal black spruce forest. *Ecological Applications*, *19*(2), 495–504. https://doi.org/10.1890/07-0771.1

Duparc, A., Garel, M., Marchand, P., Dubray, D., Maillard, D., & Loison, A. (2020). Through the taste buds of a large herbivore: Foodscape modeling contributes to an understanding of forage selection processes. *Oikos*, *129*(2), 170–183. https://doi.org/10.1111/oik.06386

Elser, J. J., Fagan, W. F., Kerkhoff, A. J., Swenson, N. G., & Enquist, B. J. (2010). Biological stoichiometry of plant production: Metabolism, scaling and ecological response to global change: Tansley review. *New Phytologist*, *186*(3), 593–608. https://doi.org/10.1111/j.1469-8137.2010.03214.x

Elser, J. J., & Hamilton, A. (2007). Stoichiometry and the new biology: The future is now. *PLoS Biology*, *5*(7), e181. https://doi.org/10.1371/journal.pbio.0050181

ESRI (10.8). (2020). [Computer software]. https://www.esri.com/en-us/arcgis/products/arcgis-pro/

Fajardo, A., & Siefert, A. (2018). Intraspecific trait variation and the leaf economics spectrum across resource gradients and levels of organization. *Ecology*, *99*(5), 1024–1030. https://doi.org/10.1002/ecy.2194

Fan, H., Wu, J., Liu, W., Yuan, Y., Hu, L., & Cai, Q. (2015). Linkages of plant and soil C:N:P stoichiometry and their relationships to forest growth in subtropical plantations. *Plant and Soil*, *392*(1), 127–138. https://doi.org/10.1007/s11104-015-2444-2

Field, C. (1983). Allocating leaf nitrogen for the maximization of carbon gain: Leaf age as a control on the allocation program. *Oecologia*, *56*(2), 341–347. https://doi.org/10.1007/BF00379710

Filipiak, M. (2018). A better understanding of bee nutritional ecology is needed to optimize conservation strategies for wild bees—The application of ecological stoichiometry. *Insects*, *9*(3). https://doi.org/10.3390/insects9030085

Forkner, R. E., & Marquis, R. J. (2004). Uneven-aged and even-aged logging alter foliar phenolics of oak trees remaining in forested habitat matrix. *Forest Ecology and Management*, *199*(1), 21–37. https://doi.org/10.1016/j.foreco.2004.03.044

Fyllas, N. M., Michelaki, C., Galanidis, A., Evangelou, E., Zaragoza-Castells, J., Dimitrakopoulos, P. G., Tsadilas, C., Arianoutsou, M., & Lloyd, J. (2020). Functional trait variation among and within species and plant functional types in mountainous mediterranean forests. *Frontiers in Plant Science*, *11*. https://doi.org/10.3389/fpls.2020.00212

Gartner, T. B., & Cardon, Z. G. (2004). Decomposition dynamics in mixed-species leaf litter. *Oikos*, *104*(2), 230–246. JSTOR.

Gimona, A., & van der Horst, D. (2007). Mapping hotspots of multiple landscape functions: A case study on farmland afforestation in Scotland. *Landscape Ecology*, *22*(8), 1255–1264. https://doi.org/10.1007/s10980-007-9105-7

Glassmire, A. E., Jeffrey, C. S., Forister, M. L., Parchman, T. L., Nice, C. C., Jahner, J. P., Wilson, J. S., Walla, T. R., Richards, L. A., Smilanich, A. M., Leonard, M. D., Morrison, C. R., Simbaña, W., Salagaje, L. A., Dodson, C. D., Miller, J. S., Tepe, E. J., Villamarin-Cortez, S., & Dyer, L. A. (2016). Intraspecific phytochemical variation shapes community and population structure for specialist caterpillars. *New Phytologist*, *212*(1), 208–219. https://doi.org/10.1111/nph.14038

Gosse, J., Hermanutz, L., McLaren, B., Deering, P., & Knight, T. (2011). Degradation of boreal forests by nonnative herbivores in Newfoundland’s National Parks: Recommendations for ecosystem restoration. *Natural Areas Journal*, *31*(4), 331–339. https://doi.org/10.3375/043.031.0403

Grime, P. J., & Pierce, S. (2012). *The evolutionary strategies that shape ecosystems*. Wiley-Blackwell.

Hallett, R. A., & Hornbeck, J. W. (1997). Foliar and soil nutrient relationships in red oak and white pine forests. *Canadian Journal of Forest Research*, *27*, 12.

Harpole, W. S., Ngai, J. T., Cleland, E. E., Seabloom, E. W., Borer, E. T., Bracken, M. E. S., Elser, J. J., Gruner, D. S., Hillebrand, H., Shurin, J. B., & Smith, J. E. (2011). Nutrient co-limitation of primary producer communities. *Ecology Letters*, *14*(9), 852–862. https://doi.org/10.1111/j.1461-0248.2011.01651.x

Harvey, E., Gounand, I., Fronhofer, E. A., & Altermatt, F. (2019). Metaecosystem dynamics drive community composition in experimental, multi-layered spatial networks. *Oikos*. https://doi.org/10.1111/oik.07037

Harvey, E., Gounand, I., Ward, C. L., & Altermatt, F. (2017). Bridging ecology and conservation: From ecological networks to ecosystem function. *Journal of Applied Ecology*, *54*(2), 371–379. https://doi.org/10.1111/1365-2664.12769

Hassell, M. P., Comins, H. N., & May, R. M. (1994). Species coexistence and self-organizing spatial dynamics. *Nature*, *370*, 290–292.

Haynes, K. J., & Cronin, J. T. (2004). Confounding of patch quality and matrix effects in herbivore movement studies. *Landscape Ecology*, *19*(2), 119–124. https://doi.org/10.1023/B:LAND.0000021721.41349.85

He, P., Fontana, S., Sardans, J., Peñuelas, J., Gessler, A., Schaub, M., Rigling, A., Li, H., Jiang, Y., & Li, M.-H. (2019). The biogeochemical niche shifts of *Pinus sylvestris var. Mongolica* along an environmental gradient. *Environmental and Experimental Botany*, *167*, 103825. https://doi.org/10.1016/j.envexpbot.2019.103825

Hemming, J. D. C., & Lindroth, R. L. (1999). Effects of light and nutrient availability on aspen: Growth, phytochemistry, and insect performance. *Journal of Chemical Ecology*, *25*(7), 1687–1714. https://doi.org/10.1023/A:1020805420160

Hessen, D. O., Ågren, G. I., Anderson, T. R., Elser, J. J., & de Ruiter, P. C. (2004). Carbon sesquestration in ecosystems: The role of stoichiometry. *Ecology*, *85*(5), 1179–1192. https://doi.org/10.1890/02-0251

Hobbie, S. E. (2015). Plant species effects on nutrient cycling: Revisiting litter feedbacks. *Trends in Ecology & Evolution*, *30*(6), 357–363. https://doi.org/10.1016/j.tree.2015.03.015

Hollinger, D. Y. (1996). Optimality and nitrogen allocation in a tree canopy. *Tree Physiology*, *16*(7), 627–634. https://doi.org/10.1093/treephys/16.7.627

Hunter, M. D. (2016). *The phytochemical landscape: Linking trophic interactions and nutrient dynamics*. Princeton University Press.

Hunter, M. D., & Schultz, J. C. (1995). Fertilization mitigates chemical induction and herbivore responses within damaged oak trees. *Ecology*, *76*(4), 1226–1232. https://doi.org/10.2307/1940929

Hussain, A., Rodriguez-Ramos, J. C., & Erbilgin, N. (2019). Spatial characteristics of volatile communication in lodgepole pine trees: Evidence of kin recognition and intra-species support. *Science of The Total Environment*, *692*, 127–135. https://doi.org/10.1016/j.scitotenv.2019.07.211

Jiang, Y., Rocha, A. V., Rastetter, E. B., Shaver, G. R., Mishra, U., Zhuang, Q., & Kwiatkowski, B. L. (2016). C–N–P interactions control climate driven changes in regional patterns of C storage on the North Slope of Alaska. *Landscape Ecology*, *31*(1), 195–213. https://doi.org/10.1007/s10980-015-0266-5

Jiang, Y., Zang, R., Lu, X., Huang, Y., Ding, Y., Liu, W., Long, W., Zhang, J., & Zhang, Z. (2015). Effects of soil and microclimatic conditions on the community-level plant functional traits across different tropical forest types. *Plant and Soil*, *390*(1), 351–367. https://doi.org/10.1007/s11104-015-2411-y

Jobbágy, E. G., & Jackson, R. B. (2004). The uplift of soil nutrients by plants: Biogeochemical consequences across scales. *Ecology*, *85*(9), 2380–2389. https://doi.org/10.1890/03-0245

Jung, V., Violle, C., Mondy, C., Hoffmann, L., & Muller, S. (2010). Intraspecific variability and trait-based community assembly. *Journal of Ecology*, *98*(5), 1134–1140. https://doi.org/10.1111/j.1365-2745.2010.01687.x

Kerkhoff, A. J., Enquist, B. J., Elser, J. J., & Fagan, W. F. (2005). Plant allometry, stoichiometry and the temperature-dependence of primary productivity. *Global Ecology and Biogeography*, *14*(6), 585–598. https://doi.org/10.1111/j.1466-822X.2005.00187.x

Kessler, A. (2015). The information landscape of plant constitutive and induced secondary metabolite production. *Current Opinion in Insect Science*, *8*, 47–53. https://doi.org/10.1016/j.cois.2015.02.002

Kichenin, E., Wardle, D. A., Peltzer, D. A., Morse, C. W., & Freschet, G. T. (2013). Contrasting effects of plant inter- and intraspecific variation on community-level trait measures along an environmental gradient. *Functional Ecology*, *27*(5), 1254–1261. https://doi.org/10.1111/1365-2435.12116

Knops, J. M. H., Bradley, K. L., & Wedin, D. A. (2002). Mechanisms of plant species impacts on ecosystem nitrogen cycling. *Ecology Letters*, *5*(3), 454–466. https://doi.org/10.1046/j.1461-0248.2002.00332.x

Kranabetter, J. M., McLauchlan, K. K., Enders, S. K., Fraterrigo, J. M., Higuera, P. E., Morris, J. L., Rastetter, E. B., Barnes, R., Buma, B., Gavin, D. G., Gerhart, L. M., Gillson, L., Hietz, P., Mack, M. C., McNeil, B., & Perakis, S. (2016). A framework to assess biogeochemical response to ecosystem disturbance using nutrient partitioning ratios. *Ecosystems*, *19*(3), 387–395. https://doi.org/10.1007/s10021-015-9934-1

Krishna, M. P., & Mohan, M. (2017). Litter decomposition in forest ecosystems: A review. *Energy, Ecology and Environment*, *2*(4), 236–249. https://doi.org/10.1007/s40974-017-0064-9

Lavorel, S., Grigulis, K., Lamarque, P., Colace, M.-P., Garden, D., Girel, J., Pellet, G., & Douzet, R. (2011). Using plant functional traits to understand the landscape distribution of multiple ecosystem services. *Journal of Ecology*, *99*(1), 135–147. https://doi.org/10.1111/j.1365-2745.2010.01753.x

Leroux, S. J. (2018). Ecological, evolutionary, and geographical correlates of variation in consumer elemental composition. *Functional Ecology*, *32*(10), 2282–2284. https://doi.org/10.1111/1365-2435.13212

Leroux, S. J. (2019). On the prevalence of uninformative parameters in statistical models applying model selection in applied ecology. *PLoS ONE*, *14*(2), 12. https://doi.org/10.1371/journal.pone.0206711

Leroux, S. J., Wal, E. V., Wiersma, Y. F., Charron, L., Ebel, J. D., Ellis, N. M., Hart, C., Kissler, E., Saunders, P. W., Moudrá, L., Tanner, A. L., & Yalcin, S. (2017). Stoichiometric distribution models: Ecological stoichiometry at the landscape extent. *Ecology Letters*, *20*(12), 1495–1506. https://doi.org/10.1111/ele.12859

Li, B., Shibuya, T., Yogo, Y., & Hara, T. (2004). Effects of ramet clipping and nutrient availability on growth and biomass allocation of yellow nutsedge. *Ecological Research*, *19*(6), 603–612. https://doi.org/10.1111/j.1440-1703.2004.00685.x

Li, Y., Reich, P. B., Schmid, B., Shrestha, N., Feng, X., Lyu, T., Maitner, B. S., Xu, X., Li, Y., Zou, D., Tan, Z.-H., Su, X., Tang, Z., Guo, Q., Feng, X., Enquist, B. J., & Wang, Z. (2020). Leaf size of woody dicots predicts ecosystem primary productivity. *Ecology Letters*, *23*(6), 1003–1013. https://doi.org/10.1111/ele.13503

Lindroth, R. L., Osier, T. L., Barnhill, H. R. H., & Wood, S. A. (2002). Effects of genotype and nutrient availability on phytochemistry of trembling aspen (*Populus tremuloides Michx.*) during leaf senescence. *Biochemical Systematics and Ecology*, *30*(4), 297–307. https://doi.org/10.1016/S0305-1978(01)00088-6

Liu, S., Yan, Z., Chen, Y., Zhang, M., Chen, J., & Han, W. (2019). Foliar pH, an emerging plant functional trait: Biogeography and variability across northern China. *Global Ecology and Biogeography*, *28*(3), 386–397. https://doi.org/10.1111/geb.12860

Lohbeck, M., Poorter, L., Lebrija-Trejos, E., Martínez-Ramos, M., Meave, J. A., Paz, H., Pérez-García, E. A., Romero-Pérez, I. E., Tauro, A., & Bongers, F. (2013). Successional changes in functional composition contrast for dry and wet tropical forest. *Ecology*, *94*(6), 1211–1216. https://doi.org/10.1890/12-1850.1

Lovell, S. T., & Johnston, D. M. (2009). Designing landscapes for performance based on emerging principles in landscape ecology. *Ecology and Society*, *14*(1). https://www.jstor.org/stable/26268059

Macek, M., Kopecký, M., & Wild, J. (2019). Maximum air temperature controlled by landscape topography affects plant species composition in temperate forests. *Landscape Ecology*, *34*(11), 2541–2556. https://doi.org/10.1007/s10980-019-00903-x

McClain, M. E., Boyer, E. W., Dent, C. L., Gergel, S. E., Grimm, N. B., Groffman, P. M., Hart, S. C., Harvey, J. W., Johnston, C. A., Mayorga, E., McDowell, W. H., & Pinay, G. (2003). Biogeochemical hot spots and hot moments at the interface of terrestrial and aquatic ecosystems. *Ecosystems*, *6*(4), 301–312. https://doi.org/10.1007/s10021-003-0161-9

Mendez, M., & Karlsson, S. P. (2005). Nutrient stoichiometry in pinguicula vulgaris: Nutrient availability, plant size, and reproductive status. *Ecology, 86*(4), 982–991.

Merems, J. L., Shipley, L. A., Levi, T., Ruprecht, J., Clark, D. A., Wisdom, M. J., Jackson, N. J., Stewart, K. M., & Long, R. A. (2020). Nutritional-landscape models link habitat use to condition of mule deer (*odocoileus hemionus*). *Frontiers in Ecology and Evolution*, *8*. https://doi.org/10.3389/fevo.2020.00098

Morquecho-Contreras, A., Zepeda-Gómez, C., & Sánchez-Sánchez, H. (2018). Plant antiherbivore defense in diverse environments. In L. Hufnagel (Ed.), *Pure and Applied Biogeography*. InTech. https://doi.org/10.5772/intechopen.70418

Müller, M., Oelmann, Y., Schickhoff, U., Böhner, J., & Scholten, T. (2017). Himalayan treeline soil and foliar C:N:P stoichiometry indicate nutrient shortage with elevation. *Geoderma, 291*, 21–32. https://doi.org/10.1016/j.geoderma.2016.12.015

Niinemets, Ü., & Kull, O. (1998). Stoichiometry of foliar carbon constituents varies along light gradients in temperate woody canopies: Implications for foliage morphological plasticity. *Tree Physiology*, *18*(7), 467–479. https://doi.org/10.1093/treephys/18.7.467

Pan, Y., Horn, J., Jenkins, J., & Birdsey, R. (2004). Importance of foliar nitrogen concentration to predict forest productivity in the mid-Atlantic region. *Forest Science*, *50*(3), 11.

Pausas, J. G., & Bond, W. J. (2019). Humboldt and the reinvention of nature. *Journal of Ecology*, *107*(3), 1031–1037. https://doi.org/10.1111/1365-2745.13109

Pellissier, L., Moreira, X., Danner, H., Serrano, M., Salamin, N., van Dam, N. M., & Rasmann, S. (2016). The simultaneous inducibility of phytochemicals related to plant direct and indirect defences against herbivores is stronger at low elevation. *Journal of Ecology, 104*(4), 1116–1125. https://doi.org/10.1111/1365-2745.12580

Peñuelas, J., Fernández-Martínez, M., Ciais, P., Jou, D., Piao, S., Obersteiner, M., Vicca, S., Janssens, I. A., & Sardans, J. (2019). The bioelements, the elementome, and the biogeochemical niche. *Ecology*, *100(5),* e02652. https://doi.org/10.1002/ecy.2652

Perry, G. L. W., Enright, N. J., Miller, B. P., & Lamont, B. B. (2013). Do plant functional traits determine spatial pattern? A test on species-rich shrublands, Western Australia. *Journal of Vegetation Science*, *24*(3), 441–452. https://doi.org/10.1111/j.1654-1103.2012.01476.x

Philben, M., Ziegler, S. E., Edwards, K. A., Kahler, R., & Benner, R. (2016). Soil organic nitrogen cycling increases with temperature and precipitation along a boreal forest latitudinal transect. *Biogeochemistry*, *127*(2–3), 397–410. https://doi.org/10.1007/s10533-016-0187-7

Pickett, S. T. A., & Cadenasso, M. L. (1995). Landscape ecology: Spatial heterogeneity in ecological systems. *Science*, *269*(5222), 331–334. https://doi.org/10.1126/science.269.5222.331

Poitevin, E. (2016). Official methods for the determination of minerals and trace elements in infant formula and milk products: A review. *Journal of AOAC International*, *99*(1), 42–52. https://doi.org/10.5740/jaoacint.15-0246

Ponette-González, A. G., Weathers, K. C., & Curran, L. M. (2010). Tropical land-cover change alters biogeochemical inputs to ecosystems in a Mexican montane landscape. *Ecological Applications*, *20*(7), 1820–1837. https://doi.org/10.1890/09-1125.1

Poorter, L., & Bongers, F. (2006). Leaf traits are good predictors of plant performance across 53 rain forest species. *Ecology*, *87*(7), 1733–1743. https://doi.org/10.1890/0012-9658(2006)87[1733:LTAGPO]2.0.CO;2

Pyakurel, A., & Wang, J. R. (2014). Leaf morphological and stomatal variations in paper birch populations along environmental gradients in Canada. *American Journal of Plant Sciences*, *05*(11), 1508–1520. https://doi.org/10.4236/ajps.2014.511166

R Core Team. (2020). *R: a language and environment for statistical computing*. R Foundation for Statistical Computing. https://www.R-project.org/

Radwan, M. A., & Harrington, C. A. (2011). Foliar chemical concentrations, growth, and site productivity relations in western red cedar. *Canadian Journal of Forest Research*. https://doi.org/10.1139/x86-185

Reich, P. B., & Oleksyn, J. (2004). Global patterns of plant leaf N and P in relation to temperature and latitude. *Proceedings of the National Academy of Sciences*, *101*(30), 11001–11006. https://doi.org/10.1073/pnas.0403588101

Richards, L. A., Dyer, L. A., Forister, M. L., Smilanich, A. M., Dodson, C. D., Leonard, M. D., & Jeffrey, C. S. (2015). Phytochemical diversity drives plant–insect community diversity. *Proceedings of the National Academy of Sciences*, *112*(35), 10973–10978. https://doi.org/10.1073/pnas.1504977112

Richardson, A. D. (2004). Foliar chemistry of balsam fir and red spruce in relation to elevation and the canopy light gradient in the mountains of the northeastern United States. *Plant and Soil*, *260*(1), 291–299. https://doi.org/10.1023/B:PLSO.0000030179.02819.85

Rijkers, T., Pons, T. L., & Bongers, F. (2000). The effect of tree height and light availability on photosynthetic leaf traits of four neotropical species differing in shade tolerance. *Functional Ecology*, *14*(1), 77–86. https://doi.org/10.1046/j.1365-2435.2000.00395.x

Rizzuto, M., Leroux, S. J., Wal, E. V., Wiersma, Y. F., Heckford, T. R., & Balluffi-Fry, J. (2019). Patterns and potential drivers of intraspecific variability in the body C, N, and P composition of a terrestrial consumer, the snowshoe hare (*Lepus americanus*). *Ecology and Evolution*, *9*(24), 14453–14464. https://doi.org/10.1002/ece3.5880

Santiago, L. S., Kitajima, K., Wright, S. J., & Mulkey, S. S. (2004). Coordinated changes in photosynthesis, water relations and leaf nutritional traits of canopy trees along a precipitation gradient in lowland tropical forest. *Oecologia*, *139*(4), 495–502. https://doi.org/10.1007/s00442-004-1542-2

Sardans, J., Alonso, R., Carnicer, J., Fernández-Martínez, M., Vivanco, M. G., & Peñuelas, J. (2016). Factors influencing the foliar elemental composition and stoichiometry in forest trees in Spain. *Perspectives in Plant Ecology, Evolution and Systematics*, *18*, 52–69. https://doi.org/10.1016/j.ppees.2016.01.001

Sardans, J., Alonso, R., Janssens, I. A., Carnicer, J., Vereseglou, S., Rillig, M. C., Fernández-Martínez, M., Sanders, T. G. M., & Peñuelas, J. (2016). Foliar and soil concentrations and stoichiometry of nitrogen and phosphorous across European *Pinus sylvestris* forests: Relationships with climate, N deposition and tree growth. *Functional Ecology*, *30*(5), 676–689. https://doi.org/10.1111/1365-2435.12541

Schmitz, O. J., Wilmers, C. C., Leroux, S. J., Doughty, C. E., Atwood, T. B., Galetti, M., Davies, A. B., & Goetz, S. J. (2018). Animals and the zoogeochemistry of the carbon cycle. *Science*, *362*(6419), eaar3213. https://doi.org/10.1126/science.aar3213

Sedio, B. E., Echeverri, J. C. R., P, C. A. B., & Wright, S. J. (2017). Sources of variation in foliar secondary chemistry in a tropical forest tree community. *Ecology*, *98*(3), 616–623. https://doi.org/10.1002/ecy.1689

Shen, W., Lin, Y., Jenerette, G. D., & Wu, J. (2011). Blowing litter across a landscape: Effects on ecosystem nutrient flux and implications for landscape management. *Landscape Ecology*, *26*(5), 629–644. https://doi.org/10.1007/s10980-011-9599-x

Shepard, E. L. C., Wilson, R. P., Rees, W. G., Grundy, E., Lambertucci, S. A., & Vosper, S. B. (2013). Energy landscapes shape animal movement ecology. *The American Naturalist*, *182*(3), 298–312. https://doi.org/10.1086/671257

Shure, D. J., & Wilson, L. A. (1993). Patch-size effects on plant phenolics in successional openings of the southern Appalachians. *Ecology*, *74*(1), 55–67. https://doi.org/10.2307/1939501

Simard, S. W., Jones, M. D., Durall, D. M., Perry, D. A., Myrold, D. D., & Molina, R. (1997). Reciprocal transfer of carbon isotopes between ectomycorrhizal *Betula papyrifera* and *Pseudotsuga menziesii*. *The New Phytologist*, *137*(3), 529–542.

Smith, C. K., Coyea, M. R., & Munson, A. D. (2000). Soil carbon, nitrogen, and phosphorus stocks and dynamics under disturbed black spruce forests. *Ecological Applications*, *10*(3), 775–788. https://doi.org/10.1890/1051-0761(2000)010[0775:SCNAPS]2.0.CO;2

Smith, N. J., McDonald, G. W., & Patterson, M. G. (2020). Biogeochemical cycling in the anthropocene: Quantifying global environment-economy exchanges. *Ecological Modelling*, *418*, 108816. https://doi.org/10.1016/j.ecolmodel.2019.108816

Smithwick, E. A. H., Harmon, M. E., & Domingo, J. B. (2003). Modeling multiscale effects of light limitations and edge-induced mortality on carbon stores in forest landscapes. *Landscape Ecology*, *18*(7), 701–721. https://doi.org/10.1023/B:LAND.0000004254.94982.67

South, R. G. (1983). *Biogeography and ecology of the island of Newfoundland* (Vol. 48). Dr. W. Junk Publishers, The Hague, The Netherlands.

Strahan, R. T., Meador, A. J. S., Huffman, D. W., & Laughlin, D. C. (2016). Shifts in community-level traits and functional diversity in a mixed conifer forest: A legacy of land-use change. *Journal of Applied Ecology*, *53*(6), 1755–1765. https://doi.org/10.1111/1365-2664.12737

Tang, Z., Xu, W., Zhou, G., Bai, Y., Li, J., Tang, X., Chen, D., Liu, Q., Ma, W., Xiong, G., He, H., He, N., Guo, Y., Guo, Q., Zhu, J., Han, W., Hu, H., Fang, J., & Xie, Z. (2018). Patterns of plant carbon, nitrogen, and phosphorus concentration in relation to productivity in China’s terrestrial ecosystems. *Proceedings of the National Academy of Sciences*, *115*(16), 4033–4038. https://doi.org/10.1073/pnas.1700295114

Turner, M. G. (1989). Landscape ecology: The effect of pattern on process. *Landscape Ecology, 20*, 171–197.

Turner, M. G. (2005). Landscape ecology: What is the state of the science? *Annual Review of Ecology, Evolution, and Systematics, 36*(1), 319–344. https://doi.org/10.1146/annurev.ecolsys.36.102003.152614

Urbina, I., Sardans, J., Grau, O., Beierkuhnlein, C., Jentsch, A., Kreyling, J., & Peñuelas, J. (2017). Plant community composition affects the species biogeochemical niche. *Ecosphere*, *8*(5), e01801. https://doi.org/10.1002/ecs2.1801

Vellend, M. (2016). *The theory of ecological communities (MPB-57)*. Princeton University Press.

Vermote, E., Justice, C., Claverie, M., & Franch, B. (2016). Preliminary analysis of the performance of the Landsat 8/OLI surface reflectance product. *Remote Sensing of Environment*, *185*, 46–56. https://doi.org/10.1016/j.rse.2016.04.008

Vitousek, P. M., Mooney, H. A., Lubchenco, J., & Melillo, J. M. (1997). Human domination of earth’s ecosystems. *Science*, *277*(5325), 494–499. https://doi.org/10.1126/science.277.5325.494

Vranken, I., Baudry, J., Aubinet, M., Visser, M., & Bogaert, J. (2015). A review on the use of entropy in landscape ecology: Heterogeneity, unpredictability, scale dependence and their links with thermodynamics. *Landscape Ecology*, *30*(1), 51–65. https://doi.org/10.1007/s10980-014-0105-0

Wam, H. K., Felton, A. M., Stolter, C., Nybakken, L., & Hjeljord, O. (2018). Moose selecting for specific nutritional composition of birch places limits on food acceptability. *Ecology and Evolution*, *8*(2), 1117–1130. https://doi.org/10.1002/ece3.3715

Weih, M., Hoeber, S., Beyer, F., & Fransson, P. (2014). Traits to ecosystems: The ecological sustainability challenge when developing future energy crops. *Frontiers in Energy Research*, *0*. https://doi.org/10.3389/fenrg.2014.00017

Wiederholt, R., Paudel, R., Khare, Y., Davis, S. E., Melodie Naja, G., Romañach, S., Pearlstine, L., & Van Lent, T. (2019). A multi-indicator spatial similarity approach for evaluating ecological restoration scenarios. *Landscape Ecology*. https://doi.org/10.1007/s10980-019-00904-w

Wilkes, M. A., Edwards, F., Jones, J. I., Murphy, J. F., England, J., Friberg, N., Hering, D., Poff, N. L., Usseglio-Polatera, P., Verberk, W. C. E. P., Webb, J., & Brown, L. E. (2020). Trait-based ecology at large scales: Assessing functional trait correlations, phylogenetic constraints and spatial variability using open data. *Global Change Biology*, *26*(12), 7255–7267. https://doi.org/10.1111/gcb.15344

Wilson, J. K., Ruiz, L., Duarte, J., & Davidowitz, G. (2019). The nutritional landscape of host plants for a specialist insect herbivore. *Ecology and Evolution*, *9*(23), 13104–13113. https://doi.org/10.1002/ece3.5730

Zhang, H., Yang, X., Wang, J., Wang, G. G., Yu, M., & Wu, T. (2017). Leaf N and P stoichiometry in relation to leaf shape and plant size for *Quercus acutissima* provenances across China. *Scientific Reports*, *7*(1). https://doi.org/10.1038/srep46133

Zhang, L.-L., & He, W.-M. (2009). Consequences of ramets helping ramets: No damage and increased nutrient use efficiency in nurse ramets of *Glechoma longituba*. *Flora -*

Morphology, Distribution, Functional Ecology of Plants, *204*(3), 182–188. https://doi.org/10.1016/j.flora.2008.02.001

Zhao, N., He, N., Wang, Q., Zhang, X., Wang, R., Xu, Z., & Yu, G. (2014). The altitudinal patterns of leaf C∶N∶P stoichiometry are regulated by plant growth form, climate and soil on Changbai mountain, China. *PLOS ONE*, *9*(4), e95196. https://doi.org/10.1371/journal.pone.0095196

3.9 Tables

Table 3.1 Hypothesis rationale for land cover, productivity, biotic (forest structure: age, height, canopy closure) and abiotic (elevation, aspect, slope) spatial covariates and their relationship to the variability of foliar elemental, stoichiometric, and phytochemical traits. For each spatial covariate we provide references to foliar ESP traits and to community level coordination of trait variability. Our approach does not consider a community weighted assessments of foliar ESP traits across species, instead we compare spatial covariates at the trait and species level to investigate potential commonalities.

Spatial covariate	Hypothesized relationship
Land cover	Land cover types, such as coniferous, deciduous, mixedwood, provide a proxy for community-level processes associated with litter-soil-nutrient feedbacks, nitrogen deposition, and competition for those elemental resources that influence foliar elemental traits (Hallett & Hornbeck, 1997; Ponette-González et al., 2010; Sardans et al., 2016); stoichiometric traits (Leroux et al., 2017; Sardans, Alonso, Carnicer, et al., 2016); and phytochemical traits (Hunter, 2016; Morquecho-Contreras et al., 2018). In addition, across species coordination of foliar trait variability has been observed for some species in response to land cover parameters (Jiang et al., 2015; Strahan et al., 2016).
Productivity	The Enhanced Vegetation Index is a Landsat derived proxy for productivity (i.e., the rate of greenness across time). Productivity is often a site level proxy associated with soil fertility, nutrient

	availability, and biomass production, as such it has been shown to influence foliar elemental traits (Ågren, 1988; Pan et al., 2004; Radwan & Harrington, 2011); stoichiometric traits (Blanes et al., 2013; Kerkhoff et al., 2005; Mendez & Karlsson, 2005); and phytochemical traits (Booker & Maier, 2001; Hunter & Schultz, 1995; Lindroth et al., 2002). As well productivity has been shown to influence foliar traits across species at the community level (Fyllas et al., 2020; Santiago et al., 2004; Tang et al., 2018).
Forest structure (biotic)	Forest structure is characterized by the structural variability of forest conditions such as dominant tree height, stand age, and canopy closure. Collectivity these parameters link structural characteristics with solar radiation interception across vertical and horizontal gradients of forest vegetation, precipitation interception, and space competition. As such, for understory vegetation these structural characteristics have been shown to influence foliar elemental traits (Becknell & Powers, 2014; Kranabetter et al., 2016; Richardson, 2004; Rijkers et al., 2000; Smithwick et al., 2003); stoichiometric traits (Fan et al., 2015; Niinemets & Kull, 1998; Sardans et al., 2016); phytochemical traits (Couture et al., 2014; Forkner & Marquis, 2004; Hemming & Lindroth, 1999; Sedio et al., 2017; Shure & Wilson, 1993); and notable examples show multi-species trait response to these structural conditions (Kichenin et al., 2013; Lohbeck et al., 2013).

Topographic (abiotic)	Topographic position defined by elevation, aspect, and slope are key parameters of the abiotic environment linked to temperature and precipitation gradients, and the incidence angle of solar radiation. Collectivity these parameters have been useful in explaining the variability of foliar elemental traits (Balzotti et al., 2016; Zhao et al., 2014); stoichiometric traits (Müller et al., 2017; Zhao et al., 2014); phytochemical traits (Glassmire et al., 2016; Pellissier et al., 2016); and there is evidence to suggest trait variability coordination across species, occurs in response to these abiotic parameters (Callis-Duehl et al., 2017; Descombes et al., 2017).

Table 3.2 List of models used to assess spatial covariates of foliar trait distribution. Land cover and productivity are derived from Landsat 8 scenes. The land cover dataset was acquired from the Commission for Environmental Cooperation and provides general classification of habitat types, i.e., coniferous, deciduous, mixed wood forests, as well as others not used in this study. Our proxy for productivity was acquired from Landsat 8 as the Enhanced Vegetation Index spectral product. Our biotic factors include grouped covariates of forest age, height, and canopy density. These variables were derived from Forest Resource Inventory datasets supplied by the Provincial Government of Newfoundland and Labrador and from the Federal Government of Canada's Park agency. These variables are grouped as the designation of these three measures are contained within a single polygon and represents associated conditions. Similarly, our abiotic factors include the grouped covariates of elevation, aspect, and slope derived from a single source, a Digital Canadian Elevation Model.

Model Number	**Explanatory Variables**
1	~ Land Cover + Productivity + Biotic + Abiotic
2	~ Productivity +Biotic + Abiotic
3	~ Land Cover + Biotic + Abiotic
4	~ Land Cover + Productivity + Abiotic
5	~ Land Cover + Productivity + Biotic
6	~ Land Cover + Biotic
7	~ Productivity + Biotic
8	~ Land Cover + Abiotic
9	~ Productivity + Abiotic
10	~ Biotic + Abiotic

11	~ Land Cover + Productivity
12	~ Land Cover
13	~ Productivity
14	~ Biotic
15	~ Abiotic
16	~ Null

3.10 Figures

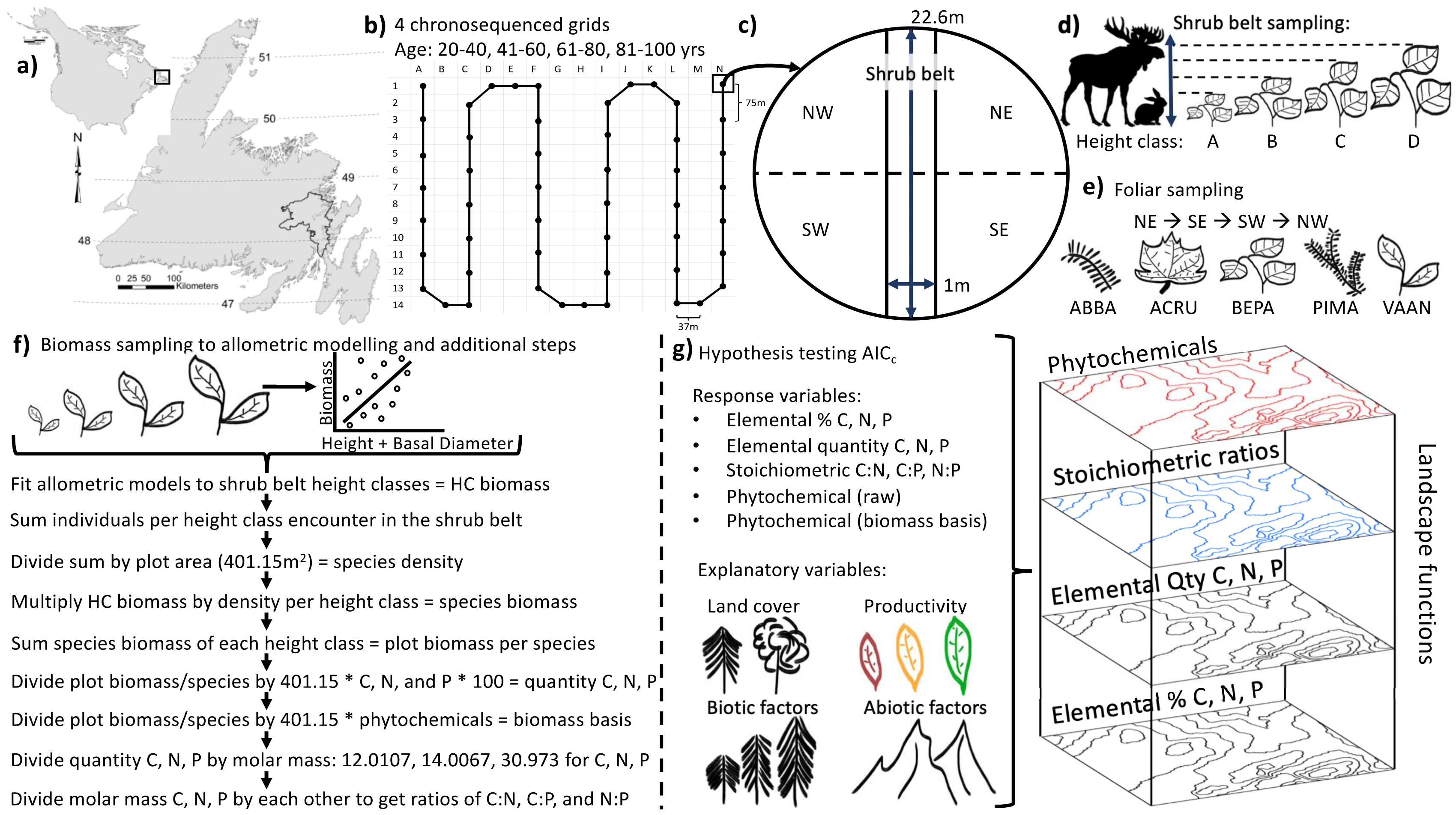

Fit allometric models to shrub belt height classes = HC biomass
Sum individuals per height class encounter in the shrub belt
Divide sum by plot area (401.15m^2) = species density
Multiply HC biomass by density per height class = species biomass
Sum species biomass of each height class = plot biomass per species
Divide plot biomass/species by 401.15 * C, N, and P * 100 = quantity C, N, P
Divide plot biomass/species by 401.15 * phytochemicals = biomass basis
Divide quantity C, N, P by molar mass: 12.0107, 14.0067, 30.973 for C, N, P
Divide molar mass C, N, P by each other to get ratios of C:N, C:P, and N:P

Response variables:

- Elemental % C, N, P
- Elemental quantity C, N, P
- Stoichiometric C:N, C:P, N:P
- Phytochemical (raw)
- Phytochemical (biomass basis)

Explanatory variables:

Figure 3.1 The roadmap of our methods adapted from Leroux et al. 2017. Our study area is located on the island of Newfoundland, Canada (a) where we set up four chronosequenced meandering transect grids each consisting of 50 sampling locations (b). At each sample location we set up 22.6 m diameter circular plots (c), and along a 22.6 m long, 1 m wide shrub belt (c) we collected density measures of our study species for a max of five per height class: 0-50 cm, 51-100 cm, 101-150 cm, 151-200 cm, coded as A, B, C, and D, respectively (d). We collected foliar samples in each intercardinal corner of the sample plot, starting in the NE corner and moving clockwise until a sufficient and representative sample was acquired (e). Species codes used: balsam fir (ABBA), red maple (ACRU), white birch (BEPA), black spruce (PIMA), and lowbush blueberry (VAAN) (e). We collected biomass samples (i.e., all new growth foliar material) on the periphery of the grids from approximately fifty individuals distributed across height classes (f). Allometric models were fit using biomass as a function of height and basal diameter, from which we parameterized shrub belt correlates to acquire plot level biomass estimates. We used these estimates to determine foliar elemental quantity, stoichiometric ratios, and phytochemical (biomass) traits relativized to biomass density at the plot level. We fit 16 models, including a null model, for response variables of foliar elemental (percent and quantity), stoichiometric, and phytochemical traits using spatially explicit covariates of land cover, productivity, biotic (stand age, height, canopy closure) and abiotic (elevation, aspect, and slope) factors (g). Using top model coefficient estimates and or average coefficients for competing top models, we constructed spatial surfaces of foliar ESP trait surfaces that link physiological properties to ecosystem processes at the landscape extent.

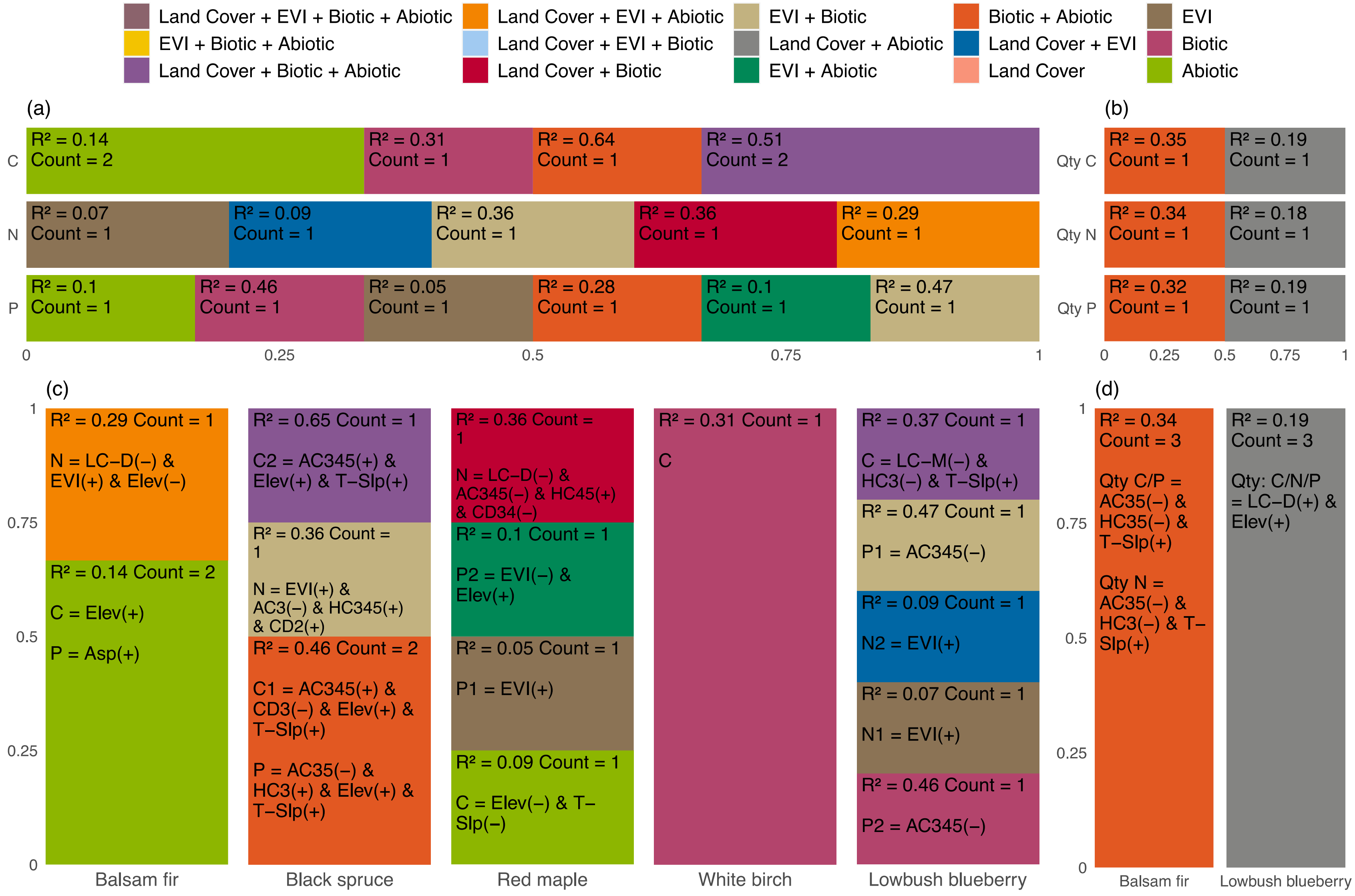
Land Cover + EVI + Biotic + Abiotic
EVI + Biotic + Abiotic
Land Cover + Biotic + Abiotic
Land Cover + EVI + Abiotic
Land Cover + EVI + Biotic
Land Cover + Biotic
EVI + Biotic
Land Cover + Abiotic
EVI + Abiotic
Biotic + Abiotic
Land Cover + EVI
Land Cover
EVI
Biotic
Abiotic
(a)
C
R² = 0.14 Count = 2
R² = 0.31 Count = 1
R² = 0.64 Count = 1
R² = 0.51 Count = 2
N
R² = 0.07 Count = 1
R² = 0.09 Count = 1
R² = 0.36 Count = 1
R² = 0.36 Count = 1
R² = 0.29 Count = 1
P
R² = 0.1 Count = 1
R² = 0.46 Count = 1
R² = 0.05 Count = 1
R² = 0.28 Count = 1
R² = 0.1 Count = 1
R² = 0.47 Count = 1
0
0.25
0.5
0.75
1
(b)
Qty C
R² = 0.35 Count = 1
R² = 0.19 Count = 1
Qty N
R² = 0.34 Count = 1
R² = 0.18 Count = 1
Qty P
R² = 0.32 Count = 1
R² = 0.19 Count = 1
0
0.25
0.5
0.75
1
(c)
1
0.75
0.5
0.25
0
R² = 0.29 Count = 1
N = LC–D(–) & EVI(+) & Elev(–)
R² = 0.14 Count = 2
C = Elev(+)
P = Asp(+)
R² = 0.65 Count = 1
C2 = AC345(+) & Elev(+) & T–Slp(+)
R² = 0.36 Count = 1
N = EVI(+) & AC3(–) & HC345(+) & CD2(+)
R² = 0.46 Count = 2
C1 = AC345(+) & CD3(–) & Elev(+) & T–Slp(+)
P = AC35(–) & HC3(+) & Elev(+) & T–Slp(+)
R² = 0.36 Count = 1
N = LC–D(–) & AC345(–) & HC45(+) & CD34(–)
R² = 0.1 Count = 1
P2 = EVI(–) & Elev(+)
R² = 0.05 Count = 1
P1 = EVI(+)
R² = 0.09 Count = 1
C = Elev(–) & T–Slp(–)
R² = 0.31 Count = 1
C
R² = 0.37 Count = 1
C = LC–M(–) & HC3(–) & T–Slp(+)
R² = 0.47 Count = 1
P1 = AC345(–)
R² = 0.09 Count = 1
N2 = EVI(+)
R² = 0.07 Count = 1
N1 = EVI(+)
R² = 0.46 Count = 1
P2 = AC345(–)
Balsam fir
Black spruce
Red maple
White birch
Lowbush blueberry
(d)
1
0.75
0.5
0.25
0
R² = 0.34 Count = 3
Qty C/P = AC35(–) & HC35(–) & T–Slp(+)
Qty N = AC35(–) & HC3(–) & T–Slp(+)
R² = 0.19 Count = 3
Qty: C/N/P = LC–D(+) & Elev(+)
Balsam fir
Lowbush blueberry

Figure 3.2 Top ranked model results (i.e., models $\Delta AIC_c < 2$) at the trait level (a, b) and species level (c, d) for foliar percent elemental (a, c) and foliar quantity elemental (b, d) traits. Results are organized to show patterns of evidence to support spatial relationships between response and explanatory variables. Superimposed descriptive text on each portion of the stacked bar graphs includes the averaged pseudo R^2 values for top models if the count > 1, if count is = 1 then only the R^2 for that model is presented. In addition, at the species level (c, d) for our response variables (i.e., C, N, and P) superimposed text indicates significant coefficients and their sign (+/-) for our explanatory variables of land cover, EVI, biotic, and abiotic. Coded values for explanatory variables represent their comprised variables and factor levels. For land cover, LC-C, LC-D, and LC-M indicate coniferous, deciduous, and mixedwood, respectively. EVI represents the Enhanced Vegetation Index. For biotic variables, AC indicates age class with 3, 4, 5 representing factor levels of 41-60, 61-80, and 81-100 years, respectively. HC indicates height class with 3, 4, 5 representing factor levels of 6.6-9.5, 9.6-12.5, 12.6-15.5 metres, respectively. CD indicates canopy density with 2, 3, 4 representing factor levels of 51-75, 26-50, 10-25 percent closed canopy, respectively. For abiotic variables, Elev, Asp, T-Slp represent elevation, aspect, and slope, respectively. If a response variable is supported by more than one top model, a sequential numbering is used to indicate the rank of that model added as a suffix to the response variable text (i.e., C2 indicates the second top ranked model in support of foliar percent carbon). The asterisk symbol (*) is used to indicate that the null model was within $\Delta AIC_c < 2$. See Appendix B.9 Table B.9.1 for a coefficient signs (+/-) and Appendix B.12, Tables B.12.1, B.12.3, and B.12.3 for coefficient estimates, standard deviations, and confidence intervals.

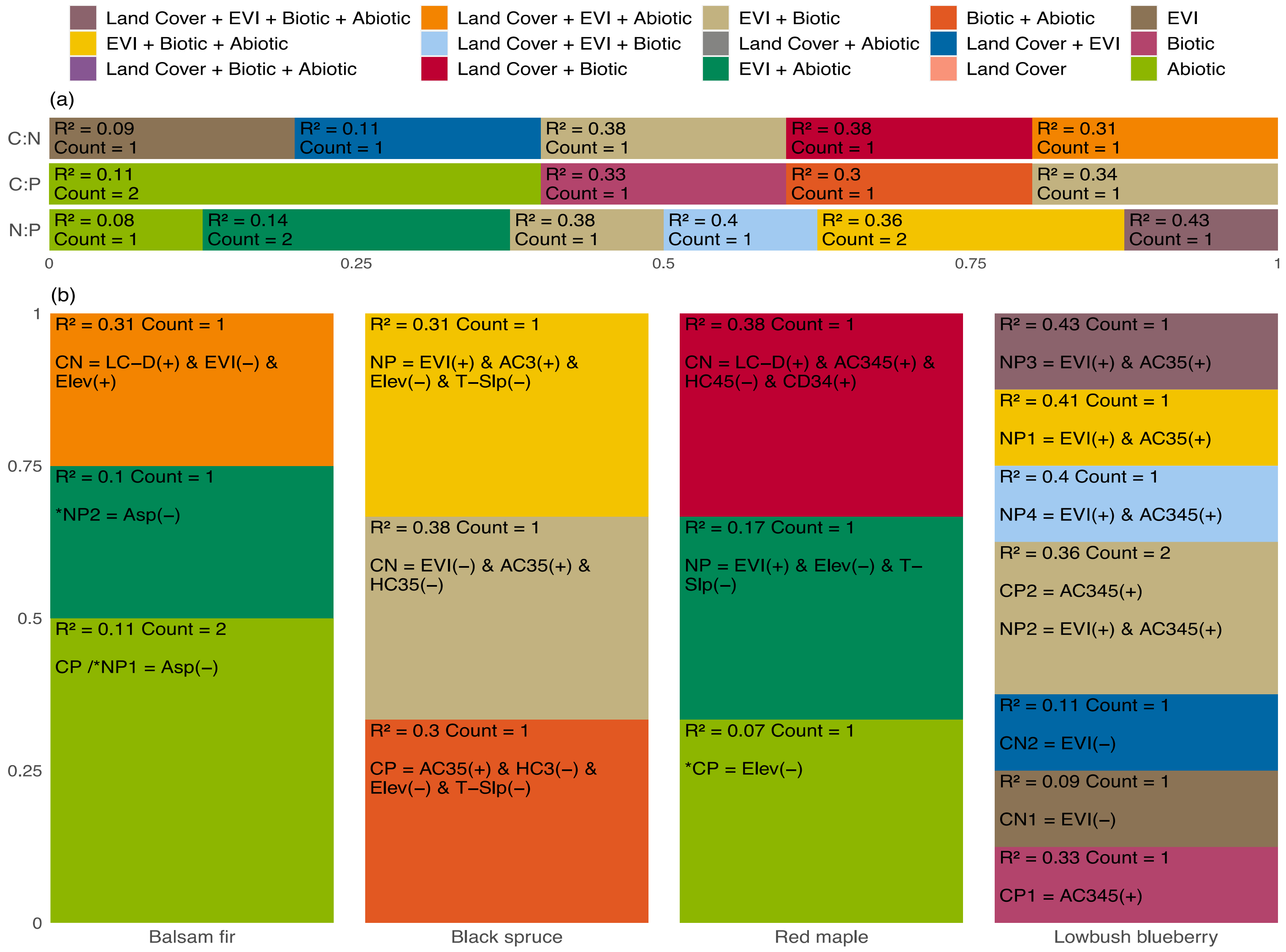
Land Cover + EVI + Biotic + Abiotic
EVI + Biotic + Abiotic
Land Cover + Biotic + Abiotic
Land Cover + EVI + Abiotic
Land Cover + EVI + Biotic
Land Cover + Biotic
EVI + Biotic
Land Cover + Abiotic
EVI + Abiotic
Biotic + Abiotic
Land Cover + EVI
Land Cover
EVI
Biotic
Abiotic
(a)
C:N
C:P
N:P
R² = 0.09 Count = 1
R² = 0.11 Count = 1
R² = 0.38 Count = 1
R² = 0.38 Count = 1
R² = 0.31 Count = 1
R² = 0.11 Count = 2
R² = 0.33 Count = 1
R² = 0.3 Count = 1
R² = 0.34 Count = 1
R² = 0.08 Count = 1
R² = 0.14 Count = 2
R² = 0.38 Count = 1
R² = 0.4 Count = 1
R² = 0.36 Count = 2
R² = 0.43 Count = 1
0
0.25
0.5
0.75
1
(b)
1
0.75
0.5
0.25
0
R² = 0.31 Count = 1
CN = LC–D(+) & EVI(–) & Elev(+)
R² = 0.1 Count = 1
*NP2 = Asp(–)
R² = 0.11 Count = 2
CP /*NP1 = Asp(–)
R² = 0.31 Count = 1
NP = EVI(+) & AC3(+) & Elev(–) & T–Slp(–)
R² = 0.38 Count = 1
CN = EVI(–) & AC35(+) & HC35(–)
R² = 0.3 Count = 1
CP = AC35(+) & HC3(–) & Elev(–) & T–Slp(–)
R² = 0.38 Count = 1
CN = LC–D(+) & AC345(+) & HC45(–) & CD34(+)
R² = 0.17 Count = 1
NP = EVI(+) & Elev(–) & T–Slp(–)
R² = 0.07 Count = 1
*CP = Elev(–)
R² = 0.43 Count = 1
NP3 = EVI(+) & AC35(+)
R² = 0.41 Count = 1
NP1 = EVI(+) & AC35(+)
R² = 0.4 Count = 1
NP4 = EVI(+) & AC345(+)
R² = 0.36 Count = 2
CP2 = AC345(+)
NP2 = EVI(+) & AC345(+)
R² = 0.11 Count = 1
CN2 = EVI(–)
R² = 0.09 Count = 1
CN1 = EVI(–)
R² = 0.33 Count = 1
CP1 = AC345(+)
Balsam fir
Black spruce
Red maple
Lowbush blueberry

Figure 3.3 Top ranked model results (i.e., models $\Delta AIC_c < 2$) at the trait level (a) and species level (b) for foliar stoichiometric traits (i.e., CN, CP, NP). All specifications as in Figure 3.2. See Appendix B.9 Table B.9.1 for a coefficient signs (+/-) and Appendix B.12 Tables B.12.5, B.12.6, and B.12.7 for coefficient estimates, standard deviations, and confidence intervals.

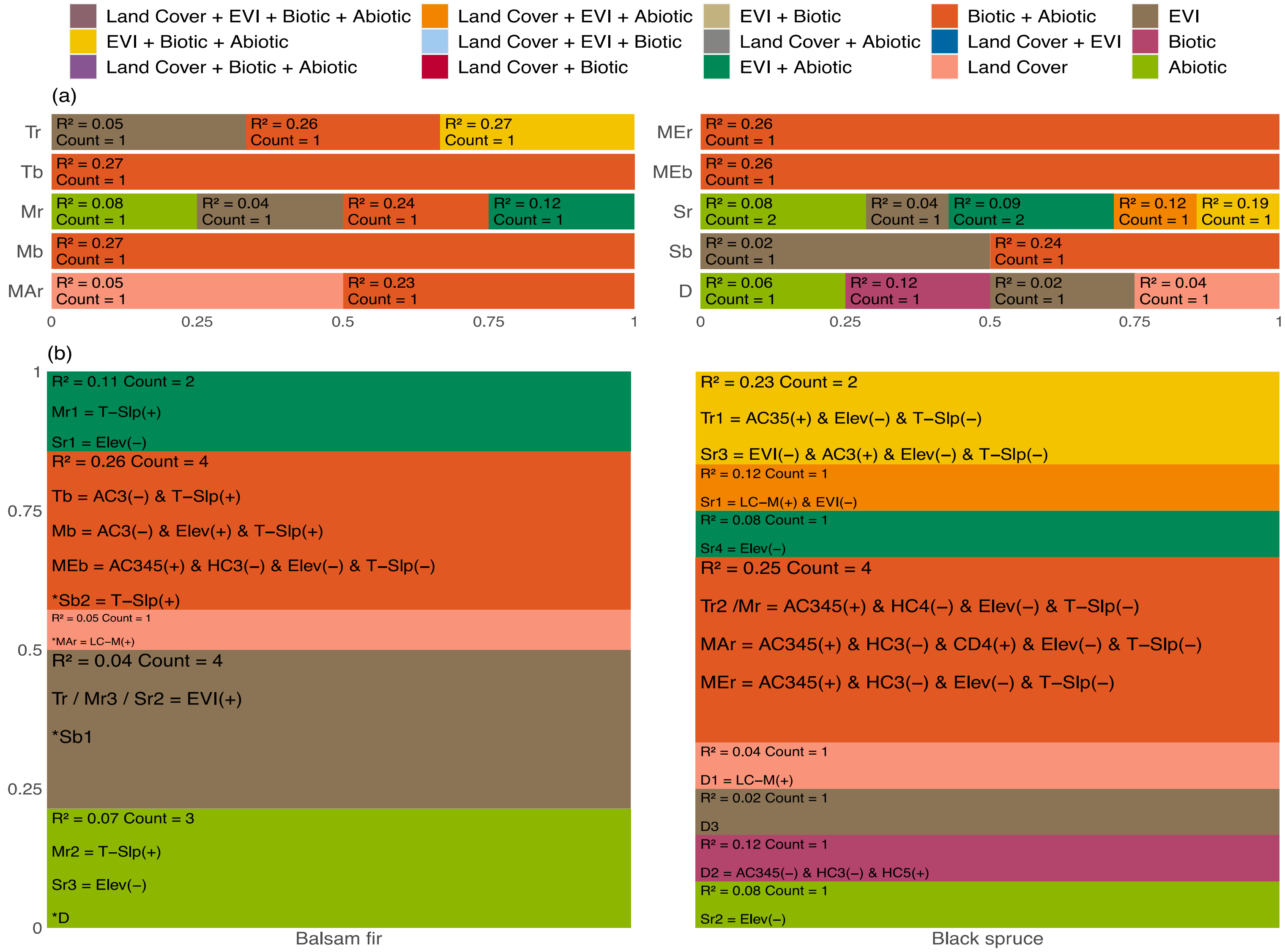
Land Cover + EVI + Biotic + Abiotic
EVI + Biotic + Abiotic
Land Cover + Biotic + Abiotic
Land Cover + EVI + Abiotic
Land Cover + EVI + Biotic
Land Cover + Biotic
EVI + Biotic
Land Cover + Abiotic
EVI + Abiotic
Biotic + Abiotic
Land Cover + EVI
Land Cover
EVI
Biotic
Abiotic
(a)
Tr
Tb
Mr
Mb
MAr
R² = 0.05 Count = 1
R² = 0.26 Count = 1
R² = 0.27 Count = 1
R² = 0.27 Count = 1
R² = 0.08 Count = 1
R² = 0.04 Count = 1
R² = 0.24 Count = 1
R² = 0.12 Count = 1
R² = 0.27 Count = 1
R² = 0.05 Count = 1
R² = 0.23 Count = 1
0
0.25
0.5
0.75
1
MEr
MEb
Sr
Sb
D
R² = 0.26 Count = 1
R² = 0.26 Count = 1
R² = 0.08 Count = 2
R² = 0.04 Count = 1
R² = 0.09 Count = 2
R² = 0.12 Count = 1
R² = 0.19 Count = 1
R² = 0.02 Count = 1
R² = 0.24 Count = 1
R² = 0.06 Count = 1
R² = 0.12 Count = 1
R² = 0.02 Count = 1
R² = 0.04 Count = 1
0
0.25
0.5
0.75
1
(b)
1
0.75
0.5
0.25
0
R² = 0.11 Count = 2
Mr1 = T–Slp(+)
Sr1 = Elev(–)
R² = 0.26 Count = 4
Tb = AC3(–) & T–Slp(+)
Mb = AC3(–) & Elev(+) & T–Slp(+)
MEb = AC345(+) & HC3(–) & Elev(–) & T–Slp(–)
*Sb2 = T–Slp(+)
R² = 0.05 Count = 1
*MAr = LC–M(+)
R² = 0.04 Count = 4
Tr / Mr3 / Sr2 = EVI(+)
*Sb1
R² = 0.07 Count = 3
Mr2 = T–Slp(+)
Sr3 = Elev(–)
*D
Balsam fir
R² = 0.23 Count = 2
Tr1 = AC35(+) & Elev(–) & T–Slp(–)
Sr3 = EVI(–) & AC3(+) & Elev(–) & T–Slp(–)
R² = 0.12 Count = 1
Sr1 = LC–M(+) & EVI(–)
R² = 0.08 Count = 1
Sr4 = Elev(–)
R² = 0.25 Count = 4
Tr2 /Mr = AC345(+) & HC4(–) & Elev(–) & T–Slp(–)
MAr = AC345(+) & HC3(–) & CD4(+) & Elev(–) & T–Slp(–)
MEr = AC345(+) & HC3(–) & Elev(–) & T–Slp(–)
R² = 0.04 Count = 1
D1 = LC–M(+)
R² = 0.02 Count = 1
D3
R² = 0.12 Count = 1
D2 = AC345(–) & HC3(–) & HC5(+)
R² = 0.08 Count = 1
Sr2 = Elev(–)
Black spruce

Figure 3.4 Top ranked model results (i.e., models $\Delta AIC_c < 2$) at the trait level (a) and species level (b) for foliar phytochemical traits. Coded values are supplied for response variables as with upper case letters representing the trait and lower-case letters representing either raw (r) or biomass basis (b). For response variables, T, M, MA, ME, S, and D indicate terpene, monoterpene, monoterpenic alcohol, monoterpenic ester, sesquiterpene, and phytochemical diversity, respectively. All specifications as in Figure 3.2. See Appendix B.9 Table B.9.1 for a coefficient signs (+/-) and Appendix B.12 Tables B.12.8, B.12.9, and B.12.10 for coefficient estimates, standard deviations, and confidence intervals.

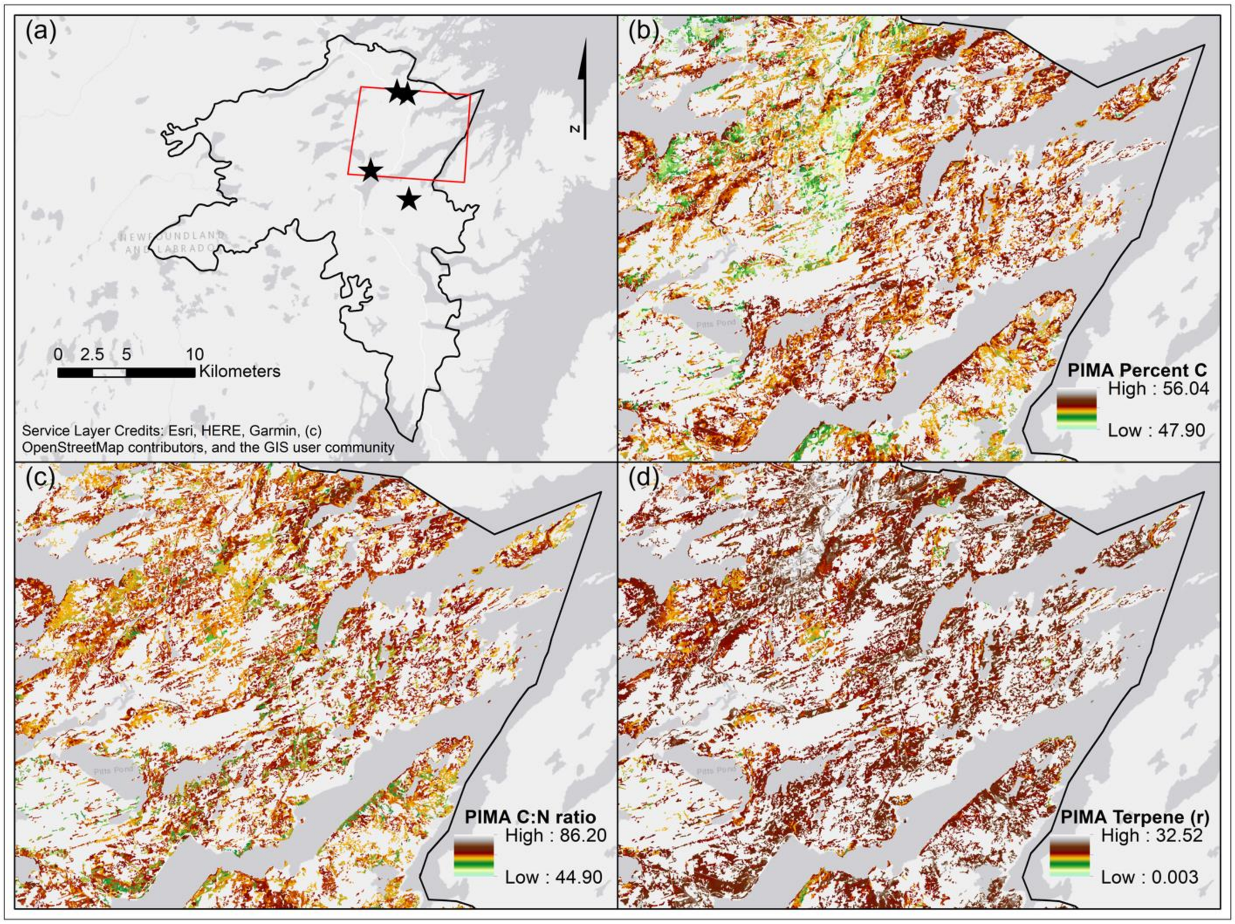

Figure 3.5 Example of spatially explicit foliar ESP trait distribution models. In (a) we show our spatial area of interest as the black outlined region (i.e., ecodistrict 468). Our grid locations are denoted in panel a using the star outline. The red box shown in panel a, is the extent of the subsequent maps provided in this figure, a close up view of spatial foliar ESP patterns for black spruce (PIMA). Foliar percent carbon (b) ranges from 47.9 to 56.04 and is predicted using spatial correlates of land cover, biotic and abiotic factors (pseudo $R^2 = 0.65$). Foliar stoichiometric C:N ranges from 44.9 to 86.2 and is predicted using spatial correlates of EVI and biotic factors (pseudo $R^2 = 0.38$). Foliar terpene raw ranges from 0.003 to 32.52 and is predicted using spatial correlates of biotic and abiotic factors (pseudo $R^2 = 0.26$). Although these traits are predicted using different spatial correlates, emerging spatial patterns in trait variability suggest different

processes are acting on trait expressions in different areas. For instance, high foliar C areas may relate to community type (land cover), forest structure (biotic), and topographic conditions (abiotic), however, patterns of C:N forest structure (biotic) and site productivity (EVI) indicate nutrient limitation areas with lower values have higher foliar nitrogen content. Moreover, foliar terpene patterns provide contours from which higher herbivore interactions results in increased terpene production. When overlaid with C and C:N we can gleam spatial patterns on the allocation of C to terpene production in terms of nutrient limitation constraints.

Chapter 4

Local scale spatial co-dispersion patterns of plant functional traits between co-occurring species

Authors: Travis R Heckford[1], Shawn J. Leroux[1], Matteo Rizzuto[1], Isabella C. Richmond[1], Eric Vander Wal[1], Juliana Balluffi-Fry[2], Yolanda F. Wiersma[1]

Author Affiliations

1: Department of Biology, Memorial University of Newfoundland. 230 Elizabeth Avenue, St. John's Canada

2: Department of Biological Sciences, University of Alberta, Edmonton, Canada

A version of this paper will be submitted to *Landscape Ecology* as

Heckford, T. R., Leroux, S. J., Vander Wal, E., Rizzuto, M., Balluffi-Fry, J., Richmond, I. C., & Wiersma, Y. F. (n.d.). "Local scale spatial co-dispersion patterns of plant functional traits between co-occurring species".

4.1 Abstract

Context: Community assembly theory predicts the traits of co-occurring species should diverge. However, little evidence exists to support this assertion in a spatially explicit context.

Objective: Using foliar elemental, stoichiometric, and phytochemical (ESP) traits we assess the spatial patterns of co-occurring understory tree species with different resource strategies from conservative conifers to acquisitive deciduous.

Methods: We collected foliar material from two chronosequenced forest sites along a grid-based sampling design. Using co-dispersion analysis, we assessed the spatial patterns of foliar ESP traits between our focal species at our two study sites. In addition, we assessed statistical significance of trait spatial relationships between species using a modified *t*-test that accounts for spatial autocorrelation.

Results: In most cases, species with similar resource strategies exhibited similar spatial trait patterns for foliar traits; however, these relationships were often site-specific. For the most part, foliar elemental and stoichiometric traits for co-occurring conifer and deciduous species were spatially aggregated, although not always significantly. No spatial relationship occurred for foliar phytochemical traits. Counter to our predictions species with dissimilar resource strategies often had significant spatial trait relationships.

Conclusions: Here we find evidence to suggest that foliar traits of co-occurring species significantly correlate. Understanding how plant functional traits co-vary between co-occurring species provides insight into how process-pattern relationships may differ within and between habitat patches.

4.2 Introduction

Community assembly theory provides a framework to potentially explain fine scale spatial co-variability patterns of plant functional traits between co-occurring species (Mcgill et al. 2006, Buckley et al. 2016a). The twin filter model of community assembly suggests that species associations are the product of a hierarchical two step filtering process, where the first filter acts to select species with (1) convergent strategies and (2) divergent traits (see Figure 4.1; Vellend 2016). Thus, traits of co-occurring species should exhibit divergent spatial patterns. However, the degree to which traits diverge between co-occurring species likely depends on how similar their resource strategies are (i.e., how and why a species acquires and uses resources) and on the spatial scale at which plants elicit similar trait responses to changes in environmental conditions (Kraft et al. 2015, Sardans et al. 2021). For instance, the spatial co-variability of traits from plants with similar resource strategies may vary in similar ways to a set of environmental conditions but as these conditions change across gradients (i.e., soil nutrient and moisture regimes) these relationships may diminish (Santiago et al. 2004). Although many studies have investigated trait co-variability at a community level along spatial gradients (see Pottier et al. 2007), very few studies have evaluated spatially explicit trait co-variability patterns between co-occurring species.

Universal traits, such as the chemical composition of foliar material allows for a direct comparison of trait spatial co-variability across species to reveal community driven patterns. For instance, aside from hydrogen and oxygen, all organisms are predominantly composed of carbon (C), nitrogen (N), and phosphorus (P) (Kaspari and Powers 2016). The ratios of C, N, and P form the basis for the field of ecological stoichiometry which focuses on the exchange of matter and energy throughout ecosystems and at a species and community level, stoichiometry provides insights on nutrient use and co-limitation (Sterner and Elser 2002). C and N also form the primary building blocks for other biological compounds (i.e., secondary metabolites, phytochemicals, proteins, and amino acids) that are key factors driving many ecosystem processes such as decomposition and nutrient cycling (Knops et al. 2002, Hobbie 2015). Moreover, organisms are elementally constrained by physiological processes to maintain an elemental homeostasis, characterized as a species elementome (amount and proportion of elements; Sterner and Elser 2002, Peñuelas et al. 2019). Across species, elementome similarity is attributed to evolutionary history via phylogenetic relatedness (Sardans et al. 2021). Thus, species that are more closely related and have similar resource strategies may exhibit similar spatial patterns of trait plasticity since they respond similarly to environmental conditions. As such foliar chemical traits of phylogenetically related species with similar resource strategies provide a useful basis to investigate spatial patterns of resource use across and between species to reveal generalities of trait patterning.

A useful approach for quantifying the spatial co-variability of foliar trait between co-occurring species is co-dispersion analysis coupled with a significance assessment of spatial correlation (Fortin and Payette 2002, Buckley et al. 2016b). Co-dispersion analysis reveals how two spatial patterns co-vary as a function of spatial lag (i.e., distance) and allows us to detect symmetries in their spatial patterns and the spatial scales at which relationships occur (Cuevas et al. 2013, Buckley et al. 2016a). For instance, the spatial patterns of plant traits between species may exhibit positive (aggregation) or negative (segregation) co-dispersion at differing distances, and this may indicate changes in environmental filtering with implications for feedbacks on ecosystem processes that determine community structure (Vallejos et al. 2015, Buckley et al. 2016a). Moreover, the change in spatial patterns, i.e., from aggregation to segregation, can indicate the effect of directionality or anisotrophic effects on these relationships. Lastly, to assess the significance of spatial relationships Dutilleul's modified *t*-test is often used as it accounts for spatial autocorrelation between variables by adjusting the effective sample size at various distances (Dutilleul et al. 1993, Fortin and Payette 2002). Although other approaches to quantify spatial point patterns exist, such as cross nearest neighbour distance and cross K-function, these approaches look for spatial relationships between two objects not sampled in the same location. With co-dispersion analysis we can assess the spatial co-variability of foliar traits between co-occurring species at a plot scale to reveal spatial patterns of interspecific interactions related to community assembly processes.

Here we use two conifer – balsam fir (*Abies balsamea* (L.) Mill.) and black spruce (*Picea mariana* (Mill.) Britton, Sterns, & Poggenb) – and two deciduous – red maple (*Acer rubrum* L.), and white birch (*Betula papyrifera* Marshall) – juvenile tree species to investigate the spatial co-dispersion of foliar elemental, stoichiometric, and phytochemical traits (hereafter referred to as foliar ESP traits). We group our focal species by conifer and deciduous resource strategies. In general, conifer species have conservative strategies and deciduous species have acquisitive strategies. These differences allow us to characterize potential linkages between elemental homeostasis, stoichiometric plasticity, and phytochemical loading. For instance, slow growing conifer species with constrained leaf morphology and growth geometry often exhibit high elemental homeostasis, low stoichiometric plasticity, and high phytochemical loading (Kessler 2015, He et al. 2019). In comparison, fast growing deciduous species with variable leaf morphology and growth geometry often exhibit low elemental homeostasis, high stoichiometric plasticity, and low phytochemical loading (Niinemets and Kull 1998, Grime and Pierce 2012, Peñuelas et al. 2019). Where any two of our focal species co-occur at the plot level, we evaluate the spatial co-variability of foliar ESP traits. We hypothesize that co-occurring species with similar resource strategies (i.e., conifer vs conifer or deciduous vs deciduous) should exhibit similar spatial patterns in foliar ESP traits (i.e., aggregation) and co-occurring species with dissimilar resource strategies (i.e., conifer vs deciduous) should exhibit dissimilar spatial patterns in foliar ESP traits (i.e., segregation; for visual hypothesis depiction and description see Figure 4.1). Moreover, we use two forest stands to assess the consistency of these spatial patterns. We expect these spatial patterns to be relatively consistent between our two stands, although we acknowledge there may be stand age specific differences such as soil nutrient build up that influences plant stoichiometry over successional time (Kranabetter et al. 2016). Our approach here aims to reveal the spatial patterns in trait co-variability between co-occurring species to better understand community assembly processes within a spatially explicit framework and to inform potential questions of herbivore forage decisions at the bite scale since our focal species are the preferred forage of moose (*Alces alces* (Linnaeus, 1758)) and snowshoe hare (*Lepus americanus* (Erxleben, 1777)).

4.3 Methods

4.3.1 Sampling area, design, and focal species description

Our study area is located in the central east region on the island of Newfoundland (Appendix C.1, Figure C.1.1). We selected two forest stands characterized by dominant canopy species (black spruce, balsam fir, with mixed deciduous); our sites, named Unicorn and Dunphy's Pond, are 61-80 and 81-100 years old, respectively. At each study site, we set up a sampling grid of 6 connected meandering transects, approximately 500 x 500 m in size (Appendix C.1, Figure C.1.1). Each grid consisted of 50 sampling locations spaced equally at 75 m intervals along the transects with closer sample locations rounding the corners at 55 and 37 m spacing (Appendix C.1, Figure C.1.1). At each sampling location, we set up 22.6 m diameter circular plots.

Our focal species consist of two conifer (balsam fir and black spruce) and two deciduous (red maple and white birch) species. The foliar material collected from these species represents available forage for two herbivores within the boreal forest ecosystem, moose and snowshoe hare. Our conifer species show close phylogenetic relatedness at the family level: Pinaceae. In comparison, our two deciduous species show phylogenetic relatedness at the clade level: Rosids.

4.3.2 Foliar ESP trait sampling and processing

Within each plot, we collected density estimates of our focal species by measuring the number of individuals encountered within a 1 m wide shrub belt transect spanning the 22.6 m diameter of the plot. Starting at the north end of the transect and moving south, we recorded the distance from the start, height, and basal diameter for each individual focal species encountered for a maximum of five individuals within each height group: 0-50 cm, 51-100 cm, 101-150 cm, and 151-200 cm. In each corner of the plot, we collected the foliar material of our focal species from individuals within a 0-2 m in height – understory juvenile tree species within a height range for common browsers noted above. Foliar material consisted of the lateral and terminal ends. We collected foliar material from one individual per corner, moving clockwise until we achieved a wet weight of 10-20 g. To estimate biomass, along the periphery of the grids and outside the sample plots, in random locations, we collected all new growth foliar material from approximately 50 individuals for each focal species with the number of samples collected stratified across the same height groups. For each individual sampled we measured height and basal diameter. To obtain estimates of biomass, we oven dried these foliar samples at 50 ºC over a 2 to 3 day period until a constant weight was achieved.

For each plot, we combined foliar samples per species until we amassed a wet weight sample of 10 g and 4 g– the amounts required for elemental and phytochemical analysis, respectively. The C and N concentration of foliar material was determined by the Agriculture Food Lab (AFL) at the University of Guelph, Ontario, Canada, using an Elementar Vario Macro Cube. Foliar P concentration was determined using a microwave acid digestion CEM MARSxpress microwave system and brought to volume using Nanopure water. The clear extract supernatant was further diluted by 10 to accurately fall within calibration range and reduce high level analyte concentration entering the inductively coupled plasma mass spectrometry detector (ICP-MS). This provides us with a measure of percent foliar C, N, and P. At the Laboratorie PhytoChemia Inc. in Quebec, Canada, the phytochemical composition of balsam fir and black spruce foliar samples were determined using a gas chromatography solvent extraction with an internal standard and a correction factor (Cachet et al. 2016). This procedure produced mg/g measures of individual terpene compounds. We did not analyze the phytochemical terpenoid composition of deciduous leaves as they exhibit compensatory strategies where chemicals are produced in response to browsing. In contrast, coniferous species exhibit constituent strategies, maintaining baseline terpenoid concentrations that may increase in response to herbivory.

Following Leroux et al. (2017), we fit allometric (i.e., linear) models using the biomass of our dried foliar samples on a natural logarithmic scale using height and basal diameter to explain biomass for each focal species (R^2 = balsam fir 0.82, black spruce 0.80, red maple 0.83, and white birch 0.79). We then used allometric model coefficients to estimate the biomass for our focal species at the plot level from shrub belt data (height and basal diameter) per height group (for biomass estimates see Heckford et al., 2022). We summed across height groups to get a total plot level biomass per species. For a given plot, if we did not encounter any individuals of our focal species on the shrub belt, but we had collected foliar samples, we used the height and basal diameter of those individuals per height group to estimate plot level biomass. To obtain foliar stoichiometric ratios, for each of our focal species, we divided plot level biomass by the area of the plot, 401.15 m^2, multiplied by foliar C, N, and P and divided C, N, and P by their respective elemental molar mass (i.e., C = 12.01, N = 14.00, P = 30.97). From here, we divided molar concentrations against each other to derived stoichiometric ratios (i.e., C/N, C/P, and N/P).

4.3.3 Spatial co-dispersion and significance testing for correlation

We used the *SpatialPack* R package and computed spatial co-dispersion coefficients at specific distances and use a modified *t*-test to assess the significance of the spatial correlations of foliar ESP traits for our focal species at our two study sites using the co-occurrence of species at the plot level (Osorio et al. 2020). Using the *codisp* function, we quantified the spatial association of two spatial sequences (i.e., foliar traits for co-occurring/pairs of our focal species) on non-rectangular grids (meandering transects) separated by distance *h* (lag). We used Sturges' formula (1 + 3.33 log(n)), where n is the number of pair observations to determine the desirable number of distance classes for which a set of spatial lags should be calculated (Osorio et al. 2020). Sturges formula is often used to determine the number of distance classes when the total number of observations is known; it is also the default formula for the co-dispersion analysis. For each distance class, we then computed a co-dispersion coefficient. We present graphs showing how the co-dispersion coefficient varied by distance where +1 indicates positive co-dispersion/correlation (spatial aggregation) and -1 indicates negative co-dispersion/correlation (spatial segregation); a 0 co-dispersion coefficient suggests there is no spatial relationship or correlation. If the co-dispersion coefficient varied between positive and negative values this indicates an anisotropic relationship where correlation is dependent on direction (as opposite to isotropic where correlation is same in all directions). We a performed a Dutilleul's modified *t*-test, using the *modified.ttest* function (Osorio et al. 2020), and assessed the significance of the observed spatial correlations between species for a given foliar ESP trait (Dutilleul et al. 1993). Dutilleul's modified *t*-test accounts for spatial dependence by estimating the effective sample size in both variables and recalculating the standard *t*-statistic (Fortin and Payette 2002). Moreover, Sturges' formula is used to determine the number of distance classes from which we estimate Moran's I coefficients for a series of distance classes. Here, statistical significance is determined by controlling for spatial non-independence of the Pearson's correlation coefficient based on geographically effective degrees of freedom using distance classes set by Sturges' formula to estimate the degree of spatial autocorrelation (Osorio et al. 2020). Lastly, the sample size, out of a maximum of 50 sample locations, for foliar elemental and stoichiometric traits of our focal species at our study sites Unicorn and Dunphy's Pond, respectively, is as follows: balsam fir (n = 41 and 40), black spruce (n = 36 and 44), red maple (n = 30 and 40), white birch (n = 25 and 20). The sample size, out of a maximum of 50 sample locations, for foliar phytochemical traits of our focal species at our study sites Unicorn and Dunphy's Pond, respectively, is as follows: balsam fir (n = 44 and 42), black spruce (n = 38 and 44).

Below we present our comparisons for groups of foliar traits: (1) elemental, (2) stoichiometric, and (3) phytochemical. We have provided figures showing how the spatial co-dispersion coefficient varies by distance (metres) for each of our focal species comparisons by study site. On each graph we have provided a study site colour-coded correlation coefficient and *p*-value as determined by the modified *t*-test, an asterisk (*) is provided for quick identification of significance at $p \leq 0.05$). In Appendix C.2, Figure C.2.1, we have provided boxplots of species traits by sites showing the range of trait variability per trait per species between the two study sites. In addition, the minimum, maximum, and average co-dispersion coefficients and distance at which the minimum and maximum occur for each species trait comparison are provided in Appendix C.3; for elemental traits see Table C.3.1; for stoichiometric see Table C.3.2; and for phytochemical see Table C.3.3. We have also provided modified *t*-test results, including the *F* statistic, degrees of freedom, *p*-value, and Pearson's correlation for spatial autocorrelation in the Appendix C.4; for elemental see Table C.4.1; for stoichiometric see Table C.4.2; and for phytochemical see Table C.4.3.

4.4 Results

4.4.1 Foliar elemental trait comparisons

Our results are consistent with our hypothesis in that our coniferous species, balsam fir and black spruce (bF-bS), should exhibit similar spatial patterns of aggregation, in foliar C, N, and P traits. However, the co-dispersion coefficient did fluctuate with increasing distance indicating that the strength of these relationships depends on scale and likely more anisotrophic than isotrophic (Figure 4.2). At our Unicorn study site, foliar C, N, and P had a maximum co-dispersion coefficient of 0.55, 0.53, and 0.61 at distances of 70 m, 239 m, and 98 m, respectively. At our Dunphy's Pond study site, C, N, and P had a maximum co-dispersion coefficient of 0.55, 0.73, 0.67 at distances of 194 m, 44 m, and 224 m, respectively. The spatial patterns of trait co-variability tended to be consistent between sites, with significant positive correlations for C, N, and P detected at our older study site, Dunphy's Pond, $R^2 = 0.385, 0.500, 0.531$, *p*-value = 0.023, 0.003, 0.002, respectively. Only foliar P was significantly correlated at our Unicorn study site $R^2 = 0.393$ and *p*-value = 0.028.

In comparison, we hypothesized that our deciduous species, red maple and white birch (rM-wB), would also exhibit similar spatial patterns of aggregation and this relationship was generally observed for foliar C, N, and P traits (Figure 4.2). However, the strength of these relationships varied with distance and direction. At our Unicorn study site foliar C, N, and P traits had a maximum co-dispersion coefficient of 1 at a 16 m distance for each trait. At our Dunphy's Pond study site, C, N, and P had a maximum co-dispersion coefficient of 0.44, 0.36, 0.30 at 48 m, 176 m, 176 m distances, respectively (Appendix C.3, Table C.3.1). Significant positive correlations were detected for foliar C, N, and P but only at our Unicorn study site, R^2 = 0.594, 0.611, 0.694, *p*-value = 0.020, 0.012, 0.010, respectively.

Our comparison of species with differing resource strategies (conifers vs deciduous) yielded mixed results that differed by trait and study site (Figure 4.2). Notably, at our Dunphy's Pond study site foliar C, N, and P for balsam fir and red maple had a maximum co-dispersion coefficient of 1 at a 16 m distance for each trait, with N and P significantly correlated (R^2 = 0.508, 0.766, and *p*-value = 0.002, 0.0001, respectively); N was significantly correlated at our Unicorn study site (R^2 = 0.412, *p*-value = 0.020). Balsam fir and white birch N and P traits were highly aggregated at close distances, with a maximum co-dispersion coefficient of 1 at a 14 m distance at our Unicorn study site; C was significantly correlated at our Dunphy's Pond study site (R^2 = 0.800, *p*-value = 3.0×10^{-5}), with a maximum co-dispersion coefficient of 0.90 at a 48 m distance. Black spruce and red maple foliar C, N, and P traits were highly aggregated, with a maximum co-dispersion coefficient of 1 at a 14 m distance; foliar N and P were significantly correlated at our Dunphy's Pond study site (R^2 = 0.568, 0.490, *p*-value = 0.006, 0.005, respectively) with a maximum co-dispersion coefficient of 0.71 and 0.66 at 104 m and 74 m, distances respectively. Although black spruce and white birch foliar C, N and P traits were highly aggregated at our Unicorn study site, with a maximum co-dispersion coefficient of 1 at a16 m distance, no significance was detected.

4.4.2 Foliar stoichiometric trait comparisons

We hypothesized our coniferous species (bF-bS) would have similar spatial patterns of aggregation. Although spatial aggregation was the dominant trend for co-dispersion in these traits, the pattern did vary with distance and direction (Figure 4.3). At our Dunphy's Pond study site foliar C:N, C:P, and N:P were significantly correlated (R^2 = 0.583, 0.542, 0.708, *p*-value = 0.0002, 0.001, 0.0004, respectively) with a maximum co-dispersion coefficient of 0.73, 0.66, 0.83 at 44 m, 224 m, 224 m distances, respectively. At our Unicorn study site foliar N:P was significantly correlated (R^2 = 0.601, *p*-value = 0.001) with a maximum co-dispersion coefficient of 0.81 at a 98 m distance. Notably, only foliar C:N and C:P traits had a negative minimum co-dispersion coefficient of -0.79, -0.3 at a 42 m distance, respectively.

We also hypothesized our deciduous species would have similar spatial patterns in foliar stoichiometric traits. Our results do not support this hypothesis for all foliar stoichiometric traits across study sites. Significant correlations were only determined for foliar C:P and N:P traits at our Unicorn study site (R^2 = 0.689, 0.841, *p*-value = 0.005, 0.0001, respectively), with a maximum co-dispersion coefficient of 1 at a 16 m distance and an average co-dispersion coefficient of 0.73 and 0.87, respectively. Foliar C:N at our Unicorn study site also had a maximum co-dispersion coefficient of 1 at a 16 m distance (R^2 = 0.313). Spatial patterns varied considerably between our two forest stands, with maximum co-dispersion coefficients of 0.34, 0.44, 0.59 at 176 m, 80 m, and 240 m distances for foliar C:N, C:P, and N:P traits at our Dunphy's Pond study site.

We expected species with differing resource strategies (conifers vs deciduous) to have dissimilar spatial patterns in foliar stoichiometric traits; however, we found significant correlations between our coniferous and deciduous traits. Balsam fir and red maple had significant correlations of C:N, C:P, and N:P at our Dunphy's Pond study site (R^2 = 0.525, 0.720, 0.787, *p*-value = 0.0002, 0.001, 0.0004, respectively) with a maximum co-dispersion coefficient of 0.84, 1, and 1 at 50 m, 16 m, and 16 m distances, respectively. Foliar C:P and N:P traits were significantly correlated at our Unicorn study site (R^2 = 0.416, 0.523, *p*-value = 0.046, 0.008, respectively), with a maximum co-dispersion coefficient of 0.59 and 0.84 at 182 m and 42 m distances, respectively. Balsam fir and white birch had significant correlations of C:P and N:P at our Unicorn study site (R^2 = 0.397, 0.500, *p*-value = 0.045, 0.004, respectively) with a maximum co-dispersion coefficient of 1 at a 14 m distance. Foliar N:P was also significantly correlated at our Dunphy's Pond study site (R^2 = 0.606, *p*-value = 0.005) with a maximum co-dispersion coefficient of 0.81 at a 176 m distance. Black spruce and red maple had significantly correlated foliar C:N, C:P, and N:P traits at our Dunphy's Pond study site (R^2 = 0.597, 0.464, 0.655, *p*-value = 0.003, 0.007, 0.003, respectively) with a maximum co-dispersion coefficient of 0.75, 0.7. 0.74 at 104 m, 194 m, and 224 m distances, respectively. Foliar C:N, C:P, and N:P traits had a maximum co-dispersion coefficient of 1 at a 14 m distance for our Unicorn study site. For black spruce and white birch comparisons, no significant relationships were determined, although foliar C:N, C:P, and N:P had a maximum co-dispersion coefficient of 1 at a 16 m distance for our Unicorn study site.

4.4.3 Foliar phytochemical trait comparisons

Although we hypothesized that balsam fir and black spruce would have similar spatial patterns of aggregation in foliar phytochemical traits, we detected no significant relationships at either study sites (Figure 4.4). In most cases, foliar phytochemical traits exhibited either weak spatial aggregation (monoterpenic alcohol and phytochemical diversity at Unicorn) or weak segregation (terpene, monoterpene, monoterpenic ester at both study sites, with sesquiterpene and phytochemical diversity at Dunphy's Pond). In general, strong spatial aggregation or segregation relationships occurred at 0 metres and diminished after 50 metres with a co-dispersion coefficient occurring close to 0 for the remaining distances.

4.5 Discussion

Community assembly theory offers a potential explanation for the spatial trait patterns of co-occurring species. Although the twin filter model conceptualizes the structure of traits via a filtering processes, it does not consider the spatial scale at which trait divergence may occur (Vellend 2016). Moreover, there are limitations in testing trait co-variability as not all traits are universal across species (Wright et al. 2005). Here we use universal and common traits across co-occurring species to evaluate trait co-variability between co-occurring species in a spatially explicit context between two forest stands. Our results demonstrate that there is scale, direction, site, and species-specific variability in the spatial relationships of foliar ESP traits. We show that the functional traits of species with similar resource strategies do not always spatially vary in similar ways, often showing anisotropic relationships. Counter to our predictions, species with dissimilar strategies often had significantly correlated spatial patterns in their traits. The spatial patterns of these traits between co-occurring species allow us to assess how ecosystem processes may vary at a small spatial extent, with consequences for resource hot spots of forage quality and changes in nutrient cycling.

4.5.1 Foliar elemental traits

The elemental composition of foliar material is often influenced by soil nutrient resources, temperature, and precipitation (Krishna and Mohan 2017, Lu et al. 2020). Across forest stands of differing ages, differences in community structure, such as the presence and abundance of species with differing litter contributions to soil nutrient resources, and tolerance for differing soil water saturation levels likely influence the foliar elemental traits of species (Urbina et al. 2017, He et al. 2019). However, species with similar resource strategies should conceivably respond in a similar way to these community gradients. Our results suggest that generalizations about community gradients may only hold for certain habitats and traits. For example, we found that foliar N and P were partially correlated despite species having dissimilar resource strategies. Thus, the way in which species with dissimilar resource strategies acquire and use soil nutrients may be similar under certain environmental conditions. By contrast, white birch and our conifer species were not spatially coordinated in foliar traits – likely attributed to differences in resource acquisition structures. For instance, Weiser et al., 2016 found that clonal species navigate spatially heterogeneous soil environments more effectively than unitary plants, as they develop highly specialized root structures that allow for the distribution of resources among connected individuals. When white birch has mycorrhizal relationships, it may behave similar to a clonal species and thus those association make it better equipped to navigate soil resource environments and disperse N and P resources to connected individuals (Simard et al., 1997). Thus, its spatial co-variability of foliar elemental traits with other species might be less constrained by environmental filters. Although we did find some spatial relationships of white birch with other species (foliar C for bF-wB), other environmental factors such as light availability via canopy gaps and species arrangements might influence the foliar elemental traits of white birch at very fine scales (Domínguez et al. 2012).

The co-variability of foliar elemental traits between our species were largely site specific and depend on scale and direction. For instance, at close distances balsam fir and black spruce exhibit no spatial relationship in foliar C, N, or P traits indicating they may be accessing different resources when positioned close together. Patterns in their foliar C, N, and P only emerge around 100 meters, and the direction of these relationships (aggregation or segregation) varies with distance suggesting that there are differences in nutrient use or competition for resources. This is a common observation. For example, Ellison et al. 2019, used co-dispersion analysis to assess the spatial relationship of foundation species with community structure (beta diversity), found that spatial segregation occurred at local scales while spatial aggregation occurred at larger scales suggesting that distance and directionality of priority effects of foundation species matters. From our results, community structure likely plays a role in influencing the foliar elemental traits of our species, given the mixed spatial patterns between sites. Nonetheless, on the landscape where differing seral stages of forests represent patches, we can hypothesize, given known community structure of those patches, that foliar elemental traits may co-vary within a patch, and thus having consequences for how pollinators, herbivores, and carnivores may navigate within habitats in search for resources (Leroux 2018, Schmitz et al. 2018, Buchkowski et al. 2019).

4.5.2 Foliar stoichiometric traits

Similar to our foliar elemental trait results, we find mixed support for our stoichiometric hypotheses, where spatial foliar stoichiometric trait relationships vary by site and for differing species comparisons. Foliar stoichiometric traits are often useful indicators of site-level differences in nutrient conditions where co-limitation of N or P constrains physiological function

(Harpole et al. 2011). For instance, differences in leaf litter input between co-occurring conifer and deciduous species may influence the relative amounts of N and P resources and in turn influence how these species retrieve these nutrients (Gartner and Cardon 2004, Persson et al. 2010). Our results suggest that there are some similarities in how species may respond to differing environmental conditions and possible distance thresholds at which co-limitation may regulate trait variability. For instance, we found that foliar C:P and N:P for balsam fir and black spruce exhibit similar spatial relationships between sites, suggesting strong symmetrical responses to environmental conditions. In comparison, our deciduous species varied in their spatial relationships widely between sites. In general, deciduous species display great flexibility in their stoichiometric phenotypes and under differing resource conditions may optimize elemental regulation differently (Wirtz and Kerimoglu 2016, Leal et al. 2017). Thus, the different spatial co-dispersion patterns between sites for our deciduous species may reflect differences in resource optimization under varying environmental conditions. For instance, our younger site had strong spatial aggregation patterns and significant relationships for our deciduous species foliar C:P and N:P traits compared to our older site. This may be due to successional climax factors in younger seral stands with a higher deciduous tree component where leaf litter results in higher N inputs to soil (Apple et al. 2009, Bergeron and Fenton 2012). Moreover, in the boreal forest, N and P limitation may offset site-level conditions that influence patterns of availability and recycling (see Goswami et al. 2018). Our results suggest that at close distances (0-50 metres) there are strong signals of spatial segregation or aggregation in foliar stoichiometric traits but these relationships, in most of our species comparisons, breakdown with increasing scale.

4.5.3 Foliar phytochemical traits

Our hypotheses for foliar phytochemical traits of conifers were not supported. We assumed that the spatial patterns of foliar phytochemical traits in our conifer species would be given their constituent strategies to maintain baseline amount of terpenoid concentrations. However, phytochemical traits have been shown to vary in response to herbivory (Karban et al. 1999), soil nutrients (Hunter 2016), community structure (Kessler 2015), and along abiotic gradients such as elevation (Callis-Duehl et al. 2017). We do find some evidence to suggest strong spatial aggregation or segregation at close distances, generally 0-50 metres. A potential explanation for this may be forage selection by moose. On the island of Newfoundland, balsam fir and black spruce, as with our other study species, commonly co-occur (South 1983). Despite the availability of both conifers as potential forage options, moose browse balsam fir considerably more over black spruce (Dodds 1960, Gosse et al. 2011). In turn, this forage preference could influence differential concentrations of induced foliar phytochemicals (Karban et al. 1999). Although limited information is available on how these phytochemicals interact to deter or inhibit moose herbivory, the spatial patterns of these traits between our conifer species suggests that at local scales (close distances) moose browsing of balsam fir may elicit a response by black spruce via aromatic chemical signaling (Hussain et al. 2019). For instance, Champagne et al. 2018 found that browsing of balsam fir by white tailed deer (*Odocoileus virginianus* (Zimmermann, 1780)) at the plot scale (small spatial extent) was spatially associated with low nutritional quality neighbourhood vegetation. Thus, as a strategy to deter being browsed, plants may allocate resources differently (i.e., C and N to terpenoid or tannin production) to disguise their nutritional value in the forage buffet.

4.6 Conclusion

Here, we show how different foliar chemical traits spatially co-vary for four common boreal tree species. We find that the traits of species with similar and dissimilar resource strategies may create spatial contours from which we can make fine scale predictions about how herbivores make spatial decisions with implications for biogeochemical processes (Schmitz et al. 2018, Rizzuto et al. 2021). Previous work has demonstrated the utility of spatial co-dispersion in determining species-environmental relationships (Buckley et al. 2016a), co-occurrence patterns (Buckley et al. 2016a), identifying ecotoxicological hot spots (Eccles et al. 2019), species-community relationships (Ellison et al. 2019), host-parasite interactions (Jorge and Poulin 2018), and community structure processes (Chi-Yu et al. 2017). Although spatial co-dispersion analysis has revealed how the different spatial patterns of ecological processes co-vary, few studies have used this approach to investigate spatial trait relationships between co-occurring species (for complementary approaches see Biswas et al. 2016). Our research demonstrates the usefulness of understanding how and where plant functional traits may co-vary between co-occurring species in an attempt to bridge gaps between community level processes and spatial ecology, with implications for forage selection. This work provides a foundation to consider other mechanisms of why plant functional traits might covary between co-occurring species. For instance, using spatial autocorrelation may reveal differences in the scale dependent properties of functional traits. As well, codispersion analysis could be coupled with plot level environmental data such as soil structure, canopy closure, micro-topography, and distance to water sources to identify factors that may drive the co-variability of functional traits or reveal co-limitation parameters between co-occurring species.

4.7 Data Availability

All data and R code used in the analyses are available via a Figshare repository at:

https://doi.org/10.6084/m9.figshare.19141856.v1

4.8 References

Apple, J. L., M. Wink, S. E. Wills, and J. G. Bishop. 2009. Successional change in phosphorus stoichiometry explains the inverse relationship between herbivory and lupin density on Mount St. Helens. PLoS ONE 4:e7807.

Bergeron, Y., and N. J. Fenton. 2012. Boreal forests of eastern Canada revisited: old growth, nonfire disturbances, forest succession, and biodiversity. Botany 90:509–523.

Biswas, S. R., A. U. Mallik, N. T. Braithwaite, and H. H. Wagner. 2016. A conceptual framework for the spatial analysis of functional trait diversity. Oikos 125:192–200.

Buchkowski, R. W., S. J. Leroux, and O. J. Schmitz. 2019. Microbial and animal nutrient limitation change the distribution of nitrogen within coupled green and brown food chains. Ecology 100:e02674.

Buckley, H. L., B. S. Case, and A. M. Ellison. 2016a. Using codispersion analysis to characterize spatial patterns in species co-occurrences. Ecology 97:32–39.

Buckley, H. L., B. S. Case, J. K. Zimmerman, J. Thompson, J. A. Myers, and A. M. Ellison. 2016b. Using codispersion analysis to quantify and understand spatial patterns in species–environment relationships. New Phytologist 211:735–749.

Cachet, T., H. Brevard, A. Chaintreau, J. Demyttenaere, L. French, K. Gassenmeier, D. Joulain, T. Koenig, H. Leijs, P. Liddle, G. Loesing, M. Marchant, Ph. Merle, K. Saito, C. Schippa, F. Sekiya, and T. Smith. 2016. IOFI recommended practice for the use of predicted relative-response factors for the rapid quantification of volatile flavouring compounds by GC-FID. Flavour and Fragrance Journal 31:191–194.

Callis-Duehl, K., P. Vittoz, E. Defossez, and S. Rasmann. 2017. Community-level relaxation of plant defenses against herbivores at high elevation. Plant Ecology 218:291–304.

Champagne, E., B. D. Moore, S. D. Côté, and J.-P. Tremblay. 2018. Spatial correlations between browsing on balsam fir by white-tailed deer and the nutritional value of neighboring winter forage. Ecology and Evolution 8:2812–2823.

Chi-Yu, W., Y. Kuoh-Cheng, H. Chang-Fu, C. Hsieh, and M.-H. Su. 2017. Local neighborhood communities in the understory play a critical role by affecting regeneration niches and subsequent community assembly in a montane cloud forest. Ecological Research; Tokyo 32:821–833.

Cuevas, F., E. Porcu, and R. Vallejos. 2013. Study of spatial relationships between two sets of variables: a nonparametric approach. Journal of Nonparametric Statistics:695–714.

Dodds, D. G. 1960. Food competition and range relationships of moose and snowshoe hare in newfoundland. The Journal of Wildlife Management 24:52.

Domínguez, M. T., C. Aponte, I. M. Pérez-Ramos, L. V. García, R. Villar, and T. Marañón. 2012. Relationships between leaf morphological traits, nutrient concentrations and isotopic signatures for Mediterranean woody plant species and communities. Plant and Soil 357:407–424.

Dutilleul, P., P. Clifford, S. Richardson, and D. Hemon. 1993. Modifying the t test for assessing the correlation between two spatial processes. Biometrics 49:305.

Eccles, K. M., B. D. Pauli, and H. M. Chan. 2019. The use of geographic information systems for spatial ecological risk assessments: an example from the Athabasca oil sands area in Canada. Environmental Toxicology and Chemistry 38:2797–2810.

Ellison, A. M., H. L. Buckley, B. S. Case, D. Cardenas, Á. J. Duque, J. A. Lutz, J. A. Myers, D. A. Orwig, and J. K. Zimmerman. 2019. Species diversity associated with foundation species in temperate and tropical forests. Forests 10:128.

Fortin, M.-J., and S. Payette. 2002. How to test the significance of the relation between spatially autocorrelated data at the landscape scale: A case study using fire and forest maps. Écoscience 9:213–218.

Gartner, T. B., and Z. G. Cardon. 2004. Decomposition dynamics in mixed-species leaf litter. Oikos 104:230–246.

Gosse, J., L. Hermanutz, B. McLaren, P. Deering, and T. Knight. 2011. Degradation of boreal forests by nonnative herbivores in Newfoundland's National Parks: recommendations for ecosystem restoration. Natural Areas Journal 31:331–339.

Goswami, S., M. C. Fisk, M. A. Vadeboncoeur, M. Garrison-Johnston, R. D. Yanai, and T. J. Fahey. 2018. Phosphorus limitation of aboveground production in northern hardwood forests. Ecology 99:438–449.

Grime, J. P., and S. Pierce. 2012. The evolutionary strategies that shape ecosystems. Wiley-Blackwell, Chichester, West Sussex, UK ; Hoboken, NJ.

Harpole, W. S., J. T. Ngai, E. E. Cleland, E. W. Seabloom, E. T. Borer, M. E. S. Bracken, J. J. Elser, D. S. Gruner, H. Hillebrand, J. B. Shurin, and J. E. Smith. 2011. Nutrient co-limitation of primary producer communities. Ecology Letters 14:852–862.

He, P., S. Fontana, J. Sardans, J. Peñuelas, A. Gessler, M. Schaub, A. Rigling, H. Li, Y. Jiang, and M.-H. Li. 2019. The biogeochemical niche shifts of *Pinus sylvestris var. mongolica* along an environmental gradient. Environmental and Experimental Botany 167:103825.

Heckford TR, Leroux SJ, Vander Wal E, et al (2022) Spatially explicit correlates of plant functional traits inform landscape patterns of resource quality. Landsc Ecol 37:59–80. https://doi.org/10.1007/s10980-021-01334-3

Hobbie, S. E. 2015. Plant species effects on nutrient cycling: revisiting litter feedbacks. Trends in Ecology & Evolution 30:357–363.

Hunter, M. D. 2016. The phytochemical landscape: linking trophic interactions and nutrient dynamics. Princeton University Press.

Hussain, A., J. C. Rodriguez-Ramos, and N. Erbilgin. 2019. Spatial characteristics of volatile communication in lodgepole pine trees: Evidence of kin recognition and intra-species support. Science of The Total Environment 692:127–135.

Jorge, F., and R. Poulin. 2018. Poor geographical match between the distributions of host diversity and parasite discovery effort. Proceedings of the Royal Society B: Biological Sciences 285:20180072.

Karban, R., A. A. Agrawal, J. S. Thaler, and L. S. Adler. 1999. Induced plant responses and information content about risk of herbivory. Trends in Ecology & Evolution 14:443–447.

Kaspari, M., and J. S. Powers. 2016. Biogeochemistry and geographical ecology: embracing all twenty-five elements required to build organisms. The American Naturalist 188:S62–S73.

Kessler, A. 2015. The information landscape of plant constitutive and induced secondary metabolite production. Current Opinion in Insect Science 8:47–53.

Knops, J. M. H., K. L. Bradley, and D. A. Wedin. 2002. Mechanisms of plant species impacts on ecosystem nitrogen cycling. Ecology Letters 5:454–466.

Kraft, N. J. B., P. B. Adler, O. Godoy, E. C. James, S. Fuller, and J. M. Levine. 2015. Community assembly, coexistence and the environmental filtering metaphor. Functional Ecology 29:592–599.

Kranabetter, J. M., K. K. McLauchlan, S. K. Enders, J. M. Fraterrigo, P. E. Higuera, J. L. Morris, E. B. Rastetter, R. Barnes, B. Buma, D. G. Gavin, L. M. Gerhart, L. Gillson, P. Hietz, M.

C. Mack, B. McNeil, and S. Perakis. 2016. A framework to assess biogeochemical response to ecosystem disturbance using nutrient partitioning ratios. Ecosystems 19:387–395.

Krishna, M. P., and M. Mohan. 2017. Litter decomposition in forest ecosystems: a review. Energy, Ecology and Environment 2:236–249.

Leal, M. C., O. Seehausen, and B. Matthews. 2017. The ecology and evolution of stoichiometric phenotypes. Trends in Ecology & Evolution 32:108–117.

Leroux, S. J. 2018. Ecological, evolutionary, and geographical correlates of variation in consumer elemental composition. Functional Ecology 32:2282–2284.

Levin, S. A. 1992. The problem of pattern and scale in ecology: the Robert H. MacArthur award lecture. Ecology 73:1943–1967.

Lu, Y., R. A. Duursma, C. E. Farrior, B. E. Medlyn, and X. Feng. 2020. Optimal stomatal drought response shaped by competition for water and hydraulic risk can explain plant trait covariation. New Phytologist 225:1206–1217.

Mcgill, B., B. Enquist, E. Weiher, and M. Westoby. 2006. Rebuilding community ecology from functional traits. Trends in Ecology & Evolution 21:178–185.

Niinemets, Ü., and O. Kull. 1998. Stoichiometry of foliar carbon constituents varies along light gradients in temperate woody canopies: implications for foliage morphological plasticity. Tree Physiology 18:467–479.

Osorio, F., R. Vallejos, F. Cuevas, and D. Manchilla. 2020. SpatialPack.

Peñuelas, J., M. Fernández-Martínez, P. Ciais, D. Jou, S. Piao, M. Obersteiner, S. Vicca, I. A. Janssens, and J. Sardans. 2019. The bioelements, the elementome, and the biogeochemical niche. Ecology 100(5):e02652.

Persson, J., P. Fink, A. Goto, J. M. Hood, J. Jonas, and S. Kato. 2010. To be or not to be what you eat: regulation of stoichiometric homeostasis among autotrophs and heterotrophs. Oikos 119:741–751.

Pottier, J., R. h. Marrs, and A. Bédécarrats. 2007. Integrating ecological features of species in spatial pattern analysis of a plant community. Journal of Vegetation Science 18:223–230.

Rizzuto, M., S. J. Leroux, E. Vander Wal, I. C. Richmond, T. R. Heckford, J. Balluffi-Fry, and Y. F. Wiersma. 2021. Forage stoichiometry predicts the home range size of a small terrestrial herbivore. Oecologia 197:327–338.

Santiago, L. S., K. Kitajima, S. J. Wright, and S. S. Mulkey. 2004. Coordinated changes in photosynthesis, water relations and leaf nutritional traits of canopy trees along a precipitation gradient in lowland tropical forest. Oecologia 139:495–502.

Sardans, J., H. Vallicrosa, P. Zuccarini, G. Farré-Armengol, M. Fernández-Martínez, G. Peguero, A. Gargallo-Garriga, P. Ciais, I. A. Janssens, M. Obersteiner, A. Richter, and J. Peñuelas. 2021. Empirical support for the biogeochemical niche hypothesis in forest trees. Nature Ecology & Evolution 5:184–194.

Schmitz, O. J., C. C. Wilmers, S. J. Leroux, C. E. Doughty, T. B. Atwood, M. Galetti, A. B. Davies, and S. J. Goetz. 2018. Animals and the zoogeochemistry of the carbon cycle. Science 362:eaar3213.

Simard, S. W., Jones, M. D., Durall, D. M., Perry, D. A., Myrold, D. D., & Molina, R. (1997). Reciprocal transfer of carbon isotopes between ectomycorrhizal *Betula papyrifera* and *Pseudotsuga menziesii*. *The New Phytologist*, *137*(3), 529–542.

South, R. G. 1983. Biogeography and ecology of the island of Newfoundland. Dr. W. Junk Publishers, The Hague, The Netherlands.

Sterner, R. W., and J. J. Elser. 2002. Ecological stoichiometry: the biology of elements from molecules to the biosphere. Princeton University Press, Princeton.

Urbina, I., J. Sardans, O. Grau, C. Beierkuhnlein, A. Jentsch, J. Kreyling, and J. Peñuelas. 2017. Plant community composition affects the species biogeochemical niche. Ecosphere 8:e01801.

Vallejos, R., F. Osorio, and D. Mancilla. 2015. The codispersion map: a graphical tool to visualize the association between two spatial variables. Statistica Neerlandica 69:298–314.

Vellend, M. 2016. The theory of ecological communities (MPB-57). Princeton University Press.

Weiser, M., T. Koubek, and T. Herben. 2016. Root foraging performance and life-history traits. Frontiers in Plant Science 7.

Wirtz, K. W., and O. Kerimoglu. 2016. Autotrophic stoichiometry emerging from optimality and variable co-limitation. Frontiers in Ecology and Evolution 4.

Wright, I. J., P. B. Reich, J. H. C. Cornelissen, D. S. Falster, E. Garnier, K. Hikosaka, B. B. Lamont, W. Lee, J. Oleksyn, N. Osada, H. Poorter, R. Villar, D. I. Warton, and M. Westoby. 2005. Assessing the generality of global leaf trait relationships. New Phytologist 166:485–496.

4.9 Figures

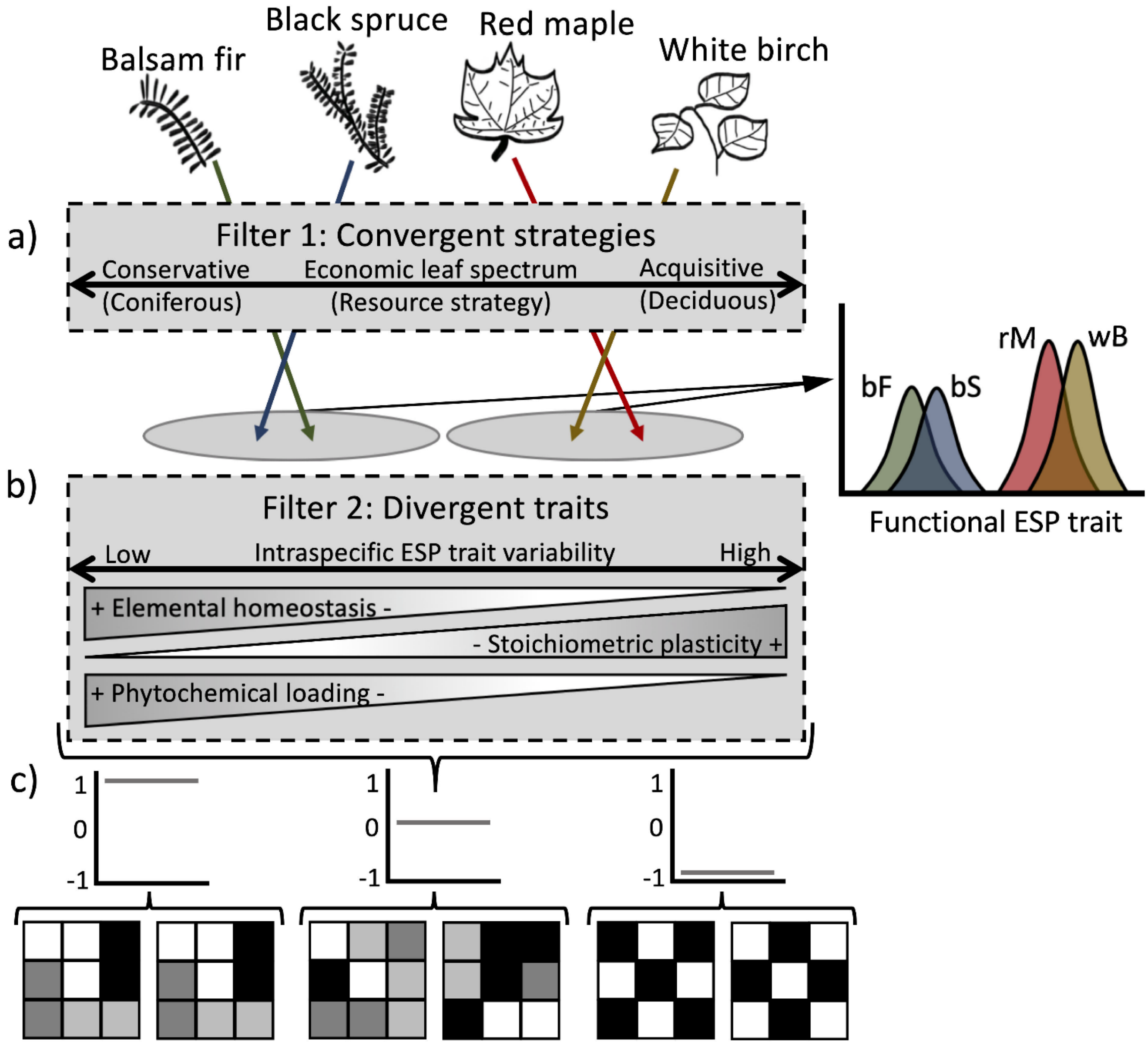

Figure 4.1 Conceptual diagram for spatially explicit trait patterns at a local scale. The twin filter model of community assembly suggests that the spatial patterns of species and their traits may be predicted by a hierarchical, two-step filtering process. The first filter (a) selects for species with convergent strategies allowing species to compete broadly within the existing community shaped by current and historic environmental conditions. In this study we group our species, generally,

by their resource strategy. For instance, slow-growing, shade-tolerant conifer species produce long-lived needles that often exhibit low morphological variability and constrained growth geometry. These differences between resources strategies reflect how these species acquire and use resources under differing environmental conditions. We use groups of coniferous (conservative strategy) species, balsam fir (bF) and black spruce (bS), and deciduous (acquisitive strategy) species, red maple (rM) and white birch (wB). The second filter (b) selects for divergent traits. Generally, coniferous species exhibit low intraspecific trait variability compared to deciduous species. In our study we compare how the foliar elemental (C, N, P), stoichiometric (C:N, C:P, N:P), and phytochemical (terpenoids) traits vary spatially among our species. Differences in resources strategies among species are reflected in their elemental homeostasis and stoichiometric plasticity. For instance, in response to environmental conditions, conifers maintain a high elemental homeostasis and low stoichiometric plasticity relative to deciduous species which exhibit a low elemental homeostasis and high stoichiometric plasticity – allowing them to persist in variable environments. Our study only looks at the foliar phytochemical traits for conifers as they exhibit constituent strategies, maintaining a baseline phytochemical composition, with increased quantities in response to herbivory. In comparison, deciduous species have a compensatory strategy and only invest in phytochemicals after an herbivory event. Thus, conifers maintain a high phytochemical loading compared to deciduous species. Here, we use species with similar and differing resource strategies to test how filter processes influence the spatial patterning of foliar elemental, stoichiometric, and phytochemical (ESP) traits. We generally, expect species with similar resource strategies to exhibit similar spatial patterns as compared to species with contrasting strategies. We apply spatial co-dispersion analysis (c) to assess these spatial relationships where a value of 1 suggests spatial aggregation, 0 represents no relationship, and -1 indicates spatial segregation. In addition, co-dispersion analysis assesses spatial relationships across distances and allows us to detect at which spatial scales relationships exist or diminish. Below part (d), we show how the spatial patterns of these relationships may look when spatialized via interpolation.

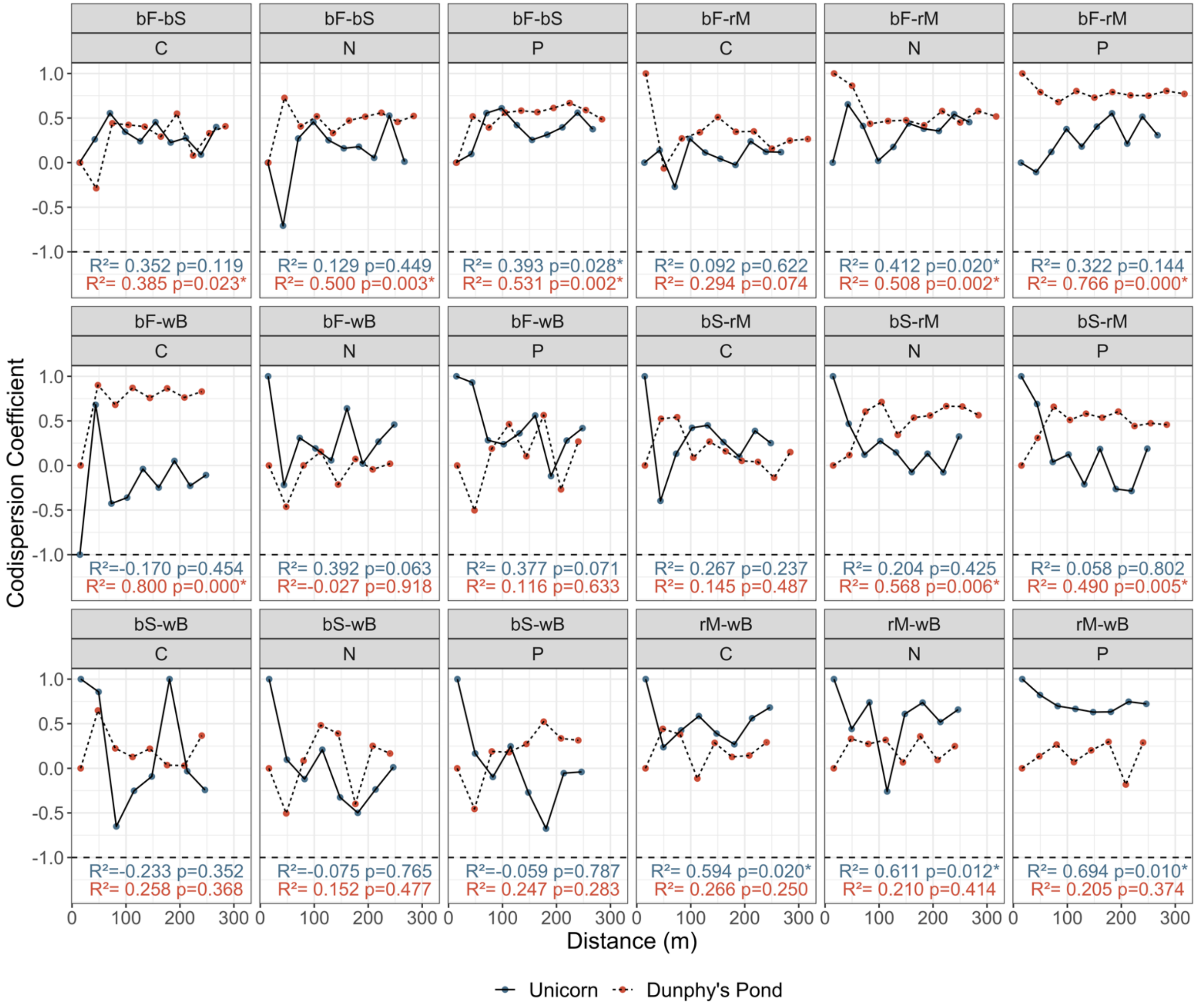
bF-bS C
R²= 0.352 p=0.119
R²= 0.385 p=0.023*
bF-bS N
R²= 0.129 p=0.449
R²= 0.500 p=0.003*
bF-bS P
R²= 0.393 p=0.028*
R²= 0.531 p=0.002*
bF-rM C
R²= 0.092 p=0.622
R²= 0.294 p=0.074
bF-rM N
R²= 0.412 p=0.020*
R²= 0.508 p=0.002*
bF-rM P
R²= 0.322 p=0.144
R²= 0.766 p=0.000*
bF-wB C
R²=-0.170 p=0.454
R²= 0.800 p=0.000*
bF-wB N
R²= 0.392 p=0.063
R²=-0.027 p=0.918
bF-wB P
R²= 0.377 p=0.071
R²= 0.116 p=0.633
bS-rM C
R²= 0.267 p=0.237
R²= 0.145 p=0.487
bS-rM N
R²= 0.204 p=0.425
R²= 0.568 p=0.006*
bS-rM P
R²= 0.058 p=0.802
R²= 0.490 p=0.005*
bS-wB C
R²=-0.233 p=0.352
R²= 0.258 p=0.368
bS-wB N
R²=-0.075 p=0.765
R²= 0.152 p=0.477
bS-wB P
R²=-0.059 p=0.787
R²= 0.247 p=0.283
rM-wB C
R²= 0.594 p=0.020*
R²= 0.266 p=0.250
rM-wB N
R²= 0.611 p=0.012*
R²= 0.210 p=0.414
rM-wB P
R²= 0.694 p=0.010*
R²= 0.205 p=0.374
Codispersion Coefficient
1.0
0.5
0.0
-0.5
-1.0
Distance (m)
0
100
200
300
Unicorn
Dunphy's Pond

Figure 4.2 Spatial co-dispersion across spatial gradients of distance (metres) for the foliar elemental (C, N, and P) traits of our focal species: balsam fir (bF), black spruce (bS), red maple (rM), and white birch (wB). Co-dispersion values range from -1 (spatial segregation) to +1 (spatial aggregation). Colour codes for data points, R^2 values, and statistical significance are used to represent our study sites (blue = Dunphy’s Pond 80-100 years old site, and red = Unicorn 60-80 years old site).

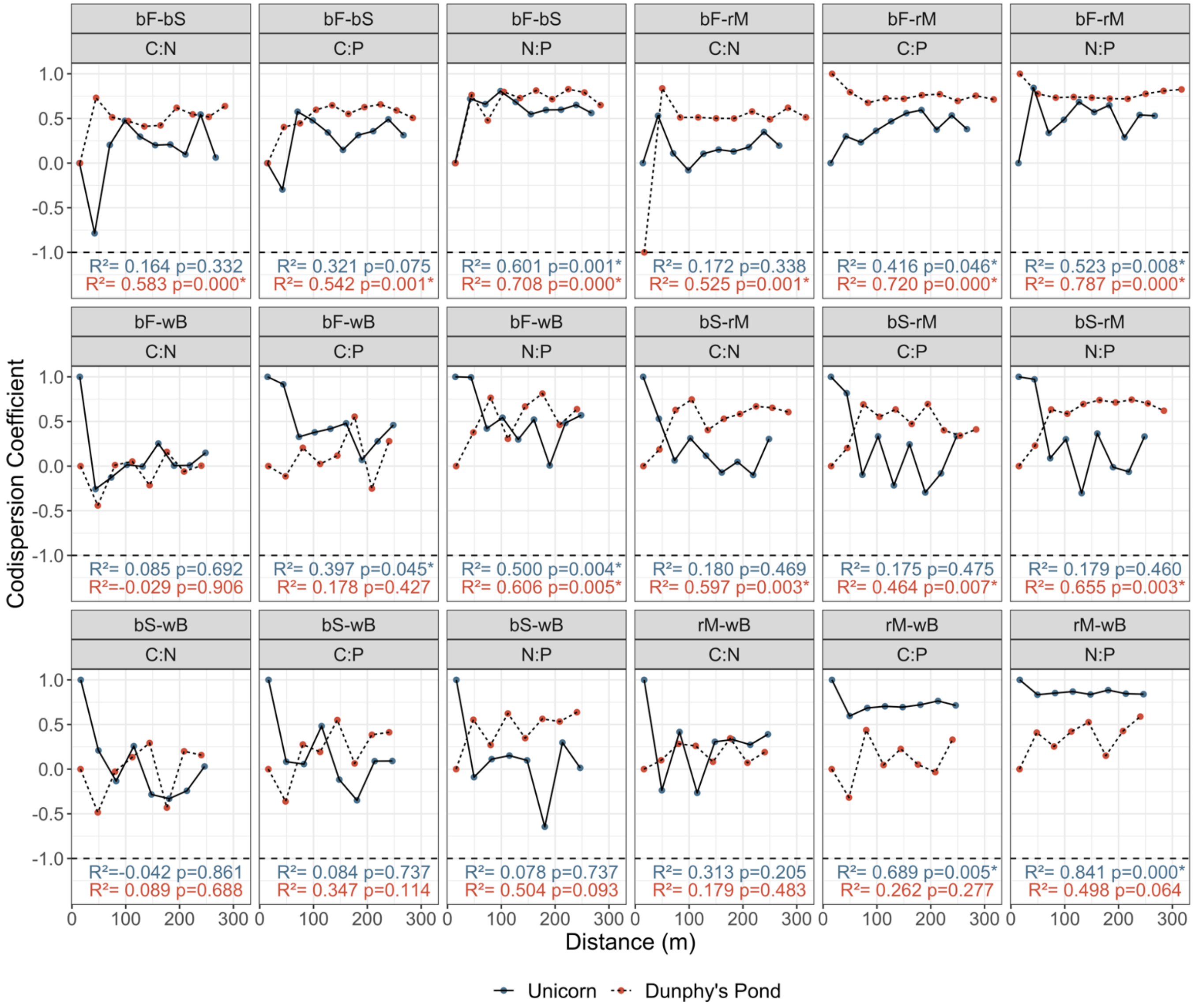
bF-bS C:N
bF-bS C:P
bF-bS N:P
bF-rM C:N
bF-rM C:P
bF-rM N:P
R²= 0.164 p=0.332
R²= 0.583 p=0.000*
R²= 0.321 p=0.075
R²= 0.542 p=0.001*
R²= 0.601 p=0.001*
R²= 0.708 p=0.000*
R²= 0.172 p=0.338
R²= 0.525 p=0.001*
R²= 0.416 p=0.046*
R²= 0.720 p=0.000*
R²= 0.523 p=0.008*
R²= 0.787 p=0.000*
bF-wB C:N
bF-wB C:P
bF-wB N:P
bS-rM C:N
bS-rM C:P
bS-rM N:P
R²= 0.085 p=0.692
R²=-0.029 p=0.906
R²= 0.397 p=0.045*
R²= 0.178 p=0.427
R²= 0.500 p=0.004*
R²= 0.606 p=0.005*
R²= 0.180 p=0.469
R²= 0.597 p=0.003*
R²= 0.175 p=0.475
R²= 0.464 p=0.007*
R²= 0.179 p=0.460
R²= 0.655 p=0.003*
bS-wB C:N
bS-wB C:P
bS-wB N:P
rM-wB C:N
rM-wB C:P
rM-wB N:P
R²=-0.042 p=0.861
R²= 0.089 p=0.688
R²= 0.084 p=0.737
R²= 0.347 p=0.114
R²= 0.078 p=0.737
R²= 0.504 p=0.093
R²= 0.313 p=0.205
R²= 0.179 p=0.483
R²= 0.689 p=0.005*
R²= 0.262 p=0.277
R²= 0.841 p=0.000*
R²= 0.498 p=0.064
Codispersion Coefficient
1.0
0.5
0.0
-0.5
-1.0
Distance (m)
0
100
200
300
Unicorn
Dunphy's Pond

Figure 4.3 Spatial co-dispersion across spatial gradients of distance (metres) for the foliar stoichiometric (C:N, C:P, and N:P) traits of our focal species: balsam fir (bF), black spruce (bS), red maple (rM), and white birch (wB). Co-dispersion values range from -1 (spatial segregation) to +1 (spatial aggregation). Colour codes for data points, R^2 values, and statistical significance are used to represent our study sites (blue = Dunphy’s Pond 80-100 years old site, and red = Unicorn 60-80 years old site).

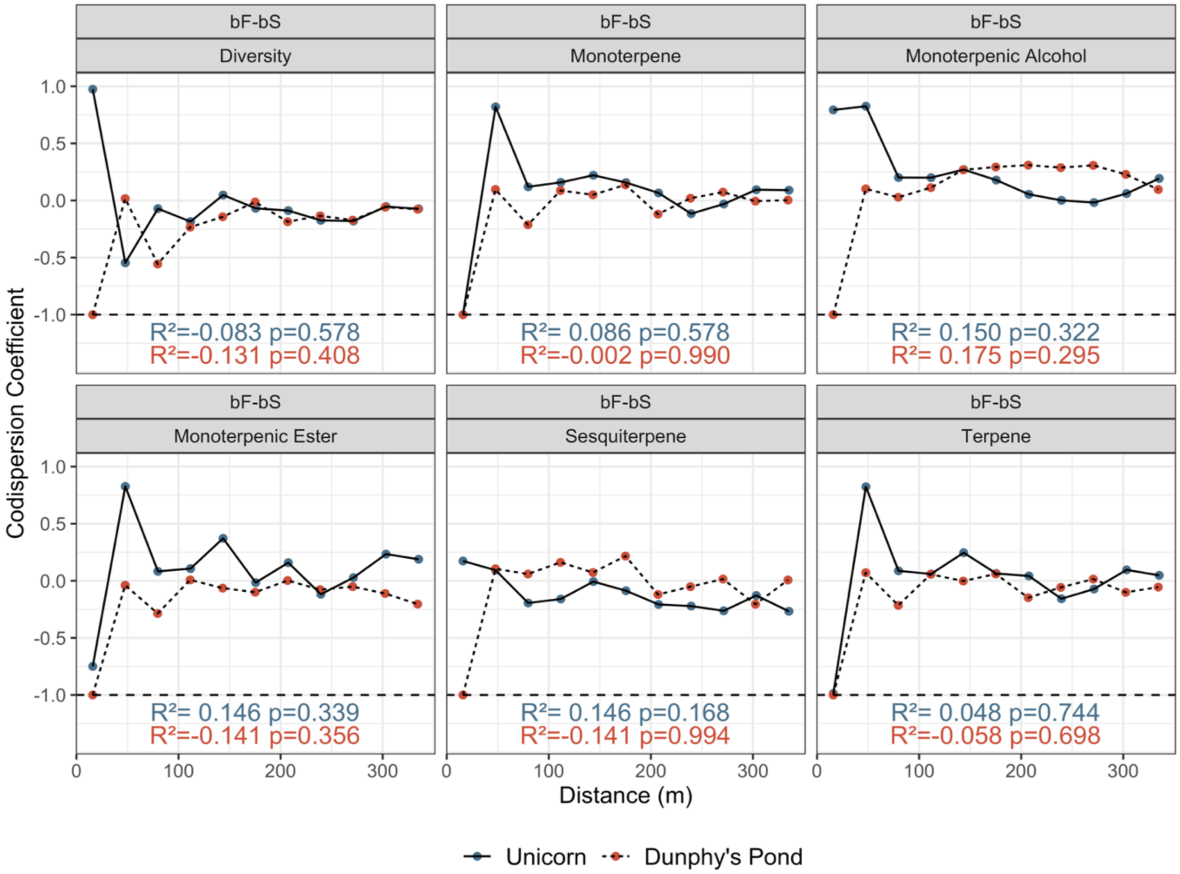

Figure 4.4 Spatial co-dispersion across spatial gradients of distance (metres) for the foliar phytochemical traits of our focal species: balsam fir (bF), and black spruce (bS). Co-dispersion values range from -1 (spatial segregation) to +1 (spatial aggregation). Colour codes for data points, R^2 values, and statistical significance are used to represent our study sites (blue = Dunphy's Pond 80-100 years old site, and red = Unicorn 60-80 years old site).

Chapter 5

Summary

The spatial variability of elemental/chemical plant traits provides a bridge between concepts in ecosystem and landscape ecology. The ebb and flow of elements between abiotic and biotic components define the ecology of ecosystems by influencing processes such as nutrient cycling, biomass production, carbon sequestration, evapotranspiration, decomposition processes, and food web structure (Barnes et al., 2018; Chapin et al., 2002). In landscape ecology a central focus is on how ecosystem processes produce and are influenced by spatial patterns (Turner, 1989). For instance, across a landscape, different ecosystem processes create variable environments. These environments influence how plants acquire and use elemental resources (i.e., resource patterns) and as such influence the variability of their foliar chemical traits that in turn influence ecosystem processes (Burton et al., 2017; Chapin, 2003). Thus, environmental drivers that influence the spatial variability of elemental/chemical plant traits provide a link to connect components of ecosystem ecology and landscape ecology to reveal pattern and process relationships and the scale at which they occur.

In this thesis, I investigate how environmental drivers influence the carbon (C), nitrogen (N), and phosphorus (P) and other molecules in foliar material to inform emergent biogeochemical properties of landscapes. The objectives of my thesis were to: i) determine the effects of geography and co-occurrence on plant foliar elemental niche space; ii) identify and compare the spatial correlates of foliar traits across, within and between a suite of focal plant species; and iii) evaluate the spatial co-variability of foliar traits between co-occurring plant species at a small spatial extent. I found that:

i) Geographic location (i.e., different ecoregions) significantly influenced the elemental niche space of balsam fir (*Abies balsamea* (L.) Mill.) and white birch (*Betula papyrifera* Marshall) (Chapter 2). In addition, comparisons of co-occurrence in niche space (i.e., conspecific vs conspecific groups from different ecoregions) also differed significantly. I found weak evidence to suggest conspecific and heterospecific niche space differed within a given ecoregion. However, white birch conspecific and heterospecific niche space did differ significantly between ecoregions and within the Central Forest ecoregion but not the Northern Peninsula ecoregion. These results suggest two things. First, the elemental niche of our focal species is geographically specific. Second, although we found weak evidence that conspecific and heterospecific niches are different within an ecoregion, these groups represent common community structure conditions of land cover classes, which may scale local effects to larger regional level patch-mosaic processes. As well, this suggests community structure is likely an important spatial predictor of foliar elemental traits.

ii) Spatial predictors of traits primarily occur at the species level with different traits influenced by different environmental conditions within a given biogeographical area (i.e., as per chapter 2 findings and in this case, we use an ecodistrict as our area of interest – a subcomponent of an ecoregion). The results of chapter 3 suggest that species respond differently to environmental conditions at the landscape extent and thus it is necessary to investigate concepts such as resource hot spots at a species level instead of a community level. For instance, across species different spatial predictors explained foliar N or P traits and thus these traits may not be reliable indicators of site productivity or forage quality in a given community. As well, although I found some commonalities in spatial predictors across species at the trait level, differences in the directionality and significance of those predictors suggest differential effects on species traits. In chapter 3, I demonstrate that we can link plot level data to accessible spatial predictors to create maps of trait variability at a landscape scale. This work demonstrates a novel spin on distribution models by predicting the spatial patterns of resource traits. By creating these maps, we can interrogate patterns of resource quality at the landscape extent and compare maps across species to inform how, where, and why herbivores make foraging decisions in these landscapes (see Balluffi-Fry et al., 2021; Balluffi-Fry et al., 2020; Richmond et al., 2021; Rizzuto et al., 2021).

iii) At a small spatial extent, the spatial co-variability of foliar traits between co-occurring species with similar resource strategies do not always vary in similar ways. The twin filter model of community assembly provides a framework, albeit spatially implicit, to justify trait relationships between species based on their resource strategies. Although in chapter 4, I expected the spatial patterns of foliar traits between species with similar resource strategies to be similar, I detected significantly similar relationships more often for species with dissimilar resource strategies. In addition, I found that there is scale, direction, site, and species-specific variability that influences the spatial relationships of foliar traits between co-occurring species. Notably, between phylogenetically-related species, balsam fir and black spruce (*Picea mariana* (Mill.) Britton, Sterns, & Poggenb) with

> similar resource strategies, foliar phytochemical traits did not co-vary in similar ways, except at close distances (i.e., 0 meters). In this system, moose (*Alces alces* (Linnaeus, 1758)) preferentially browse balsam fir over black spruce. These patterns suggest that black spruce may actively disguise its nutritional quality to evade browsing. This work opens up novel directions to further bridge the gap between community and spatial ecology with implications for ecosystem functionality.

Overall, my thesis advances research on species-trait-environmental relationships using spatially implicit and explicit approaches to merge concepts of ecosystem ecology and landscape ecology. I present evidence of large-scale biophysical controls on the variability of foliar elemental traits, including and how these traits vary via the co-occurrence of different species, the environmental spatial covariates that drive spatial traits patterns at the landscape extent, and how traits spatially co-vary between species at a fine scale local extent. Insights gained in my thesis help understand species-trait responses to different environmental drivers and the scale at which they operate. Using universal elemental/chemical traits I demonstrate how the spatial patterning of traits potentially relates to differences in ecosystem processes thus, connecting process to pattern relationships that underpin the discipline of landscape ecology.

5.1 The main ingredients: traits, space, and scale

A central focus of trait-based ecology is investigating trait-species-environment relationships using functional traits as opposed to taxonomic based traits (Levine, 2016). Although there is debate on what constitutes a functional trait, they are broadly considered traits that are inherent to an organism and linked to ecosystem processes (Cadotte & Tucker, 2017;

Violle et al., 2007). For instance, soil decomposition rates are often influenced by the elemental/chemical composition of plant litter (Gartner & Cardon, 2004; Hobbie, 2015); primary productivity can reflect foliar carbon gains or biomass production (Becknell & Powers, 2014); changes to foliar N and P can indicate differences in soil nutrient retention (Bosatta & Agren, 1991). These relationships are often circular with trait variability influenced by the strength of feedback forces (i.e., negative and positive reinforcement; Bruelheide et al., 2018). Thus, the variability of functional traits—as measured in my thesis using elemental and chemical composition—along environmental gradients are useful indicators to describe the spatial heterogeneity of ecosystem processes occurring across a landscape at different scales.

Describing the spatial heterogeneity of functional traits can be achieved using spatially implicit and explicit approaches. Although many studies have demonstrated differences and specific uses between spatially implicit and explicit approaches (DeAngelis & Yurek, 2017), both approaches are useful to resolve pattern and scale problems in ecology (Levin, 1992). Spatially implicit approaches, where we are not concerned with the geographic position of data (i.e., spatially disjunct/discrete or spatially autocorrelated data), have been useful for understanding large scale processes such as vegetation patterns (Bugmann, 2001), disturbance regimes (Seidl et al., 2011), population dynamics (Hanski & Ovaskainen, 2003), and food web structure (Paine, 1980). However, in recent years, assessing trait-species-environment relationships in a spatially explicit context has become an emerging challenge in ecology (Perry et al., 2013; Wilkes et al., 2020). With advancements in spatial statistics, spatially explicit approaches (i.e., where we are concerned with the geographic position of data) have allowed for the identification of spatial patterns at local and regional scales that create amplifying effects to inform processes that structure landscape patterns (DeAngelis & Yurek, 2017).

Still, deriving generalizations of spatial heterogeneity as it relates to ecosystem processes via individual level mechanisms, has been a long-standing challenge for landscape ecologists (Newman et al., 2019; Wiens et al., 1993). However, ecological stoichiometry potentially provides a lens to resolve aspects of this issue. Ecological stoichiometry offers a framework to reveal how the movement or location of energy and matter influences ecosystem processes such as trophic interactions via currency interactions of C, N, and P (Kaspari & Powers, 2016; Meunier et al., 2017). Only recently have spatially explicit approaches been used to quantify spatial heterogeneity within an ecological stoichiometric framework (Leroux et al., 2017). In my second chapter, I show how biogeographical patterns of foliar C, N, and P vary at a species level in response to biophysical geographical signals (i.e., ecoregion conditions). With this, we can paint a picture of how the foliar stoichiometry of species differs across broad scale gradients of environmental conditions that describe landscapes by their ecological classification (i.e., ecoregion, ecodistrict). At these scales, we can form broad-brush generalizations of spatial heterogeneity as it pertains to individual level C, N, and P traits. Specifically, in this case, foliar C, N, and P traits of species from the northern ecoregion operate in different trait space and with increased variability compared to a southern ecoregion.

Although ecological stoichiometry provides a powerful parsimonious framework to explain complex system properties via elemental traits, the spatial variability of traits is still constrained by the scale at which environmental drivers operate (Meunier et al., 2017). For instance, the ecoregions differences described in my second chapter show that major physiographic and minor macroclimatic environmental factors ultimately influence the elemental trait space of our focal species. However, within a given ecoregion, differences in certain environmental drivers may influence trait variability in different ways. For instance, in my third chapter, stoichiometric traits are among the functional traits I used to spatially predict trait patterns via environmental drivers with a specific ecodistrict (e.g., a local subcomponent of an ecoregion). In this chapter, I take a novel spin on distribution modelling to determine which environmental covariate or combination of covariates explained trait variability and used this information to produce species-trait specific maps of resource/forage quality on the landscape. These maps provide direct linkages to inform third and fourth order selection by herbivores (Johnson, 1980; Rizzuto et al., 2021). As well, future work could use these maps to cue into additional site level covariates such as soil moisture and nutrient regimes to determine causal spatial patterns, thus revealing additional biogeochemical and ecological spatial dimensions. Moreover, this work demonstrates that trait variability is species-specific and different traits are influenced by different environmental covariates. As such, this work acts as a cautionary flag to studies which group forage material by plant functional groups or community conditions; lumping at this scale may produce potentially inaccurate estimates of resource quality and generalizations of bite scale herbivore decisions (Balluffi-Fry et al., 2021; Merems et al., 2020). Taken together my second and third chapter demonstrate the spatial hierarchy of environmental conditions that potentially influence a species trait variability.

However, within species, traits can be correlated, such as increasing foliar N with foliar P and this potentially confounds species-trait-environmental relationships (Dray & Legendre, 2008). Although there are many ways to aspatially and spatially assess these relationships (e.g., spatially explicit fourth corner analysis), in my third chapter I took the approach to model traits individually by species and select parsimonious spatial predictors. As a precursor to fitting linear models of traits, I evaluated for correlation between traits. Although I observed that the strength of correlation varied between certain traits at a species level, I found that not all traits were correlated. As such, species-trait-environment relationships are likely trait-specific. Indeed, this is what the results support; at a species level, different spatial predictors explain different traits. Nonetheless between species, similar traits may co-vary, and if so this would provide justification to group species at a trait level to explain patterns of resource quality.

Understanding spatial co-variability of foliar traits between species remains a central challenge for ecologists to connect community processes to the ecology of the landscape (Buckley et al., 2016; Schöb et al., 2012). Although spatially implicit analysis of trait co-variability has been well studied at a community level and for groups of plant functional types, these relationships in a spatially explicit context remain unresolved (Armbruster et al., 2014; Dézerald et al., 2018). Many tools exist to evaluate these spatial relationships, largely under the umbrella of point-pattern analyses (Velázquez et al., 2016). In Chapter 4, I use spatial co-dispersion to investigate trait co-variability between species using plot level, grid-based data. I expected trait divergence for species with dissimilar resource strategies and trait convergence for species with similar resource strategies. Counter to these expectations, the strength of spatial co-variability of foliar traits between co-occurring species varied by trait, species, scale, and site. These results suggest that some generalizations can be made about species-trait-environment relationships between species for specific traits, however, a single species foliar trait may not indicate a resource hot spot at a community level. Thus, the spatial contours of forage quality via foliar traits for different species likely influence how, where, and why an herbivore uses different habitats when selecting for different resources. For instance, in my third chapter I found that although certain species had similar spatial predictors of traits, they did not co-vary at a small spatial extent as assessed in chapter four. However, foliar C:P and N:P for balsam fir and red maple appear to maintain trait co-variability at both stand and landscape extents. By placing these trait-species-environment relationships into a spatial context, I was able to demonstrate the role scale plays in these relationships.

Differences in the scales in which processes operate, such as those occurring at the level of the individual, within a forest stand or between stands, create a spatial mosaic of variability via ecosystem processes at the landscape extent. This is similar to the hierarchical scales of processes that influence habitat selection i.e., where an animal is, their home range size, location of feeding sites, and usage of forage within feeding site (Johnson, 1980). A common conceptualization of a landscape is of a patch-mosaic model where composition and configuration of landscapes are described by the interaction of distinct patch types (Costanza et al., 2019). In forested ecosystems, forest patches represent a set of similar conditions such as stand age and species composition, thus, at a higher level of organization than individuals, we can characterize patches as distinct ecological communities. By linking the elemental/chemical functional trait-environment relationships of species within a given patch/community we can operationalize the patch-mosaic model to obtain estimates of ecosystem processes at the landscape extent. My thesis attempts to add information about ecological functions in response to the landscape mosaic using trait variability. In Chapter 2, I show how the co-occurrence of two dominant species in this landscape influences their elemental niche space and hence between patch differences in elemental composition. In Chapter 3, I map trait variability at the landscape extent and demonstrate differences between species in terms of spatial patch patterns. In Chapter 4, I take a spatially explicit approach to investigate within-patch trait co-variability of co-occurring species and find that site characteristics (e.g., stand age) play an important role in determining spatial trait patterns. Taken together, these findings suggest that trait variability for a given species occurs within and between patches and this contributes to differences in how the patch mosaic influences ecosystems processes at the landscape extent. Moreover, this work lays the foundation for future researchers to investigate the spatial scales at which herbivores cue into forage quality within implications for population dynamics and habitat controls on density thresholds (see Balluffi-Fry et al., 2020; Behmer et al., 2002; Merems et al., 2020; Rizzuto et al., 2021).

5.2 Future directions

1. Spatial variability of functional traits that inform resource quality; throughout my thesis I identify the linkages that foliar elemental, stoichiometric, and phytochemical traits have to herbivore space/resource use. The foliar traits we used largely define the availability of resource quality to herbivores, primarily moose and snowshoe hare (*Lepus americanus* (Erxleben, 1777); Dodds, 1960). Thus, the spatial distribution of these traits may help land managers cue in on resource hot spots and aid in delineating habitat that captures a range of forage quality and diversity (Crandall et al., 2000). However, future work is needed to link strategic planning and operational scales of resource hot spots between producer, herbivore, and predator trophic groups which promote food web and habitat integrity (Borer et al., 2015).
2. Spatial stoichiometry to inform landscape functionality; ecological stoichiometry offers a unified framework to assess ecosystem processes as it provides predictable responses to changes in resources of elemental ratios (Sitters et al., 2015; Sterner & Elser, 2002). At different scales, ecosystems are spatially connected through the transfer of energy and matter. For instance, animals make decisions at different scales about where to consume, defecate, and sleep based on the mosaic of different habitats, their resource

characteristics, and suitability to a specific function (Hutchinson, 1991; Shepard et al., 2013). The use of and movement through different forest and non-forest patches facilitates the transfer of energy and matter over space and time (Schmitz et al., 2018). Moreover, elemental resources can flow within and between ecosystem via hydrological systems, thus connecting ecosystem at very large scales (Schade et al., 2005). Elemental resources often regulate ecosystem processes (i.e., productivity via biogeochemical dynamics) and as such, placing these components in a spatially explicit context provides an opportunity to characterize patches within a mosaic that inform differences in functionality (i.e., nutrient inputs, changes in productivity, movement and directionality of elemental resources). Future work could consider how changes to landscape structure via industrial forestry, urbanization, and agriculture alter biogeochemical pathways via spatially explicit stoichiometric assessments of elemental flows. This work could be applied to mitigate impacts to ecosystem integrity and services.

3. Managing for integrity via landscape resiliency and stoichiometric recovery; in recent years resiliency concepts have been increasingly applied to landscape management (Cushman & McGarigal, 2019). For instance, in western North America increasingly frequent incidents of catastrophic wildfires and flooding events have warranted a re-evaluation of how we currently use and strategize for the recruitment and maintenance of forest landscape resources (Hessburg et al., 2015; McWethy et al., 2019). Research suggests that landscape resiliency can be achieved by restoring landscape structure back to pre-colonial contact conditions (Keane et al., 2018). However, this “back to the future” approach in some cases is unattainable given current climate shifts and the ecological departure of landscapes via structural alterations (i.e., impacts from industrialized

forestry; Larson et al., 2022). A fundamental component of managing towards resiliency is understanding ecosystem recovery at multiple scales. At the stand scale, recovery time is often less on productive sites (i.e., those where trees are not limited by nutrient and water constraints; DeAngelis, 1980). At the landscape scale, the surrounding matrix can increase ecosystem recovery rates via subsidises of elemental resources (Allen et al., 2016). Thus, understanding spatial stoichiometry at the patch level via soil and vegetation nutrients and managing for a resilient mosaic configuration that supports the flow of energy and material may buffer the effects resource extraction and lessen stand and landscape level recovery time to future disturbances. Future work may consider the use of joint species distribution model methods to develop stoichiometric patch models using vegetation and soil community trait data to inform resilient landscape structure under different perturbation scenarios.

5.3 Conclusion

In this thesis, I present empirical assessments to determine the scale of spatial patterns for functional foliar traits from commonly occurring boreal forest species. Aside from the linkages these traits have to ecosystem processes, the species we used are commonly consumed by moose and snowshoe hare and thus contribute to understanding spatial dynamics for these primary consumers and food web interactions. The results of my thesis contribute to a growing discussion in the field of trait-based ecology, and more broadly in community, ecosystem, and landscape ecology. My findings suggest that (1) the elemental composition of foliar material is likely constrained by biogeographical/biophysical factors and thus trait variability is geographically specific; (2) foliar elemental, stoichiometric, and chemical traits are largely predicted by different spatial covariates for traits and species, and by identifying these covariates we can make maps that relate trait patterns to ecosystem processes; (3) the strength of spatial co-variability of foliar traits between co-occurring species varies by distance, direction, and site and as such, delineating resource quality hot spots on the landscape and in different habitats requires careful consideration of indicator traits between species.

5.4 References

Allen, C. R., Angeler, D. G., Cumming, G. S., Folke, C., Twidwell, D., & Uden, D. R. (2016). Quantifying spatial resilience. *Journal of Applied Ecology*, *53*(3), 625–635. https://doi.org/10.1111/1365-2664.12634

Armbruster, W. S., Pélabon, C., Bolstad, G. H., & Hansen, T. F. (2014). Integrated phenotypes: Understanding trait covariation in plants and animals. *Philosophical Transactions of the Royal Society B: Biological Sciences*, *369*(1649), 20130245. https://doi.org/10.1098/rstb.2013.0245

Balluffi-Fry, J., Leroux, S. J., Wiersma, Y. F., Heckford, T. R., Rizzuto, M., Richmond, I. C., & Vander Wal, E. (2020). Quantity–quality trade-offs revealed using a multiscale test of herbivore resource selection on elemental landscapes. *Ecology and Evolution*, *10*(24), 13847–13859. https://doi.org/10.1002/ece3.6975

Balluffi-Fry, J., Leroux, S. J., Wiersma, Y. F., Richmond, I. C., Heckford, T. R., Rizzuto, M., Kennah, J. L., & Vander Wal, E. (2021). Integrating plant stoichiometry and feeding experiments: State-dependent forage choice and its implications on body mass. *Oecologia*. https://doi.org/10.1007/s00442-021-05069-5

Barnes, A. D., Jochum, M., Lefcheck, J. S., Eisenhauer, N., Scherber, C., O'Connor, M. I., de Ruiter, P., & Brose, U. (2018). Energy flux: The link between multitrophic biodiversity and ecosystem functioning. *Trends in Ecology & Evolution*. https://doi.org/10.1016/j.tree.2017.12.007

Becknell, J., M., & Powers, J., S. (2014). Stand age and soils as drivers of plant functional traits and aboveground biomass in secondary tropical dry forest. *Canadian Journal of Forest Research*. https://doi.org/10.1139/cjfr-2013-0331

Behmer, S. T., Simpson, S. J., & Raubenheimer, D. (2002). Herbivore foraging in chemically heterogeneous environments: Nutrients and secondary metabolites. *Ecology*, *83*(9), 2489–2501.

Borer, E. T., Lind, E. M., Ogdahl, E. J., Seabloom, E. W., Tilman, D., Montgomery, R. A., & Kinkel, L. L. (2015). Food-web composition and plant diversity control foliar nutrient content and stoichiometry. *Journal of Ecology*, *103*(6), 1432–1441. https://doi.org/10.1111/1365-2745.12461

Bosatta, E., & Agren, G. I. (1991). Dynamics of carbon and nitrogen in the organic matter of the soil: A generic theory. *The American Naturalist*, *138*(1), 227–245. https://doi.org/10.1086/285213

Bruelheide, H., Dengler, J., Purschke, O., Lenoir, J., Jiménez-Alfaro, B., Hennekens, S. M., Botta-Dukát, Z., Chytrý, M., Field, R., Jansen, F., Kattge, J., Pillar, V. D., Schrodt, F., Mahecha, M. D., Peet, R. K., Sandel, B., van Bodegom, P., Altman, J., Alvarez-Dávila, E., … Jandt, U. (2018). Global trait–environment relationships of plant communities. *Nature Ecology & Evolution*, *2*(12), 1906–1917. https://doi.org/10.1038/s41559-018-0699-8

Buckley, H. L., Case, B. S., & Ellison, A. M. (2016). Using codispersion analysis to characterize spatial patterns in species co-occurrences. *Ecology*, *97*(1), 32–39. https://doi.org/10.1890/15-0578.1

Bugmann, H. (2001). A review of forest gap models. *Climatic Change*, *51*(3), 259–305. https://doi.org/10.1023/A:1012525626267

Burton, J. I., Perakis, S. S., McKenzie, S. C., Lawrence, C. E., & Puettmann, K. J. (2017). Intraspecific variability and reaction norms of forest understorey plant species traits. *Functional Ecology*, *31*(10), 1881–1893. https://doi.org/10.1111/1365-2435.12898

Cadotte, M. W., & Tucker, C. M. (2017). Should environmental filtering be abandoned? *Trends in Ecology & Evolution*, *32*(6), 429–437. https://doi.org/10.1016/j.tree.2017.03.004

Chapin, F. S. (2003). Effects of plant traits on ecosystem and regional processes: A conceptual framework for predicting the consequences of global change. *Annals of Botany*, *91*(4), 455–463. https://doi.org/10.1093/aob/mcg041

Chapin, F. S., Matson, P. A., & Mooney, H. A. (2002). *Principles of terrestrial ecosystem ecology*. Springer.

Costanza, J. K., Riitters, K., Vogt, P., & Wickham, J. (2019). Describing and analyzing landscape patterns: Where are we now, and where are we going? *Landscape Ecology*, *34*(9), 2049–2055. https://doi.org/10.1007/s10980-019-00889-6

Crandall, K. A., Bininda-Emonds, O. R., Mace, G. M., & Wayne, R. K. (2000). Considering evolutionary processes in conservation biology. *Trends in Ecology & Evolution*, *15*(7), 290–295.

Cushman, S. A., & McGarigal, K. (2019). Metrics and models for quantifying ecological resilience at landscape scales. *Frontiers in Ecology and Evolution*, *7*. https://doi.org/10.3389/fevo.2019.00440

DeAngelis, D. L. (1980). Energy flow, nutrient cycling, and ecosystem resilience. *Ecology*, *61*(4), 764–771. https://doi.org/10.2307/1936746

DeAngelis, D. L., & Yurek, S. (2017). Spatially explicit modeling in ecology: A review. *Ecosystems*, *20*(2), 284–300. https://doi.org/10.1007/s10021-016-0066-z

Dézerald, O., Srivastava, D. S., Céréghino, R., Carrias, J.-F., Corbara, B., Farjalla, V. F., Leroy, C., Marino, N. A. C., Piccoli, G. C. O., Richardson, B. A., Richardson, M. J., Romero, G. Q., & González, A. L. (2018). Functional traits and environmental conditions predict community isotopic niches and energy pathways across spatial scales. *Functional Ecology*, *32*(10), 2423–2434. https://doi.org/10.1111/1365-2435.13142

Dray, S., & Legendre, P. (2008). Testing the species traits–environment relationships: The fourth-corner problem revisited. *Ecology*, *89*(12), 3400–3412.

Gartner, T. B., & Cardon, Z. G. (2004). Decomposition dynamics in mixed-species leaf litter. *Oikos*, *104*(2), 230–246. JSTOR.

Hanski, I., & Ovaskainen, O. (2003). Metapopulation theory for fragmented landscapes. *Theoretical Population Biology*, *64*(1), 119–127. https://doi.org/10.1016/s0040-5809(03)00022-4

Hessburg, P. F., Churchill, D. J., Larson, A. J., Haugo, R. D., Miller, C., Spies, T. A., North, M. P., Povak, N. A., Belote, R. T., Singleton, P. H., Gaines, W. L., Keane, R. E., Aplet, G. H., Stephens, S. L., Morgan, P., Bisson, P. A., Rieman, B. E., Salter, R. B., & Reeves, G. H. (2015). Restoring fire-prone Inland Pacific landscapes: Seven core principles. *Landscape Ecology*, *30*(10), 1805–1835. https://doi.org/10.1007/s10980-015-0218-0

Hobbie, S. E. (2015). Plant species effects on nutrient cycling: Revisiting litter feedbacks. *Trends in Ecology & Evolution*, *30*(6), 357–363. https://doi.org/10.1016/j.tree.2015.03.015

Hutchinson, G. E. (1991). Population studies: Animal ecology and demography. *Bulletin of Mathematical Biology*, *53*(1–2), 193–213.

Johnson, D. H. (1980). The comparison of usage and availability measurements for evaluating resource preference. *Ecology*, *61*(1), 65–71. https://doi.org/10.2307/1937156

Kaspari, M., & Powers, J. S. (2016). Biogeochemistry and geographical ecology: Embracing all twenty-five elements required to build organisms. *The American Naturalist*, *188*(S1), S62–S73. https://doi.org/10.1086/687576

Keane, R. E., Loehman, R. A., Holsinger, L. M., Falk, D. A., Higuera, P., Hood, S. M., & Hessburg, P. F. (2018). Use of landscape simulation modeling to quantify resilience for ecological applications. *Ecosphere*, *9*(9), e02414. https://doi.org/10.1002/ecs2.2414

Larson, A. J., Jeronimo, S. M. A., Hessburg, P. F., Lutz, J. A., Povak, N. A., Cansler, C. A., Kane, V. R., & Churchill, D. J. (2022). Tamm Review: Ecological principles to guide post-fire forest landscape management in the Inland Pacific and Northern Rocky Mountain regions. *Forest Ecology and Management*, *504*, 119680. https://doi.org/10.1016/j.foreco.2021.119680

Leroux, S. J., Wal, E. V., Wiersma, Y. F., Charron, L., Ebel, J. D., Ellis, N. M., Hart, C., Kissler, E., Saunders, P. W., Moudrá, L., Tanner, A. L., & Yalcin, S. (2017). Stoichiometric distribution models: Ecological stoichiometry at the landscape extent. *Ecology Letters*, *20*(12), 1495–1506. https://doi.org/10.1111/ele.12859

Levin, S. A. (1992). The problem of pattern and scale in ecology: The Robert H. MacArthur award lecture. *Ecology*, *73*(6), 1943–1967.

Levine, J. M. (2016). A trail map for trait-based studies. *Nature*, *529*(7585), 163–164. https://doi.org/10.1038/nature16862

McWethy, D. B., Schoennagel, T., Higuera, P. E., Krawchuk, M., Harvey, B. J., Metcalf, E. C., Schultz, C., Miller, C., Metcalf, A. L., Buma, B., Virapongse, A., Kulig, J. C., Stedman, R. C., Ratajczak, Z., Nelson, C. R., & Kolden, C. (2019). Rethinking resilience to wildfire. *Nature Sustainability*. https://doi.org/10.1038/s41893-019-0353-8

Merems, J. L., Shipley, L. A., Levi, T., Ruprecht, J., Clark, D. A., Wisdom, M. J., Jackson, N. J., Stewart, K. M., & Long, R. A. (2020). Nutritional-landscape models link habitat use to condition of mule deer (*odocoileus hemionus*). *Frontiers in Ecology and Evolution, 8*. https://doi.org/10.3389/fevo.2020.00098

Meunier, C. L., Boersma, M., El-Sabaawi, R., Halvorson, H. M., Herstoff, E. M., Van de Waal, D. B., Vogt, R. J., & Litchman, E. (2017). From elements to function: Toward unifying ecological stoichiometry and trait-based ecology. *Frontiers in Environmental Science*, *5*(18). https://doi.org/10.3389/fenvs.2017.00018

Newman, E. A., Kennedy, M. C., Falk, D. A., & McKenzie, D. (2019). Scaling and complexity in landscape ecology. *Frontiers in Ecology and Evolution*, *7*. https://doi.org/10.3389/fevo.2019.00293

Paine, R. T. (1980). Food webs: Linkage, interaction strength and community infrastructure. *Journal of Applied Ecology*, *49*, 667–685.

Perry, G. L. W., Enright, N. J., Miller, B. P., & Lamont, B. B. (2013). Do plant functional traits determine spatial pattern? A test on species-rich shrublands, Western Australia. *Journal of Vegetation Science*, *24*(3), 441–452. https://doi.org/10.1111/j.1654-1103.2012.01476.x

Richmond, I. C., Balluffi-Fry, J., Vander Wal, E., Leroux, S. J., Rizzuto, M., Heckford, T. R., Kennah, J. L., Riefesel, G. R., & Wiersma, Y. F. (2021). Individual snowshoe hares manage risk differently: Integrating stoichiometric distribution models and foraging ecology. *Journal of Mammalogy*. https://doi.org/10.1093/jmammal/gyab130

Rizzuto, M., Leroux, S. J., Vander Wal, E., Richmond, I. C., Heckford, T. R., Balluffi-Fry, J., & Wiersma, Y. F. (2021). Forage stoichiometry predicts the home range size of a small terrestrial herbivore. *Oecologia*, *197*(2), 327–338. https://doi.org/10.1007/s00442-021-04965-0

Schade, J. D., Espeleta, J. F., Klausmeier, C. A., McGroddy, M. E., Thomas, S. A., & Zhang, L. (2005). A conceptual framework for ecosystem stoichiometry: Balancing resource supply and demand. *Oikos*, *109*(1), 40–51. https://doi.org/10.1111/j.0030-1299.2005.14050.x

Schmitz, O. J., Wilmers, C. C., Leroux, S. J., Doughty, C. E., Atwood, T. B., Galetti, M., Davies, A. B., & Goetz, S. J. (2018). Animals and the zoogeochemistry of the carbon cycle. *Science*, *362*(6419), eaar3213. https://doi.org/10.1126/science.aar3213

Schöb, C., Butterfield, B. J., & Pugnaire, F. I. (2012). Foundation species influence trait-based community assembly. *New Phytologist*, *196*(3), 824–834. https://doi.org/10.1111/j.1469-8137.2012.04306.x

Seidl, R., Fernandes, P. M., Fonseca, T. F., Gillet, F., Jönsson, A. M., Merganičová, K., Netherer, S., Arpaci, A., Bontemps, J.-D., Bugmann, H., González-Olabarria, J. R., Lasch, P., Meredieu, C., Moreira, F., Schelhaas, M.-J., & Mohren, F. (2011). Modelling natural disturbances in forest ecosystems: A review. *Ecological Modelling*, *222*(4), 903–924. https://doi.org/10.1016/j.ecolmodel.2010.09.040

Shepard, E. L. C., Wilson, R. P., Rees, W. G., Grundy, E., Lambertucci, S. A., & Vosper, S. B. (2013). Energy landscapes shape animal movement ecology. *The American Naturalist*, *182*(3), 298–312. https://doi.org/10.1086/671257

Sitters, J., Atkinson, C. L., Guelzow, N., Kelly, P., & Sullivan, L. L. (2015). Spatial stoichiometry: Cross-ecosystem material flows and their impact on recipient ecosystems and organisms. *Oikos*, *124*(7), 920–930. https://doi.org/10.1111/oik.02392

Sterner, R. W., & Elser, J. J. (2002). *Ecological stoichiometry: The biology of elements from molecules to the biosphere*. Princeton University Press.

Turner, M. G. (1989). Landscape ecology: The effect of pattern on process. *Landscape Ecology, 20*, 171–197.

Velázquez, E., Martínez, I., Getzin, S., Moloney, K. A., & Wiegand, T. (2016). An evaluation of the state of spatial point pattern analysis in ecology. *Ecography*, *39*(11), 1042–1055. https://doi.org/10.1111/ecog.01579

Violle, C., Navas, M.-L., Vile, D., Kazakou, E., Fortunel, C., Hummel, I., & Garnier, E. (2007). Let the concept of trait be functional! *Oikos*, *116*(5), 882–892. https://doi.org/10.1111/j.2007.0030-1299.15559.x

Wiens, J. A., Stenseth, N. Chr., Van Horne, B., & Ims, R. A. (1993). Ecological mechanisms and landscape ecology. *Oikos*, *66*(3), 369–380. https://doi.org/10.2307/3544931

Wilkes, M. A., Edwards, F., Jones, J. I., Murphy, J. F., England, J., Friberg, N., Hering, D., Poff, N. L., Usseglio-Polatera, P., Verberk, W. C. E. P., Webb, J., & Brown, L. E. (2020). Trait-based ecology at large scales: Assessing functional trait correlations, phylogenetic constraints and spatial variability using open data. *Global Change Biology*, *26*(12), 7255–7267. https://doi.org/10.1111/gcb.15344

Appendices

Appendix A Supplemental Information for Chapter 2: Ecoregion and community structure influences on the foliar elemental niche of balsam fir (*Abies balsamea* (L.) Mill.) and white birch (*Betula papyrifera* Marshall)

A.1 Distribution map of focal species and ecoregion map for the island of Newfoundland

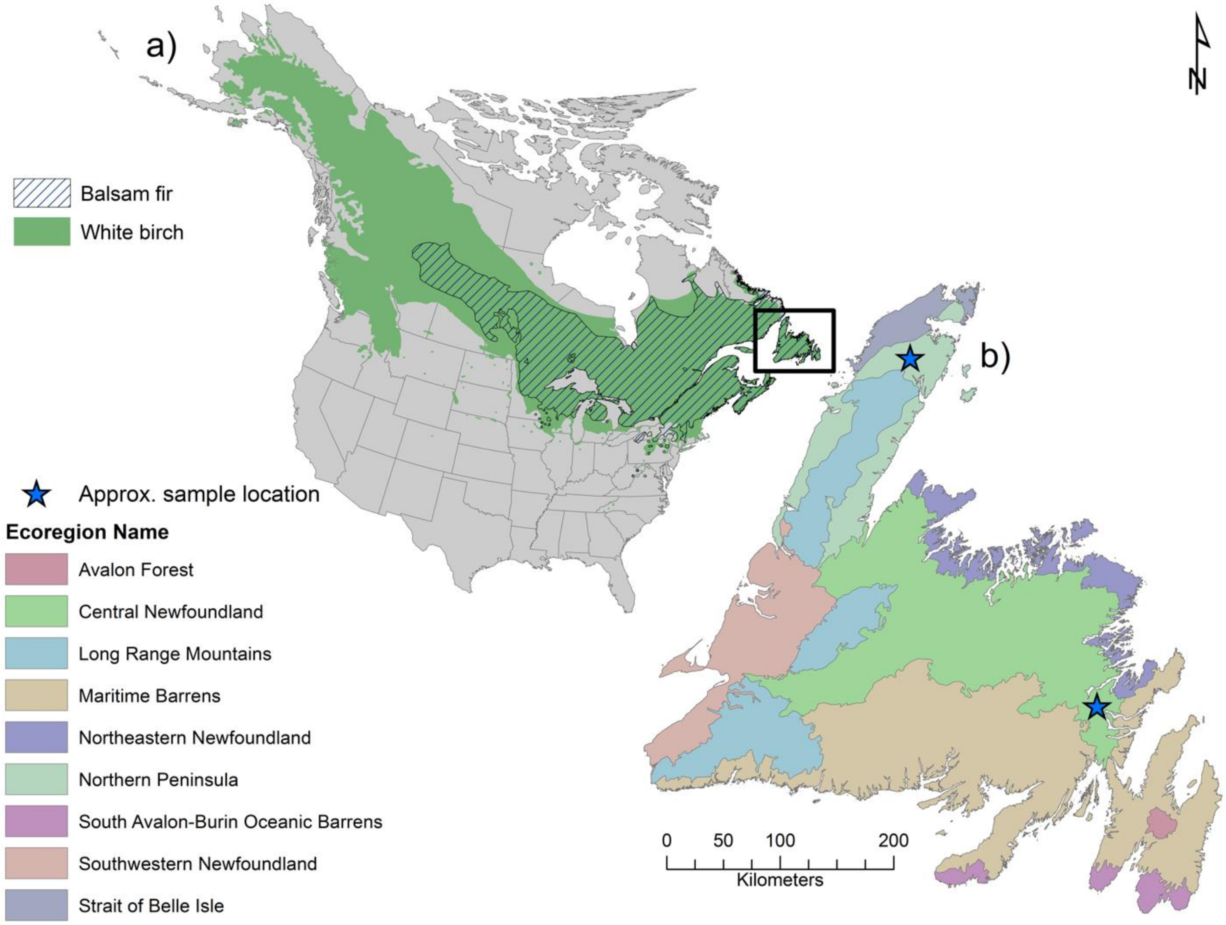

Figure A.1.1 Study maps showing the (a) geographic distribution of our focal species balsam fir and white birch across North America (Prasad & Iverson, 2003). We sampled balsam fir and white birch individuals from (b) the Island of Newfoundland, at locations indicated by stars in the Northern Peninsula and Central Forest ecoregions.

A.2 Full PERMANOVA results for niche comparisons

Table A.2.1 PERMANOVA results for each of our niche comparisons for balsam fir and white birch. Our ecoregion comparison of Northern Peninsula (NP) and Central Forest (CF) niches are presented first. Followed by across, within and between ecoregion comparisons of comparisons of conspecific (con) and heterospecific (hetero) niches. Conspecific and heterospecific niche comparisons between our Northern Peninsula and Central Forest populations are present last. Significant *p*-values are bolded.

	Balsam fir					White birch				
Between ecoregions	Df	SS	R2	F	*p*-value	Df	SS	R2	F	*p*-value
NP vs CF	1	0.002	0.0362	14.5919	**0.001**	1	0.0185	0.2508	75.9986	**0.001**
Residual	388	0.0535	0.9638			227	0.0554	0.7492		
Total	389	0.0556	1			228	0.0739	1		
Across ecoregions										
Con vs Hetero	1	1.00E-04	0.0017	0.6457	0.458	1	0.0013	0.0176	4.0752	**0.021**
Residual	388	0.0555	0.9983			227	0.0726	0.9824		
Total	389	0.0556	1			228	0.0739	1		
Within ecoregion										
NP: Con vs Hetero	1	1.00E-04	0.0015	0.4501	0.57	1	1.00E-04	0.0031	0.4798	0.577
Residual	293	0.0505	0.9985			156	0.0456	0.9969		
Total	294	0.0506	1			157	0.0458	1		
Within ecoregion										
CF: Con vs Hetero	1	0	0.0033	0.3055	0.726	1	0.0011	0.1172	9.1626	**0.001**
Residual	93	0.0029	0.9967			69	0.0085	0.8828		
Total	94	0.0029	1			70	0.0096	1		

Con: between ecoregion	1	0.001	0.039	7.5813	**0.005**	1	0.0015	0.2362	8.0383	**0.001**
Residual	187	0.0254	0.961			26	0.0049	0.7638		
Total	188	0.0264	1			27	0.0065	1		
Hetero: between ecoregion	1	0.001	0.0337	6.9427	**0.004**	1	0.017	0.2566	68.7019	**0.001**
Residual	199	0.028	0.9663			199	0.0492	0.7434		
Total	200	0.029	1			200	0.0661	1		

A.3 Sample size niche effects

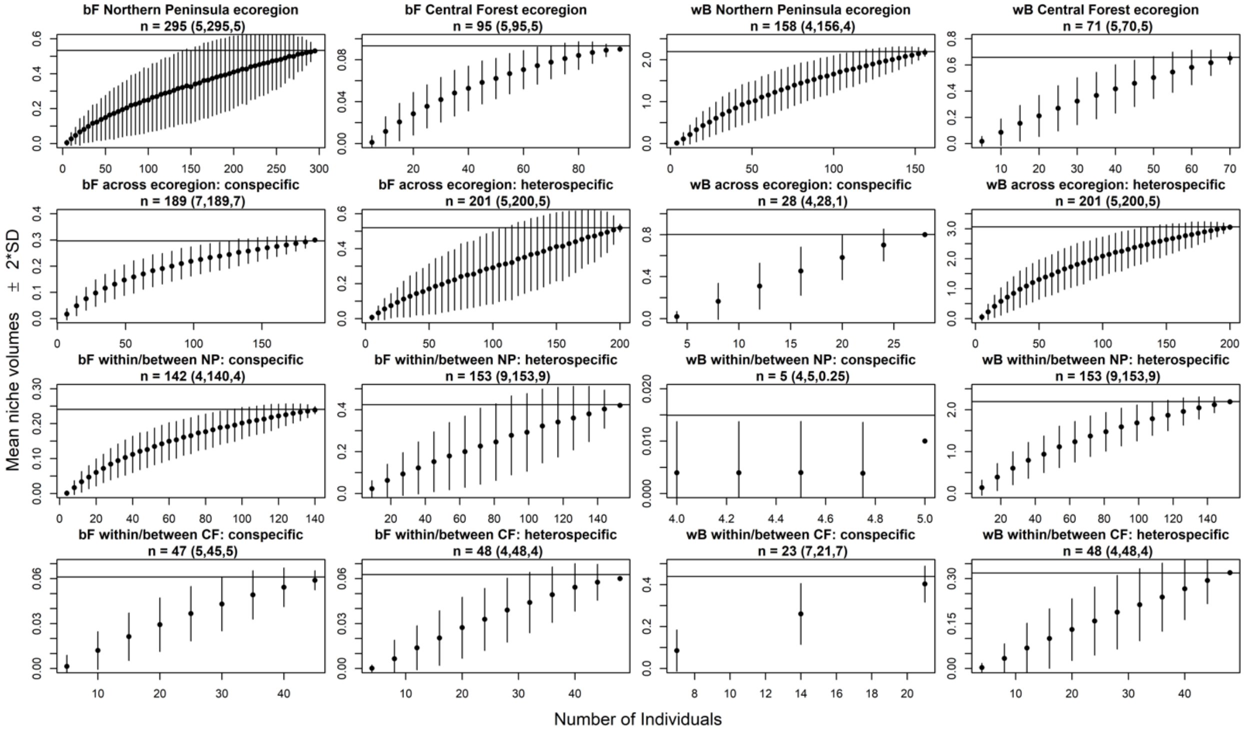

Figure A.3.1 The effect of increasing sample size on determining niche volume. Results for species level comparisons across ecoregions are shown in the top row of plots (H1). The second row of plots show results for community level comparisons across ecoregions (H2/H3) and the third and fourth row of plots show results for within (H4/H5) and between (H6) ecoregion comparisons. For each plot we provide the total sample size (n) and the maximum number of samples used to estimate niche volume using 999 randomized permutations at a specified interval of increasing individuals used (i.e., 5, 295, 5 from the first plot indicates a starting samples size of 5, an end sample size of 295, at an interval of 5). The range of variation in our randomized niche volumes was quantified using 95% confidence interval (2 standard deviations from the randomized niche mean). Horizontal lines indicate the total niche volume computed for a given group (i.e., ecoregion, conspecific, heterospecific).

A.4 Sample size, Shapiro-Wilk results, and niche volumes

Table A.4.1 The sample size for each niche (n), the MVW and *p*-value results of a Shapiro-Wilk test for multivariate normality, here a significant *p*-value indicates these data are not normally distributed. To perform a PERMANOVA test, data must exhibit a non-normal structure. We further investigate this with Levene's test for multivariate homogeneity of variance for each of our niche comparisons. This aids in our interpretation of PERMANOVA results. In addition, we provide niche volume as a percentage, relative to the total available niche space. This was calculated following steps outlined by González et al., 2017. Forward slashes (/) indicate insufficient samples sizes needed for calculation. Calculating the Shapiro-Wilk measure requires a minimum of 12 data points (Shapiro & Wilk, 1965) and niche volume requires a minimum of 2 data points (González et al., 2017).

Balsam fir	n	Shapiro-Wilk (MVW)	*p*-value	Niche volume (%)
Northern Peninsula	295	0.942	**3.42x10^{-22}**	85.49
Central Forest	95	0.942	**3.41x10^{-8}**	14.52
Across ecoregions: conspecific	189	0.979	**4.93x10^{-5}**	48.39
Across ecoregions: heterospecific	201	0.942	**2.98x10^{-16}**	83.88
Northern Peninsula: conspecific	142	0.980	**0.003**	38.71
Northern Peninsula: heterospecific	153	0.902	**4.38x10^{-20}**	67.75
Central Forest: conspecific	47	0.937	**2.72x10^{-4}**	9.68
Central Forest: heterospecific	48	0.928	**3.84x10^{-5}**	9.68
White birch	n	Shapiro-Wilk (MVW)	*p*-value	Niche volume (%)
Northern Peninsula	158	0.973	**1.30x10^{5}**	66.78
Central Forest	71	0.958	**5.67x10^{-4}**	20.13
Across ecoregions: conspecific	28	0.975	0.894	24.39
Across ecoregions: heterospecific	201	0.977	**2.78x10^{-6}**	93.31
Northern Peninsula: conspecific	5	/	/	0.30
Northern Peninsula: heterospecific	153	0.972	**7.80x10^{-6}**	66.78
Central Forest: conspecific	23	0.963	0.657	13.42
Central Forest: heterospecific	48	0.924	**1.67x10^{-5}**	9.76

A.5 Scatter plots for species and community level niche comparisons

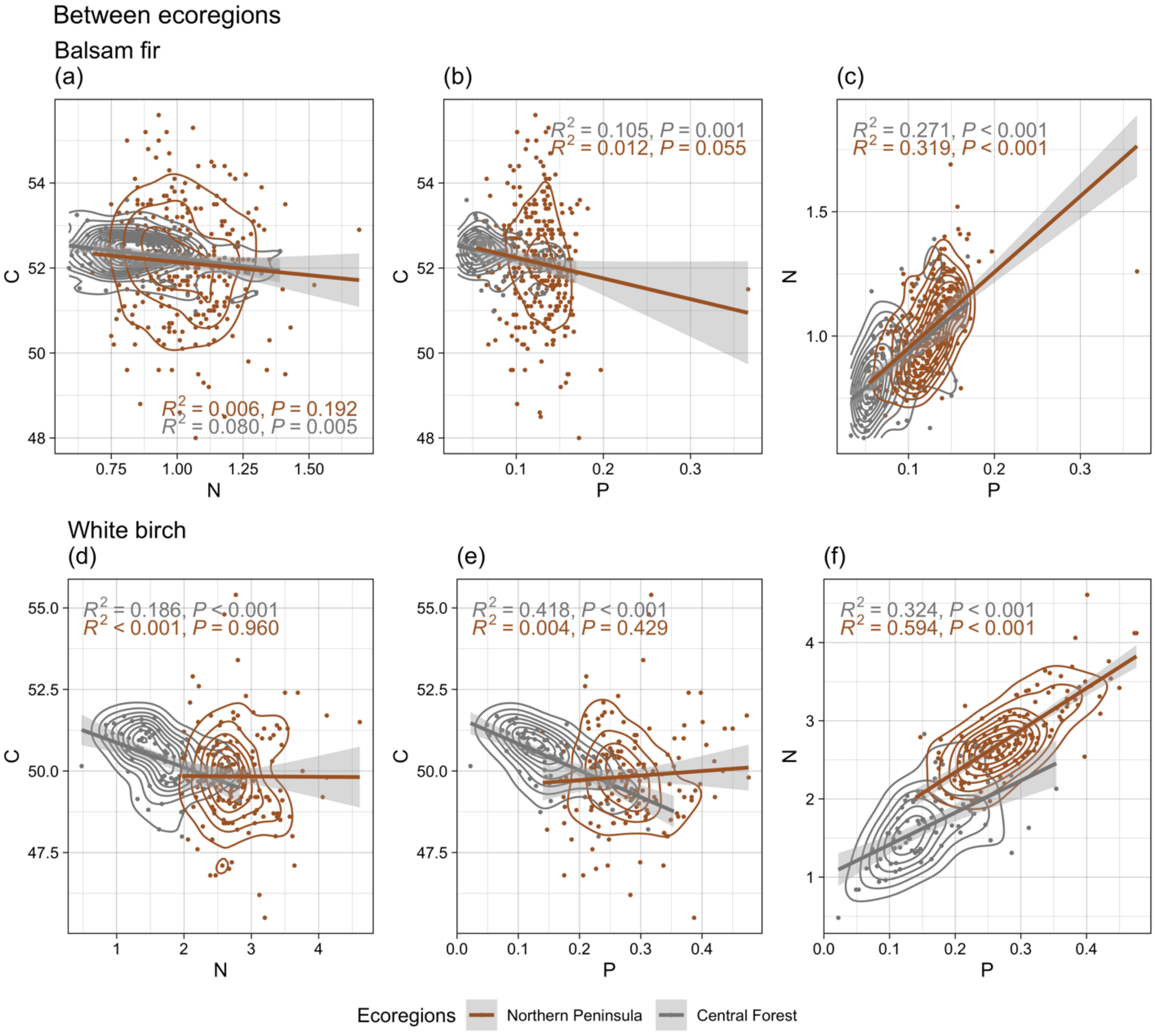

Figure A.5.1 Species level between ecoregion scatter plots with kernel density estimations presented using Gaussian approximation contour lines for individual pair-wise comparisons of foliar C, N, and P traits for balsam fir (a, b, and c) and white birch (d, e, and f). Colour-coded R^2 and *p*-values are presented for each trait comparison by ecoregion. This figure aids to complements spherical representations of niches found in Figure 2.3.

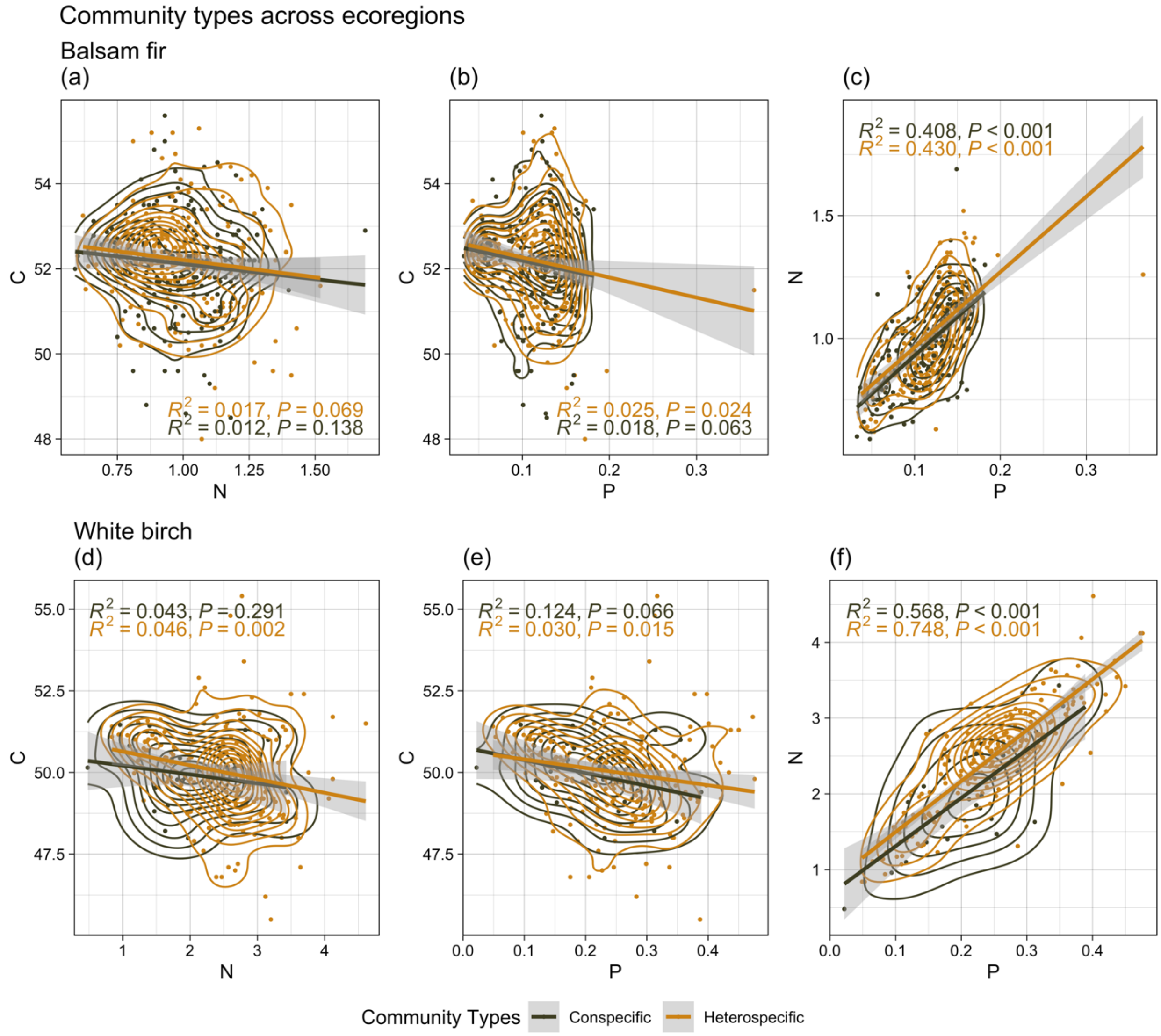

Figure A.5.2 Community level across ecoregion scatter plots with kernel density estimations presented using Gaussian approximation contour lines for individual pair-wise comparisons of foliar C, N, and P traits for balsam fir (a, b, and c) and white birch (d, e, and f). Colour-coded R^2 and *p*-values are presented for each trait comparison by ecoregion. This figure aids to complements spherical representations of niches found in Figure 2.4.

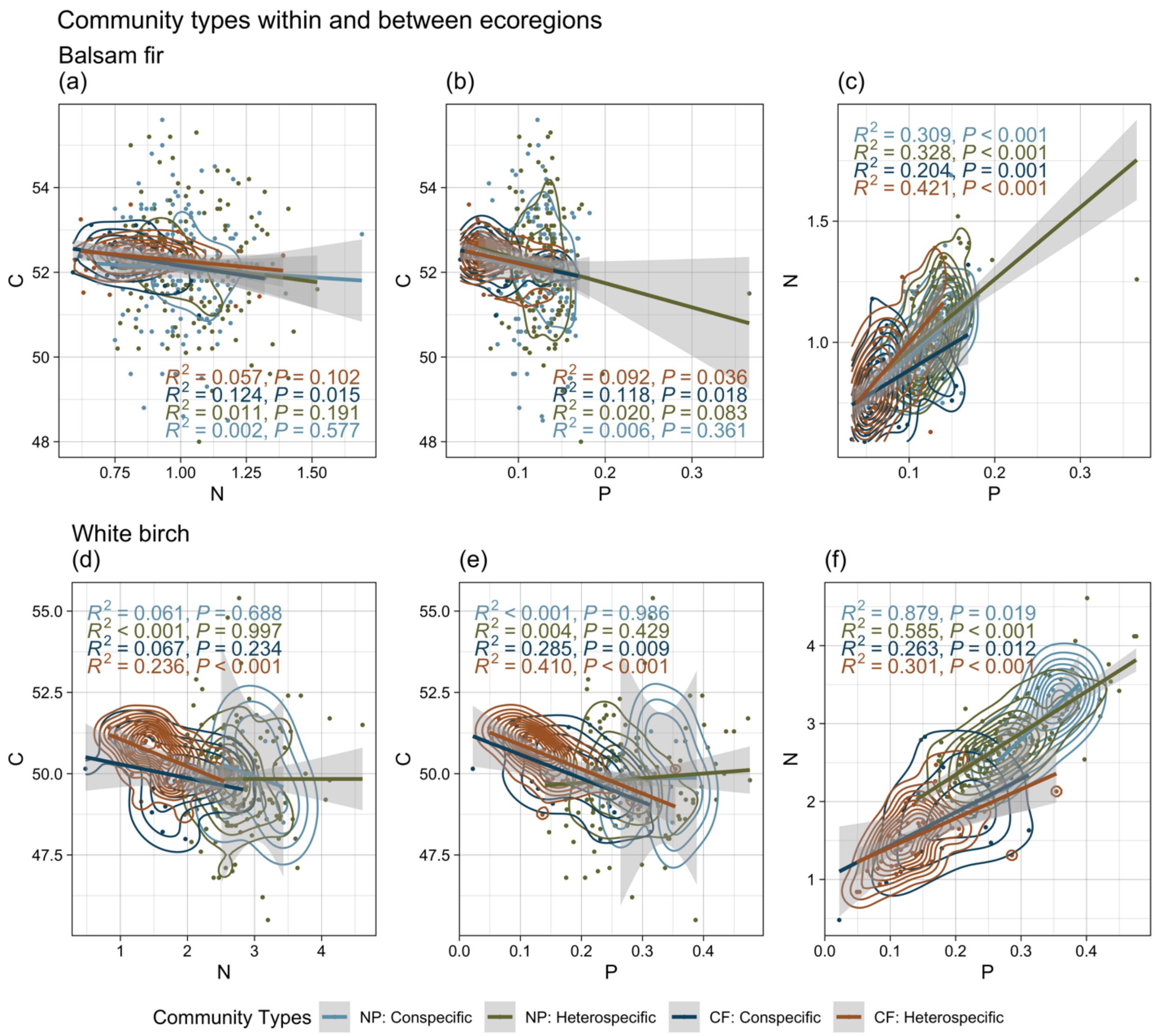

Figure A.5.3 Community level within and between ecoregion scatter plots with kernel density estimations presented using Gaussian approximation contour lines for individual pair-wise comparisons of foliar C, N, and P traits for balsam fir (a, b, and c) and white birch (d, e, and f). Colour-coded R^2 and p-values are presented for each trait comparison by community type and ecoregion. This figure aids to complements spherical representations of niches found in Figure 2.5.

A.6 Addition results: temporal niche comparisons

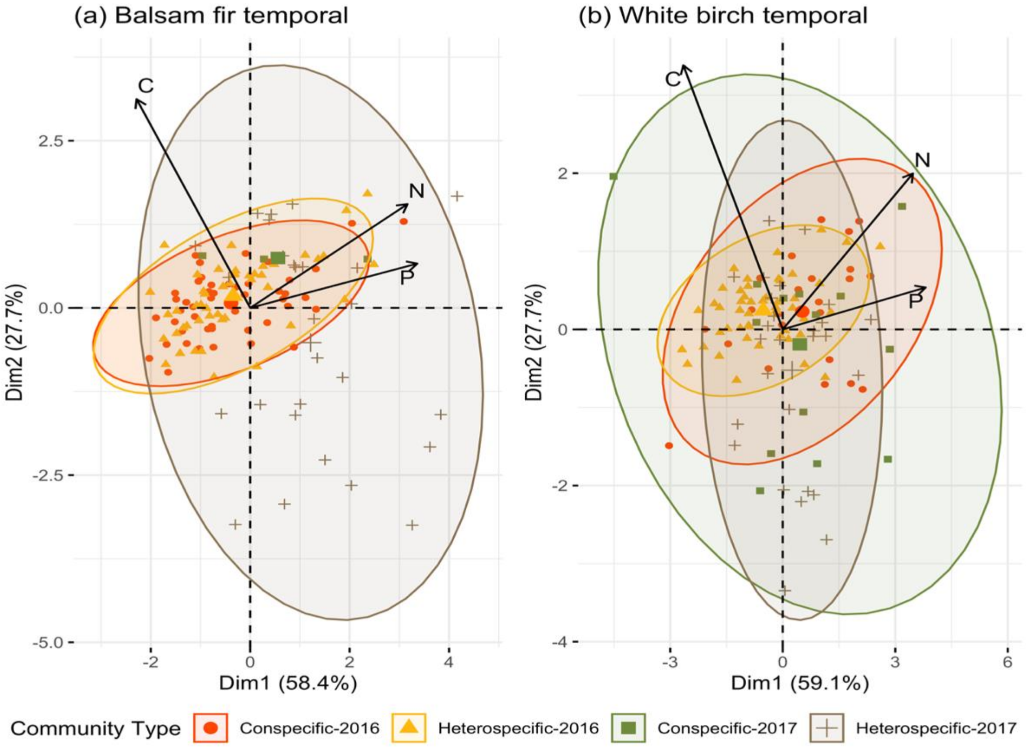

Figure A.6.1 Principal component analysis (PCA) for our 2016 and 2017 temporal comparison of balsam fir (a) and white birch (b) in the Central Forest ecoregion. Ellipses with a 95 % probability are shown for conspecific 2016, heterospecific 2016, conspecific 2017, and heterospecific 2017 niches with individuals depicted as circles, triangles, squares, and crosshairs, respectively. In both cases the variance is similar for dimension 1 and 2. In all cases N and P highly influence dimension 1 while C influences dimension 2. There was insufficient sample size to construct a balsam fir conspecific 2017 niche.

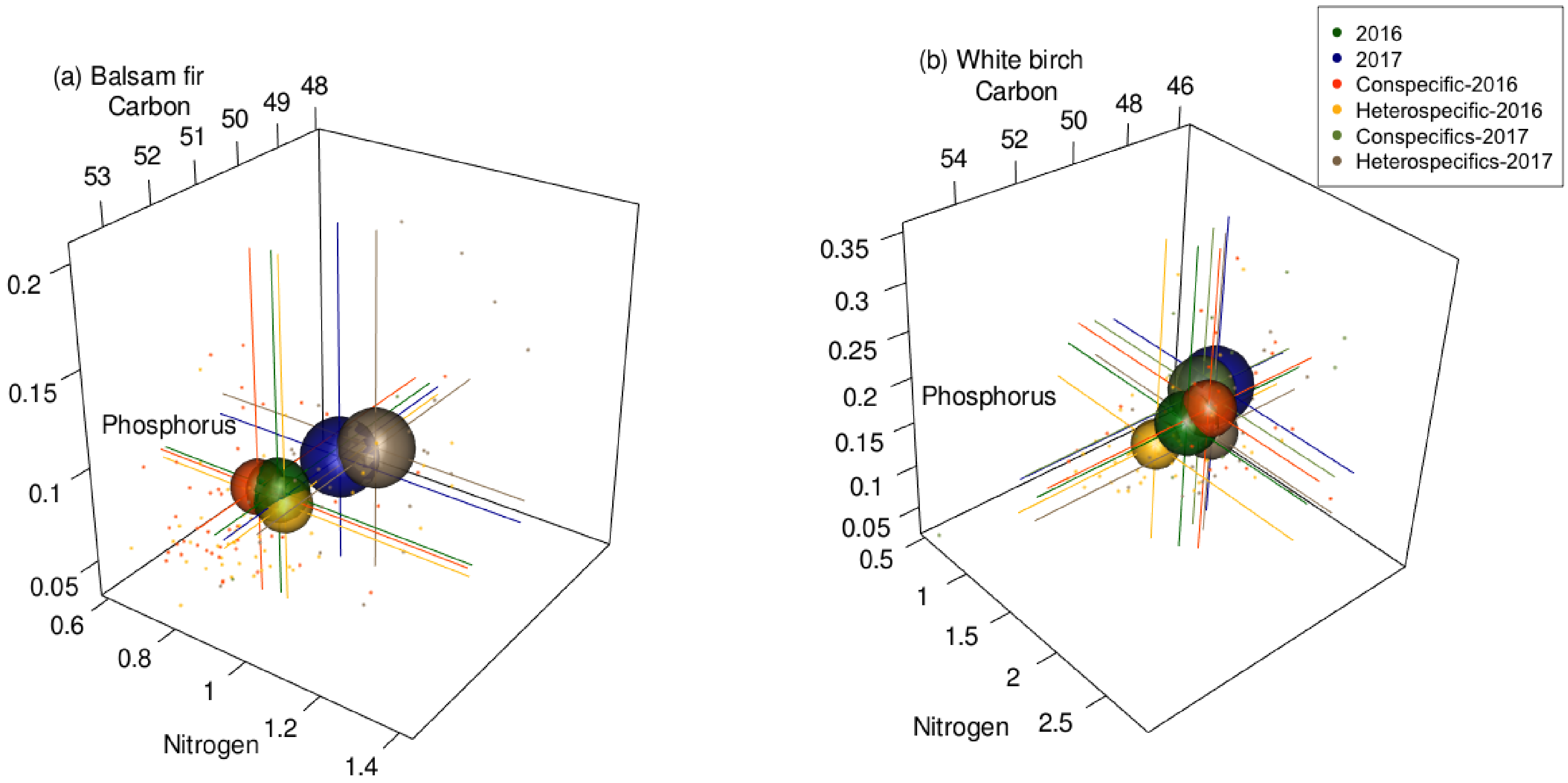

Figure A.6.2 Spherical representations of temporal foliar C, N, and P niche hypervolumes for balsam fir (a) and white birch (b). For each species we depicted niches as spheres and show average C, N, and P values with droplines for 2016 (n = 95 for fir and n = 71 for birch) and 2017 (n = 30 for fir and n = 41 for birch) niches; 2016 conspecific (n = 47 for fir and n = 23 for birch) and heterospecific (n = 48 for fir and n = 48 for birch) niches; and 2017 conspecific (n = 3 for fir and n = 14 for birch) and heterospecific (n = 27 for fir and n = 27 for birch) niches. Plot size represents the total stoichiometric volume of C, N, and P between years.

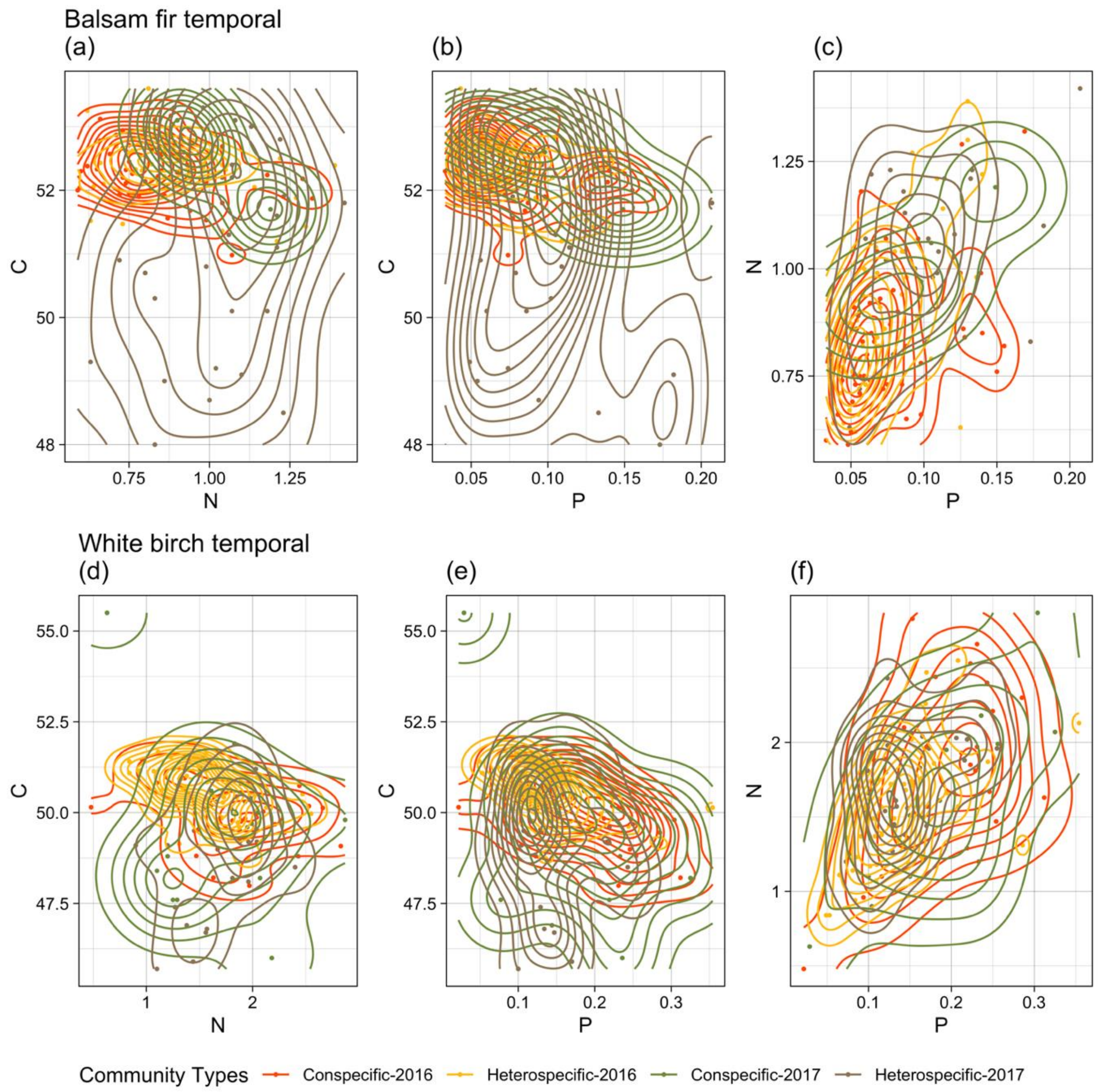

Figure A.6.3 Scatter plots for our temporal comparisons with kernel density estimations presented using Gaussian approximation contour lines for balsam fir (a, b, and c) and white birch (d, e, and f) showing 2016 and 2017 conspecific and heterospecific groups. This figure aids to complements spherical representations of niches found in Figure A.6.2.

Table A.6.1 For our temporal comparisons we report the sample size of each niche (n), the MVW and *p*-value results of a Shapiro-Wilk test for multivariate normality, here a significant *p*-value indicates these data are not normally distributed. To perform a PERMANOVA test, data must exhibit a non-normal structure. We further investigate this with Levene's test for multivariate homogeneity of variance for each of our niche comparisons. This aids in our interpretation of PERMANOVA results. In addition, we provide niche volume as a percentage, relative to the total available niche space. This was calculated following steps outlined by González et al., 2017. Forward slashes (/) indicate insufficient samples sizes needed for calculation. Shapiro-Wilk requires a minimum of 12 data points (Shapiro & Wilk, 1965) and niche volume requires a minimum of 2 data points (González et al., 2017). Significant *p*-values are bolded.

Balsam fir	n	Shapiro-Wilk (MVW)	*p*-value	Niche volume (%)
2017 conspecific	3	/	/	/
2017 heterospecific	27	0.957	0.299	61.420
2016 con/heterospecific	95	0.942	**3.41×10^{-8}**	29.090
2017 con/heterospecific	30	0.960	0.270	61.420
White birch	**n**	**Shapiro-Wilk (MVW)**	***p*-value**	**Niche volume (%)**
2017 conspecific	14	0.929	0.266	47.120
2017 heterospecific	27	0.972	0.838	25.280
2016 con/heterospecific	71	0.958	**0.001**	37.920
2017 con/heterospecific	41	0.968	0.269	69.520

Table A.6.2 Summary of temporal niche comparison results for balsam fir and white birch. Results for balsam fir and white birch are separated within the table. The first column indicates the level of comparison and the second column indicates the year or community type groups being compared for that level. For instance, in the first column we compare groups in the second column at the ecoregion, in this case Central Forest, the community type of conspecific (con) and heterospecific (hetero), or the year level. For the other columns we present the Multivariate Homogeneity test of Dispersion (MHD) for each niche, the Permutation test for Homogeneity of Multivariate Dispersion (PT-MHD) with *F* value and *p*-value for the comparison of dispersion between two niches. As well, we report the Permutational Multivariate Analysis of Variance (PERMANOVA) showing a R^2, *F* statistic, and *p*-value for each comparison, followed by our hypervolume similarity assessment which reports the Jaccard similarity index. Lastly, we report niche metrics of overlap, nestedness and ITV. The sign of the ITV indicates if ITV increased (+) or decreased (-). For our 2016 and 2017 comparisons in the Central Forest ecoregion, conspecific, and heterospecific niches, ITV is calculated by subtracting niche volumes of 2017 by 2016. For our 2017 comparison of conspecific and heterospecific niches, ITV is calculated by subtracting niche volumes of heterospecific by conspecific. Bolded *p*-value indicate significant results. Forward slashes indicate insufficient samples sizes to compute.

Balsam fir	MHD		PT-MHD		PERMANOVA			Hypervolume	Niche volume metrics		
Comparisons	**2016**	**2017**	*F* value	*p*-value	R2	*F* statistic	*p*-value	Jaccard	Overlap (%)	Nestedness	ITV (%)
Central Forest	0.005	0.015	87.405	**0.001**	0.245	40.003	**0.001**	0.163	21.739	0.167	+ 32.33
Conspecific	0.005	0.006	0.583	0.458	0.019	0.936	0.363	0.329	/	/	/

Heterospecific	0.005	0.015	55.961	**0.001**	0.273	27.409	**0.001**	0.160	13.636	0.197	+ 42.02
Comparisons	**Con**	**Hetero**	*F* value	*p*-value	R2	*F* statistic	*p*-value	Jaccard	Overlap (%)	Nestedness	ITV (%)
2017	0.006	0.015	3.147	0.088	0.069	2.077	0.151	0.310	/	/	/

White birch	MHD		PT-MHD		PERMANOVA			Hypervolume	Niche volume metrics		
Comparisons	**2016**	**2017**	*F* value	*p*-value	R2	*F* statistic	*p*-value	Jaccard	Overlap (%)	Nestedness	ITV (%)
Central Forest	0.010	0.017	15.731	**0.001**	0.137	17.510	**0.001**	0.302	37.500	0.255	+ 31.6
Conspecific	0.011	0.020	4.239	**0.041**	0.028	0.989	0.374	0.273	35.484	0.245	+ 21.84
Heterospecific	0.008	0.016	15.316	**0.001**	0.263	26.059	**0.001**	0.272	18.750	0.043	+ 6.89
Comparisons	**Con**	**Hetero**	*F* value	*p*-value	R2	*F* statistic	*p*-value	Jaccard	Overlap (%)	Nestedness	ITV (%)
2017	0.020	0.016	0.738	0.424	0.013	0.516	0.564	0.258	27.273	0.170	- 21.84

Table A.6.3 PERMANOVA results for each of our temporal niche comparisons with balsam fir in the first and white birch in the second column. Our temporal comparison of conspecific (con) niches is presented first followed by our temporal comparison of heterospecific (hetero) niches. Thirdly, we present a 2017 conspecific versus heterospecific comparison. A comparison for 2016 and 2017 is presented last. Significant *p*-values are bolded. Temporal comparison of conspecific niches for balsam fir is limited due to low sample size (n=3).

	Balsam fir					White birch				
	Df	SS	R2	F	*p*-value	Df	SS	R2	F	*p*-value
Temporal con	1	0	0.0191	0.9357	0.363	1	4.00E-04	0.0275	0.9888	0.374
Residual	48	0.0015	0.9809			35	0.0129	0.9725		
Total	49	0.0016	1			36	0.0133	1		
Temporal hetero	1	0.0034	0.273	27.409	**0.001**	1	0.005	0.2631	26.0589	**0.001**
Residual	73	0.0091	0.727			73	0.0141	0.7369		
Total	74	0.0125	1			74	0.0191	1		
2017 con vs hetero	1	6.00E-04	0.069	2.0765	0.151	1	2.00E-04	0.0131	0.5161	0.564
Residual	28	0.0077	0.931			39	0.0185	0.9869		
Total	29	0.0083	1			40	0.0188	1		
2016 vs 2017	1	0.0036	0.2454	40.0025	**0.001**	1	0.0045	0.1373	17.5104	**0.001**
Residual	123	0.0112	0.7546			110	0.0284	0.8627		
Total	124	0.0149	1			111	0.0329	1		

A.7 References

González, A. L., Dézerald, O., Marquet, P. A., Romero, G. Q., & Srivastava, D. S. (2017). The multidimensional stoichiometric niche. *Frontiers in Ecology and Evolution*, *5*, 110. https://doi.org/10.3389/fevo.2017.00110

Prasad, A. M., & Iverson, L. R. (2003). *Little's range and FIA importance value database for 135 eastern US tree species* [Map]. http://www.fs.fed.us/ne/delaware/4153/global/littlefia/index.html

Shapiro, S. S., & Wilk, M. B. (1965). An analysis of variance test for normality (complete samples). *Biometrika*, *52*(3–4), 591–611. https://doi.org/10.1093/biomet/52.3-4.591

Appendix B Supplemental Information for Chapter 3: Spatially explicit correlates of plant functional traits inform landscape patterns of resource quality

B.1 Detailed description of Figure 3.1: the roadmap of our methods

Our study area (a) is location on the eastern side of the island of Newfoundland, Canada, as shown by the outlined area – ecodistrict 468. Generally, bounded between the 47th and 48th latitude this biogeographical area is composed of boreal forest conditions primarily dominated by intermediate-aged, closed canopy, forest stands of black spruce (*Picea mariana* (Mill.) Britton, Sterns, & Poggenb), balsam fir (*Abies balsamea* (L.) Mill.), white birch (*Betula papyrifera* Marshall), and trembling aspen (*Populus tremuloides* Michx.) (Ecological Stratification Working Group, 1996; South, 1983). Within this area we set up four chronosequenced grids, consisting of connected meandering transects. Age classes and grid layout shown in panel b. Grids were originally designed for snowshoe hare (*Lepus americanus* (Erxleben, 1777)) trapping and to allow us to relate foliar resource quality to hare home range size and ecology. Each grid is comprised of 50 sampling locations, spaced equally apart by 75 m with closer sample location rounding the corners (b). At each sample location we set up 22.6 m diameter circular plots (c). Within each plot we collected density estimates for each of our study species along a 22.6 m long and 1 m wide shrub belt transect (c/d). Moving in a north to south direction, along the belt, for each of our study species encountered we measured their height and basal diameter, and the distance at which it was encountered, for a maximum of five individuals per height class: 0-50 cm, 51-100 cm, 101-150 cm, and 151-200 cm, denoted as A, B, C, and D respectively (d). We restricted our sampling to species within 0-2 m heights (d) as these individuals represent the available forage for common boreal herbivores, moose (*Alces alces* (Linnaeus, 1758)) and snowshoe hare. Within each plot, starting in the NE corner (e), we moved in a clockwise direction and collected foliar samples of our study species, as well we measured their height and basal diameter. In panel e, we use coded names for our study species, balsam fir (ABBA), red maple (ACRU), white birch (BEPA), black spruce (PIMA), and lowbush blueberry (VAAN). We collect foliar material for our study species until we had a sufficient sample size of approximately 10-20 g. Using foliar samples for each of our study species, we combined representative units of foliar material until a wet weight sample of 10 g and 4 g was amassed – the amount required for elemental and phytochemical analysis, respectively. At the Agriculture Food Lab (AFL) at the University of Guelph Ontario, Canada the carbon and nitrogen composition of foliar material determined using an Elementar Vario Macro Cube. Foliar phosphorus content was determined using a microwave acid digestion CEM MARSxpress microwave system and brought to volume using Nanopure water. The clear extract supernatant was further diluted by 10 to accurately fall within calibration range and reduce high level analyte concentration entering the inductively coupled plasma mass spectrometry (ICP-MS) detector (Poitevin, 2016). This provides us with a measure of percent foliar C, N, and P. At the Laboratorie PhytoChemia Inc in Quebec, Canada, the phytochemical composition of balsam fir and black spruce foliar samples were determined using a gas chromatography solvent extraction with an internal standard and a correction factor (Cachet et al., 2016). This procedure produced mg/g measures of individual terpene compounds, see Appendix B.3 Table B.3.1 for a complete list of identified terpene compounds and groups. In addition, along the periphery of our study grids and outside of the sample plots, in randomly selected locations we collected all new growth foliar material for each of our study species from approximately 50 individuals, the number of samples distributed across the height classes listed above (f). As well, we measured the height and basal diameter for each individual sampled. The foliar material was dried, providing a measure of biomass from which we fit linear allometric models using covariates of height and basal diameter (f). Using coefficient estimates from our allometric models we predicted biomass estimates for our study species per height class from shrub belt measurements. In the few instances where we had obtained foliar samples but did not encounter individuals on the shrub belt we augmented the total number of individuals per height class as the total number of foliar samples in that height class. We subsequently summed biomass estimates per height class for each of our study species and divided this measure by the area of the circular plot (401.15 m^2) to get a density estimate. We then multiplied biomass by density for each height class to get a species biomass estimate, which was summed together, providing a plot level biomass estimate per species. To obtain elemental quantity estimates we divided biomass by the plot area multiplied by the foliar percentage of carbon, nitrogen, and phosphorus. As well, we did the same for phytochemicals to obtain a plot level biomass basis estimate of foliar phytochemicals. To determine stoichiometric ratios, we divided quantity C, N, and P estimates by their corresponding molar mass and then divided the resulting value together to get foliar C:N, C:P, and N:P for each study species. Using response variables of foliar percent elemental, quantity elemental, stoichiometric, and phytochemical we constructed sixteen plausible model combinations with spatially explicit covariates of land cover, productivity, abiotic, and biotic factors and used Akaike Information Criterion to determine parsimonious explanations (g). We then assessed top models and extracted coefficient estimates for use in constructing of distribution models of foliar elemental, stoichiometric, and phytochemical traits which provides us surfaces to inform landscape function (g). To do so, we sum coefficient values multiple against their corresponding spatial predictor which consists of binary raster layers for categorical variables (i.e., landcover and biotic) and continuous raster layers for the Enhanced Vegetation Index and topographic variables (i.e., elevation, aspect, and slope).

B.2 Spatial sample representation of biotic factors relative to their landscape availability

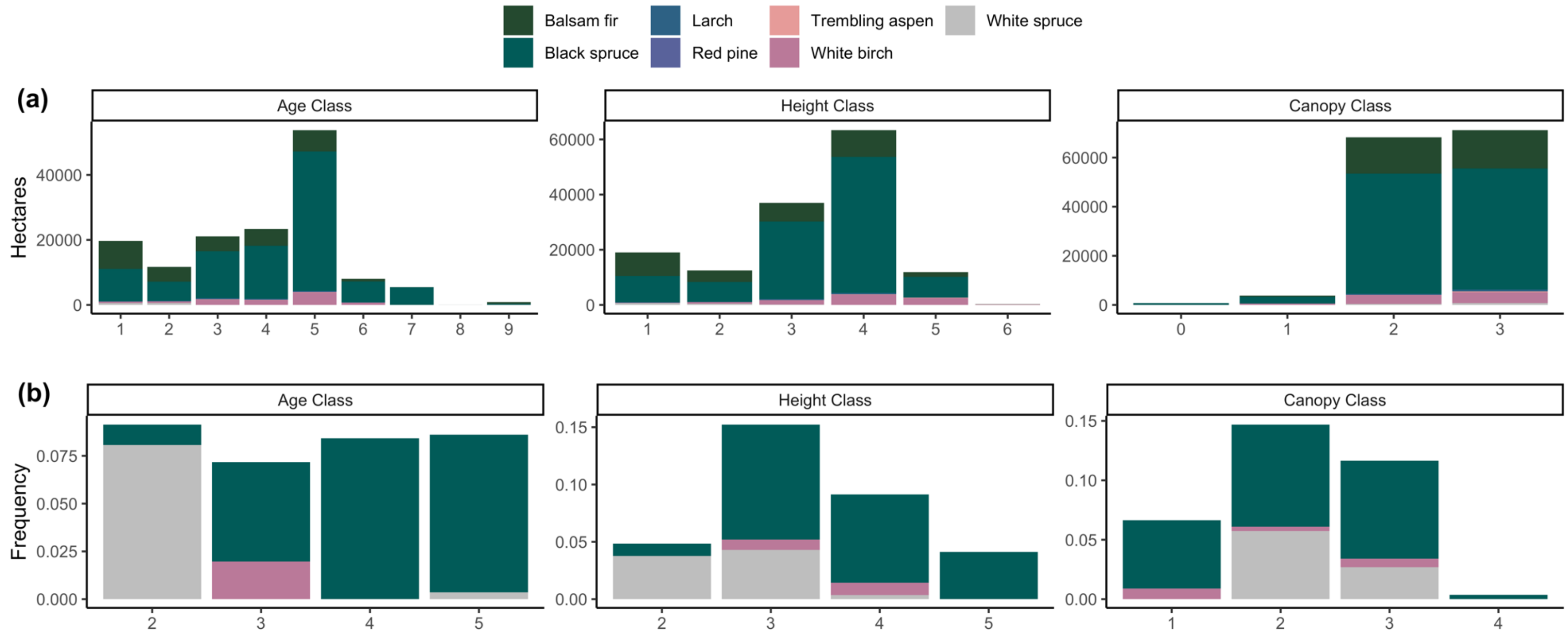

Figure B.2.1 The top (a) shows the total number of hectares for each dominant species forest type within our landscape area of interest, for stand metrics of age, height, and canopy class. Age class codes represent 20-year intervals ranging from 1 (0-20 years) to 9 (161+ years). Height class codes represent 3.5 m intervals of tree heights ranging from 1 (0-3.5 m) to 6 (15.6-18.5 m). Canopy class codes represent 25 % intervals of canopy closeness where 0 indicates a regenerating stand that is 100 % closed and 4 indicates a 10-25% closed canopy conditions. The bottom (b) shows the frequency in which these dominant species forest stands were sampled for foliar ESP traits of our study species. Here we show that although our sampling design is not ideal for spatial distribution modelling, we sampled within representative units of forest types available on the landscape, thus strengthening our inference for the spatial distribution of foliar ESP traits on this landscape.

B.3 List of phytochemical compounds used to make our terpenoid groups between conifer species

Table B.3.1 A complete list of phytochemical compounds and classes for terpenes identified in balsam fir and black spruce foliar samples. Only common terpene groups between these two coniferous species were used: terpene (includes all compounds identified), monoterpene, monoterpenic alcohol, monoterpenic ester, sesquiterpene, and diversity (computed using all compounds identified).

Group	Balsam fir	Black spruce
	Chemical Name	*Chemical Name*
Monoterpene	Tricyclene	Tricyclene
	α-Pinene	α-Pinene
	Camphene	Camphene
	β-Pinene (main) + Sabinene	β-Pinene (main) + Sabinene
	Myrcene	Myrcene
	Δ-Carene	Δ-Carene
	Limonene (main) + β-Phellandrene	α-Phellandrene
	γ-Terpinene	Limonene (main) + 1,8-cineole
	Terpinolene	Terpinolene
Monoterpenic Alcohol	Linalool	Linalool
	Camphene hydrate	Camphene hydrate
	Borneol	Citronellol

	α-Terpineol	α-Terpineol
	Thymol	---
Monoterpenic Ester	Bornyl acetate	Unknown "PIMA 6"
		Bornyl acetate (main) + Isobornyl acetate
		endo-Fenchyl acetate
		trans-Pinocarvyl acetate
		cis-Piperityl acettae
		Geranyl acetate
Sesquiterpene	Longifolene	β-Elemene
	β-Caryophyllene	β-Caryophyllene
	α-Humulene	α-Humulene
	(E)-β-Farnesene	Germacrene D
	Unknown sesquiterpene	γ-Cadinene (main) + Cubebol
	α-Muurolene	α-Muurolene
	(Z)-α-Bisabolene	δ-Cadinene
	β-Bisabolene	Unknown sesquiterpene
	(E)-α-Bisabolene	(E)-α-Bisabolene
Sesquiterpenic alcohol	**--**	Germacrene D-4-ol
		τ-Cadinol + τ-Muurolol (approx 1:1)
		α-Cadinol
		Oplopanone

Sesquiterpenic ether	Caryophyllene oxide	
Monoterpenic aldehyde	**--**	α-Campholenal
Monoterpenic ketone	Piperitone	--
Maltol	Maltol	--
Oxygenated sesquiterpene	**--**	Unknown "PIMA 18"
Unknown	**--**	Unknown "PIMA 9"

B.4 Allometric modelling results

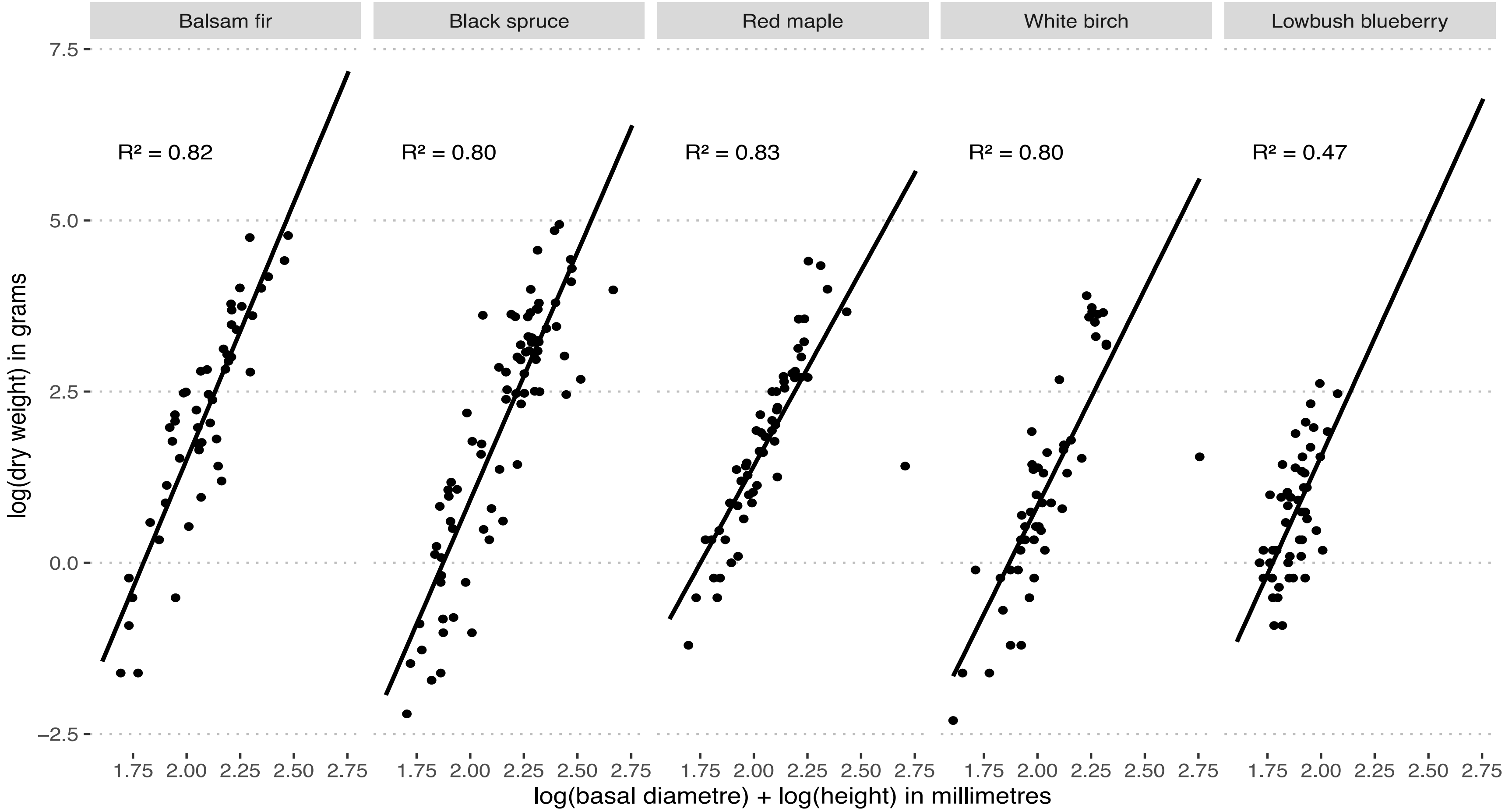

Figure B.4.1 Allometric modelling of biomass in terms of basal diameter and height for each of our study species, balsam fir, black spruce, red maple, white birch, and lowbush blueberry. The goodness of fit (adjusted R^2) is superimposed on each species regression plot.

B.5 Number of samples augmented to estimate plot density

Table B.5.1 The number of individuals that we augmented using foliar samples to obtain density measures when individuals of that species were not encountered on the shrub belt. Numbers are shown for each species per height class relative to the total number of individuals used in that height class. Height class is coded as A = 0-50 cm, B = 51-100 cm, C = 101-150 cm, and D = 151-200 cm.

Species	Height Class	Elemental Sample	Phytochemical Sample
ABBA	A	29/326	30/310
ABBA	B	6/89	9/91
ABBA	C	2/6	1/5
ABBA	D	0/1	0/1
ACRU	A	13/217	
ACRU	B	26/164	
ACRU	C	6/28	
ACRU	D	1/3	
BEPA	A	10/34	
BEPA	B	33/63	
BEPA	C	11/14	
BEPA	D	3/6	
PIMA	A	8/127	8/120
PIMA	B	33/229	35/223
PIMA	C	43/206	44/199

PIMA	D	28/136	29/135
VAAN	A	14/852	
VAAN	B	2/160	
VAAN	C	0/2	

B.6 Detailed description of spatial predictors and processing steps

Our spatial resolution was constrained by our coarsest dataset, Landsat 8, i.e., 30 m resolution. In ArcGIS, we resampled our Digital Elevation Model from a 20 m to a 30 m resolution. The Forest Resource Inventory vector dataset was rasterized at a 30 m resolution.

Enhanced Vegetation Index (EVI): Landsat 8 satellite imagery was acquired from the Earth Resources Observation (EROS) and Science, Centre Science Processing Architecture (ESPA). There were three Landsat 8 scenes available during our 2016 sampling time period; June 28, August 15, and September 16, 2016 with 0.46%, 20.18%, 4.39% land cloud cover respectively. As a standard product, Landsat 8 acquisitions contain a preprocessed EVI surface reflectance scene. Newfoundland boreal forest demonstrably receives a greater amount of precipitation and experiences shorter growing seasons due to Atlantic Ocean influences creating colder climatic conditions compared to continental boreal forest conditions (South, 1983). Under these conditions, the EVI as a measure of biological productivity performs better than the Normalized Difference Vegetation Index which commonly saturates early in the season and does not account for the structural complexity of vegetative canopies (Muraoka et al., 2013; Requena-Mullor et al., 2017; Waring et al., 2006). Using the Landsat Quality Assurance ArcGIS toolbox, publicly accessible software from the U.S. Geological Survey, we extracted the following cloud coded bits from the pixel QA band: cloud shadow, snow, cloud, high cloud confidence and high cirrus confidence (Jones et al., 2013; U.S. Geological Survey, 2017). Using the ‘Extract by Mask’ ArcGIS function we removed cloudy pixels from our EVI scenes. In R, we rescaled EVI scenes by dividing by 0.0001. Using the ‘approxNA’ function from the ‘raster’ R package (Hijmans, 2020), we computed a linear interpolation across our temporal scenes to fill cloud removed pixels, see Appendix B.7 Figure B.7.1, for before and after interpolation maps and pixel histograms. We average our temporal EVI scene to obtain an estimated seasonal measure of productivity. Using the ‘raster.transformation’ function from the ‘spatialEco’ R package, we standardized the EVI annual productivity scene by subtracting the scene mean from each pixel and dividing by the scene standard deviation (Evans, 2020).

Elevation, Aspect, Slope and Land Cover: A Canadian Digital Elevation Model (DEM) was retrieved from Natural Resources Canada. Using ArcGIS, we combined DEM images together to create a seamless raster. In ArcGIS, using the ‘Clip’ function we limited our DEM raster to our AOI. Using the ‘terrain’ function from the ‘raster’ R package we constructed aspect and slope rasters. We normalized our aspect raster by replacing any value > 180 by subtracting -180 (e.g., an aspect of 240 is now an aspect of 60; changing the scale from 0-360 to 0-180). We used the base R ‘subs’ function with a legend of corresponding values to normalize the aspect raster. As we did for the EVI raster, we standardized elevation, aspect, and slope rasters using the ‘raster.transformation’ function from the ‘spatialEco’ R package. In addition, we used the freely accessible Commission for Environmental Cooperation Land Cover dataset; derived from Landsat images, to obtain categorical values of forest type: coniferous, deciduous, mixed coniferous and deciduous.

Forest Resource Inventory: our AOI covers a national park, Terra Nova National Park (TNNP) and public land. Spatial information regarding forest stand attributes, Forest Resource Inventory (spatial vector), were supplied to us from two sources: Parks Canada and the Provincial Government of Newfoundland and Labrador. Using unique forest polygon identifiers, we attributed spatial covariates to the FRI datasets (attributes also contained non-interest covariates). To construct a seamless FRI layer across our AOI we combined the two sets of Forest Resource Inventory together. In ArcGIS, using the ‘clip’ function we constrained the geographic extents of the two FRI datasets to our AOI; to alleviate spatial data processing time. Using the ‘erase’ function in ArcGIS we removed any spatially overlapping boundaries between the two FRI datasets. Using the ‘merge’ ArcGIS function we create a single FRI dataset by spatially joining the two FRI datasets together. In R, we subset the FRI dataset to only include covariates of interest: forest stand age class, height class, and crown density – categorical properties that likely influence growing conditions and thus the elemental and phytochemical properties of our plants. In R, we further cleaned the FRI dataset by removing any non-intention ‘white space’ in the text of the categorical data. For each co-variate we extracted unique values and re-coding text values as integers. Using the ‘rasterize’ function from the ‘raster’ R package, we convert our FRI vector data into a raster for each co-covariate, using the integer values as a coded legend for our categories. In addition, we created binary layers for each factor in the age class, height class, and crown density variables. Binary layers were used when model average estimates were extracted as the predict function in the ‘raster’ package is limited to single model objects.

Inference Mask: Using species composition codes derived from the FRI dataset for each of our sample points, we create a vector mask of forest polygons types for which we have spatial inference. These codes represent community types dominated by either black spruce, white spruce, and white birch. In R, we used the ‘mask’ function from the ‘raster’ package to clip spatial covariate surfaces.

Spatial Data Extraction: At each plot location, using the ‘extract’ function from the ‘raster’ R package we spatially extracted pixel values from each of our raster datasets: elevation, aspect, slope, and land cover. We used the ‘intersect’ function from the ‘raster’ R package to extract polygon forest stand attributes from the FRI dataset: age class, height class, and crown density. At some sample locations the FRI was either inaccurate or our sample location was within a wetland type area with no attributes. For these instances, we attributed our sample locations with the values from the closest forest stand polygon. In total there were 14, 3, and 5 incorrect spatial designations for age class, height class, and crown density, however the adjacent forested polygon reflected observed conditions at the plot level.

B.7 Temporal interpolation figures of EVI surfaces

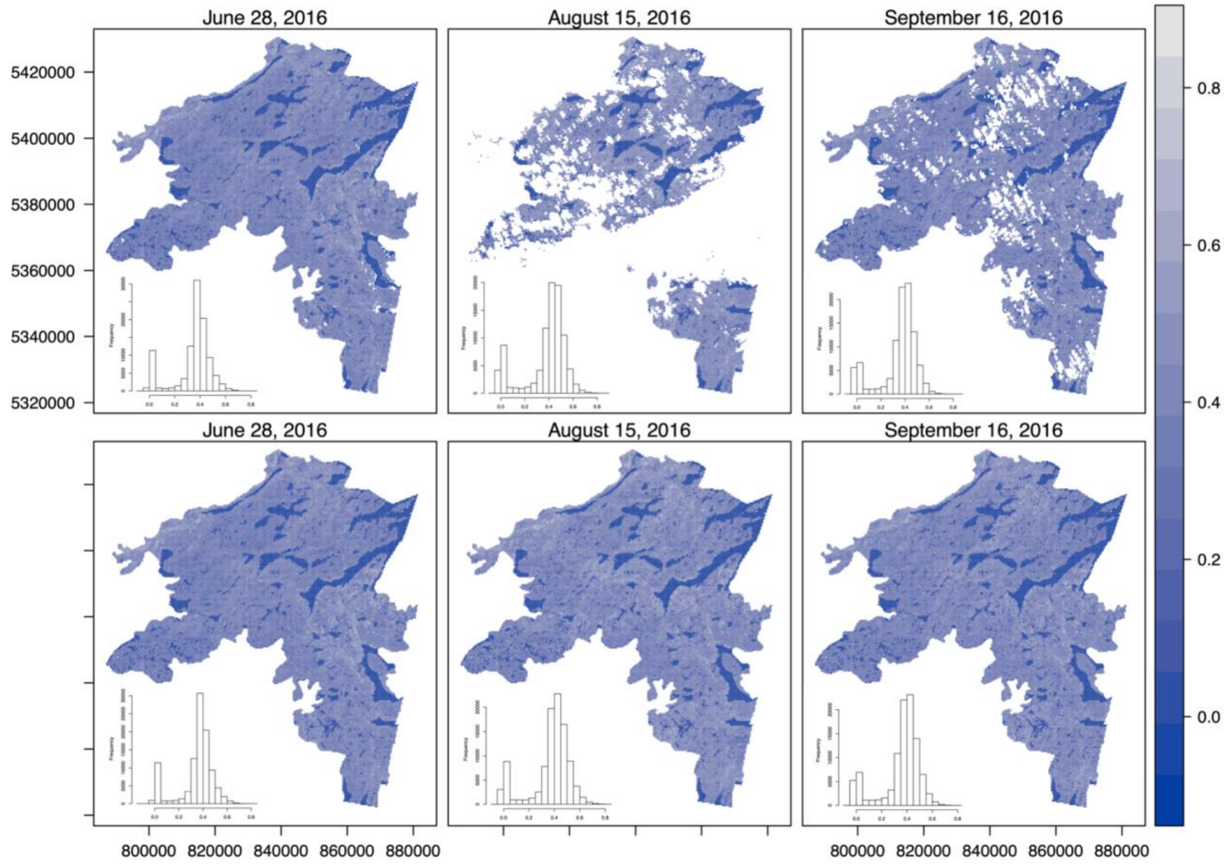

Figure B.7.1 Using the ‘approxNA’ function from the ‘raster’ package in R, we performed a linear temporal interpolation to determine pixel values for areas of cloud cover for our three Enhanced Vegetation Index scenes, June 28, August 15, and September 16, 2016. The top panel shows each scene before interpolation and the bottom panel shows each scene after interpolation. Accompanying histograms are provided for each EVI scene, demonstrating the change in pixel value distribution after interpolation.

B.8 Top model AICc results

Table B.8.1 AIC_c results for foliar elemental (percent and quantity), stoichiometric, and phytochemical traits. Explanatory variables include land cover, EVI, biotic, and abiotic. Land cover is a categorical variable with three factor levels which include coniferous, deciduous, and mixed. EVI is the Enhanced Vegetation Index and performs better than NDVI (Normalized Difference Vegetation Index) under wet conditions. Our biotic variable represents forest structural conditions and is comprised of three variables, age class, height class, and canopy density, each containing four factors levels of increasing age, height, and canopy density. Abiotic is comprised of three continuous variables for elevation, aspect, and slope. Results are shown for models within 2 delta AIC_c, K is the number of parameters, LL represents the model log likelihood, ΔAIC_c for the interpretation of model ranking, ωAIC_c for model weights, and R^2 is presented as Efron's goodness of fit. Pretending variables are denoted with an asterisk and were removed from any model averaging. Biomass basis phytochemical models are identified with (bm).

Species	**Explanatory Variables**	**K**	**LL**	**ΔAIC_c**	**ωAIC_c**	**R^2**
Elemental: percent carbon						
ABBA	Abiotic	5	-47.96	0.00	0.52	0.19
	EVI* + Abiotic	6	-47.36	1.08	0.31	0.20
ACRU	Abiotic	5	-51.43	0.00	0.37	0.09
	EVI* + Abiotic	6	-50.54	0.52	0.28	0.11
BEPA	Biotic	10	-72.14	0.00	0.48	0.31
PIMA	Biotic + Abiotic	14	-202.13	0.00	0.38	0.64
	Land Cover + Biotic + Abiotic	16	-199.88	0.42	0.31	0.65

VAAN	Land Cover + Biotic + Abiotic	16	-92.50	0.00	0.44	0.37
	Land Cover + EVI* + Biotic + Abiotic	17	-91.78	1.06	0.26	0.37
Elemental: percent nitrogen						
ABBA	Land Cover + EVI + Abiotic	8	48.53	0.00	0.62	0.29
ACRU	Land Cover + Biotic	13	20.02	0.00	0.36	0.36
	Land Cover + EVI* + Biotic	14	21.05	0.75	0.25	0.37
BEPA	Intercept	2	-45.13	0.00	0.41	0.00
	Abiotic	5	-42.47	1.43	0.20	0.07
	EVI	3	-44.96	1.85	0.16	0.00
PIMA	EVI + Biotic	12	112.91	0.00	0.68	0.36
VAAN	EVI	3	33.08	0.00	0.45	0.07
	Land Cover + EVI	5	34.82	0.76	0.31	0.09
Elemental: percent phosphorus						
ABBA	Abiotic	5	199.02	0.00	0.52	0.10
ACRU	EVI	3	134.27	0.00	0.39	0.05
	EVI + Abiotic	6	136.95	1.35	0.20	0.10
BEPA	Intercept	2	94.94	0.00	0.51	0.00
	EVI	3	95.44	1.19	0.28	0.01
PIMA	Biotic + Abiotic	14	345.69	0.00	0.42	0.28
	EVI* + Biotic + Abiotic	15	346.63	0.57	0.32	0.29
VAAN	EVI + Biotic	12	419.42	0.00	0.60	0.47
	Biotic	11	417.36	1.78	0.25	0.46

Elemental: quantity carbon						
ABBA	Biotic + Abiotic	14	-158.93	0.00	0.68	0.35
ACRU	Intercept	2	-190.97	0.00	0.60	0.00
	EVI	3	-190.84	1.87	0.23	0.00
BEPA	Intercept	2	10.10	0.00	0.60	0.00
PIMA	Intercept	2	-497.69	0.00	0.43	0.00
	Abiotic	5	-495.20	1.34	0.22	0.03
VAAN	Land Cover + Abiotic	7	-444.06	0.00	0.56	0.19
Elemental: quantity nitrogen						
ABBA	Biotic + Abiotic	14	227.46	0.00	0.68	0.35
ACRU	Intercept	2	121.64	0.00	0.58	0.00
	EVI	3	121.87	1.67	0.25	0.01
BEPA	Intercept	2	251.05	0.00	0.62	0.00
PIMA	Intercept	2	146.79	0.00	0.38	0.00
	Abiotic	5	149.56	0.79	0.25	0.03
	EVI	3	146.97	1.74	0.16	0.00
VAAN	Land Cover + Abiotic	7	166.00	0.00	0.54	0.18
	Land Cover + EVI* + Abiotic	8	166.19	1.84	0.22	0.19
Elemental: quantity phosphorus						
ABBA	Biotic + Abiotic	14	449.29	0.00	0.53	0.32
ACRU	Intercept	2	334.15	0.00	0.61	0.00
	EVI	3	334.24	1.96	0.23	0.00
BEPA	Intercept	2	433.74	0.00	0.62	0.00

PIMA	Intercept	2	470.41	0.00	0.48	0.00
VAAN	Land Cover + Abiotic	7	581.16	0.00	0.72	0.19
Stoichiometric: C:N ratio						
ABBA	Land Cover + EVI + Abiotic	8	-364.16	0.00	0.72	0.31
ACRU	Land Cover + Biotic	13	-267.39	0.00	0.40	0.39
	Land Cover + EVI* + Biotic	14	-266.49	0.99	0.24	0.40
BEPA	Intercept	2	-291.69	0.00	0.48	0.00
	EVI	3	-291.22	1.25	0.26	0.01
PIMA	EVI + Biotic	12	-559.84	0.00	0.70	0.38
VAAN	EVI	3	-539.51	0.00	0.44	0.09
	Land Cover + EVI	5	-537.79	0.79	0.30	0.11
Stoichiometric: C:P ratio						
ABBA	Abiotic	5	-755.06	0.00	0.63	0.14
ACRU	Abiotic	5	-665.73	0.00	0.26	0.07
	Intercept	2	-669.06	0.07	0.25	0.00
	EVI + Abiotic	6	-664.89	0.61	0.19	0.09
	EVI	3	-668.32	0.75	0.18	0.02
BEPA	Intercept	2	-568.29	0.00	0.49	0.00
	EVI	3	-567.62	0.85	0.32	0.02
PIMA	Biotic + Abiotic	14	-1095.54	0.00	0.59	0.30
	EVI* + Biotic + Abiotic	15	-1095.19	1.75	0.25	0.30
VAAN	Biotic	11	-1189.78	0.00	0.40	0.33
	EVI + Biotic	12	-1188.63	0.03	0.39	0.34

Stoichiometric: N:P ratio						
ABBA	Abiotic	5	-331.11	0.00	0.31	0.08
	EVI + Abiotic	6	-330.06	0.18	0.28	0.10
	Intercept	2	-334.87	0.99	0.19	0.00
ACRU	EVI + Abiotic	6	-324.45	0.00	0.54	0.17
BEPA	Intercept	2	-245.07	0.00	0.44	0.00
	EVI	3	-244.16	0.36	0.37	0.03
PIMA	EVI + Biotic + Abiotic	15	-410.79	0.00	0.73	0.31
VAAN	EVI + Biotic + Abiotic	15	-541.26	0.00	0.32	0.41
	EVI + Biotic	12	-544.89	0.04	0.31	0.39
	Land Cover + EVI + Biotic + Abiotic	17	-539.24	0.94	0.20	0.43
	Land Cover + EVI + Biotic	14	-543.20	1.44	0.15	0.40
Phytochemical: terpene (raw)						
ABBA	EVI	3	-269.49	0.00	0.52	0.05
PIMA	EVI + Biotic + Abiotic	15	-471.87	0.00	0.47	0.27
	Biotic + Abiotic	14	-473.22	0.28	0.41	0.26
Phytochemical: terpene (bm)						
ABBA	Biotic + Abiotic	14	-516.39	0.00	0.54	0.27
PIMA	Intercept	2	-1126.03	0.00	0.40	0.00
	Abiotic	5	-1123.40	1.05	0.24	0.03
	EVI	3	-1125.99	2.00	0.15	0.00
Phytochemical: monoterpene (raw)						

ABBA	EVI + Abiotic	6	-229.81	0.00	0.44	0.12
	Abiotic	5	-231.81	1.75	0.18	0.08
	EVI	3	-234.08	1.93	0.17	0.04
PIMA	Biotic + Abiotic	14	-290.67	0.00	0.67	0.24
Phytochemical: monoterpene (bm)						
ABBA	Biotic + Abiotic	14	-461.32	0.00	0.57	0.27
PIMA	Intercept	2	-944.97	0.00	0.41	0.00
	Abiotic	5	-942.37	1.12	0.23	0.03
Phytochemical: monoterpenic alcohol (raw)						
ABBA	Land Cover	4	42.49	0.00	0.26	0.05
	Intercept	2	40.04	0.61	0.19	0.00
	Land Cover + EVI	5	43.01	1.17	0.15	0.06
	Land Cover + Abiotic	7	45.16	1.42	0.13	0.09
	Abiotic	5	42.64	1.90	0.10	0.05
PIMA	Biotic + Abiotic	14	149.34	0.00	0.53	0.23
Phytochemical: monoterpenic alcohol (bm)						
ABBA	Intercept	2	-179.59	0.00	0.30	0.00
	EVI	3	-178.87	0.67	0.21	0.01
	Biotic + Abiotic	14	-165.76	0.94	0.19	0.23
PIMA	Intercept	2	-487.60	0.00	0.42	0.00
	Abiotic	5	-485.08	1.27	0.22	0.03
	EVI	3	-487.49	1.86	0.16	0.00
Phytochemical: monoterpenic ester (raw)						

ABBA	Intercept	2	-115.95	0.00	0.21	0.00
	Land Cover	4	-113.88	0.13	0.19	0.04
	Land Cover + EVI	5	-112.80	0.19	0.19	0.06
	Abiotic	5	-113.31	1.22	0.11	0.05
	EVI	3	-115.73	1.67	0.09	0.00
PIMA	Biotic + Abiotic	14	-310.53	0.00	0.57	0.27
	EVI* + Biotic + Abiotic	15	-309.93	1.23	0.31	0.27
Phytochemical: monoterpenic ester (bm)						
ABBA	Biotic + Abiotic	14	-332.19	0.00	0.47	0.27
PIMA	Intercept	2	-926.76	0.00	0.42	0.00
	Abiotic	5	-924.24	1.26	0.22	0.03
Phytochemical: sesquiterpene (raw)						
ABBA	EVI + Abiotic	6	-61.73	0.00	0.33	0.10
	EVI	3	-65.31	0.54	0.25	0.04
	Abiotic	5	-63.51	1.31	0.17	0.07
PIMA	Land Cover + EVI + Abiotic	8	4.46	0.00	0.28	0.12
	Abiotic	5	0.93	0.50	0.22	0.08
	EVI + Biotic + Abiotic	15	11.98	1.29	0.15	0.19
	EVI + Abiotic	6	1.53	1.45	0.13	0.08
Phytochemical: sesquiterpene (bm)						
ABBA	EVI	3	-284.44	0.00	0.23	0.02
	Biotic + Abiotic	14	-271.25	0.08	0.22	0.24
	Intercept	2	-285.69	0.36	0.19	0.00

PIMA	Intercept	2	-566.61	0.00	0.38	0.00
	Abiotic	5	-563.89	0.86	0.25	0.03
	EVI	3	-566.55	1.95	0.15	0.00
Phytochemical: diversity						
ABBA	Abiotic	5	113.25	0.00	0.31	0.06
	Intercept	2	109.95	0.11	0.30	0.00
	EVI	3	110.17	1.79	0.13	0.00
	EVI + Abiotic	6	113.45	1.85	0.12	0.07
PIMA	Land Cover	4	189.24	0.00	0.31	0.04
	Biotic	11	196.43	1.11	0.18	0.12
	EVI	3	187.20	1.98	0.11	0.02

B.9 Top model coefficient signs (+/-) and significance

Table B.9.1 Coefficient signs (+/-) for all for top ranked models. Top models are presented in order of rank with Efron pseudo R^2 presented in the last column. We use red coloured coefficients signs to indicate statistical significance at $p \leq 0.05$. For land cover, Decid, and Mix indicate, deciduous, and mixed cover types respectively. EVI represents the Enhanced Vegetation Index. For biotic variables, AC indicates age class with 3, 4, 5 representing factor levels of 41-60, 61-80, and 81-100 years, respectively. HC indicates height class with 3, 4, 5 representing factor levels of 6.6-9.5, 9.6-12.5, 12.6-15.5 metres, respectively. CD indicates canopy density with 2, 3, 4 representing factor levels of 51-75, 26-50, 10-25 percent closed. For abiotic variables, E, A, and S represent elevation, aspect, and slope, respectively.

	Land cover		Prod	Biotic factors									Abiotic factors			
Species	Decid	Mix	EVI	AC3	AC4	AC5	HC3	HC4	HC5	CD2	CD3	CD4	E	A	S	R^2
Elemental: percent carbon																
ABBA													+	−	+	0.19
ACRU													−	−	−	0.09
BEPA				+	+	+	−	−	−	−	−					0.31
PIMA				+	+	+	−	−	−	+	−	−	+	+	+	0.64

PIMA	−	−		+	+	+	−	−	−	+	−	−	+	+	+	0.65
VAAN	−	−		+	+	+	−	−	−	−	+	+	+	−	+	0.37
Elemental: percent nitrogen																
ABBA	−	−	+										−	+	+	0.29
ACRU	−	−		−	−	−	+	+	+	−	−	−				0.36
PIMA			+	−	−	−	+	+	+	+	+	+				0.36
VAAN			+													0.07
VAAN	−	−	+													0.09
Elemental: percent phosphorus																
ABBA													+	+	+	0.1
ACRU			+													0.05
ACRU			−										+	+	+	0.1
PIMA				−	−	−	+	+	+	+	+	−	+	+	+	0.28
VAAN			−	−	−	−	−	−	+	−	−	−				0.47
VAAN				−	−	−	−	−	−	+	−	−				0.46
Elemental: quantity carbon																

ABBA				−	−	−	−	−	−	−	+	+	+	−	+	0.35
VAAN	+	+											+	+	−	0.19
Elemental: quantity nitrogen																
ABBA				−	−	−	−	−	−	−	+	+	+	−	+	0.35
VAAN	+	+											+	+	−	0.18
Elemental: quantity phosphorus																
ABBA				−	−	−	−	−	−	+	+	+	+	+	+	0.32
VAAN	+	+											+	+	−	0.19
Stoichiometric: C:N ratio																
ABBA	+	+	−										+	−	−	0.31
ACRU	+	+		+	+	+	−	−	−	+	+	+				0.39
PIMA			−	+	+	+	−	−	−	−	−	−				0.38
VAAN			−													0.09
VAAN	+	+	−													0.11
Stoichiometric: C:P ratio																
ABBA													+	−	−	0.14

*ACRU													−	−	−	0.07
PIMA				+	+	+	−	−	−	−	−	+	−	−	−	0.3
VAAN				+	+	+	+	+	−	−	+	+				0.33
VAAN			+	+	+	+	+	+	−	−	+	+				0.34
Stoichiometric: N:P ratio																
*ABBA													−	−	−	0.08
*ABBA			+										−	−	−	
ACRU			+										−	−	−	0.17
PIMA			+	+	+	+	−	+	−	+	−	+	−	−	−	0.31
VAAN			+	+	+	+	−	+	−	−	−	−	−	−	+	0.41
VAAN			+	+	+	+	−	+	−	−	−	+				0.39
VAAN	−	−	+	+	+	+	−	+	−	−	−	+	−	−	+	0.43
VAAN	−	−	+	+	+	+	−	+	−	−	−	+				0.4
Phytochemical: terpene (raw)																
ABBA			+													0.05
PIMA			−	+	+	+	−	−	−	+	+	+	−	−	−	0.27

PIMA				+	+	+	−	−	−	+	+	+	−	−	−	0.26
Phytochemical: terpene (bm)																
ABBA				−	−	−	−	−	−	+	+	+	+	−	+	0.27
Phytochemical: monoterpene (raw)																
ABBA			+										+	−	+	0.12
ABBA													+	−	+	0.08
ABBA			+													0.04
PIMA				+	+	+	−	−	−	+	+	+	−	−	−	0.24
Phytochemical: monoterpene (bm)																
ABBA				−	−	−	−	−	−	+	+	+	+	−	+	0.27
Phytochemical: monoterpenic alcohol (raw)																
*ABBA	+	+														0.05
PIMA				+	+	+	−	−	−	+	+	+	−	−	−	0.23
Phytochemical: monoterpenic ester (raw)																
PIMA				+	+	+	−	−	−	+	+	+	−	−	−	0.27
Phytochemical: monoterpenic ester (bm)																

ABBA				−	−	−	−	−	−	+	+	+	+	−	+	0.27
Phytochemical: sesquiterpene (raw)																
ABBA			+										−	−	−	0.1
ABBA			+													0.04
ABBA													−	−	−	0.07
PIMA	−	+	−										−	−	−	0.12
PIMA													−	−	−	0.08
PIMA			−	+	−	+	−	−	−	−	−	+	−	+	−	0.19
PIMA			−										−	−	−	0.08
Phytochemical: sesquiterpene (bm)																
*ABBA			+													0.02
*ABBA				−	−	−	−	−	−	+	+	+	+	−	+	0.24
Phytochemical: diversity																
*ABBA													−	−	+	0.06
PIMA	+	+														0.04
PIMA				−	−	−	−	+	+	−	−	−				0.12

PIMA			+													0.02

B.10 Distribution of pseudo R^2 of top models at the species and trait level

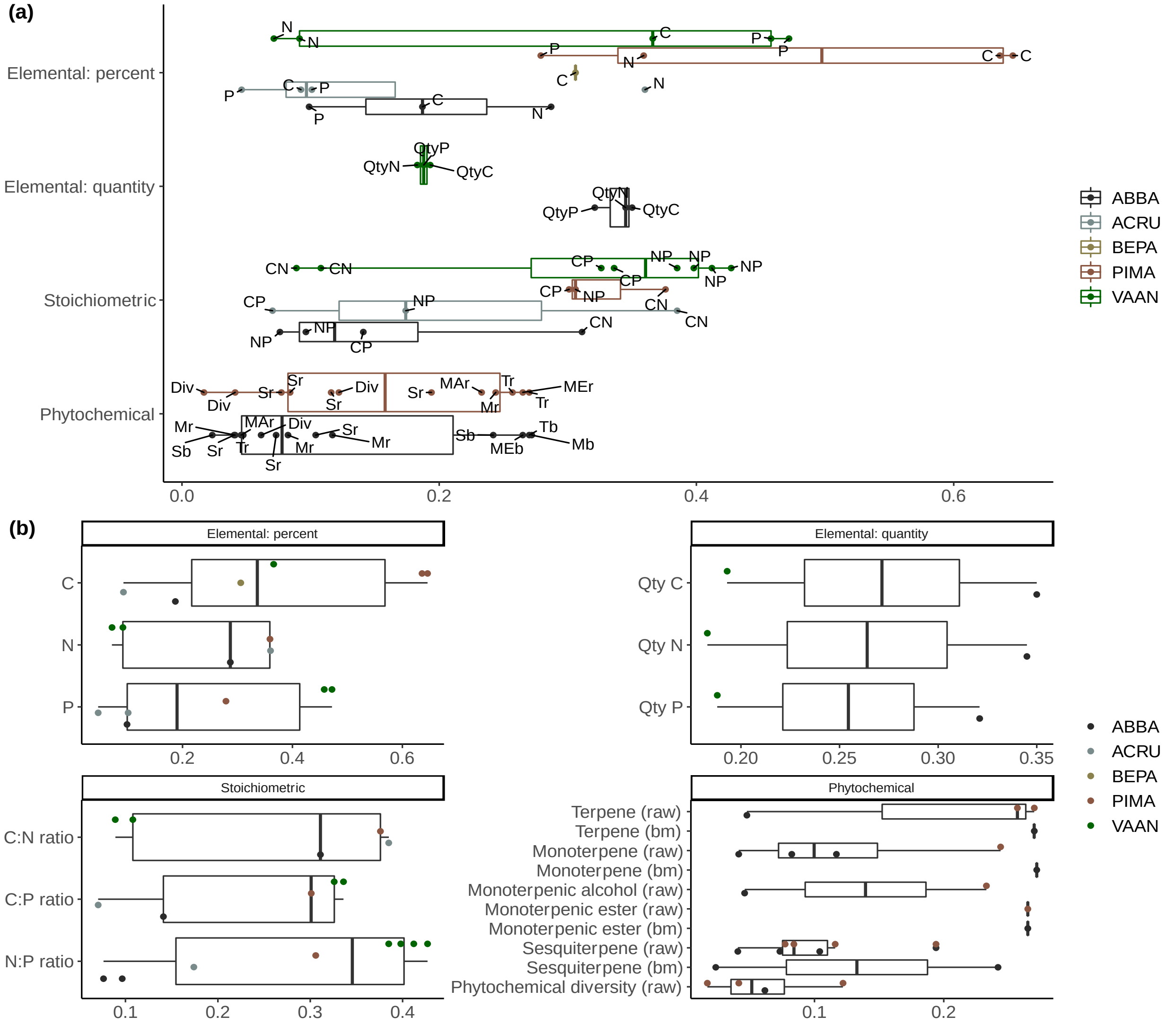

Figure B.10.1 Distribution of pseudo R^2 values across species, at the trait type level (a) and at the trait level (b), for all top ranked models. At trait type level, we show pseudo R^2 values for element percent and quantity, stoichiometric, and phytochemical traits. At the trait level we show individual traits of percent elemental (i.e., %C, %N, and %P), quantity elemental (i.e., C, N, and P on a g/m^2 biomass basis), stoichiometric ratios (i.e., C:N, C:P, and N:P), and phytochemical groups (terpene, monoterpene, monoterpenic alcohol, monoterpenic ester, sesquiterpene, and phytochemical diversity) on a raw of biomass basis, indicated as either (raw) or (bm) suffixes, respectively. Species bar and point colours are the same between plots. In addition, labels are provided in (a) to identify individual traits for a given species within a trait type.

B.11 Comparison of observed data and predicted raster data

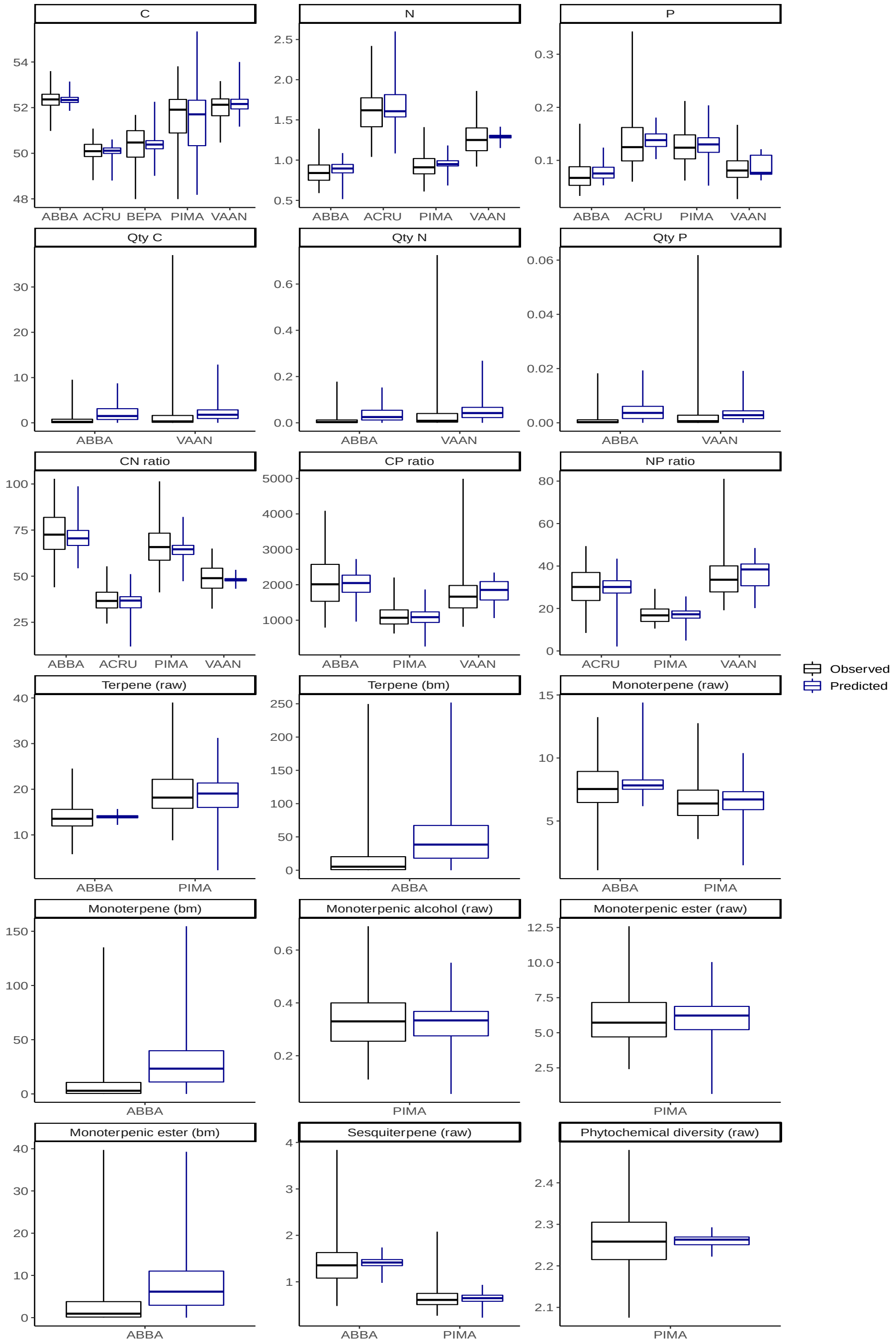

Figure B.11.1 Comparison of observed (data) and predicted (raster values) data for foliar elemental, stoichiometric, and phytochemical traits for each of our study species where a parsimonious explanation was determined. Generally, medians are consistent between observed and predicted data, however, ranges differ between observed and predicted variability.

B.12 Coefficient estimates, confidence intervals, and standard error values to top ranked models

Table B.12.1 Foliar percent carbon trait coefficient estimates, confidence intervals, and standard error values for top ranked models (< 2 ΔAIC_c). Species codes are used for balsam fir (ABBA), red maple (ACRU), white birch (BEPA), black spruce (PIMA), and lowbush blueberry (VAAN). If there is more than one top ranked model per species, we present in order of ΔAIC_c rank. Model numbers are supplied beside the species code in the top row (see Table 3.2 for model descriptions). Predictors include land cover (LandCover5 and LandCover6 represent deciduous and mixedwood conditions), EVI (i.e., proxy for productivity), abiotic factors (aspect, slope, elevation), and biotic factors: AgeClss3 (41-60 years old), AgeClss 4 (61-80 years old), AgeClss5 (81-100 years old), HghtCls3 (6.6 - 9.5 m), HghtCls4 (9.6-12.5 m), HghtCls5 (12.6-15.5m), CrwnDns2 (51-75 % closed), CrwnDns3 (26-50%), CrwnDn4 (10-25 % closed). Total number of observations are provided in the bottom row. In addition, asterisks are used to indicate coefficient significance as follows: * $p<0.05$ ** $p<0.01$ *** $p<0.001$.

	ABBA 15	**ABBA 9**	**ACRU 15**	**ACRU 9**	**BEPA 14**	**PIMA 10**	**PIMA 3**	**VAAN 3**	**VAAN 1**
Predictors									
Intercept	52.33 ***	52.33 ***	50.12 ***	50.12 ***	51.00 ***	49.93 ***	50.40 ***	52.45 ***	52.50 ***
	(52.24-52.41)	(52.24 -52.41)	(50.03 -50.21)	(50.03-50.21)	(50.08 -51.93)	(49.16 -50.70)	(49.50-51.29)	(51.97-52.93)	(52.01-52.98)
	(0.04)	(0.04)	(0.05)	(0.05)	(0.47)	(0.39)	(0.46)	(0.24)	(0.25)

Aspect	-0.09	-0.10	-0.08	-0.08		0.14	0.16	-0.05	-0.05
	(-0.19-0.01)	(-0.20-0.01)	(-0.18-0.03)	(-0.19-0.03)		(-0.07-0.35)	(-0.05-0.37)	(-0.15-0.05)	(-0.15-0.05)
	(0.05)	(0.05)	(0.06)	(0.06)		(0.11)	(0.11)	(0.05)	(0.05)
Slope	0.07	0.06	-0.11 *	-0.12 *		0.24 *	0.28 **	0.16 **	0.17 **
	(-0.03-0.18)	(-0.04-0.17)	(-0.22--0.00)	(-0.23--0.01)		(0.04-0.44)	(0.08-0.49)	(0.06-0.27)	(0.06-0.27)
	(0.05)	(0.05)	(0.05)	(0.06)		(0.10)	(0.10)	(0.05)	(0.05)
Elevation	0.14 **	0.14 **	-0.16 **	-0.15 **		0.28 **	0.26 *	0.08	0.06
	(0.04-0.25)	(0.04-0.25)	(-0.26--0.05)	(-0.26--0.05)		(0.08-0.48)	(0.06-0.46)	(-0.02-0.17)	(-0.04-0.16)
	(0.05)	(0.05)	(0.05)	(0.05)		(0.10)	(0.10)	(0.05)	(0.05)
EVI		0.05		0.06					-0.06
		(-0.04-0.13)		(-0.03-0.15)					(-0.17-0.04)
		(0.04)		(0.05)					(0.05)
AgeClss3					1.25 ***	2.03 ***	1.97 ***	0.34	0.30
					(0.62-1.88)	(1.28-2.79)	(1.21-2.73)	(-0.04-0.72)	(-0.09-0.69)
					(0.32)	(0.39)	(0.39)	(0.20)	(0.20)
AgeClss4					0.71	2.97 ***	2.52 ***	0.08	-0.06
					(-0.14-1.55)	(2.18-3.77)	(1.61-3.42)	(-0.39-0.56)	(-0.59-0.47)
					(0.43)	(0.41)	(0.46)	(0.24)	(0.27)

AgeClss5	0.78	2.54 ***	2.37 ***	0.27	0.20
	(0.00-1.56)	(1.89-3.18)	(1.71-3.03)	(-0.05-0.59)	(-0.14-0.55)
	(0.40)	(0.33)	(0.34)	(0.17)	(0.18)
HghtCls3	-1.39 **	-0.47	-0.46	-0.49 ***	-0.49 ***
	(-2.18--0.60)	(-1.03-0.08)	(-1.02-0.09)	(-0.76--0.23)	(-0.76--0.23)
	(0.40)	(0.28)	(0.28)	(0.14)	(0.14)
HghtCls4	-0.80	-0.11	-0.09	-0.31	-0.28
	(-1.66-0.06)	(-0.74-0.52)	(-0.72-0.53)	(-0.62--0.00)	(-0.60-0.03)
	(0.44)	(0.32)	(0.32)	(0.16)	(0.16)
HghtCls5	-0.98	-0.06	-0.02	-0.24	-0.18
	(-1.95--0.02)	(-0.81-0.69)	(-0.76-0.73)	(-0.61-0.12)	(-0.56-0.20)
	(0.49)	(0.38)	(0.38)	(0.19)	(0.19)
CrwnDns2	-0.36	0.04	0.17	-0.07	-0.10
	(-1.01-0.29)	(-0.62-0.70)	(-0.52-0.85)	(-0.45-0.30)	(-0.48-0.28)
	(0.33)	(0.34)	(0.35)	(0.19)	(0.19)
CrwnDns3	-0.60	-0.67 *	-0.48	0.20	0.20
	(-1.28-0.07)	(-1.29--0.05)	(-1.14-0.17)	(-0.15-0.55)	(-0.16-0.55)
	(0.34)	(0.32)	(0.34)	(0.18)	(0.18)

CrwnDns4						-0.14	-0.03	0.14	0.14
						(-1.14-0.87)	(-1.03-0.98)	(-0.33-0.60)	(-0.32-0.61)
						(0.51)	(0.51)	(0.24)	(0.24)
LandCover5							-0.14	-0.40	-0.37
							(-1.02-0.73)	(-0.87-0.08)	(-0.84-0.11)
							(0.45)	(0.24)	(0.24)
LandCover6							-0.57	-0.44**	-0.43**
							(-1.17-0.03)	(-0.75--0.14)	(-0.73--0.12)
							(0.31)	(0.16)	(0.16)
Observations	95	95	91	91	71	157	157	160	160

Table B.12.2 Foliar percent nitrogen trait coefficient estimates, confidence intervals, and standard error values for top ranked models (< 2 ΔAIC_c). Species codes are used for balsam fir (ABBA), red maple (ACRU), white birch (BEPA), black spruce (PIMA), and lowbush blueberry (VAAN). If there is more than one top ranked model per species, we present in order of ΔAIC_c rank. Model numbers are supplied beside the species code in the top row (see Table 3.2 for model descriptions). Predictors include land cover (LandCover5 and LandCover6 represent deciduous and mixedwood conditions), EVI (i.e., proxy for productivity), abiotic factors (aspect, slope, elevation), and biotic factors: AgeClss3 (41-60 years old), AgeClss 4 (61-80 years old), AgeClss5 (81-100 years old), HghtCls3 (6.6-9.5 m), HghtCls4 (9.6-12.5 m), HghtCls5 (12.6-15.5m), CrwnDns2 (51-75 % closed), CrwnDns3 (26-50%), CrwnDn4 (10-25 % closed). Total number of observations are provided in the bottom row. In addition, asterisks are used to indicate coefficient significance as follows: * $p<0.05$ ** $p<0.01$ *** $p<0.001$.

	ABBA 4	**ACRU 6**	**ACRU 5**	**PIMA 7**	**VAAN 13**	**VAAN 11**
Predictors						
Intercept	0.90 ***	2.17 ***	2.11 ***	0.84 ***	1.27 ***	1.29 ***
	(0.80-0.99)	(1.87-2.47)	(1.80-2.42)	(0.74-0.94)	(1.24-1.30)	(1.21-1.37)
	(0.05)	(0.15)	(0.16)	(0.05)	(0.02)	(0.04)

LandCover5	-0.20 *	-0.32 *	-0.33 *			-0.17
	(-0.35--0.05)	(-0.57--0.07)	(-0.57--0.08)			(-0.35-0.02)
	(0.08)	(0.13)	(0.12)			(0.09)
LandCover6	-0.02	-0.10	-0.10			-0.02
	(-0.12-0.08)	(-0.29-0.09)	(-0.28-0.09)			(-0.11-0.07)
	(0.05)	(0.09)	(0.09)			(0.05)
EVI	0.04 *		0.04	0.05 ***	0.05 ***	0.06 **
	(0.00-0.07)		(-0.02-0.09)	(0.02-0.07)	(0.02-0.09)	(0.02-0.10)
	(0.02)		(0.03)	(0.01)	(0.02)	(0.02)
Aspect	0.02					
	(-0.02-0.06)					
	(0.02)					
Slope	0.00					
	(-0.04-0.04)					
	(0.02)					

Elevation	-0.07 **			
	(-0.11--0.03)			
	(0.02)			
AgeClss3		-0.45 **	-0.43 **	-0.16 ***
		(-0.76--0.14)	(-0.74--0.13)	(-0.23--0.08)
		(0.16)	(0.16)	(0.04)
AgeClss4		-0.63 ***	-0.56 **	-0.08
		(-0.95--0.30)	(-0.89--0.22)	(-0.19-0.03)
		(0.16)	(0.17)	(0.06)
AgeClss5		-0.51 ***	-0.47 ***	-0.07
		(-0.77--0.25)	(-0.73--0.21)	(-0.16-0.01)
		(0.13)	(0.13)	(0.04)
HghtCls3		0.12	0.14	0.14 ***
		(-0.16-0.40)	(-0.14-0.43)	(0.07-0.21)
		(0.14)	(0.14)	(0.04)

HghtCls4		0.23 *	0.23 *	0.09 *		
		(0.02-0.45)	(0.02-0.44)	(0.00-0.17)		
		(0.11)	(0.11)	(0.04)		
HghtCls5		0.43 ***	0.40 ***	0.17 **		
		(0.23-0.64)	(0.19-0.61)	(0.07-0.27)		
		(0.10)	(0.11)	(0.05)		
CrwnDns2		-0.18	-0.15	0.09 *		
		(-0.37--0.00)	(-0.34-0.04)	(0.00-0.18)		
		(0.09)	(0.10)	(0.04)		
CrwnDns3		-0.25 *	-0.23 *	0.06		
		(-0.46--0.05)	(-0.43--0.03)	(-0.02-0.15)		
		(0.10)	(0.10)	(0.04)		
CrwnDns4		-0.30 *	-0.28 *	0.02		
		(-0.54--0.05)	(-0.53--0.04)	(-0.11-0.16)		
		(0.13)	(0.13)	(0.07)		
Observations	95	91	91	157	160	160

Table B.12.3 Foliar percent phosphorus trait coefficient estimates, confidence intervals, and standard error values for top ranked models (< 2 ΔAIC_c). Species codes are used for balsam fir (ABBA), red maple (ACRU), white birch (BEPA), black spruce (PIMA), and lowbush blueberry (VAAN). If there is more than one top ranked model per species, we present in order of ΔAIC_c rank. Model numbers are supplied beside the species code in the top row (see Table 3.2 for model descriptions). Predictors include land cover (LandCover5 and LandCover6 represent deciduous and mixedwood conditions), EVI (i.e., proxy for productivity), abiotic factors (aspect, slope, elevation), and biotic factors: AgeClss3 (41-60 years old), AgeClss 4 (61-80 years old), AgeClss5 (81-100 years old), HghtCls3 (6.6-9.5 m), HghtCls4 (9.6-12.5 m), HghtCls5 (12.6-15.5m), CrwnDns2 (51-75 % closed), CrwnDns3 (26-50%), CrwnDn4 (10-25 % closed). Total number of observations are provided in the bottom row. In addition, asterisks are used to indicate coefficient significance as follows: * $p<0.05$ ** $p<0.01$ *** $p<0.001$.

	ABBA 15	**ACRU 13**	**ACRU 9**	**PIMA 10**	**PIMA 2**	**VAAN 7**	**VAAN 14**
Predictors							
Intercept	0.08 ***	0.14 ***	0.14 ***	0.13 ***	0.13 ***	0.12 ***	0.11 ***
	(0.07-0.08)	(0.13-0.15)	(0.13-0.15)	(0.10-0.15)	(0.11-0.15)	(0.10-0.13)	(0.10-0.13)
	(0.00)	(0.01)	(0.01)	(0.01)	(0.01)	(0.01)	(0.01)

Aspect	0.01 **		0.01	0.00	0.00		
	(0.00-0.02)		(-0.00-0.02)	(-0.01-0.01)	(-0.01-0.01)		
	(0.00)		(0.01)	(0.00)	(0.00)		
Slope	0.00		0.01	0.01 *	0.01 *		
	(-0.00-0.01)		(-0.01-0.02)	(0.00-0.01)	(0.00-0.01)		
	(0.00)		(0.01)	(0.00)	(0.00)		
Elevation	0.00		0.02 *	0.01 **	0.01 **		
	(-0.01-0.01)		(0.00-0.03)	(0.00-0.02)	(0.00-0.02)		
	(0.00)		(0.01)	(0.00)	(0.00)		
EVI		-0.01 *	-0.01 *		-0.00	-0.00	
		(-0.02--0.00)	(-0.02--0.00)		(-0.01-0.00)	(-0.01--0.00)	
		(0.01)	(0.01)		(0.00)	(0.00)	
AgeClss3				-0.06 ***	-0.06 ***	-0.04 ***	-0.04 ***
				(-0.09--0.04)	(-0.09--0.04)	(-0.05--0.03)	(-0.05--0.03)
				(0.01)	(0.01)	(0.01)	(0.01)

AgeClss4	-0.01	-0.02	-0.04 ***	-0.03 ***
	(-0.03-0.01)	(-0.05-0.01)	(-0.06--0.02)	(-0.05--0.02)
	(0.01)	(0.01)	(0.01)	(0.01)
AgeClss5	-0.02 *	-0.02 *	-0.04 ***	-0.03 ***
	(-0.04--0.00)	(-0.05--0.00)	(-0.05--0.02)	(-0.05--0.02)
	(0.01)	(0.01)	(0.01)	(0.01)
HghtCls3	0.02 *	0.02 *	-0.00	-0.00
	(0.00-0.04)	(0.00-0.04)	(-0.01-0.01)	(-0.01-0.01)
	(0.01)	(0.01)	(0.01)	(0.01)
HghtCls4	0.00	0.00	-0.00	-0.01
	(-0.02-0.02)	(-0.02-0.02)	(-0.02-0.01)	(-0.02-0.01)
	(0.01)	(0.01)	(0.01)	(0.01)
HghtCls5	0.02	0.02 *	0.00	-0.00
	(-0.00-0.04)	(0.00-0.05)	(-0.01-0.02)	(-0.02-0.01)
	(0.01)	(0.01)	(0.01)	(0.01)

CrwnDns2				0.01	0.01	-0.00	0.00
				(-0.01-0.03)	(-0.01-0.03)	(-0.01-0.01)	(-0.01-0.02)
				(0.01)	(0.01)	(0.01)	(0.01)
CrwnDns3				0.01	0.01	-0.00	-0.00
				(-0.01-0.03)	(-0.01-0.03)	(-0.02-0.01)	(-0.02-0.01)
				(0.01)	(0.01)	(0.01)	(0.01)
CrwnDns4				-0.00	-0.00	-0.01	-0.01
				(-0.03-0.03)	(-0.03-0.03)	(-0.03-0.01)	(-0.03-0.01)
				(0.02)	(0.02)	(0.01)	(0.01)
Observations	95	91	91	157	157	160	160

Table B.12.4 Foliar elemental quantity trait coefficient estimates, confidence intervals, and standard error values for top ranked models (< 2 ΔAIC$_c$). Species codes are used for balsam fir (ABBA), red maple (ACRU), white birch (BEPA), black spruce (PIMA), and lowbush blueberry (VAAN). If there is more than one top ranked model per species, we present in order of ΔAIC$_c$ rank. Model numbers are supplied beside the species code in the top row (see Table 3.2 for model descriptions). Predictors include land cover (LandCover5 and LandCover6 represent deciduous and mixedwood conditions), EVI (i.e., proxy for productivity), abiotic factors (aspect, slope, elevation), and biotic factors: AgeClss3 (41-60 years old), AgeClss 4 (61-80 years old), AgeClss5 (81-100 years old), HghtCls3 (6.6-9.5 m), HghtCls4 (9.6-12.5 m), HghtCls5 (12.6-15.5m), CrwnDns2 (51-75 % closed), CrwnDns3 (26-50%), CrwnDn4 (10-25 % closed). In addition, asterisks are used to indicate coefficient significance as follows: * $p<0.05$ ** $p<0.01$ *** $p<0.001$.

	ABBA QtyC 10	**VAAN QtyC 8**	**ABBA QtyN 10**	**VAAN QtyN 8**	**VAAN QtyN 4**	**ABBA QtyP 10**	**VAANQtyP 8**
Predictors							
Intercept	4.07 ***	1.58 *	0.07 ***	0.04 *	0.04 *	0.01 ***	0.00 *
	(2.40-5.75)	(0.21-2.95)	(0.04-0.10)	(0.01-0.07)	(0.01-0.08)	(0.00-0.01)	(0.00-0.00)
	(0.86)	(0.70)	(0.01)	(0.02)	(0.02)	(0.00)	(0.00)
AgeClss3	-2.53 *		-0.04 **			-0.00 *	
	(-4.42--0.64)		(-0.08--0.01)			(-0.01--0.00)	
	(0.97)		(0.02)			(0.00)	

AgeClss4	-1.77	-0.03		-0.00
	(-3.65-0.11)	(-0.06-0.00)		(-0.01-0.00)
	(0.96)	(0.02)		(0.00)
AgeClss5	-2.17**	-0.04**		-0.00*
	(-3.72--0.63)	(-0.07--0.01)		(-0.01--0.00)
	(0.79)	(0.01)		(0.00)
HghtCls3	-1.81*	-0.03*		-0.00*
	(-3.38--0.24)	(-0.06--0.00)		(-0.01--0.00)
	(0.80)	(0.01)		(0.00)
HghtCls4	-1.26	-0.02		-0.00
	(-2.56-0.05)	(-0.04-0.00)		(-0.00-0.00)
	(0.67)	(0.01)		(0.00)
HghtCls5	-1.44*	-0.02		-0.00
	(-2.86--0.03)	(-0.05-0.00)		(-0.00-0.00)
	(0.72)	(0.01)		(0.00)

CrwnDns2	-0.08		-0.00			0.00	
	(-1.26-1.09)		(-0.02-0.02)			(-0.00-0.00)	
	(0.60)		(0.01)			(0.00)	
CrwnDns3	0.39		0.01			0.00	
	(-0.92-1.70)		(-0.02-0.03)			(-0.00-0.00)	
	(0.67)		(0.01)			(0.00)	
CrwnDns4	1.68		0.02			0.00	
	(-0.21-3.57)		(-0.01-0.05)			(-0.00-0.00)	
	(0.96)		(0.02)			(0.00)	
Aspect	-0.29	0.26	-0.00	0.01	0.01	0.00	0.00
	(-0.78-0.21)	(-0.43-0.95)	(-0.01-0.01)	(-0.01-0.02)	(-0.01-0.02)	(-0.00-0.00)	(-0.00-0.00)
	(0.25)	(0.35)	(0.00)	(0.01)	(0.01)	(0.00)	(0.00)
Slope	0.67 **	-0.17	0.01 **	-0.00	-0.00	0.00 ***	-0.00
	(0.27-1.07)	(-0.84-0.49)	(0.00-0.02)	(-0.02-0.01)	(-0.02-0.01)	(0.00-0.00)	(-0.00-0.00)
	(0.20)	(0.34)	(0.00)	(0.01)	(0.01)	(0.00)	(0.00)

Elevation	0.15	1.44 ***	0.00	0.03 ***	0.03 ***	0.00	0.00 **
	(-0.32-0.62)	(0.71-2.17)	(-0.01-0.01)	(0.02-0.05)	(0.02-0.05)	(-0.00-0.00)	(0.00-0.00)
	(0.24)	(0.37)	(0.00)	(0.01)	(0.01)	(0.00)	(0.00)
LandCover5		7.27 ***		0.14 ***	0.14 **		0.01 ***
		(3.80-10.73)		(0.07-0.22)	(0.05-0.22)		(0.01-0.02)
		(1.77)		(0.04)	(0.04)		(0.00)
LandCover6		0.06		0.01	-0.00		0.00
		(-1.51-1.63)		(-0.03-0.04)	(-0.04-0.04)		(-0.00-0.00)
		(0.80)		(0.02)	(0.02)		(0.00)
EVI					0.01		
					(-0.01-0.02)		
					(0.01)		
Observations	95	160	95	160	160	95	160

Table B.12.5 Foliar stoichiometric C:N trait coefficient estimates, confidence intervals, and standard error values for top ranked models (< 2 ΔAIC_c). Species codes are used for balsam fir (ABBA), red maple (ACRU), white birch (BEPA), black spruce (PIMA), and lowbush blueberry (VAAN). If there is more than one top ranked model per species, we present in order of ΔAIC_c rank. Model numbers are supplied beside the species code in the top row (see Table 3.2 for model descriptions). Predictors include land cover (LandCover5 and LandCover6 represent deciduous and mixedwood conditions), EVI (i.e., proxy for productivity), abiotic factors (aspect, slope, elevation), and biotic factors: AgeClss3 (41-60 years old), AgeClss 4 (61-80 years old), AgeClss5 (81-100 years old), HghtCls3 (6.6-9.5 m), HghtCls4 (9.6-12.5 m), HghtCls5 (12.6-15.5m), CrwnDns2 (51-75 % closed), CrwnDns3 (26-50%), CrwnDn4 (10-25 % closed). Total number of observations are provided in the bottom row. In addition, asterisks are used to indicate coefficient significance as follows: * $p<0.05$ ** $p<0.01$ *** $p<0.001$.

	ABBA 4	**ACRU 6**	**ACRU 5**	**PIMA 7**	**VAAN 13**	**VAAN 11**
Predictors						
Intercept	70.34 ***	23.77 ***	25.12 ***	70.61 ***	48.81 ***	48.14 ***
	(63.17-77.51)	(16.69-30.85)	(17.75-32.48)	(63.24-77.99)	(47.71-49.91)	(45.35-50.93)
	(3.66)	(3.61)	(3.76)	(3.76)	(0.56)	(1.42)

LandCover5	15.56 *	7.80 *	7.92 **			5.87
	(3.85-27.27)	(2.01-13.59)	(2.15-13.70)			(-0.62-12.37)
	(5.98)	(2.95)	(2.95)			(3.31)
LandCover6	2.24	3.02	2.98			0.60
	(-5.59-10.08)	(-1.36-7.40)	(-1.39-7.34)			(-2.67-3.86)
	(4.00)	(2.24)	(2.23)			(1.66)
EVI	-3.48 **		-0.80	-3.26 ***	-2.21 ***	-2.45 ***
	(-6.00--0.96)		(-2.05-0.45)	(-5.16--1.36)	(-3.31--1.11)	(-3.79--1.11)
	(1.29)		(0.64)	(0.97)	(0.56)	(0.68)
Aspect	-1.99					
	(-4.90-0.92)					
	(1.48)					
Slope	-0.15					
	(-3.25-2.96)					
	(1.58)					

Elevation	4.90 **			
	(1.75-8.05)			
	(1.61)			
AgeClss3		12.05 **	11.68 **	11.75 ***
		(4.81-19.29)	(4.45-18.92)	(6.23-17.27)
		(3.69)	(3.69)	(2.82)
AgeClss4		16.38 ***	14.80 ***	8.10
		(8.79-23.97)	(6.84-22.75)	(0.00-16.19)
		(3.87)	(4.06)	(4.13)
AgeClss5		13.51 ***	12.62 ***	7.42 *
		(7.45-19.58)	(6.42-18.82)	(1.15-13.69)
		(3.09)	(3.16)	(3.20)
HghtCls3		-4.60	-5.15	-9.44 ***
		(-11.19-1.98)	(-11.77-1.47)	(-14.70--4.17)
		(3.36)	(3.38)	(2.69)

HghtCls4		-7.48 **	-7.36 **	-5.10		
		(-12.45--2.50)	(-12.32--2.41)	(-11.21-1.01)		
		(2.54)	(2.53)	(3.12)		
HghtCls5		-11.94 ***	-11.30 ***	-11.42 **		
		(-16.77--7.10)	(-16.22--6.38)	(-18.77--4.08)		
		(2.47)	(2.51)	(3.75)		
CrwnDns2		4.10	3.38	-6.14		
		(-0.20-8.40)	(-1.05-7.81)	(-12.52-0.24)		
		(2.19)	(2.26)	(3.26)		
CrwnDns3		6.04 *	5.51 *	-5.22		
		(1.28-10.79)	(0.70-10.32)	(-11.22-0.77)		
		(2.43)	(2.45)	(3.06)		
CrwnDns4		6.98 *	6.67 *	-1.90		
		(1.19-12.77)	(0.88-12.47)	(-11.52-7.73)		
		(2.96)	(2.96)	(4.91)		
Observations	95	91	91	157	160	160

Table B.12.6 Foliar stoichiometric C:P trait coefficient estimates, confidence intervals, and standard error values for top ranked models (< 2 ΔAIC_c). Species codes are used for balsam fir (ABBA), red maple (ACRU), white birch (BEPA), black spruce (PIMA), and lowbush blueberry (VAAN). If there is more than one top ranked model per species, we present in order of ΔAIC_c rank. Model numbers are supplied beside the species code in the top row (see Table 3.2 for model descriptions). Predictors include land cover (LandCover5 and LandCover6 represent deciduous and mixedwood conditions), EVI (i.e., proxy for productivity), abiotic factors (aspect, slope, elevation), and biotic factors: AgeClss3 (41-60 years old), AgeClss 4 (61-80 years old), AgeClss5 (81-100 years old), HghtCls3 (6.6-9.5 m), HghtCls4 (9.6-12.5 m), HghtCls5 (12.6-15.5m), CrwnDns2 (51-75 % closed), CrwnDns3 (26-50%), CrwnDn4 (10-25 % closed). Total number of observations are provided in the bottom row. In addition, asterisks are used to indicate coefficient significance as follows: * *p<0.05* ** *p<0.01* *** *p<0.001*.

	ABBA 15	**PIMA 10**	**PIMA 2**	**VAAN 14**	**VAAN 7**
Predictors					
Intercept	2060.13 ***	1050.36 ***	1023.84 ***	1236.55 ***	1188.23 ***
	(1919.44-2200.82)	(822.39-1278.32)	(786.47-1261.22)	(871.64-1601.45)	(819.07-1557.39)
	(71.78)	(116.31)	(121.11)	(186.18)	(188.35)

Aspect	-251.44 **	-17.44	-16.83		
	(-424.38--78.50)	(-79.52-44.63)	(-79.00-45.34)		
	(88.24)	(31.67)	(31.72)		
Slope	-85.87	-87.56 **	-88.31 **		
	(-263.30-91.56)	(-146.45--28.67)	(-147.30--29.32)		
	(90.53)	(30.05)	(30.10)		
Elevation	69.19	-96.17 **	-88.44 **		
	(-108.96-247.33)	(-155.76--36.57)	(-151.06--25.83)		
	(90.89)	(30.41)	(31.95)		
AgeClss3		660.74 ***	671.90 ***	600.19 ***	653.17 ***
		(436.52-884.95)	(445.73-898.08)	(347.73-852.65)	(391.96-914.39)
		(114.40)	(115.40)	(128.81)	(133.28)
AgeClss4		195.92	255.05	438.81 *	578.27 **
		(-39.39-431.22)	(-21.81-531.91)	(82.57-795.06)	(177.66-978.87)
		(120.06)	(141.26)	(181.76)	(204.39)

AgeClss5	250.32*	276.94**	585.00***	652.94***
	(58.96-441.68)	(74.47-479.42)	(305.37-864.64)	(360.03-945.85)
	(97.64)	(103.31)	(142.67)	(149.45)
HghtCls3	-204.19*	-201.20*	18.98	18.95
	(-368.92--39.45)	(-366.30--36.09)	(-224.77-262.73)	(-223.87-261.76)
	(84.05)	(84.24)	(124.37)	(123.89)
HghtCls4	-15.32	-22.18	118.38	84.36
	(-201.75-171.10)	(-209.61-165.24)	(-170.51-407.27)	(-206.97-375.69)
	(95.12)	(95.63)	(147.39)	(148.64)
HghtCls5	-198.13	-219.18	-6.08	-90.02
	(-420.27-24.01)	(-447.55-9.18)	(-335.39-323.23)	(-436.61-256.58)
	(113.34)	(116.52)	(168.02)	(176.84)
CrwnDns2	-74.85	-64.88	-48.19	-33.56
	(-269.80-120.10)	(-261.61-131.85)	(-384.27-287.89)	(-368.91-301.79)
	(99.47)	(100.37)	(171.47)	(171.10)

CrwnDns3		-109.94	-109.96	49.93	45.40
		(-293.56-73.68)	(-293.82-73.89)	(-265.13-365.00)	(-268.51-359.31)
		(93.69)	(93.81)	(160.75)	(160.16)
CrwnDns4		65.42	66.59	204.86	190.11
		(-231.27-362.11)	(-230.49-363.67)	(-224.67-634.39)	(-238.21-618.44)
		(151.38)	(151.58)	(219.15)	(218.54)
EVI			25.14		69.94
			(-36.66-86.93)		(-23.29-163.18)
			(31.53)		(47.57)
Observations	95	157	157	160	160

Table B.12.7 Foliar stoichiometric N:P trait coefficient estimates, confidence intervals, and standard error values for top ranked models (< 2 ΔAIC_c). Species codes are used for balsam fir (ABBA), red maple (ACRU), white birch (BEPA), black spruce (PIMA), and lowbush blueberry (VAAN). If there is more than one top ranked model per species, we present in order of ΔAIC_c rank. Model numbers are supplied beside the species code in the top row (see Table 3.2 for model descriptions). Predictors include land cover (LandCover5 and LandCover6 represent deciduous and mixedwood conditions), EVI (i.e., proxy for productivity), abiotic factors (aspect, slope, elevation), and biotic factors: AgeClss3 (41- 60 years old), AgeClss 4 (61- 80 years old), AgeClss5 (81-100 years old), HghtCls3 (6.6-9.5 m), HghtCls4 (9.6-12.5 m), HghtCls5 (12.6-15.5m), CrwnDns2 (51-75 % closed), CrwnDns3 (26-50%), CrwnDn4 (10-25 % closed). Total number of observations are provided in the bottom row. In addition, asterisks are used to indicate coefficient significance as follows: * $p<0.05$ ** $p<0.01$ *** $p<0.001$.

	ACRU 9	**PIMA 2**	**VAAN 2**	**VAAN 7**	**VAAN 1**	**VAAN 5**
Predictors						
Intercept	29.44 ***	14.38 ***	29.35 ***	27.62 ***	31.58 ***	29.27 ***
	(27.63-31.25)	(11.34-17.42)	(22.46-36.24)	(21.02-34.23)	(23.67-39.50)	(21.88-36.66)
	(0.92)	(1.55)	(3.52)	(3.37)	(4.04)	(3.77)

EVI	2.37*	1.45***	2.44**	3.05***	2.63**	3.26***
	(0.52-4.21)	(0.66-2.24)	(0.70-4.19)	(1.38-4.72)	(0.89-4.37)	(1.58-4.94)
	(0.94)	(0.40)	(0.89)	(0.85)	(0.89)	(0.86)
Aspect	-1.87	-0.42	-1.33		-1.30	
	(-4.07-0.33)	(-1.22-0.37)	(-3.00-0.34)		(-2.96-0.36)	
	(1.12)	(0.41)	(0.85)		(0.85)	
Slope	-2.52*	-1.22**	0.05		0.26	
	(-4.72--0.33)	(-1.98--0.47)	(-1.59-1.69)		(-1.42-1.94)	
	(1.12)	(0.38)	(0.84)		(0.86)	
Elevation	-3.67**	-0.88*	-1.72*		-1.74*	
	(-5.84--1.50)	(-1.68--0.08)	(-3.36--0.08)		(-3.38--0.11)	
	(1.11)	(0.41)	(0.84)		(0.83)	
AgeClss3		6.38***	11.99***	13.24***	11.98***	13.57***
		(3.48-9.27)	(5.63-18.35)	(8.57-17.91)	(5.58-18.37)	(8.89-18.25)
		(1.48)	(3.24)	(2.38)	(3.26)	(2.39)

AgeClss4	2.45	7.76	10.93 **	6.42	10.27 **
	(-1.10-5.99)	(-0.20-15.73)	(3.76-18.10)	(-2.25-15.10)	(2.64-17.90)
	(1.81)	(4.06)	(3.66)	(4.43)	(3.89)
AgeClss5	2.48	11.98 ***	13.45 ***	12.28 ***	14.00 ***
	(-0.11-5.07)	(6.45-17.51)	(8.21-18.69)	(6.64-17.91)	(8.69-19.32)
	(1.32)	(2.82)	(2.67)	(2.88)	(2.71)
HghtCls3	-0.55	-1.98	-1.26	-2.28	-1.61
	(-2.66-1.56)	(-6.35-2.39)	(-5.61-3.08)	(-6.65-2.09)	(-5.96-2.74)
	(1.08)	(2.23)	(2.22)	(2.23)	(2.22)
HghtCls4	0.93	1.17	1.20	0.62	0.64
	(-1.47-3.33)	(-3.99-6.32)	(-4.02-6.41)	(-4.55-5.79)	(-4.59-5.88)
	(1.22)	(2.63)	(2.66)	(2.64)	(2.67)
HghtCls5	-0.06	-2.31	-2.89	-2.30	-2.85
	(-2.98-2.86)	(-8.54-3.92)	(-9.09-3.31)	(-8.50-3.89)	(-9.03-3.33)
	(1.49)	(3.18)	(3.16)	(3.16)	(3.15)

CrwnDns2		0.55	-2.84	-2.39	-1.37	-0.95
		(-1.97-3.06)	(-8.86-3.19)	(-8.39-3.61)	(-7.56-4.81)	(-7.16-5.27)
		(1.28)	(3.07)	(3.06)	(3.16)	(3.17)
CrwnDns3		-0.52	-1.46	-1.84	-0.06	-0.58
		(-2.87-1.83)	(-7.02-4.10)	(-7.46-3.77)	(-5.83-5.71)	(-6.41-5.26)
		(1.20)	(2.84)	(2.87)	(2.94)	(2.98)
CrwnDns4		0.66	-0.13	0.06	0.48	0.62
		(-3.14-4.46)	(-7.71-7.44)	(-7.60-7.73)	(-7.10-8.06)	(-7.07-8.31)
		(1.94)	(3.86)	(3.91)	(3.87)	(3.92)
LandCover5					-7.48	-7.02
					(-15.25-0.29)	(-14.86-0.83)
					(3.97)	(4.00)
LandCover6					-3.46	-3.00
					(-8.47-1.56)	(-7.92-1.91)
					(2.56)	(2.51)
Observations	91	157	160	160	160	160

Table B.12.8 Part one of three for foliar phytochemical trait coefficient estimates, confidence intervals, and standard error values for top ranked models (< 2 $\Delta \mathrm{AIC_c}$). Species codes are used for balsam fir (ABBA), red maple (ACRU), white birch (BEPA), black spruce (PIMA), and lowbush blueberry (VAAN). If there is more than one top ranked model per species, we present in order of $\Delta \mathrm{AIC_c}$ rank. Model numbers are supplied beside the species code in the top row (see Table 3.2 for model descriptions). Models denoted with the suffix "r" and "b" represent raw and biomass basis respectively. Predictors include land cover (LandCover5 and LandCover6 represent deciduous and mixedwood conditions), EVI (i.e., proxy for productivity), abiotic factors (aspect, slope, elevation), and biotic factors: AgeClss3 (41-60 years old), AgeClss 4 (61-80 years old), AgeClss5 (81-100 years old), HghtCls3 (6.6-9.5 m), HghtCls4 (9.6-12.5 m), HghtCls5 (12.6-15.5m), CrwnDns2 (51-75 % closed), CrwnDns3 (26-50%), CrwnDn4 (10-25 % closed). Total number of observations are provided in the bottom row. In addition, asterisks are used to indicate coefficient significance as follows: * *p<0.05 ** p<0.01 *** p<0.001*.

	ABBA Terpene 13r	**PIMA Terpene 2r**	**PIMA Terpene 10r**	**ABBA Terpene 10b**	**ABBA Monoterpene 9r**	**ABBA Monoterpene 15r**	**ABBA Monoterpene 13r**	**PIMA Monoterpene 10r**	**ABBA Monoterpene 10b**
Predictors									
Intercept	13.69 ***	16.02 ***	15.17 ***	73.58 ***	7.63 ***	7.63 ***	7.63 ***	5.12 ***	41.28 ***
	(13.07-	(12.11-	(11.38-	(33.79-	(7.20-8.07)	(7.19-8.07)	(7.19-8.08)	(3.88-6.35)	(17.85-64.71)
					(0.22)	(0.22)	(0.23)	(0.63)	(11.95)

	14.32) (0.32)	19.93) (2.00)	18.96) (1.93)	113.37) (20.30)					
EVI	0.73 * (0.10-1.36) (0.32)	-0.83 (-1.85-0.20) (0.52)			0.45 (0.00-0.90) (0.23)		0.48 * (0.03-0.93) (0.23)		
AgeClss3		8.84 *** (5.10-12.59) (1.91)	9.28 *** (5.55-13.00) (1.90)	-49.73 * (-97.16--2.31) (24.20)				2.66 *** (1.44-3.87) (0.62)	-30.43 * (-58.35--2.50) (14.25)
AgeClss4		4.11 (-0.47-8.70) (2.34)	6.09 ** (2.19-9.99) (1.99)	-24.13 (-70.13-21.87) (23.47)				2.29 *** (1.02-3.56) (0.65)	-14.26 (-41.35-12.83) (13.82)
AgeClss5		5.41 ** (2.05-8.77) (1.71)	6.31 *** (3.12-9.49) (1.62)	-37.93 (-75.56--				1.83 *** (0.79-2.87) (0.53)	-22.02 (-44.17-0.14) (11.30)

			0.31) (19.20)					
HghtCls3	-2.67 (-5.35-0.00) (1.37)	-2.65 (-5.34-0.04) (1.37)	-30.52 (-71.55-10.51) (20.93)				-1.09* (-1.97--0.21) (0.45)	-15.95 (-40.11-8.21) (12.33)
HghtCls4	-2.86 (-5.97-0.25) (1.59)	-3.14* (-6.25--0.03) (1.59)	-23.45 (-57.58-10.68) (17.41)				-1.04* (-2.06--0.03) (0.52)	-12.72 (-32.82-7.37) (10.25)
HghtCls5	-2.06 (-5.89-1.78) (1.95)	-2.79 (-6.53-0.95) (1.91)	-31.17 (-68.43-6.09) (19.01)				-0.86 (-2.08-0.36) (0.62)	-18.03 (-39.97-3.91) (11.19)
CrwnDns2	1.05 (-2.24-	1.40 (-1.88-	3.75 (-27.06-				0.90 (-0.17-1.97) (0.55)	2.67 (-15.47-

	4.33) (1.68)	4.67) (1.67)	34.55) (15.72)					20.81) (9.25)
CrwnDns3	1.56 (-1.52-4.65) (1.57)	1.57 (-1.54-4.67) (1.58)	12.28 (-21.71-46.27) (17.34)				0.76 (-0.25-1.77) (0.52)	8.56 (-11.45-28.57) (10.21)
CrwnDns4	4.20 (-0.81-9.21) (2.56)	4.24 (-0.80-9.27) (2.57)	46.34 (-3.47-96.14) (25.41)				1.37 (-0.28-3.01) (0.84)	29.79 * (0.46-59.11) (14.96)
Aspect	-0.11 (-1.14-0.92) (0.52)	-0.11 (-1.15-0.92) (0.53)	-2.23 (-14.14-9.69) (6.08)	-0.09 (-0.62-0.44) (0.27)	-0.00 (-0.53-0.53) (0.27)		-0.19 (-0.53-0.15) (0.17)	-1.55 (-8.57-5.47) (3.58)
Slope	-1.60 ** (-2.61--	-1.61 ** (-2.63--	20.40 *** (9.52-31.28) (5.55)	0.67 * (0.11-1.22) (0.28)	0.75 ** (0.19-1.30) (0.28)		-0.38 * (-0.71--0.04) (0.17)	12.61 *** (6.20-19.02) (3.27)

		0.59)	0.60)						
		(0.52)	(0.52)						
Elevation		-2.69 ***	-2.45 ***	7.45	0.29	0.28		-0.70 ***	4.55
		(-3.69--	(-3.41--	(-4.62-	(-0.26-0.85)	(-0.28-0.84)		(-1.01--0.38)	(-2.55-11.66)
		1.68)	1.49)	19.52)	(0.28)	(0.29)		(0.16)	(3.63)
		(0.51)	(0.49)	(6.16)					
Observations	104	163	163	104	104	104	104	163	104

Table B.12.9 Part two of three for foliar phytochemical trait coefficient estimates, confidence intervals, and standard error values for top ranked models (< 2 ΔAIC_c). Species codes are used for balsam fir (ABBA), red maple (ACRU), white birch (BEPA), black spruce (PIMA), and lowbush blueberry (VAAN). If there is more than one top ranked model per species, we present in order of ΔAIC_c rank. Model numbers are supplied beside the species code in the top row (see Table 3.2 for model descriptions). Codes are used for monoterpenic alcohol (MA) and monoterpenic ester (ME). Models denoted with the suffix "r" and "b" represent raw and biomass basis respectively. Predictors include land cover (LandCover5 and LandCover6 represent deciduous and mixedwood conditions), EVI (i.e., proxy for productivity), abiotic factors (aspect, slope, elevation), and biotic factors: AgeClss3 (41-60 years old), AgeClss 4 (61-80 years old), AgeClss5 (81-100 years old), HghtCls3 (6.6-9.5 m), HghtCls4 (9.6-12.5 m), HghtCls5 (12.6-15.5m), CrwnDns2 (51-75 % closed), CrwnDns3 (26-50%), CrwnDn4 (10-25 % closed). Total number of observations are provided in the bottom row. In addition, asterisks are used to indicate coefficient significance as follows: * $p<0.05$ ** $p<0.01$ *** $p<0.001$.

	PIMA MA 10r	**PIMA ME 10r**	**PIMA ME 2r**	**ABBA ME 10b**
Predictors				
Intercept	0.23 ***	4.37 ***	4.57 ***	12.89 ***
	(0.15-0.31)	(2.97-5.76)	(3.13-6.02)	(6.12-19.66)
	(0.04)	(0.71)	(0.74)	(3.45)

AgeClss3	0.19 ***	3.21 ***	3.10 ***	-7.81
	(0.10-0.27)	(1.84-4.58)	(1.72-4.49)	(-15.88-0.26)
	(0.04)	(0.70)	(0.71)	(4.12)
AgeClss4	0.17 ***	2.66 ***	2.17 *	-3.97
	(0.09-0.26)	(1.22-4.09)	(0.47-3.87)	(-11.80-3.85)
	(0.04)	(0.73)	(0.87)	(3.99)
AgeClss5	0.13 ***	2.17 ***	1.95 **	-6.36
	(0.06-0.20)	(1.00-3.35)	(0.71-3.20)	(-12.76-0.04)
	(0.04)	(0.60)	(0.63)	(3.27)
HghtCls3	-0.08 **	-1.33 **	-1.33 **	-5.78
	(-0.14--0.02)	(-2.32--0.34)	(-2.33--0.34)	(-12.76-1.20)
	(0.03)	(0.51)	(0.51)	(3.56)
HghtCls4	-0.06	-0.99	-0.92	-4.38
	(-0.13-0.00)	(-2.13-0.16)	(-2.07-0.23)	(-10.18-1.43)
	(0.03)	(0.58)	(0.59)	(2.96)

HghtCls5	-0.04	-0.67	-0.49	-5.86
	(-0.13-0.04)	(-2.05-0.71)	(-1.91-0.93)	(-12.19-0.48)
	(0.04)	(0.70)	(0.72)	(3.23)
CrwnDns2	0.05	0.87	0.79	0.53
	(-0.02-0.12)	(-0.33-2.08)	(-0.43-2.01)	(-4.71-5.77)
	(0.04)	(0.62)	(0.62)	(2.67)
CrwnDns3	0.04	0.69	0.69	1.89
	(-0.02-0.11)	(-0.45-1.83)	(-0.45-1.83)	(-3.90-7.67)
	(0.03)	(0.58)	(0.58)	(2.95)
CrwnDns4	0.14 *	1.16	1.15	6.61
	(0.03-0.25)	(-0.69-3.02)	(-0.70-3.01)	(-1.86-15.09)
	(0.06)	(0.95)	(0.95)	(4.32)
Aspect	-0.00	-0.08	-0.08	-0.06
	(-0.02-0.02)	(-0.47-0.30)	(-0.46-0.30)	(-2.08-1.97)
	(0.01)	(0.19)	(0.19)	(1.03)

Slope	-0.03 **	-0.42 *	-0.42 *	3.15 **
	(-0.05--0.01)	(-0.79--0.05)	(-0.79--0.04)	(1.30-5.01)
	(0.01)	(0.19)	(0.19)	(0.94)
Elevation	-0.03 *	-0.73 ***	-0.79 ***	1.32
	(-0.05--0.00)	(-1.08--0.37)	(-1.16--0.41)	(-0.73-3.38)
	(0.01)	(0.18)	(0.19)	(1.05)
EVI			-0.20	
			(-0.58-0.18)	
			(0.19)	
Observations	163	163	163	104

Table B.12.10 Part three of three for foliar phytochemical trait coefficient estimates, confidence intervals, and standard error values for top ranked models (< 2 ΔAIC_c). Species codes are used for balsam fir (ABBA), red maple (ACRU), white birch (BEPA), black spruce (PIMA), and lowbush blueberry (VAAN). If there is more than one top ranked model per species, we present in order of ΔAIC_c rank. Model numbers are supplied beside the species code in the top row (see Table 3.2 for model descriptions). Sesquesterpene is truncated as sesq. Models denoted with the suffix "r" and "b" represent raw and biomass basis respectively. Predictors include land cover (LandCover5 and LandCover6 represent deciduous and mixedwood conditions), EVI (i.e., proxy for productivity), abiotic factors (aspect, slope, elevation), and biotic factors: AgeClss3 (41-60 years old), AgeClss 4 (61-80 years old), AgeClss5 (81-100 years old), HghtCls3 (6.6-9.5 m), HghtCls4 (9.6-12.5 m), HghtCls5 (12.6-15.5m), CrwnDns2 (51-75 % closed), CrwnDns3 (26-50%), CrwnDn4 (10-25 % closed). Total number of observations are provided in the bottom row. In addition, asterisks are used to indicate coefficient significance as follows: * *p<0.05* ** *p<0.01* *** *p<0.001*.

Predictors	**ABBA Sesq 9r**	**ABBA Sesq 13r**	**ABBA Sesq 15r**	**PIMA Sesq 4r**	**PIMA Sesq 15r**	**PIMA Sesq 2r**	**PIMA Sesq 9r**	**PIMA Diversity 12**	**PIMA Diversity 14**	**PIMA Diversity 13**
Intercept	1.38 ***	1.38 ***	1.38 ***	0.58 ***	0.66 ***	0.66 ***	0.66 ***	2.23 ***	2.28 ***	2.26 ***
	(1.30-1.47)	(1.29-1.47)	(1.30-1.47)	(0.48-0.67)	(0.63-0.70)	(0.46-0.86)	(0.63-0.70)	(2.21-2.26)	(2.22-2.34)	(2.25-2.27)
	(0.04)	(0.04)	(0.04)	(0.05)	(0.02)	(0.10)	(0.02)	(0.01)	(0.03)	(0.01)

EVI	0.08 (-0.00-0.17) (0.05)	0.09 * (0.01-0.18) (0.05)		-0.05 * (-0.10-0.00) (0.02)		-0.06 * (-0.11- -0.01) (0.03)	-0.02 (-0.06-0.02) (0.02)			0.01 (-0.00-0.02) (0.01)
Aspect	-0.05 (-0.15-0.06) (0.05)		-0.03 (-0.13-0.08) (0.05)	-0.03 (-0.07-0.01) (0.02)	-0.03 (-0.07-0.02) (0.02)	0.01 (-0.04-0.07) (0.03)	-0.03 (-0.07-0.02) (0.02)			
Slope	-0.06 (-0.17-0.05) (0.06)		-0.04 (-0.15-0.07) (0.06)	-0.03 (-0.07-0.02) (0.02)	-0.02 (-0.06-0.02) (0.02)	-0.06 * (-0.11--0.01) (0.03)	-0.02 (-0.06-0.02) (0.02)			
Elevation	-0.15 * (-0.25--0.04) (0.06)		-0.15 * (-0.26--0.04) (0.06)	-0.09 *** (-0.14--0.05) (0.02)	-0.08 *** (-0.13--0.04) (0.02)	-0.13 *** (-0.19--0.08) (0.03)	-0.08 *** (-0.13--0.04) (0.02)			
LandCover5				-0.02 (-0.23-0.18) (0.10)				0.03 (-0.04-0.09) (0.03)		
LandCover6				0.12 * (0.00-0.23) (0.06)				0.04 ** (0.01-0.07) (0.01)		

AgeClss3	0.26 **	-0.04 *
	(0.07-0.46)	(-0.09--0.00)
	(0.10)	(0.02)
AgeClss4	-0.06	-0.09 **
	(-0.30-0.17)	(-0.15--0.03)
	(0.12)	(0.03)
AgeClss5	0.15	-0.05 *
	(-0.02-0.32)	(-0.10--0.00)
	(0.09)	(0.03)
HghtCls3	-0.03	0.05 *
	(-0.17-0.10)	(0.01-0.09)
	(0.07)	(0.02)
HghtCls4	-0.08	0.04
	(-0.24-0.08)	(-0.02-0.09)
	(0.08)	(0.03)
HghtCls5	-0.07	0.06 *
	(-0.27-0.13)	(0.00-0.12)
	(0.10)	(0.03)

CrwnDns2					-0.05			-0.01		
					(-0.22-0.12)			(-0.06-0.04)		
					(0.09)			(0.03)		
CrwnDns3					-0.03			-0.00		
					(-0.19-0.13)			(-0.05-0.05)		
					(0.08)			(0.03)		
CrwnDns4					0.07			-0.04		
					(-0.19-0.32)			(-0.12-0.05)		
					(0.13)			(0.04)		
Observations	104	104	104	163	163	163	163	163	163	163

B.13 Correlation plot for data space and spatial explicit comparisons of foliar ESP traits across species

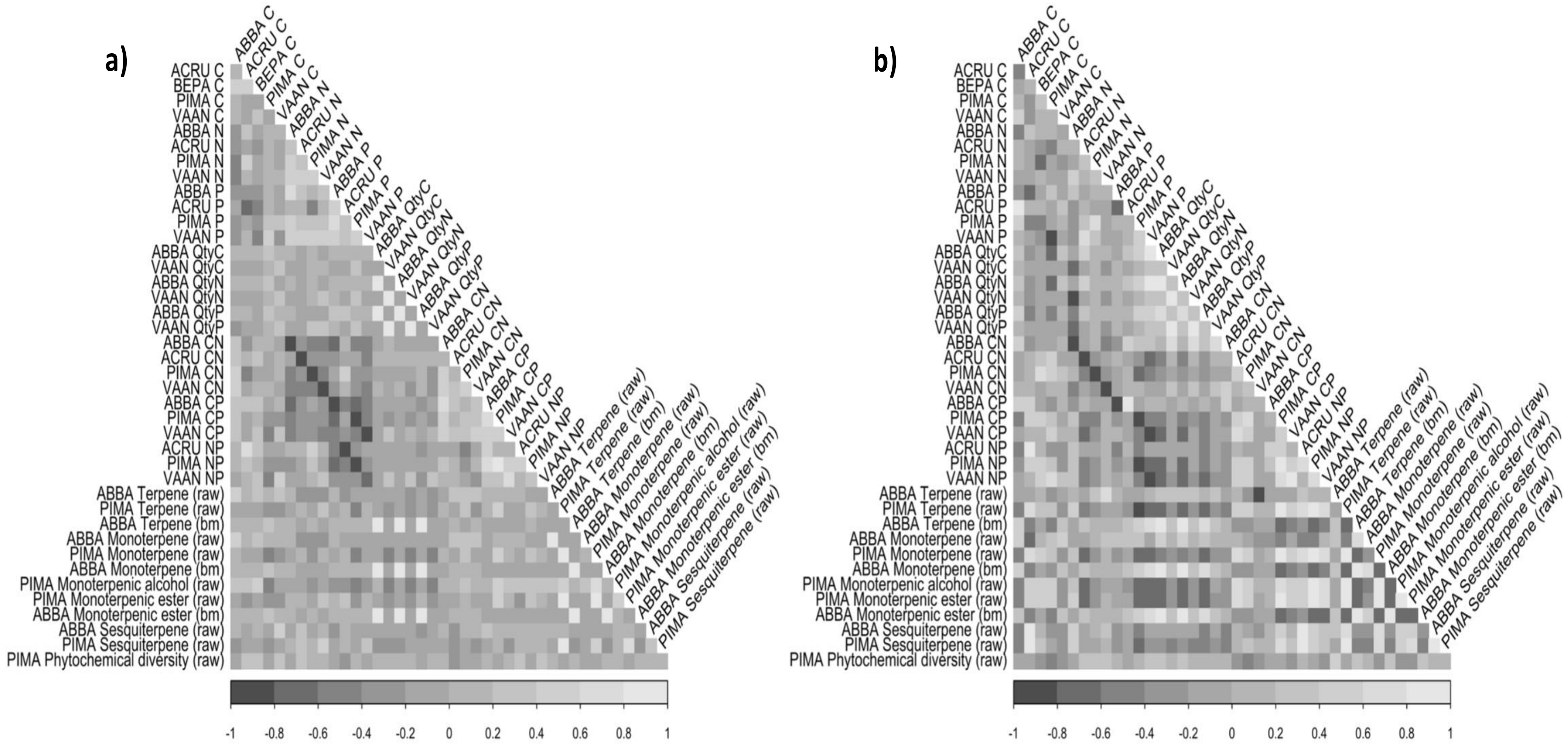

Figure B.13.1 Correlation plot showing the relationships between our study species foliar elemental, stoichiometric, and phytochemical traits for top ranked models where the intercept was not with < 2 ΔAIC_c. The left correlation plot (a) shows data space comparisons, for this we only compared plots in which all species were present (n = 29). The right correlation plot (b) shows spatial comparisons of predictive trait raster/surfaces. Correlation in data space is limited to co-occurrence of observations, while spatial correlation considers all pixels. In panel (b), we can see emergent patterns that are less apparent in data space comparisons (a).

B.14 References

Cachet, T., Brevard, H., Chaintreau, A., Demyttenaere, J., French, L., Gassenmeier, K., Joulain, D., Koenig, T., Leijs, H., Liddle, P., Loesing, G., Marchant, M., Merle, Ph., Saito, K., Schippa, C., Sekiya, F., & Smith, T. (2016). IOFI recommended practice for the use of predicted relative-response factors for the rapid quantification of volatile flavouring compounds by GC-FID. *Flavour and Fragrance Journal*, *31*(3), 191–194. https://doi.org/10.1002/ffj.3311

Ecological Stratification Working Group. (1996). *A national ecological framework for Canada*. Centre for Land and Biological Resources Research, Research Branch, Agriculture and Agri-Food Canada.

Evans, J. (2020). *spatialEco. R package* (1.3-3) [Computer software]. https://github.com/jeffreyevans/spatialEco

Hijmans, R., J. (2020). *Raster: Geographic Data Analysis and Modeling. R package* (3.4-5) [Computer software].

Jones, J. W., Starbuck, M. J., & Jenkerson, C. B. (2013). *Landsat surface reflectance quality assurance extraction (version 1.7): U.S. Geological Survey Techniques and Methods*. https://pubs.usgs.gov/tm/11/c07

Muraoka, H., Noda, H. M., Nagai, S., Motohka, T., Saitoh, T. M., Nasahara, K. N., & Saigusa, N. (2013). Spectral vegetation indices as the indicator of canopy photosynthetic productivity in a deciduous broadleaf forest. *Journal of Plant Ecology*, *6*(5), 393–407. https://doi.org/10.1093/jpe/rts037

Poitevin, E. (2016). Official methods for the determination of minerals and trace elements in infant formula and milk products: A review. *Journal of AOAC International*, *99*(1), 42–52. https://doi.org/10.5740/jaoacint.15-0246

Requena-Mullor, J. M., López, E., Castro, A. J., Alcaraz-Segura, D., Castro, H., Reyes, A., & Cabello, J. (2017). Remote-sensing based approach to forecast habitat quality under climate change scenarios. *PLOS ONE*, *12*(3), e0172107. https://doi.org/10.1371/journal.pone.0172107

South, R. G. (1983). *Biogeography and ecology of the island of Newfoundland* (Vol. 48). Dr. W. Junk Publishers, The Hague, The Netherlands.

U.S. Geological Survey. (2017). *Landsat Quality Assurance ArcGIS Toolbox*. US Department of the Interior. doi: 10.5066/F7JM284N

Waring, R. H., Coops, N. C., Fan, W., & Nightingale, J. M. (2006). MODIS enhanced vegetation index predicts tree species richness across forested ecoregions in the contiguous U.S.A. *Remote Sensing of Environment*, *103*(2), 218–226. https://doi.org/10.1016/j.rse.2006.05.007

Appendix C Supplemental Information for Chapter 4: Local scale spatial co-dispersion patterns of plant functional traits between co-occurring species

C.1 Overview map of sample locations and sampling grid design

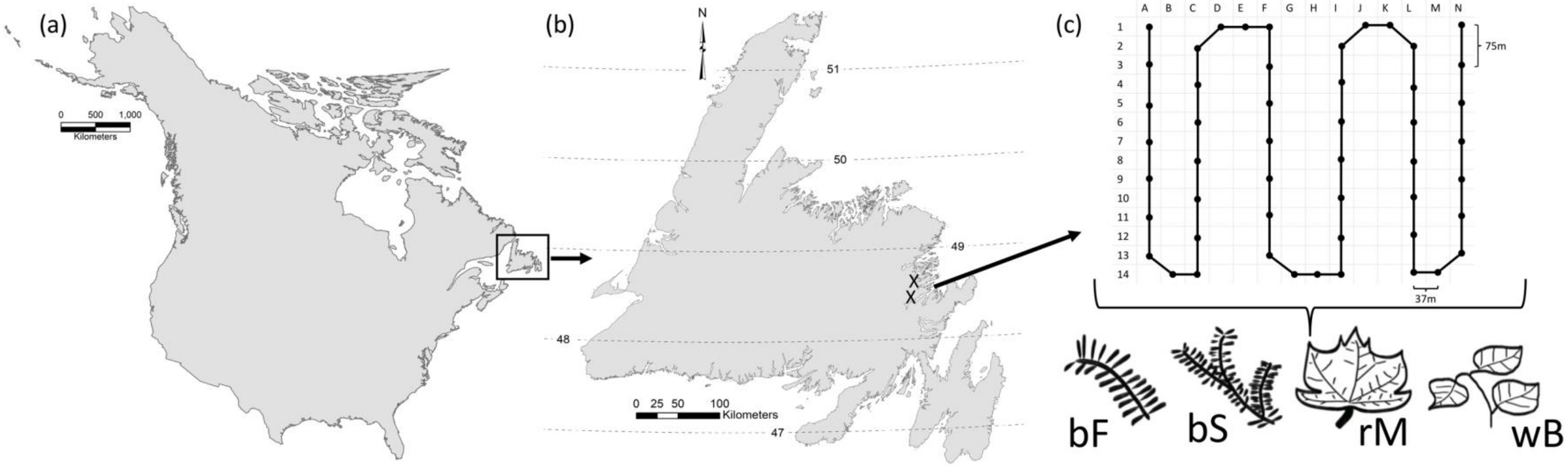

Figure C.1.1 Our study is located in North America (a) on the island of Newfoundland, Canada (b). Within two forest types of similar species composition but of different age (b, denoted with X), we set up a meandering transect sampling grid that consists of 50 sampling locations (c). At each location we sampled we collected foliage from four different species, if they were present: balsam fir (bF), black spruce (bS), red maple (rM), and white birch (wB).

C.2 Species trait variability by study site

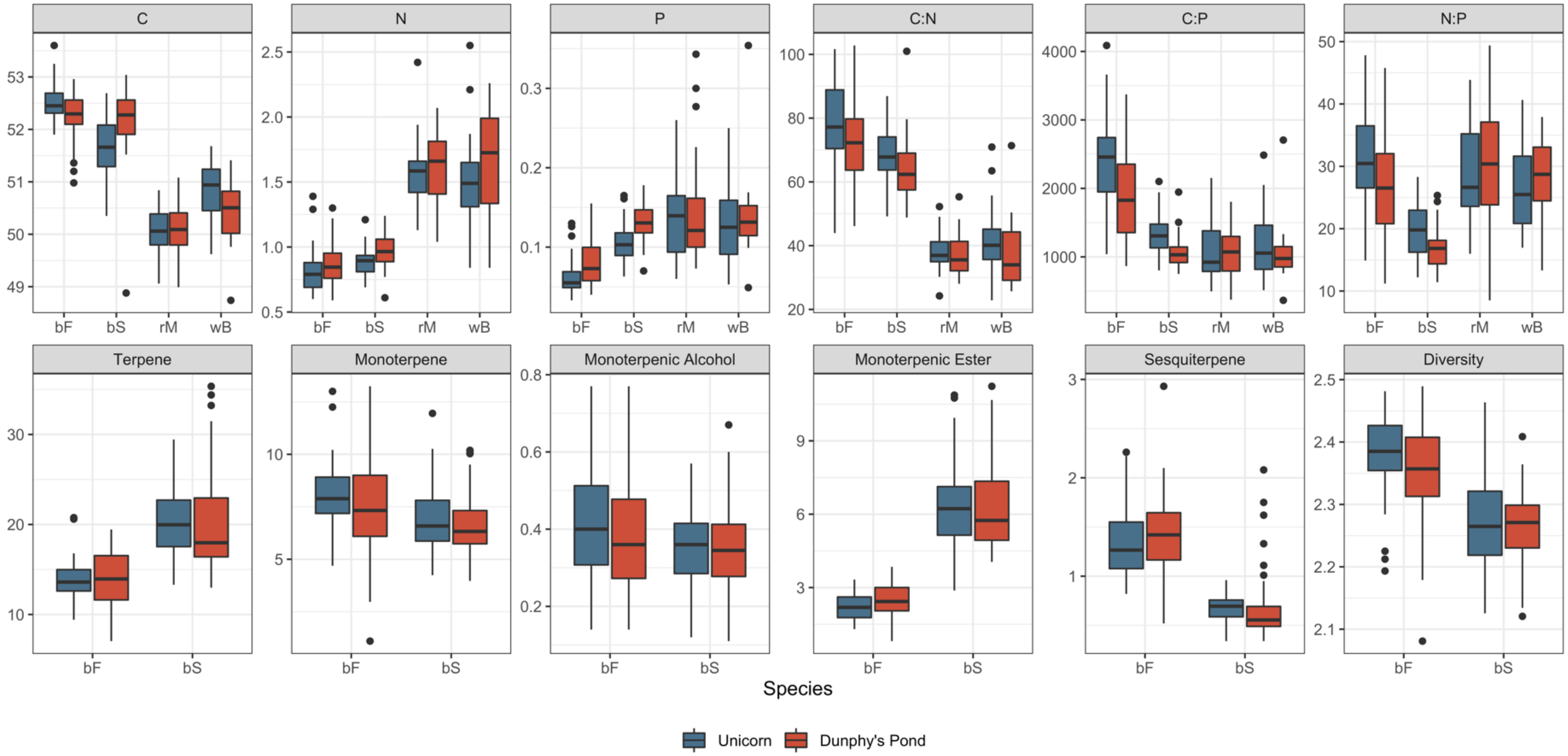

Figure C.2.1 Species trait distribution comparisons by site: Unicorn (age: 60-80 years old) and Dunphy’s Pond (80-100 years old). Foliar elemental traits are expressed in percentages. Foliar stoichiometric traits are expression in ratios on a molar mass basis. Foliar phytochemical traits are expressed on a mg/g basis. Species codes definitions; bF: balsam fir, bS: black spruce, rM: red maple, wB: white birch. Note: data presented are for all plots at which a species occurred. Co-dispersion comparisons are for where two of our focal species co-occurred and as such represent a smaller sample size.

C.3 Range of co-dispersion coefficient for species elemental, stoichiometric, and phytochemical trait comparisons

Table C.3.1 Foliar elemental trait minimum, maximum, and average co-dispersion coefficient (CC) values and corresponding distances (dist) for our species comparisons between two forest stands, Unicorn (40-60 years old) and Dunphy's (80-100 years old). Bolded rows indicate significant relationships at $p \leq 0.05$. Species codes: balsam fir (bF), black spruce (bS), red maple (rM), and white birch (wB).

		Unicorn					Dunphy's Pond				
Species	Trait	Min CC	Min Dist (m)	Max CC	Max Dist (m)	Avg CC	Min CC	Min Dist (m)	Max CC	Max Dist (m)	Avg CC
bF-bS	C	0.00	14	0.55	70	0.28	**-0.29**	**44**	**0.55**	**194**	**0.26**
	N	-0.71	42	0.53	239	0.12	**0.00**	**14**	**0.73**	**44**	**0.45**
	P	**0.00**	**14**	**0.61**	**98**	**0.36**	**0.00**	**14**	**0.67**	**224**	**0.50**
bF-rM	C	-0.27	70	0.27	98	0.07	-0.06	50	1.00	16	0.34
	N	**0.00**	**14**	**0.65**	**42**	**0.34**	**0.42**	**183**	**1.00**	**16**	**0.58**
	P	-0.11	42	0.55	182	0.26	**0.68**	**83**	**1.00**	**16**	**0.79**
bF-wB	C	-1.00	14	0.68	43	-0.19	**0.00**	**16**	**0.90**	**48**	**0.71**
	N	-0.22	43	1.00	14	0.30	-0.46	48	0.15	112	-0.06
	P	-0.12	189	1.00	14	0.44	-0.50	48	0.56	176	0.10

	C	-0.40	43	1.00	14	0.29	-0.14	254	0.54	74	0.17
bS-rM	N	-0.08	219	1.00	14	0.26	**0.00**	**14**	**0.71**	**104**	**0.48**
	P	-0.29	219	1.00	14	0.16	**0.00**	**14**	**0.66**	**74**	**0.46**
	C	-0.65	82	1.00	16	0.20	0.00	16	0.65	48	0.21
bS-wB	N	-0.50	180	1.00	16	0.02	-0.51	48	0.48	112	0.06
	P	-0.68	180	1.00	16	0.03	-0.46	48	0.52	176	0.17
	C	**0.24**	**49**	**1.00**	**16**	**0.52**	-0.11	112	0.44	48	0.19
rM-wB	N	**-0.26**	**114**	**1.00**	**16**	**0.56**	0.00	16	0.36	176	0.21
	P	**0.63**	**147**	**1.00**	**16**	**0.74**	-0.18	208	0.30	176	0.13

Table C.3.2 Foliar stoichiometric trait minimum, maximum, and average co-dispersion coefficient (CC) values and corresponding distances (dist) for our species comparisons between two forest stands, Unicorn (40-60 years old) and Dunphy's (80-100 years old). Bolded rows indicate significant relationships at $p \leq 0.05$. Species codes: balsam fir (bF), black spruce (bS), red maple (rM), and white birch (wB).

		Unicorn					Dunphy's Pond				
Species	Trait	Min CC	Min Dist (m)	Max CC	Max Dist (m)	Avg CC	Min CC	Min Dist (m)	Max CC	Max Dist (m)	Avg CC
bF-bS	C:N	-0.79	42	0.54	239	0.13	**0.00**	**14**	**0.73**	**44**	**0.49**
	C:P	-0.30	42	0.58	70	0.27	**0.00**	**14**	**0.66**	**224**	**0.50**
	N:P	**0.00**	**14**	**0.81**	**98**	**0.58**	**0.00**	**14**	**0.83**	**224**	**0.66**
bF-rM	C:N	-0.08	98	0.53	42	0.17	**-1.00**	**16**	**0.84**	**50**	**0.41**
	C:P	**0.00**	**14**	**0.59**	**182**	**0.38**	**0.68**	**83**	**1.00**	**16**	**0.76**
	N:P	**0.00**	**14**	**0.84**	**42**	**0.49**	**0.72**	**216**	**1.00**	**16**	**0.78**
bF-wB	C:N	-0.26	43	1.00	14	0.12	-0.44	48	0.16	176	-0.06
	C:P	**0.07**	**189**	**1.00**	**14**	**0.48**	-0.25	208	0.55	176	0.10
	N:P	**0.01**	**189**	**1.00**	**14**	**0.54**	**0.00**	**16**	**0.81**	**176**	**0.50**
bS-rM	C:N	-0.10	219	1.00	14	0.25	**0.00**	**14**	**0.75**	**104**	**0.50**

	C:P	-0.29	189	1.00	14	0.23	**0.00**	**14**	**0.70**	**194**	**0.44**
	N:P	-0.30	131	1.00	14	0.30	**0.00**	**14**	**0.74**	**224**	**0.57**
bS-wB	C:N	-0.33	180	1.00	16	0.06	-0.48	48	0.29	144	-0.02
	C:P	-0.35	180	1.00	16	0.17	-0.36	48	0.55	144	0.19
	N:P	-0.65	180	1.00	16	0.12	0.00	16	0.64	240	0.44
rM-wB	C:N	-0.27	114	1.00	16	0.28	0.00	16	0.34	176	0.17
	C:P	**0.60**	**49**	**1.00**	**16**	**0.73**	-0.32	48	0.44	80	0.09
	N:P	**0.83**	**49**	**1.00**	**16**	**0.87**	0.00	16	0.59	240	0.35

Table C.3.3 Foliar phytochemical trait minimum, maximum, and average co-dispersion coefficient (CC) values and corresponding distances (dist) for our species comparisons between two forest stands, Unicorn (40-60 years old) and Dunphy's (80-100 years old). Bolded rows indicate significant relationships at $p \leq 0.05$. Species codes: balsam fir (bF), black spruce (bS), red maple (rM), and white birch (wB).

		Unicorn					Dunphy's Pond				
Species	Trait	Min CC	Min Dist (m)	Max CC	Max Dist (m)	Avg CC	Min CC	Min Dist (m)	Max CC	Max Dist (m)	Avg CC
bF-bS	Diversity	-0.55	47	0.97	15	-0.04	-1	15	0.02	47	-0.23
	Monoterpene	-1.00	15	0.82	47	0.05	-1	15	0.14	175	-0.08
	Monoterpenic Alcohol	-0.02	271	0.83	47	0.25	-1	15	0.31	206	0.09
	Monoterpenic Ester	-0.75	15	0.83	47	0.10	-1	15	0.01	111	-0.17
	Sesquiterpene	-0.27	335	0.17	15	-0.12	-1	15	0.22	175	-0.07
	Terpene	-0.99	15	0.82	47	0.02	-1	15	0.07	47	-0.13

C.4 Modified *t*-test results for species elemental, stoichiometric, and phytochemical trait comparisons

Table C.4.1 Foliar elemental trait modified *t*-test, *F*-statistic, degrees of freedom (DoF), *p*-values (bolded indicates significance at $p \leq 0.05$) and Pearson's correlation coefficient for spatial autocorrelation (R^2) for species comparisons between our two forest stands, Unicorn (40-60 years old) and Dunphy's Pond (80-100 years old). Species codes: balsam fir (bF), black spruce (bS), red maple (rM), and white birch (wB).

		Unicorn				Dunphy's Pond			
Species	Trait	*F*-statistic	DoF	*p*-value	R^2	*F*-statistic	DoF	*p*-value	R^2
bF-bS	C	2.663	18.786	0.119	0.352	5.658	32.444	**0.023**	0.385
	N	0.588	34.854	0.449	0.129	10.598	31.793	**0.003**	0.500
	P	5.378	29.384	**0.028**	0.393	11.041	28.102	**0.002**	0.531
bF-rM	C	0.248	28.868	0.622	0.092	3.387	35.892	0.074	0.294
	N	6.047	29.665	**0.020**	0.412	10.965	31.541	**0.002**	0.508
	P	2.317	20.030	0.144	0.322	24.705	17.449	**0.0001**	0.766
bF-wB	C	0.585	19.583	0.454	-0.170	30.610	17.169	**0.00003**	0.800
	N	3.837	21.147	0.063	0.392	0.011	15.535	0.918	-0.027
	P	3.614	21.869	0.071	0.377	0.236	17.212	0.633	0.116
bS-rM	C	1.489	19.381	0.237	0.267	0.499	23.085	0.487	0.145

	N	0.672	15.550	0.425	0.204	9.568	20.068	**0.006**	0.568
	P	0.064	18.944	0.802	0.058	9.057	28.698	**0.005**	0.490
bS-wB	C	0.919	15.988	0.352	-0.233	0.872	12.194	0.368	0.258
	N	0.092	16.443	0.765	-0.075	0.523	22.041	0.477	0.152
	P	0.075	21.557	0.787	-0.059	1.223	18.745	0.283	0.247
rM-wB	C	7.050	12.937	**0.020**	0.594	1.410	18.510	0.250	0.266
	N	8.383	14.073	**0.012**	0.611	0.706	15.270	0.414	0.210
	P	9.921	10.706	**0.010**	0.694	0.828	18.784	0.374	0.205

Table C.4.2 Modified *t*-test results for foliar stoichiometric trait comparisons between our focal species, including the *F*-statistic, degrees of freedom (DoF), *p*-values (bolded indicates significance at $p \leq 0.05$) and Pearson's correlation coefficient for spatial autocorrelation (R^2). Results are presented to show comparisons between our two chronosequenced forest study sites, Unicorn (40 – 60 years) and Dunphy's Pond (80 – 100 years). Species codes are used for balsam fir (bF), black spruce (bS), red maple (rM), and white birch (wB).

		Unicorn				Dunphy's Pond			
Species	Trait	*F*-statistic	DoF	*p*-value	R^2	F-statistic	DoF	*p*-value	R^2
bF-bS	C:N	0.967	34.826	0.332	0.164	16.508	32.083	**0.0002**	0.583
	C:P	3.415	29.622	0.075	0.321	13.377	32.170	**0.001**	0.542
	N:P	14.325	25.279	**0.001**	0.601	18.555	18.418	**0.0004**	0.708
bF-rM	C:N	0.947	31.087	0.338	0.172	13.695	35.945	**0.001**	0.525
	C:P	4.481	21.407	**0.046**	0.416	19.504	18.081	**0.0003**	0.720
	N:P	8.554	22.711	**0.008**	0.523	23.254	14.314	**0.0002**	0.787
bF-wB	C:N	0.161	22.398	0.692	0.085	0.015	17.588	0.906	-0.029
	C:P	4.484	23.936	**0.045**	0.397	0.657	20.180	0.427	0.178
	N:P	9.914	29.755	**0.004**	0.500	10.453	18.041	**0.005**	0.606

bS-rM	C:N	0.549	16.409	0.469	0.180	11.467	20.719	**0.003**	0.597
	C:P	0.533	16.898	0.475	0.175	8.279	30.095	**0.007**	0.464
	N:P	0.570	17.260	0.460	0.179	12.117	16.100	**0.003**	0.655
bS-wB	C:N	0.032	18.105	0.861	-0.042	0.166	20.949	0.688	0.089
	C:P	0.117	16.423	0.737	0.084	2.737	20.030	0.114	0.347
	N:P	0.116	19.139	0.737	0.078	3.437	10.081	0.093	0.504
rM-wB	C:N	1.748	16.136	0.205	0.313	0.517	15.667	0.483	0.179
	C:P	11.303	12.500	**0.005**	0.689	1.260	17.110	0.277	0.262
	N:P	29.879	12.328	**0.0001**	0.841	4.115	12.451	0.064	0.498

Table C.4.3 Modified *t*-test results for foliar phytochemical trait comparisons between our focal species, including the *F*-statistic, degrees of freedom (DoF), *p*-values (bolded indicates significance at $p \leq 0.05$) and Pearson's correlation coefficient for spatial autocorrelation (R^2). Results are presented to show comparisons between our two chronosequenced forest study sites, Unicorn (40 – 60 years) and Dunphy's Pond (80 – 100 years). Species codes are used for balsam fir (bF), black spruce (bS), red maple (rM), and white birch (wB).

		Unicorn				Dunphy's Pond			
Species	Trait	*F*-statistic	DoF	*p*-value	R^2	*F*-statistic	DoF	*p*-value	R^2
bF-bS	Terpene	0.108	46.621	0.744	0.048	0.152	44.951	0.698	-0.058
	Monoterpene	0.315	42.726	0.578	0.086	0.000	42.373	0.990	-0.002
	Monoterpenic Alcohol	1.002	43.294	0.322	0.150	1.128	35.847	0.295	0.175
	Monoterpenic Ester	0.934	42.686	0.339	0.146	0.872	42.967	0.356	-0.141
	Sesquiterpene	1.960	44.254	0.168	0.146	0.000	48.686	0.994	-0.141
	Diversity	0.314	45.698	0.578	-0.083	0.698	40.162	0.408	-0.131